Handling and Final Storage of Unreprocessed Spent Nuclear Fuel

Volume

I General

II Technical

KÄRN -
BRÄNSLE -
SÄKERHET

Handling and Final Storage of Unreprocessed Spent Nuclear Fuel

Volume

I General

II Technical

KÄRN-
BRÄNSLE-
SÄKERHET

MAILING ADDRESS: Kärnbränslesäkerhet, Fack, S-102 40 Stockholm, Sweden.

TABLE OF CONTENTS FOR TECHNICAL VOLUME

1 INTRODUCTION

KBS' first report entitled "Handling of Spent Nuclear Fuel and Final Storage of Vitrified High Level Reprocessing Waste" was published in November 1977. This second report deals with the second alternative given by the Stipulation Law, i.e. the handling and final storage of spent nuclear fuel which has not been reprocessed, the so-called "direct disposal alternative".

Some of the background material for this report is the same as that used for the preceding report. In its general principles, the proposed handling chain is also similar for the two alternatives. In both cases, it is proposed that the waste be encapsulated in a corrosion-resistant material, after which final deposition of the canisters shall take place in vertical boreholes drilled from tunnels at great depth in the crystalline bedrock. Prior to final disposal, a supervised intermediate storage period is proposed for the direct disposal alternative as well. The purpose of this intermediate storage period is to allow the heat flux of the waste to decrease so that the maximum temperature in the final repository can be kept well below $100^{\circ}C$. During the period of intermediate storage, freedom of choice will be retained with regard to the question of reprocessing, while time will be provided for the development and improvement of methods for encapsulation and final storage.

The different properties of the two types of waste, vitrified reprocessing waste and spent nuclear fuel, do, however, entail considerable differences with respect to certain aspects of the handling procedures and the design of the facilities.

The Stipulation Law refers to spent nuclear fuel. This includes the fuel rods with their zircaloy cladding as well as certain metal structural components which hold the fuel rods together in fuel assemblies. The fuel rods and the metal components represent different types of waste whose handling and storage is described in the following.

Appendix 1 to the preceding KBS report presented a status report on the direct disposal of spent nuclear fuel. The more exhaustive studies which have been conducted since then have led to certain modifications in the proposal sketched there. This applies above all with regard to the following three points.

- Now completed studies have shown that the fuel's zircaloy cladding can be expected to remain intact even in contact with water for considerably longer periods of time than the

intermediate storage period of about 40 years proposed here. It has therefore been possible to omit the previously proposed stainless steel container in which the fuel was to be enclosed to prevent it from coming into contact with water.
- The canister is surrounded with highly-compacted bentonite instead of a mixture of bentonite and quartz sand in order to provide the canister with even better protection against the action of the groundwater.
- In order to make the best possible use of the favourable effects of the highly-compacted bentonite, the canisters are positioned vertically in the borehole - in the same manner as the vitrified waste - and not horizontally in storage tunnels as shown in the status report.

The work carried out within the KBS project has gradually expanded the available body of knowledge, and the background material is now considerably better than when the report on vitrified waste was published. This applies especially with regard to:

- the properties of the buffer material (the bentonite)
- the physical-chemical conditions which determine a) the durability of the canister material and b) the solubility and dispersal of the radioactive elements in the groundwater
- calculation models for groundwater movements in the bedrock
- age data on groundwater from great depths

Consequently, the safety analysis presented in this report has a more secure basis, and some of the premises specified in the previous report have now been found to be overly cautious.

The proposed handling chain for the spent fuel from the power stations to the final repository (see fig. 1-1) encompasses a number of stages, each of which is based on known technology which has already been applied within the industry, although in other areas. In some cases - electron beam welding of the copper canister lid, lead filling of cavities in the canister, preparation and compaction of bentonite application of quartz-bentonite mixture in tunnels - the applicability of the methods has been verified by special trials.

The described facilities have been designed for a total spent fuel quantity corresponding to 9 000 tonnes of uranium, which is the product of 30 years of operation of 13 reactors. Changes in the design capacity will not affect the basic principles of the technical solutions. It is also possible to design the facilities so that both vitrified reprocessing waste and spent fuel can be processed and stored.

As in the preceding report, the Finnsjö area 16 km west-southwest of Forsmark has been selected as the hypothetical site of a final repository. This does not mean that the Finnsjö area is being proposed as the site where a final repository should be built. A final site choice is not necessary at this point in time and should not be made for many years. Further extensive studies of a number of possible sites should be carried out first. A suitable goal would seem to be to decide on the site for a final repository around the year 2 000.

The two materials copper and bentonite have an important function for the safety of the proposed final repository. There are cur-

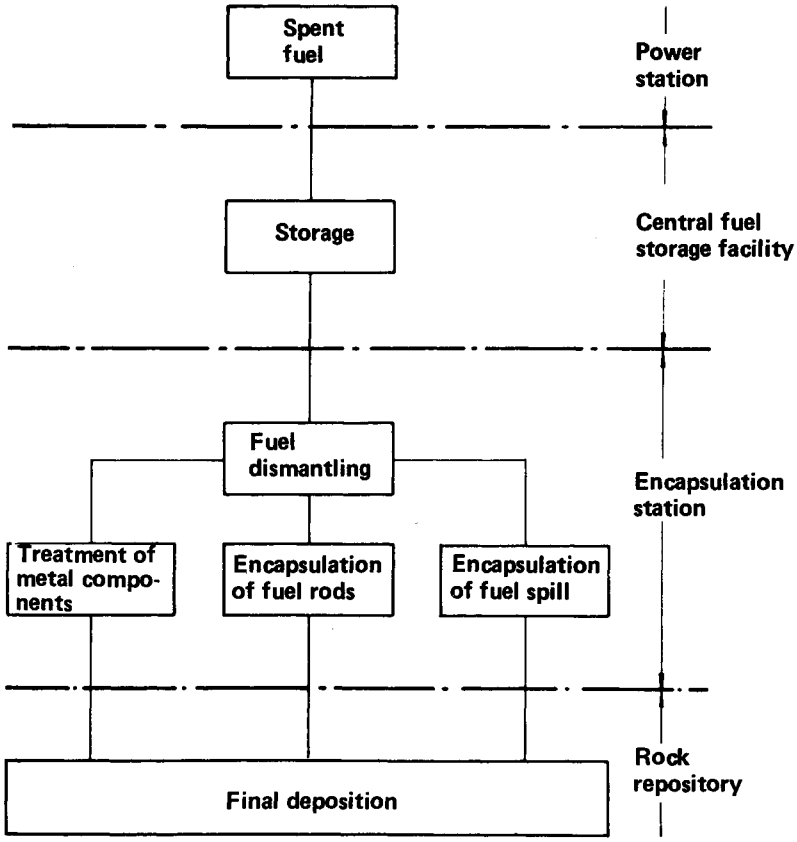

Figure 1-1. Handling chain for the spent fuel from the power station to the final repository.

rently about 400 million tonnes of known copper reserves in the world which are worth mining. World production is about 9 million tonnes per year, and Sweden produces about 0.05 million tonnes per year and consumes about 0.1 million tonnes per year. The total weight of copper in the proposed final repository would be about 0.1 million tons. If the repository is filled at a uniform pace over a period of 30 years, the annual requirement corresponds to about 3% of the aforementioned annual consumption in Sweden.

World production of bentonite averaged 4.2 million tonnes per year during the period 1973-75. A total of about 0.25 million tonnes, or an average of about 8 000 tonnes per year if the filling work proceeds for 30 years, will be required to fill boreholes, tunnels and shafts in the proposed final repository. This corresponds to about 0.2% of annual production.

The various facilities incorporated in the proposed handling chain are described in the following chapter 2. The transport system and the central fuel storage facility are of basically the same design as was described in the preceding report on vitrified waste, so they are not dealt with here.

Chapter 3 describes the geological conditions which are essential for a final repository. With regard to the site surveys, the reader is often referred to the previous report while the material regarding bedrock movements, groundwater conditions and the chemical environment is new in many respects.

Chapters 4 and 5 describe the buffer and canister materials and how they contribute towards a long-term isolation of the spent fuel.

Chapter 6 deals with leaching of the deposited fuel in the event that the canister is penetrated as well as the transport mechanisms which determine the migration of the radioactive substances through the buffer material. The dispersal processes in the geosphere and the biosphere are described in chapter 7, where the transfer mechanisms to the ecological systems as well as radiation doses are also dealt with.

Finally, chapter 8 summarizes the safety analysis of the proposed method for the handling and final storage of the spent fuel.

A special appendix provides a report on the status of current development work aimed at developing a highly durable ceramic canister for spent nuclear fuel.

2 FACILITIES

2.1 GENERAL

2.1.1 Description of spent fuel

The fuel for a nuclear reactor consists of cylindrical pellets of uranium dioxide enclosed in zirconium alloy (zircaloy) cladding tubes. The tubes with pellets are called fuel rods. They are bound together in fuel assemblies, which are handled as units. The fuel assemblies are of varying design, depending on the type of reactors for which they are intended.

Fig. 2-1 shows a fuel assembly for an ASEA-ATOM BWR reactor. It contains 64 rods (3), one of which is a spacer-capture rod. The rods are held in position by a top tie plate (4), a bottom tie plate (8) and seven spacer-grids (6). Four of the fuel rods are tie-rods (5) and are screwed into the top and bottom tie plates. The ends of the other rods are stuck into holes in the tie plates. The fuel bundle is lifted by means of a handle (1) attached to the top tie plate. The bundle is enclosed by a box (7) with lifting lugs at the top for handling and a transition piece (9) on the bottom on which the assembly rests in the reactor. Springs (2) hold the fuel assembly in place in the reactor core. One BWR assembly weighs about 300 kg.

Fig. 2-2 shows a fuel assembly for a Westinghouse PWR reactor. It contains 289 positions with 264 fuel rods (3), 24 control rod guide tubes (4) and one guide tube for neutron flow measurement. The guide tubes are welded to a top tie plate (2) and screwed by means of weld-locked screws in a bottom tie plate (6). They are also rigidly bound by eight spacers (5). The fuel rods are attached to the spacers by springs and are not connected to the bottom or top tie plate. The fuel bundle is handled via a grip in the top tie plate. Springs on the top tie plate (1) restrain the fuel in the reactor core. No box is used for PWR fuel. One PWR element weighs about 670 kg.

The structural components in BWR and PWR assemblies are made of stainless steel, inconel or zircaloy. Some fuel assemblies in the first core in a PWR reactor contain power-regulating boron glass rods in the control rod guide tubes which accompany the assembly at discharge.

The facilities described in the following are designed for spent fuel from 30 years of operation of 10 BWR and 3 PWR reactors. The

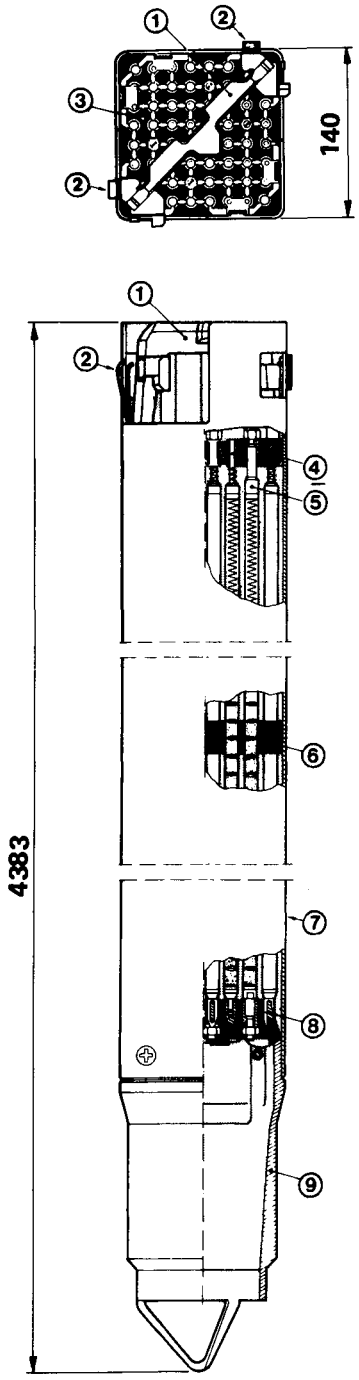

1 Handle
2 Springs
3 Fuel rod bundle
4 Top tie plate
5 Tie rod
6 Spacer-grid
7 Box
8 Bottom tie plate
9 Transition piece

Figure 2-1. Fuel assembly for a BWR reactor. (ASEA-ATOM).

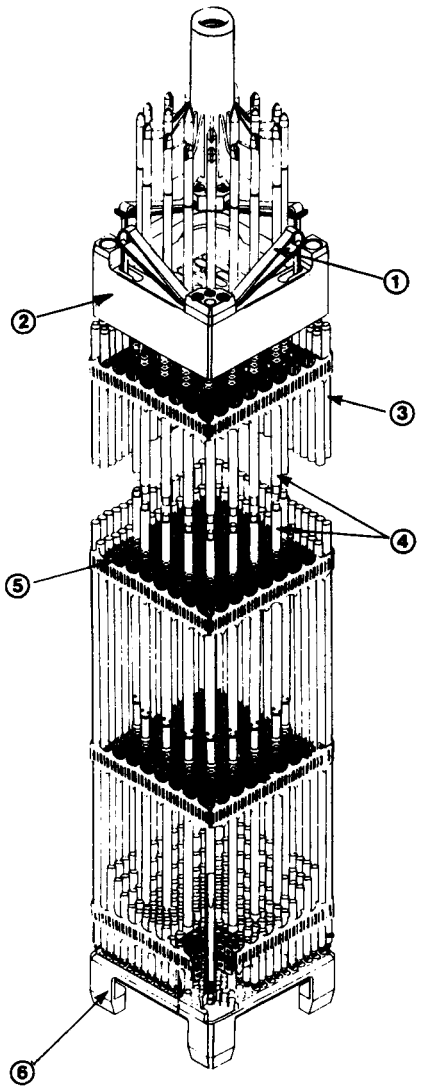

1 Spring
2 Top tie plate
3 Fuel rod
4 Control rod guide tube
5 Spacer-grid
6 Bottom tie plate

Figure 2-2. Fuel assembly for a PWR reactor. (Westinghouse Ringhals 3 and 4).

total amount of fuel discharged from the reactor is estimated to be about 40 000 BWR assemblies containing 2.5 million fuel rods and about 4 700 PWR assemblies containing 1.1 million fuel rods, equivalent to a total of about 9 000 tonnes of uranium.

2.1.2 Necessary facilities

The facilities which are required for the handling, storage and final disposal of unreprocessed spent fuel are:

- a central fuel storage facility in which the fuel can be stored while awaiting final disposal
- an encapsulation station in which the fuel and the metal components of the fuel assemblies are provided with a durable encapsulation prior to final storage
- a final repository
- a transportation system for transporting the fuel from the nuclear power stations to the central fuel storage facility and from there to the encapsulation station at the final repository

The central fuel storage facility and the transportation system are described in the appendix to the siting and licensing application for the central fuel storage facility submitted by the Swedish Nuclear Fuel Supply Company (SKBF) in November of 1977 to the Government /2-1/. During transport, the fuel is contained in special transport casks which fulfill the requirements stipulated by current international regulations - see also chapter 2, Volume III of the KBS report on vitrified waste from reprocessing.

2.2 CENTRAL FUEL STORAGE FACILITY

Regardless of whether the spent fuel is to be reprocessed or disposed of without reprocessing, additional storage capacity is required for spent fuel. The reason for this is that the storage spaces which are presently available at the nuclear power stations and which only correspond to spent fuel from a few years of operation will be full before sufficient reprocessing capacity or facilities for the final disposal of spent fuel are available. For economic reasons, a central storage facility is preferable to an expansion of storage capacity at the individual nuclear power plants.

The design of the central fuel storage facility which is described in the forementioned siting and licensing application is now being further refined by SKBF. The goal is a completed facility by 1984. Planned storage capacity will be equivalent to 3 000 tonnes of uranium, which covers needs up to 1990. The storage period will be up to 20 years.

The age of the fuel at the time of deposition in the final repository is an important factor in the design of a final repository for spent fuel. The longer the fuel has been stored prior to final deposition, the lower is its heat flux.

In the final repository, the fuel is enclosed in a copper canister. The amount of heat emitted by the fuel determines how much fuel can be stored in each canister in order that a given maximum

canister temperature is not exceeded and how densely the canisters can be deposited in the rock in order that a given maximum temperature increase in the rock around the final repository is not exceeded.

An excessively high canister temperature can have an adverse effect on the buffer material which surrounds the canister. A large temperature increase in the rock can lead to undesirable rock stresses and groundwater movements. In order to limit these effects, the KBS project has made it an essential design prerequisite that the heat load be kept at a low level.

In the proposal presented here, it has been assumed that the fuel is stored for 40 years prior to deposition in the final repository. However, the storage period can be varied, and its length is largely a technical-economical optimization question. A shorter storage period requires more canisters and a larger final repository and vice versa. The proposed length of the storage period is not based on detailed studies, but rather on a general judgement that it entails a reasonable optimization of handling and final storage.

The storage principle for the spent fuel in the central storage facility is the same as at the power stations, i.e. the fuel assemblies are stored in water pools, whereby the water provides sufficient cooling and radiation shielding. In order to determine whether the same storage principle can be applied with adequate safety for a storage time of 40 years, a study has been carried out /2-2/ whose conclusions can be summarized as follows:

The integrity of the fuel in connection with storage in water is dependent upon the durability of the material (zircaloy) which is used for the cladding on the fuel rods.

Zircaloy has been used as a cladding material for fuel in light water reactors since the 1950s. Zircaloy-4 is preferred for PWR fuel and Zircaloy-2 for BWR fuel. The alloys are zirconium-based (approx. 98%) with additions of Sn, Fe and Cr. Zircaloy-2 also contains approx. 0.05% Ni. As far as corrosion is concerned, the two alloys can be considered to be equivalent for pool storage.

The alloys possess high resistance to corrosion in water, owing to their ability to form an impervious insulating oxide layer on the surface. The growth of this layer takes place by diffusion of oxygen ions (O^{2-}) and electrons (e^{-}) through the layer. Owing to the fact that the general corrosion is thereby diffusion-controlled, it is exponentially temperature-dependent. At the relatively low temperatures which prevail during storage, oxidation is very slow. After 40 years of storage in the pools, it can be expected that less than 0.1% of the canister wall will have oxidized. The effects of irradiation on general corrosion can be expected to be negligible compared to the conditions which prevail during reactor operation, when the dose rates are of quite another order of magnitude.

In the environment which prevails during pool storage, zircaloy possesses satisfactory resistance to local corrosion. Zircaloy, for example, has a higher tolerance to chloride in the water than aluminium or stainless steel.

The chemical compatibility between the canister material and the fission products formed during reactor operation is also good. Extensive studies have been conducted of the effects of the fission products (I_2, Br_2, Cs and Cd), which are of special importance in this context, on the canister material. The stresses which exist in the canister after reactor operation are too low for stress corrosion to occur under the influence of the fission products.

Experiences of the storage of spent fuel in water pools are extensive and good. Degradation mechanisms which could jeopardize the integrity of the fuel within 40 years have not been identified.

For a more detailed description of the long-term properties of the fuel in connection with pool storage and of experiences of such storage, the reader is referred to the above-cited study /2-2/.

There is thus no reason to depart from the storage principle which is applied at the power plants and at the proposed central fuel storage facility if the storage period is 40 years. An extension of this storage period is also possible. If all fuel from 13 reactors, each operating over a period of 30 years, is to be disposed of without reprocessing - which is the hypothetical premise for this report - a storage capacity of about 9 000 tonnes is required. A trebling of the planned capacity of the central fuel storage facility would thereby be required, and the facility would have a design as illustrated by fig. 2-3.

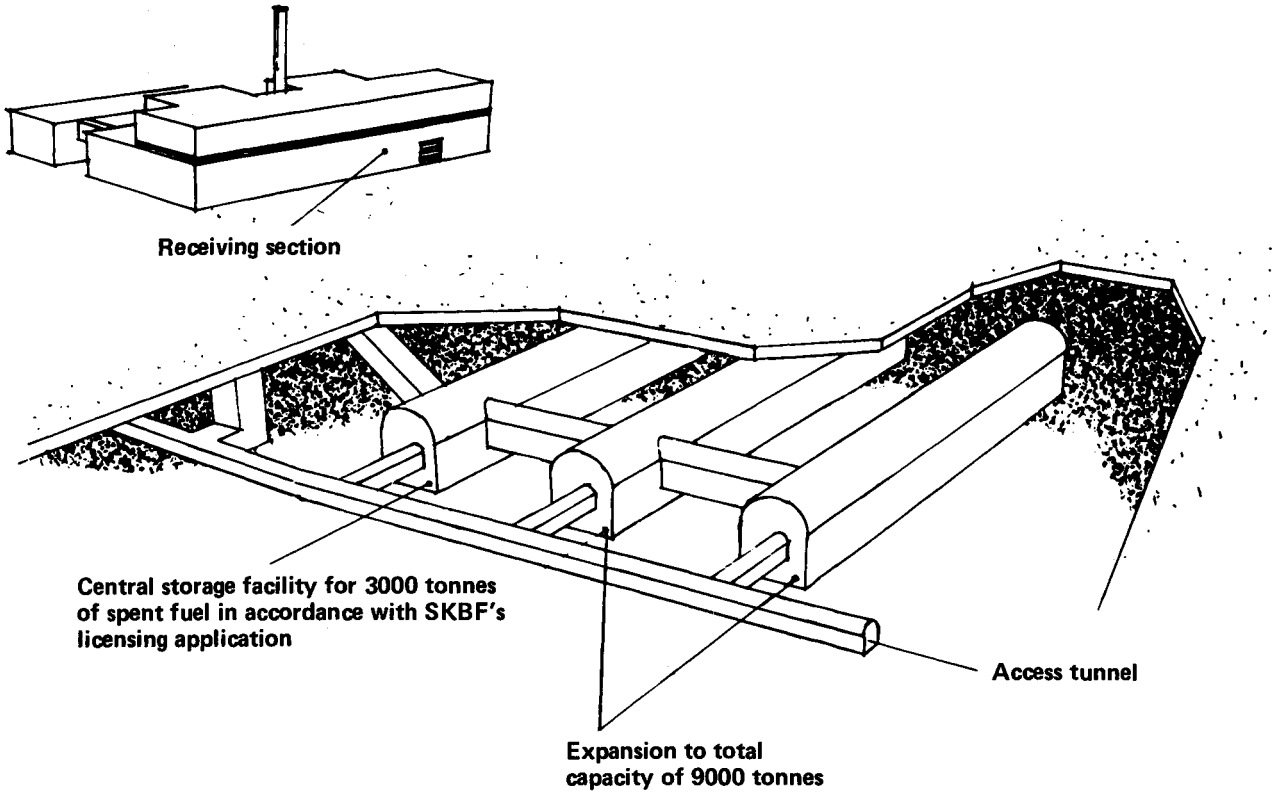

Figure 2-3. Central fuel storage facility expanded to capacity of 9000 tonnes.

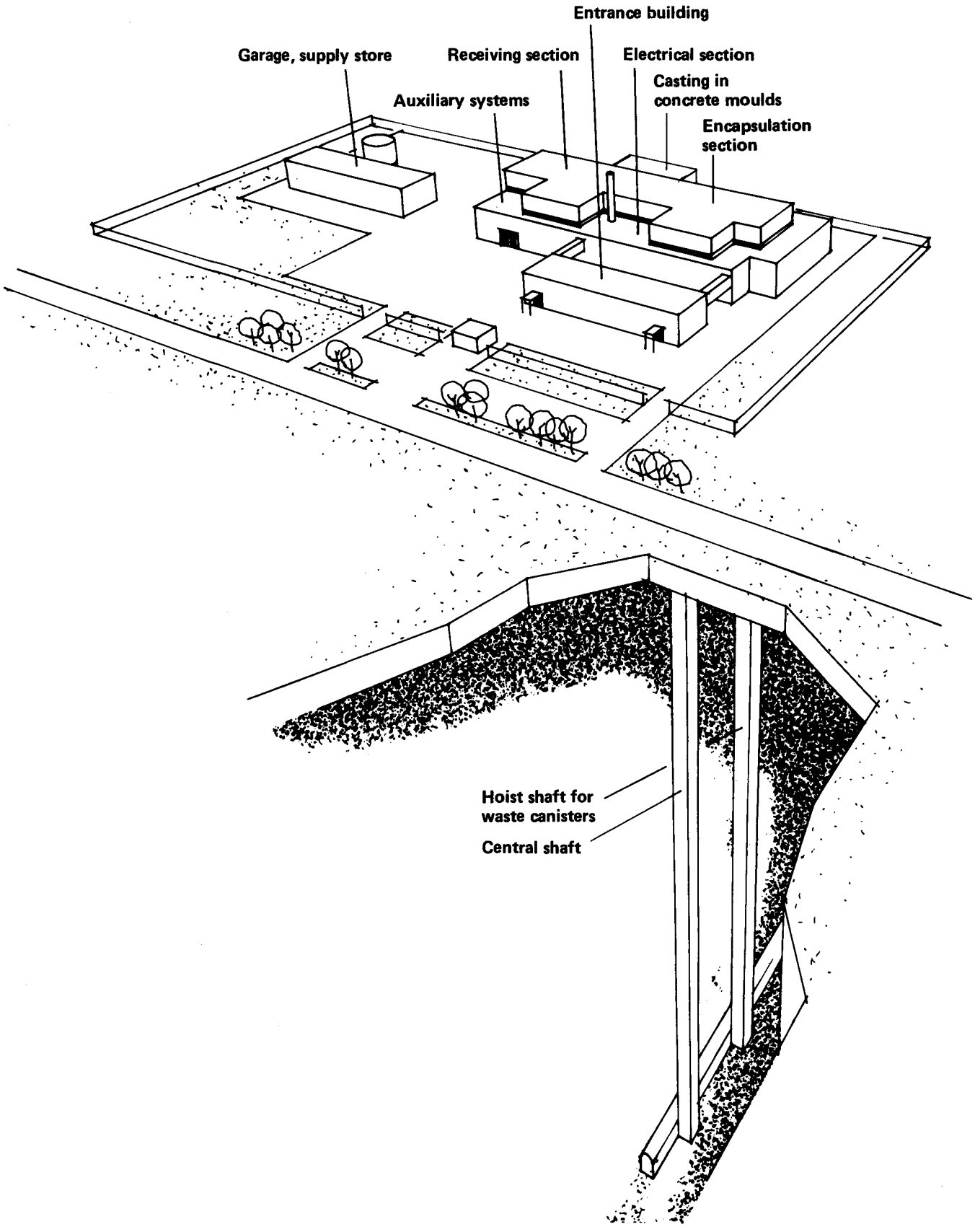

Figure 2-4. Encapsulation station for spent nuclear fuel. The facility is located at ground level above the final repository.

For a more detailed description of the design of the facility, the reader is referred to the siting and licensing application referred to under 2.1.

2.3 ENCAPSULATION STATION

2.3.1 General

An encapsulation station will be built in connection with the final repository. The facility will consist of process and service buildings located above ground, see fig. 2-4.

The spent fuel arrives at the encapsulation station following storage in the central fuel storage facility. Here, the fuel rods are enclosed in copper canisters and the metal parts of the assemblies in concrete moulds prior to final disposal. The copper canister provides a long-term protection against the groundwater in the final repository. It also affords radiation shielding which simplifies handling and reduces radiolysis of the groundwater around the copper canister to a low level, which is important in limiting corrosion. The concrete also affords radiation protection, which simplifies handling. In addition, it provides protection against the effects of the groundwater, primarily by raising the pH of the water, which limits the rate of dissolution of nickel-59, which is the most important isotope in the metal components of the fuel assemblies from the viewpoint of safety.

The facility has a capacity of 8 canisters per week, each containing fuel corresponding to approximately 1.4 tonnes (BWR) or 1.1 tonnes (PWR) of uranium, which provides a good margin to a deposition pace which corresponds to the flow of fuel from 13 reactors (approx. 300 tonnes/year).

Prior to encapsulation, the fuel assemblies are dismantled in order to permit better utilization of the canister's cavity. Only the fuel rods and fuel spill are sealed in copper canisters, while boxes, spacers, tie plates and other parts of the fuel assemblies are cast in concrete moulds in a part of the facility specially equipped for this purpose.

The total number of canisters is about 7 000 and the number of concrete moulds is 1 200.

For a more detailed description of the encapsulation station, see the drawings appended to the end of this section and to /2-3/.

2.3.2 Description of facility

The layout of the process building is shown in fig. 2-5. It can be functionally divided into a receiving section with associated storage and fuel dismantling stations, an encapsulation section including a casting cell, a cooling cell and a welding cell and an auxiliary systems section. It also contains equipment for handling metal components etc. from the fuel assemblies and for fuel spill.

Connected to the process building are buildings for administra-

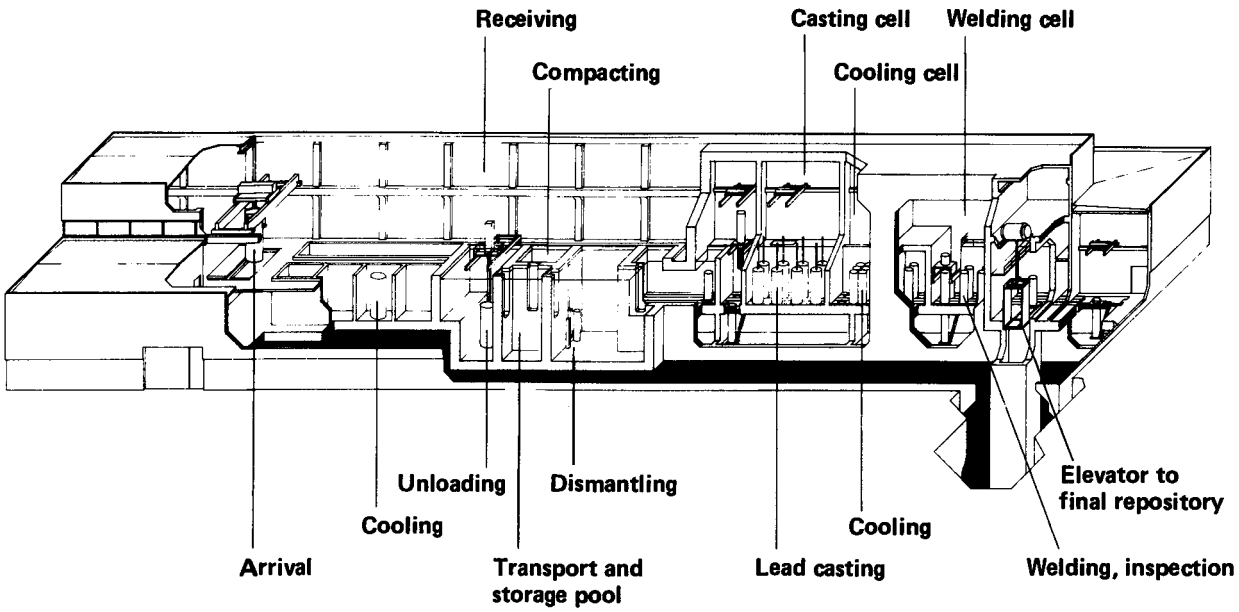

Figure 2-5. Perspective drawing of encapsulation station's process building.

tion and service. The process building, which is classified as a controlled area, is entered via the entrance building. From here, a connection is provided to the final repository via a hoist shaft.

The fuel arrives at the facility in a transport cask on a trailer (or on a railway wagon). A cask contains the equivalent of about 3 tonnes of uranium. The flow of fuel from 13 reactors corresponds to about 100 casks per year.

Receiving

The various operations included in the handling sequence in the receiving section are illustrated in fig. 2-6.

In the arrival hall, the transport cask is lifted from its trailer and transferred to the cooling and washing positions. It is then lifted in two stages down into a pool in which it is placed in a vertical position. After the lid has been removed, the container is emptied and the fuel assemblies are placed in mobile cassettes. The empty cask can then be returned and, after washing and inspection, leave the facility.

The fuel cassettes are transported under water by an overhead crane either directly to the dismantling pool or to the intermediate storage pool to await dismantling.

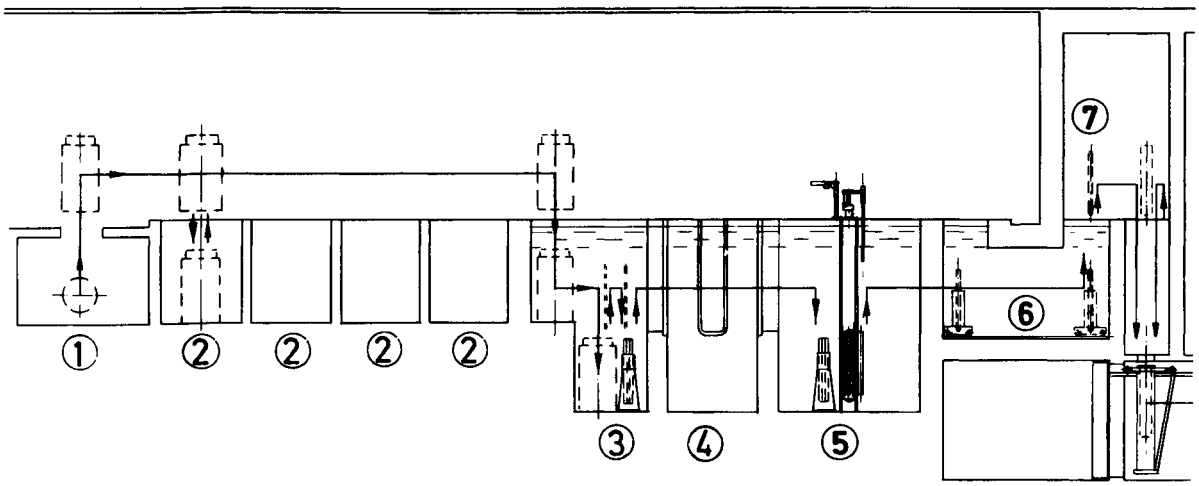

1 **Arrival hall**
2 **Cooling and washing**
3 **Unloading of transport casks**
4 **Transport and storage pool**
5 **Dismantling of fuel assemblies**
6 **Transfer carriage**
7 **Drying of fuel rack. Drying and compacting of fuel spill**

Figure 2-6. Schematic illustration of handling procedure in receiving section of process building.

In the dismantling pool, the fuel assemblies are lifted one at a time to one of the five dismantling stations, of which four are intended for BWR assemblies and one for PWR assemblies. The cassette is designed so that the BWR assemblies' boxes are retained in the cassette when the assemblies are lifted.

In the dismantling position, fig. 2-7, the bottom nuts on the BWR assembly are milled off. Metal chip and fragments which may be dislodged from the fuel are collected and removed by suction to a cyclone separator in the storage pool in the receiving section for further processing as described under "handling of fuel spill" below. The top nuts are then unscrewed and the top tie plate is lifted off. The rods are held in position by fork-shaped devices. After the spacer-capture rod has been lifted away, the fuel rods are lifted one by one and placed in a copper rack.

This handling sequence is employed for BWR assemblies of the type manufactured by ASEA-ATOM. Exxon fuel has a somewhat different structure. This type of BWR assembly has four centre rods made of solid zircaloy and eight of the outer fuel rods function as tie-rods. When such fuel is dismantled, the top tie plate is released by undoing the bayonet type lock on the tie rods with a special tool. The top tie plate is then lifted off, whereby the rods are kept in position by means of fork-like tools. After the centre rods have been lifted away, the fuel rods are transferred to the copper rack as described above. The tie rods must first be unscrewed from the bottom tie plate by means of a tool with a rotating motion. Rods which seize and require such great twisting

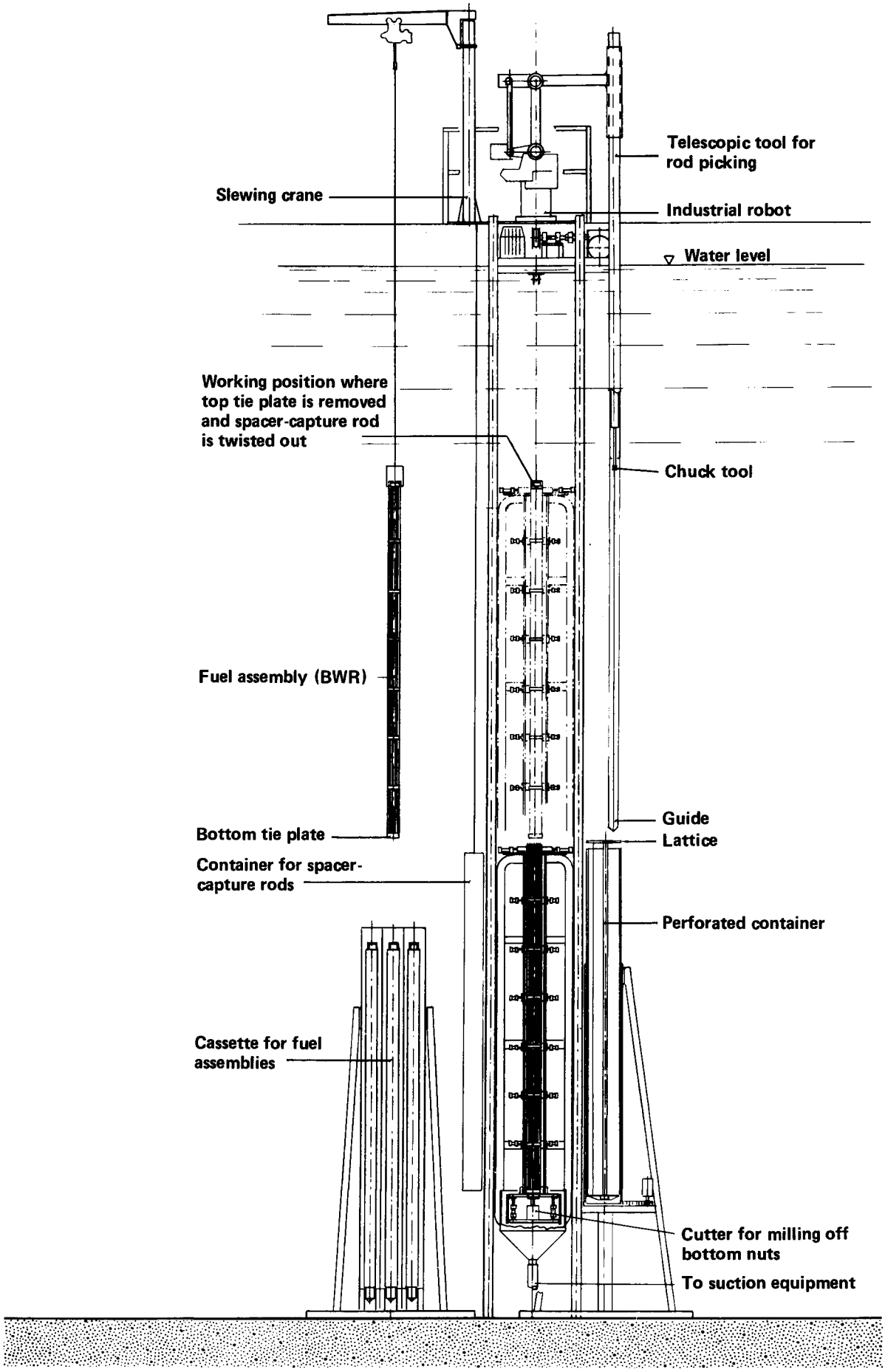

Figure 2-7. Equipment for dismantling of fuel assemblies.

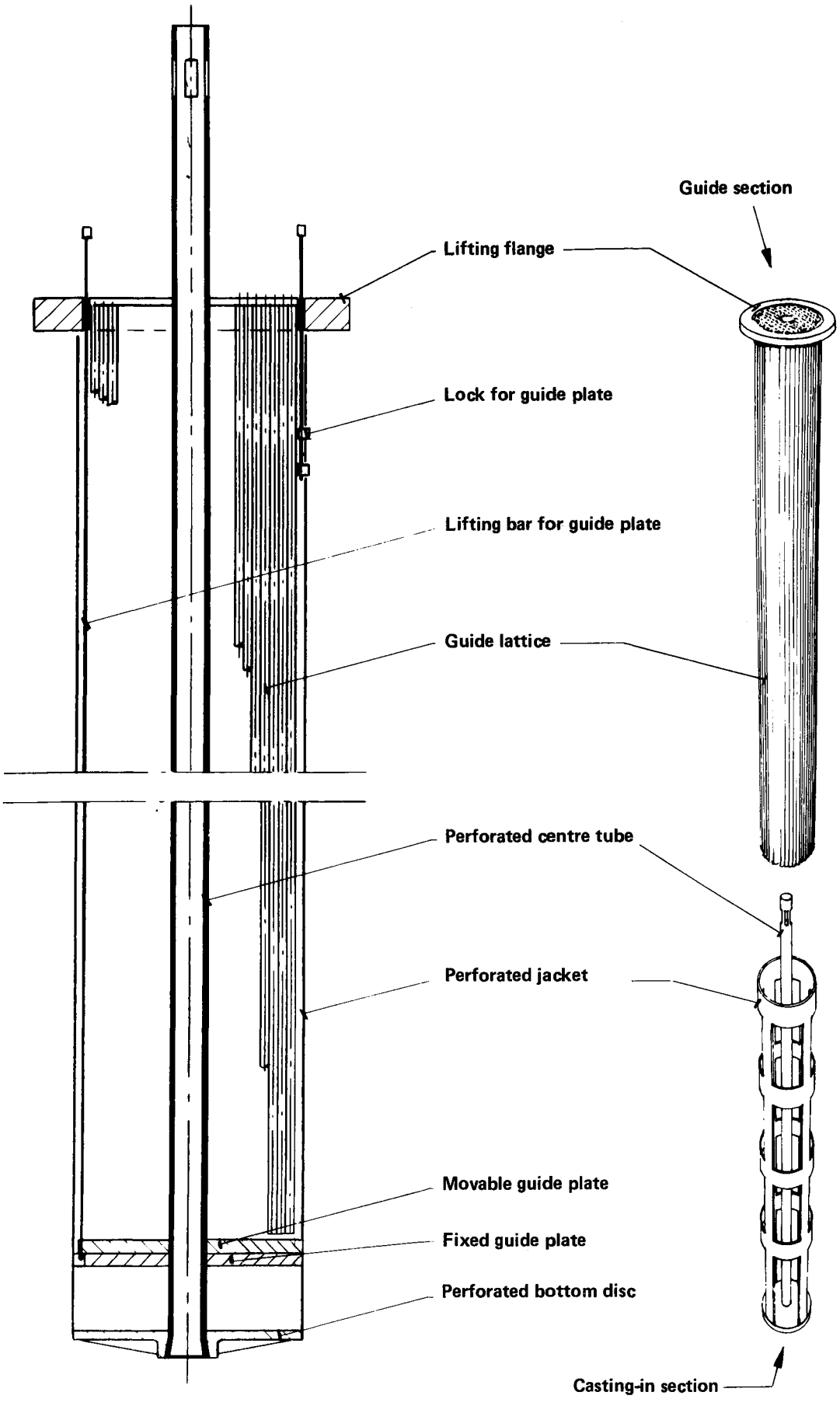

Figure 2-8. Copper rack for fuel rods. The guide section is used to pack the rods into the casting-in section.

force that the rod can be damaged are instead released from the bottom tie plate by a tubular milling cutter which machines off the material around the threads.

The copper rack, fig. 2-8, consists of a casting-in section in which the fuel is transferred to the canister (and which is encapsulated together with the fuel) and a guide section which permits a high packing density for the fuel rods in the canister. All component parts are made of copper.

The casting-in section consists of a bottom disc on which the rods stand, a centre tube by which the rack is lifted, a jacket which encloses the fuel rods and two guide plates which hold the rods in place.

The guide section consists of a hexagonal lattice which, for BWR rods (rod diameter 12.25 or 11.75 mm), consists of tubes with inner diameter 13 mm and wall thickness 0.5 mm. Some of the tubes in the lattice have a larger diameter so that they can receive fuel rods which have swollen, been deformed or are broken off. The number of positions is 498.

The fuel rods are set down one by one in the lattice tubes, whereby coordinate control ensures that they are lowered into an empty position. When a rod is lifted up out of the fuel assembly, it is checked to see if it is broken, swollen or deformed, in which case it must be placed in the special positions for such rods. A minicomputer records the filling of the lattice. The lower parts of broken rods are handled by special tools.

The metal components from the fuel assembly - spacers, bottom and top tie plate etc. - are placed in a transport box and transferred, together with the fuel boxes, to the compacting pool in the receiving section pending further processing as described under "Handling of radioactive metal components etc." below.

After the copper rack has been filled, the lattice is lifted by means of a lifting tool and transferred to a new casting-in section. The lifting tool is equipped with ejector rods which prevent rods (which may get stuck in the lattice tubes) from being lifted along with the lattice. At the same time, the moveable guide plate is lifted to its upper position, where it is fixed by means of a locking device. Finally, a lid is placed on the copper rack in order to stiffen the rack and hold the fuel rods in place during the lead casting operation included in the encapsulation process (see below).

In the case of PWR fuel, the assembly is turned upside down after the screw heads in the bottom tie plates have been milled off. (Alternatively, only the weld lock at the screw heads is milled off.) The above-described handling sequence then follows with minor modifications. In the case of PWR rods of diameter 10.7 mm, the same lattice is used as for BWR rods as described above. For rods with diameter 9.7 mm, a lattice with 636 positions is used, but this lattice has the same external dimensions as the BWR lattice. This permits the same copper canister to be used for all existing types of fuel.

With PWR fuel, the space in the canister would permit a larger number of lattice positions. In order to keep heat the flux at

the same level (about 0.8 kW) for all canisters, however, the PWR rods are packed less densely. An alternative possibility is to reduce the diameter of the PWR canister, which would reduce canister cost.

Encapsulation

The various operations included in the handling sequence in the encapsulation section are illustrated in fig. 2-9.

The casting-in section of the copper rack, filled with fuel rods, is transferred by a transfer carriage to the casting cell in the encapsulation section through a pool which also serves as a water lock between the dismantling area and the casting cell. Up to this point, the fuel has been handled and stored under water with sufficent water coverage to provide adequate radiation shielding. From now on, the fuel is handled in air in cells via remote control, whereby thick concrete walls provide sufficient radiation shielding.

The copper rack is lifted up from the transfer carriage in the pool by an overhead crane, after which the water is allowed to run off and the rack is allowed to dry in the air. It is then lowered into a copper canister, which has been brought in via a hatch in the floor of the lock, and placed in a transport wagon by the crane. The transport wagon serves one of the two handling lines in the casting cell.

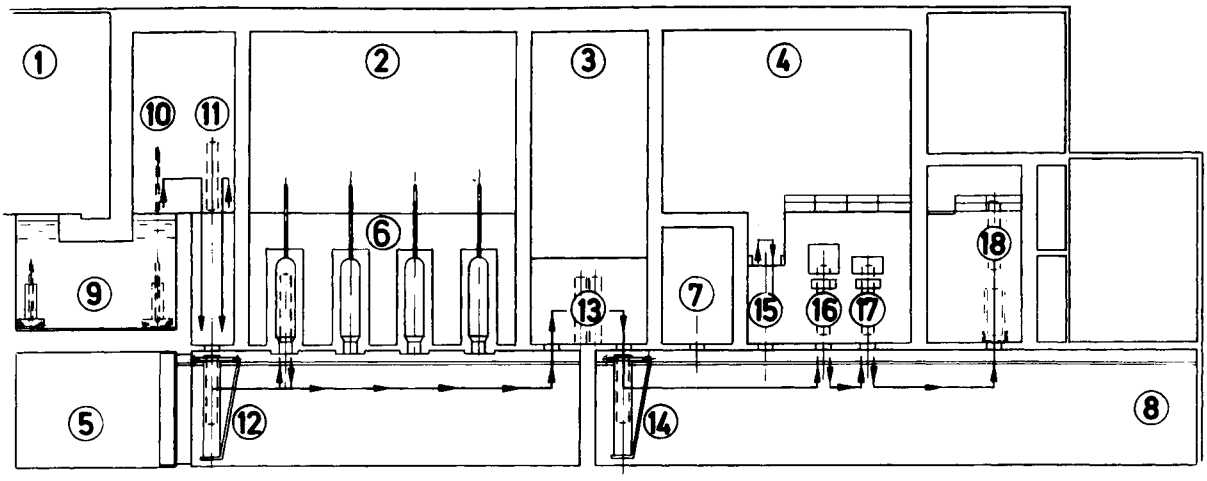

1 Receiving section
2 Casting cell
3 Cooling cell
4 Welding cell
5 Service area for transport wagon 12
6 Furnaces for filling canister with lead
7 Cell for opening sealed canister
8 Service area for transport wagon 14
9 Transport lock
10 Drying of fuel rack. Drying and compacting of fuel spill
11 Arrival of copper canister from store
12 Transport wagon
13 Cooling station
14 Transport wagon
15 Mounting station for lid
16 Welding station
17 Inspection station
18 Dispatch station

Figure 2-9. Schematic illustration of handling sequence in encapsulation section of process building.

The canister, fig. 2-10, is fabricated from pure copper by the forging of a copper ingot which is then turned down to its final external dimensions. After drilling of the internal cavity, the input end is machined for the lid /2-4/.

The transport wagon transfers the canister to one of the four casting positions in the handling line. A casting position consists of a vacuum bell into which the canister can be brought from below. The bell is surrounded by a furnace by which the canister can be heated and its cooling controlled.

The canister is brought into the bell by a hydraulic hoist on the transport wagon. The canister stands on the lid of the bell (plunger), which is simultaneously lifted up and joined airtightly to the bell. The centre tube in the fuel rack is connected by means of an automatic coupling to a tube for lead casting, fig. 2-11.

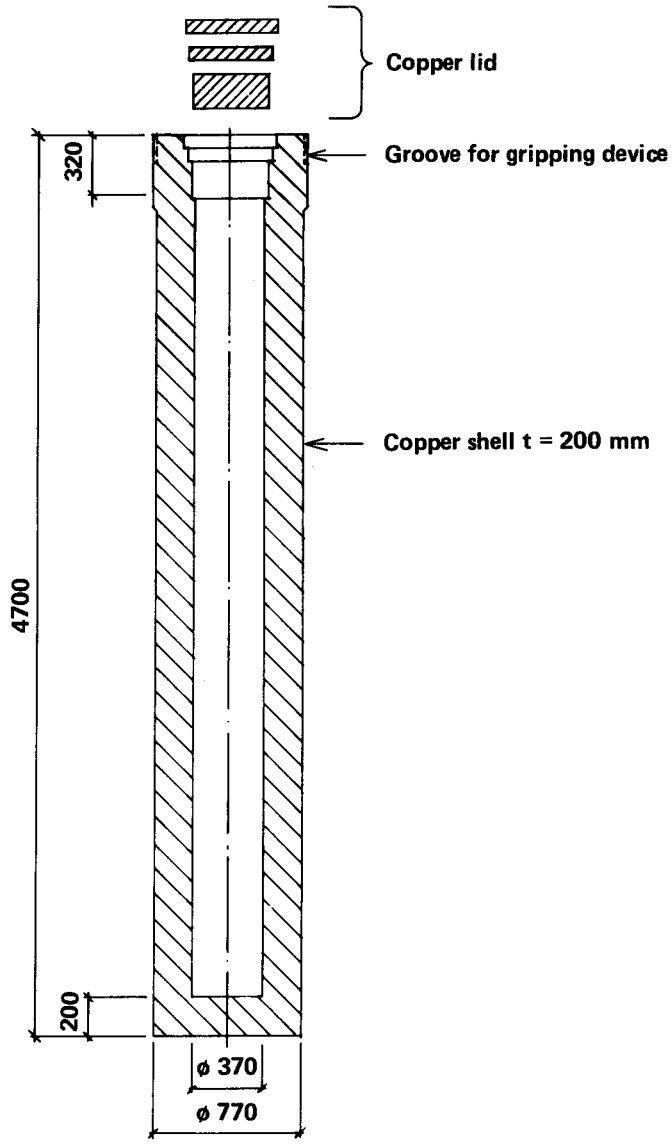

Figure 2-10. Longitudinal section of copper canister.

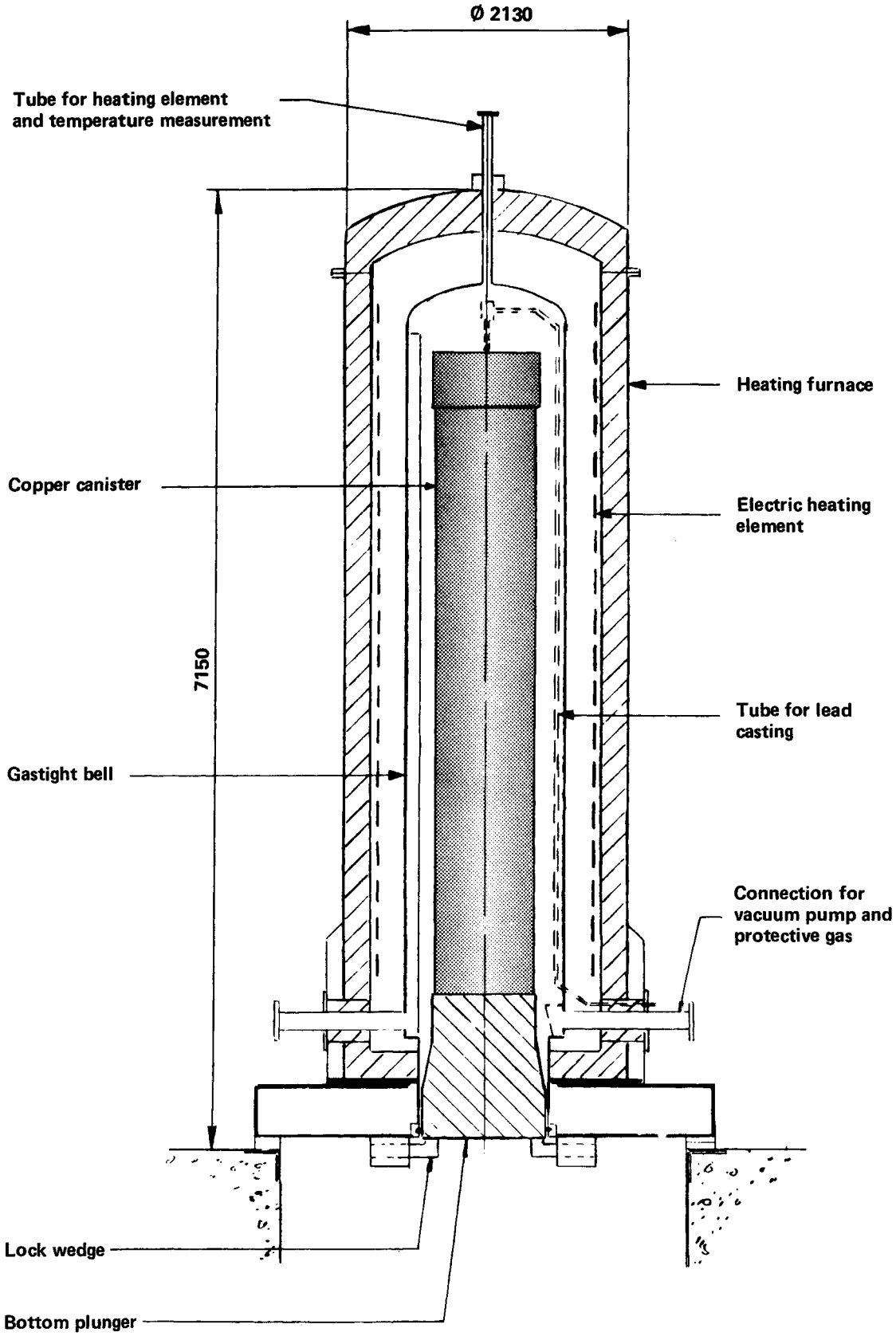

Figure 2-11. Longitudinal section of furnace for lead casting. Casting of lead into the canister takes place in a gastight bell surrounded by a heating furnace.

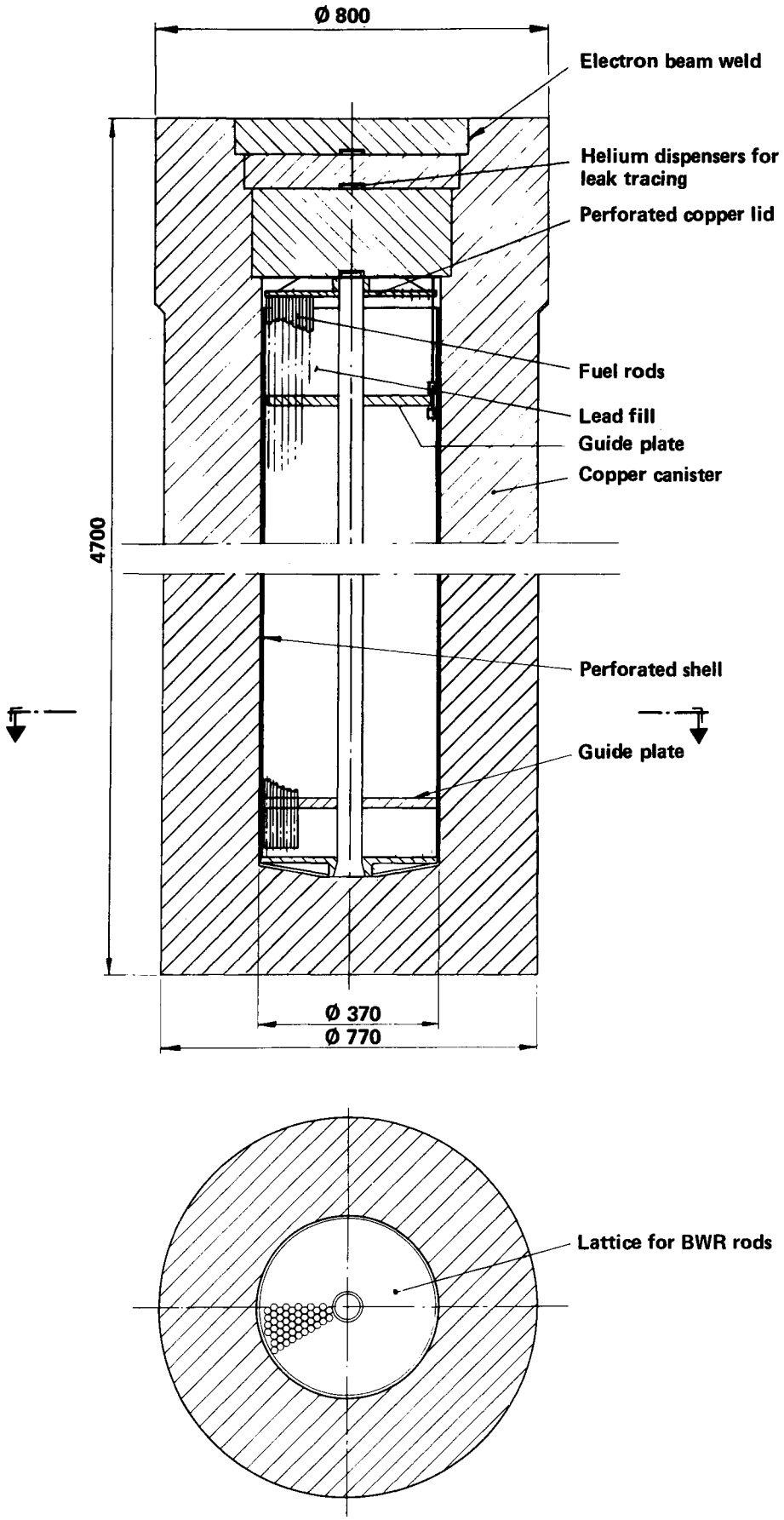

Figure 2-12. Longitudinal section and cross-section of copper canister filled with fuel rods from a BWR reactor.

The bell is then evacuated and the canister is heated for 48 hours, partially by radiated heat from the furnace and partially by the heat generated by the fuel. Heating is interrupted at 380-400°C and molten lead is pumped into the centre tube in the copper rack from a melting furnace outside of the cell. The centre tube, like the bottom disc, the lid and the jacket, is perforated to permit the lead to flow out and fill all cavities in the canister. When the lead is poured, the fuel rods are lifted up towards the lid on the rack due to the fact that the rods are of lower density than the lead. Lead pouring is interrupted on a signal from level detectors. A heating element is inserted into the centre tube and keeps the lead hot in and around the tube during the solidification process. This prevents "piping", i.e. the formation of pores, by allowing lead to run in from above during solidification. For this reason, lead is "heaped" a few centimeters above the lowest shoulder for the copper lid.

The bell is now filled with nitrogen gas, which circulates in a closed circuit and is cooled in a heat exchanger. The temperature of the canister is gradually reduced over a period of 48 hours down to about 150°C. When the temperature has dropped to just above the melting point of lead (327°C), the heating element is slowly pulled up out of the lead in the centre tube and additional lead is pumped in to compensate for shrinkage.

The purpose of the vacuum and the nitrogen gas is to prevent the copper, the lead and the fuel from oxidizing while the canister is at a high temperature. Vacuum during lead pouring also prevents gas inclusions. Since the bell is hermetically sealed, airborne radioactivity cannot escape into the cell.

After cooling, the canister is transferred by the transport carriage to a cooling cell. The cooling cell also serves as an airlock between the casting cell and the welding cell. In the cooling cell, the temperature of the canister is allowed to drop further to about 80°C. The canister is then moved to a position in the cell where the excess lead and the projecting centre tube are removed by machining so that the top surface of the lead is at the same level as the lowest shoulder for the canister lid. The surfaces of the shoulders are then also polished. Chip from machining and polishing is collected and transferred to a melting furnace in a separate room below the cooling cell. Here, the lead is recovered and returned to the system for lead casting into the canisters. The slag formed during melting, which may contain radioactive material from the fuel, is separated and embedded after cooling in concrete moulds in the same manner as radioactive metal components as described below.

The canister is now placed by the overhead crane in the cooling cell into one of the cooling cell's transport carriages, which serves the cell's two handling lines with welding and inspection stations. If required, the canister can first be cleaned externally in a cell which is also used for opening sealed canisters which have been found to be defective upon inspection. In the welding cell, the canister is filled with a lid which is fastened by means of electron beam welding. The lid consists of three parts, since the welding method does not presently permit the welding of 20 cm metal with full penetration. The weld is checked by means of ultrasound and helium leakage tracing. The finished

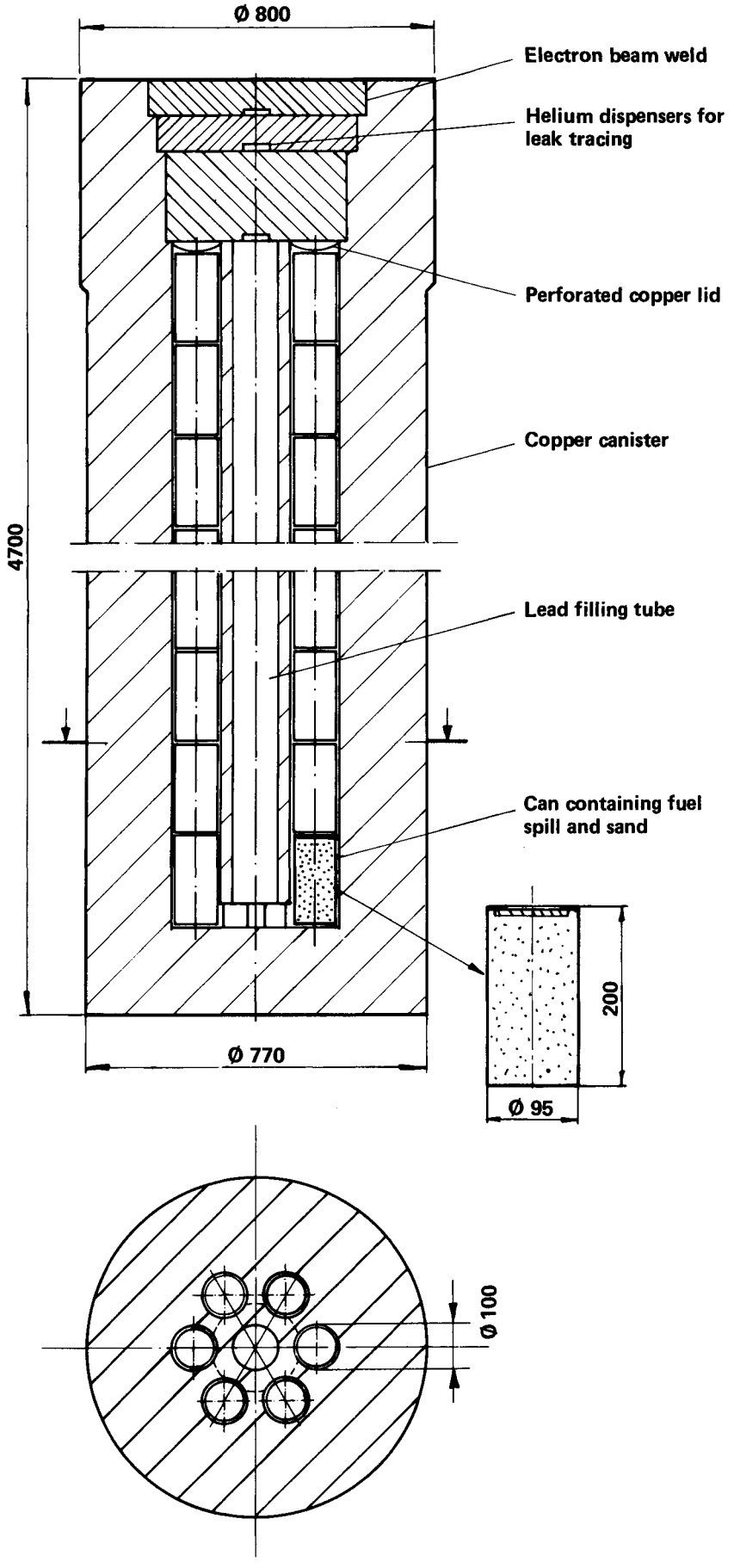

Figure 2-13. Longitudinal section and cross-section of copper canister for can with fuel spill.

canister (fig. 2-12) is then transferred to a wagon for transport down to the final repository.

Regarding the properties of the canister material, see chapter 5.

Handling of fuel spill

Fuel spill which can become dislodged from damaged fuel rods during handling in the encapsulation station, mainly during dismantling, is collected by means of sludge suction and delivered to a cyclone separator in a pool in the receiving section. There, particles down to a size of 0.5 mm, which are expected to comprise at least 99% of the fuel spill, are separated. From the cyclone separator, the suction water is delivered to a tank in which the fine-grained fuel spill is allowed to settle.

The fuel spill which is separated in the cyclone separator is collected in a copper can with a volume of about one litre in the bottom of which a layer of sand has been deposited. When the can is full, it is transferred to the cell above the transport lock, where it is allowed to dry. After all water has evaporated, a layer of sand is deposited on top of the fuel spill. The sand and the fuel spill are then mixed by means of vibration and the mixture is compacted by a copper lid being pressed down on the top surface by a piston. The sand is graded so that it fills the voids between the larger fuel fragments and gives the compacted mixture a high density. It will then be able to withstand the high pressures to which it may be subjected in the final repository without being deformed. After compaction, the edges of the can are folded down over the lid so that the lid is fixed in position.

The copper can with the fuel spill is placed in a copper canister in which seven holes of diameter 100 mm and length 4 metres have been drilled, see fig. 2-13. The cans are placed on top of one another in the holes, but the centre hole is left open to permit subsequent lead casting to be carried out from the bottom upwards. The canister is kept in the cell above the transport lock until it is filled with cans.

The fine-graned fuel spill is transferred after sedimentation from the collection tank in the form of a sludge to an evaporator. The dry material is collected in a copper can and handled in the same manner as described above for the coarser fractions. The water from the tank is delivered to the filters in the cleaning system for pool water.

After the canister's holes have been filled, a copper lid is placed over the uppermost cans. The lid is intended to prevent the cans from floating up when the spaces around the can are filled with lead by means of the same procedure as described above for the canisters containing fuel rods. The subsequent handling procedure is identical to that used for the canisters for fuel rods.

One canister is expected to be able to hold all of the fuel spill (approx. 130 kg) from the handling of all fuel from 30 years of operation of 13 reactors. This assessment is based on the extensive experience from the handling of fuel. Only one per cent or

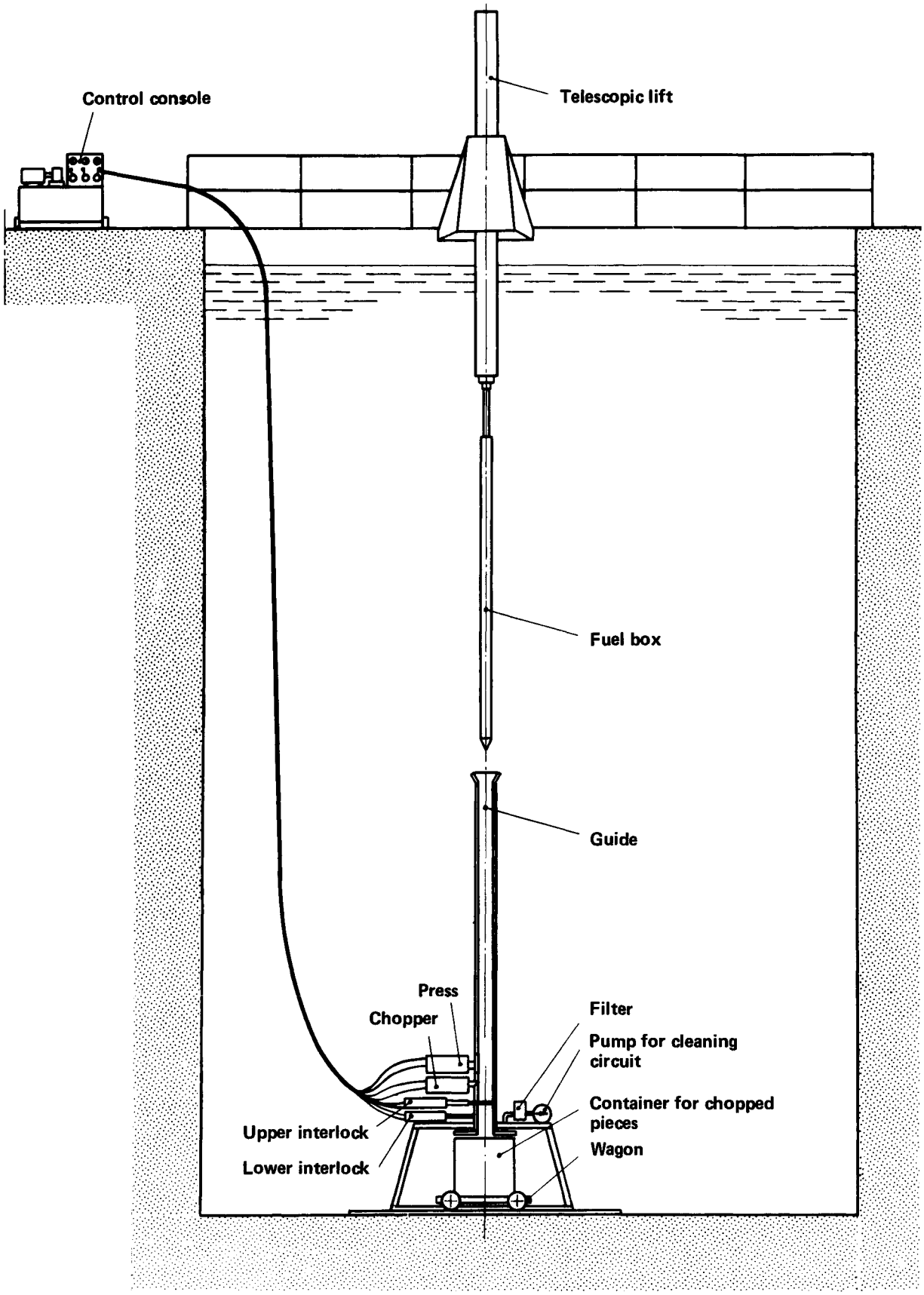

Figure 2-14. Equipment for compacting boxes from BWR assemblies.

so of the fuel rods can be expected to be damaged, and it has been found that the amount of uranium dioxide which can drop out from severely damaged or even broken rods is very limited.

Handling of radioactive metal components etc.

In connection with the dismantling of the fuel assemblies in the encapsulation station, metal components etc. are collected in transport boxes, which, when they have been filled, are transferred to a pool in the receiving section. The boxes for the BWR assemblies are also brought here and placed in a rack awaiting compaction.

Prior to compaction of the boxes, the transition piece is detached in a fixture. The boxes are moved to a machine which compacts them and chops them up, see fig. 2-14. The transition piece is compacted in a press.

Other components are processed in the following manner:

BWR assemblies: The spacer-grids are compacted in a press. The spacer-capture rod and the centre rods from the Exxon fuel are cut up in a chopping tool. Handles and springs are cut or milled off from the top tie plate. The bottom tie plate is not compacted.

PWR assemblies: Spacer-grids, top tie plate and control rod guide tubes are held together in a skeleton which is taken to a chopping tool. The guide tubes are chopped off on both sides of the spacers and at the top tie plate. The spacers are compacted in a press. The springs on the top tie plate are cut off. The boron glass rods are also cut up in a chopping tool. The bottom tie plate is not compacted.

The material is collected in stainless steel baskets which are taken via a water lock from the compacting pool into a cell with radiation-shielded walls, where they are lifted out of the water and allowed to dry, see fig. 2-15. Chip and spill from the handling procedure are sucked into a special basket with an internal filter. The baskets are taken via an airlock down into concrete moulds positioned underneath openings in the floor of the lock. The moulds stand on wagons equipped with jacks by means of which the moulds can be lifted up and connected tightly to the openings. Mortar is then injected into the mould until it is filled to a level just above the top of the basket. The technique used here is the same as that used within the construction industry for grouting by the injection of concrete.

After completed injection, the mould is lowered into the wagon and moved to a position where a concrete lid is mounted by the overhead crane. The cavity underneath and the space around the lid are then injected with mortar.

The moulds are cubical, 1.6 m on a side. The walls are 0.3 m thick for the moulds used for BWR assembly boxes and for the slag from the melting of the chip from machining after lead casting, and 0.4 m for the moulds used for the other components of the fuel assemblies (whose radiation level is higher). The surface

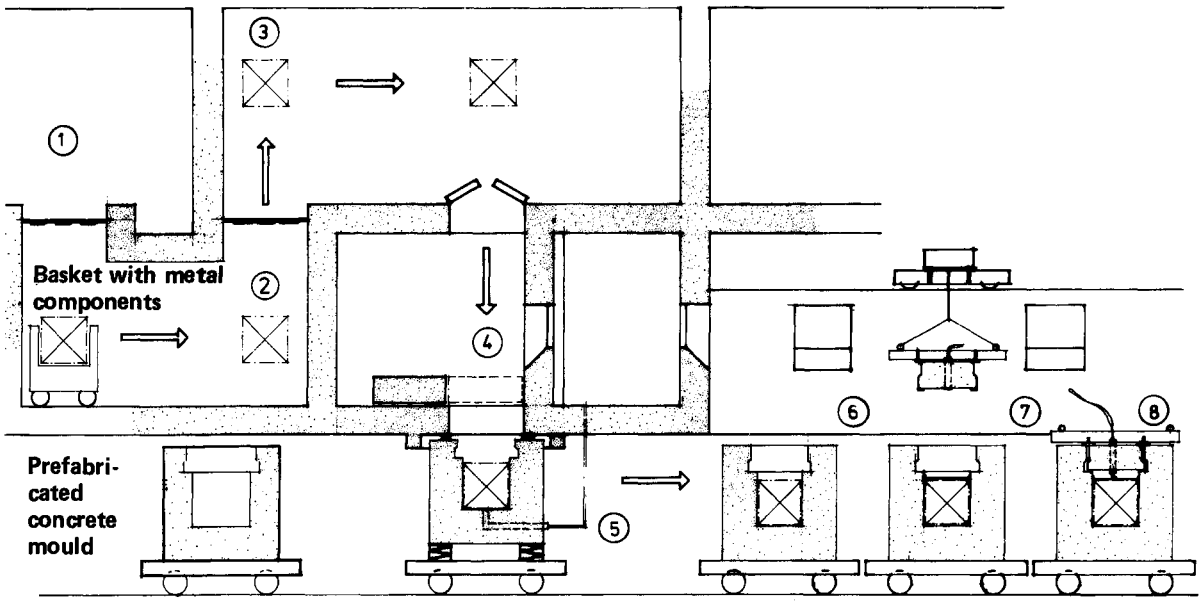

1 Station for reception, chopping and compaction of metal components
2 Transfer via water pool
3 Drainage of transport basket
4 Placement of transport basket in concrete mould
5 Injection-grouting of transport basket in concrete mould
6 Transport to sealing station
7 Mounting of lid
8 Injection-grouting of space around lid

Figure 2-15. Schematic illustration of handling procedure for injection-grouting of radioactive metal components from the fuel assemblies in concrete moulds.

dose rate on the moulds is normally lower than 1 rem/h but can in extreme cases reach maximum 2 rem/h. One mould weighs about 10 tonnes. A total of about 1 200 moulds is required.

Mould fabrication is remote-controlled from a radiation-shielded control room.

For a more detailed account of the handling of radioactive metal components, see /2-5/.

Auxiliary systems

The facility will include auxiliary systems for:

- cleaning and cooling of transport cask
- pouring of lead
- welding and weld inspection of canisters
- lifts and transports
- ventilation
- heating of premises
- electric power supply
- drainage
- sludge suction
- water treatment
- treatment of filter and ion exchange masses from cleaning systems
- water supply and compressed air supply

These systems are similar to those in a nuclear power station or other industrial plants. Practical tests with the embedding of fuel rods in lead and with the electron beam welding of copper have been conducted and have verified that the technique described here is applicable, see /2-4/.

In order to limit the disruptions caused by an external power failure and thereby increase the operational availability of the facility, the facility is equipped with a diesel-powered generating plant to which certain process systems as well as personnel elevators are connected.

The ventilation system in the process building maintains a lower pressure in areas with a higher risk of contamination in relation to areas with a lower risk. The incoming air is filtered an conditioned to provide pleasant working conditions. Outgoing air is radiation-monitored and cleaned when necessary by filters. The ventilation systems for the casting and welding cells contain so-called "absolute filters".

2.3.3 Operation of facility

The process premises will be classified as a controlled area and divided into zones with respect to radiation levels and potential risk for contamination in a manner similar to that applied in a nuclear power station.

All handling of fuel and fuel assembly components will be effected via remote control either under water, whereby the water provides adequate radiation shielding, or in special cells with concrete walls which provide the necessary radiation shielding. Ventilation and filter systems prevent radioactivity from spreading to the environment.

Known technology and experiences from similar systems in existing facilities will be applied in the facility's operating systems. The dismantling facility has been designed on the basis of experiences from the dismantling of fuel at nuclear power stations, e.g. in connection with the rebuilding of fuel assemblies (more than 1 000 fuel assemblies have been rebuilt at the Swedish stations).

All equipment in the cells can be given service and maintenance by lifting the equipment out of the cells or taking it to a separate service cell.

Maintenance can also be carried out in a cell after it has been emptied of fuel and, if necessary, decontaminated.

The design and operation of the facility will be examined and inspected by authorities such as the Swedish Nuclear Power Inspectorate and the National Institute of Radiation Protection in the same way as a nuclear power station. It will be designed in accordance with the directives issued by these authorities and in consultation with concerned personnel organizations.

With regard to working environment and occupational safety, see 2.5.

2.3.4 Quality control

In order to satisfy the stringent requirements on safety and operational availability which are imposed on the activities described here and in order to ensure absolute safe final storage, the quality of plant and material must conform to a sufficiently high standard. This requires effective quality assurance, which entails that all measures aimed at achieving and maintaining the necessary level of quality shall be planned, systematic and documented.

The owner of the facility shall also be responsible for ensuring that quality control and quality assurance activities are organized and executed in a satisfactory manner. The execution and documentation of various quality-guaranteeing measures should be divided between the owner and an official institution, such as the Swedish Plants Inspectorate, in a manner similar to that which is followed in the case of nuclear power plants. This division shall be based on competence and on safety considerations and shall be approved by the Swedish Nuclear Power Inspectorate (SKI). Responsibility for coordinating such activities shall rest with the owner, who shall also submit periodic reports to SKI.

The owner shall also submit a report to SKI, in good time before the start of construction, specifying a programme for the organization and functions of quality control and quality assurance. Supplementary instructions shall subsequently be issued as required and the programme shall be subjected to continuous follow-up by SKI. The programme shall include the following points:

- Definition of the application of the programme to various building sections and installations based on safety classes.
- Description of the owner's organization and cooperating organizations, with specification of areas of responsibility and channels of contact.
- Directives for design examination. Designs should be examined by an independent body.
- Purchasing directives with respect to quality requirements.
- Inspection and identification of purchased material.
- Production and installation control appropriate to the importance of the product for plant safety and operational availability.
- Programme for recurrent periodic testing and inspection of certain plant components.
- Directives for operation and maintenance of the facility, including comprehensive instructions for abnormal operational situations and events.
- Routines for the submitting of reports to the supervisory authority.

A quality control plan for the encapsulation procedure for spent fuel should include the following points:

Lead filling:

- Compositional analysis of lead
- Temperature measurement in connection with filling
- Level check in connection with filling

- Vacuum check in casting bell
- Check of nitrogen gas pressure

Copper cylinder and lid:

- Compositional analysis of material
- Tensile testing of material
- Grain size determination of material
- Material identification
- Dimensional check
- Visual inspection of final surface
- Ultrasonic testing of material
- Penetrant testing of final surface
- Welding procedure check
- Functional test of automatic welding equipment
- Purity check prior to welding
- Supervision of welding work
- Ultrasonic testing of welds
- Penetrant testing of welds
- Tightness testing by means of He
- Marking and issuing of testing certificate

Some of these quality control procedures may take the form of spot checks, the frequency of which shall be determined on the basis of the probability of defects.

Concrete mould fabrication is subject to the provisions of applicable regulations governing concrete work. Appropriate quality control measures are practiced.

2.3.5 Decommissioning

When the facility is no longer required and there is no fuel left in it, the facility shall be decontaminated and all "home" radioactive waste, contaminated scrap and building materials shall be taken away to facilities which are equipped to receive and process such material. The facility can then be modified for other use or demolished.

Decommissioning is not expected to present any great problems, since the encapsulation station does not contain any heavy equipment or permanent installations which are contaminated, but rather only systems and building materials which can be regarded as inactive after cleaning.

2.4 FINAL REPOSITORY

2.4.1 General

The final repository for the fuel canisters is situated in rock underneath the encapsulation station at a level approximately 500 metres below the surface. (With regard to the final storage of concrete moulds containing radioactive metal components, see 2.4.5 below.) The facility consists basically of a system of parallel storage tunnels with appurtenant transport tunnels and shafts for communication with the surface and with the encapsula-

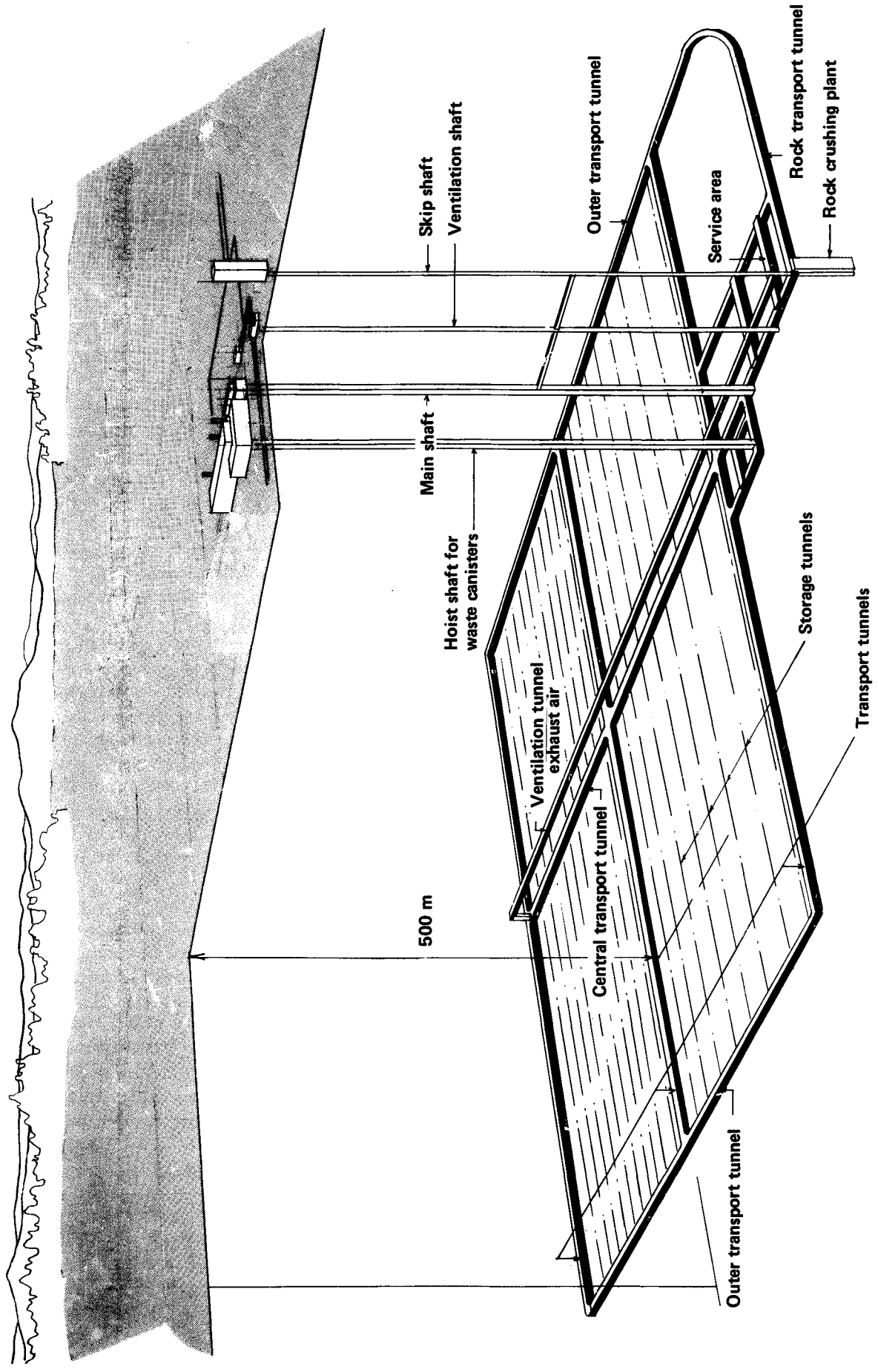

Figure 2-16. Perspective drawing of final repository. The encapsulation station is located at ground level. The final repository consists of a system of parallel storage tunnels situated 500 metres below the surface.

tion station, see fig. 2-16. The tunnel system, which occupies an area of about 1 km^2, also contains diverse service areas. The fuel canisters are deposited in vertical holes drilled in the floors of the storage tunnels. The design of the final repository is similar to that described in the KBS report on vitrified waste from reprocessing, with the principal difference that the canister in the storage hole is surrounded by highly compacted pure bentonite instead of a sand/bentonite mixture. The reason for this and for the fact that the fuel is encapsulated in copper instead of lead and titanium is that the radioactivity of the spent fuel decays at a much slower rate than that of vitrified waste from reprocessing. The design of the canister ensures the longer life which is commensurate with the higher demans on the durability of the containment which isolates the unreprocessed spent fuel from the biosphere.

The dispersal of radioactive substances from a final repository can only occur via the groundwater. In order to prevent and retard such dispersal, the final repository is provided with a series of consecutive barriers.

In order for the groundwater to come into contact with the fuel, it must first penetrate the copper canister, the lead and the zircaloy cladding which enclose the fuel rods. These materials possess very high resistance to corrosion. The canisters are placed in holes drilled in rock of good quality with low water flow. They are surrounded by a buffer material of highly compacted clay (bentonite) with such low water permeability that diffusion is the controlling transport mechanism through the buffer material.

Even if the groundwater were to penetrate to the fuel, the fuel is extremely poorly soluble in water, since the fuel pellets are made of a ceramic material.

Chemical processes in the buffer material and in the system of fissures in the rock, the imperviousness of the buffer material, the low flow rate of the water and the long path which the water must travel in order to reach the biosphere constitute additional barriers which prevent and retard the dispersal of radioactive substances. Furthermore prior to outflow into the biosphere such substances would be diluted in large volumes of groundwater.

The dispersal mechanisms are described in chapter 7. An evaluation of the safety of the final repository is presented in chapter 8.

The final repository has been designed for a total capacity of approximately 7 000 canisters, including 5 300 with BWR fuel (1.4 tonnes of uranium/canister) and 1 700 with PWR fuel (1.1 tonnes of uranium/canister).

The design of the facility is illustrated by the drawings appended to the end of this chapter.

2.4.2 Description of facility

The final repository for the fuel canisters is designed in the form of a tunnel system situated within a roughly square area of

slightly more than 1 km^2 at a level of about 500 metres below the surface. Its geometric configuration will, however, be modified in accordance with the geological conditions at the chosen site.

The fuel canisters are deposited in vertical holes drilled in the floors of the storage tunnels. The distances between the tunnels (25 metres) and between the storage holes (6 metres, see fig. 2-17) have been determined on the basis of considerations of rock mechanics and the heat flux of the fuel in the canisters (approx. 0.8 kW per canister at the time of deposition). With the chosen distances, the specific heat load in the initial phase will be the same (5.25 watts per m^2) as that in the final repository for vitrified reprocessing waste proposed by KBS. The heat flux of the fuel will not give rise to any new fractures in the rock or new flow paths for the groundwater which could affect the safety of the final repository. Furthermore, the effects of the final repository at the surface of the ground on the climate, land uplift etc. will not be noticeable /2-6/.

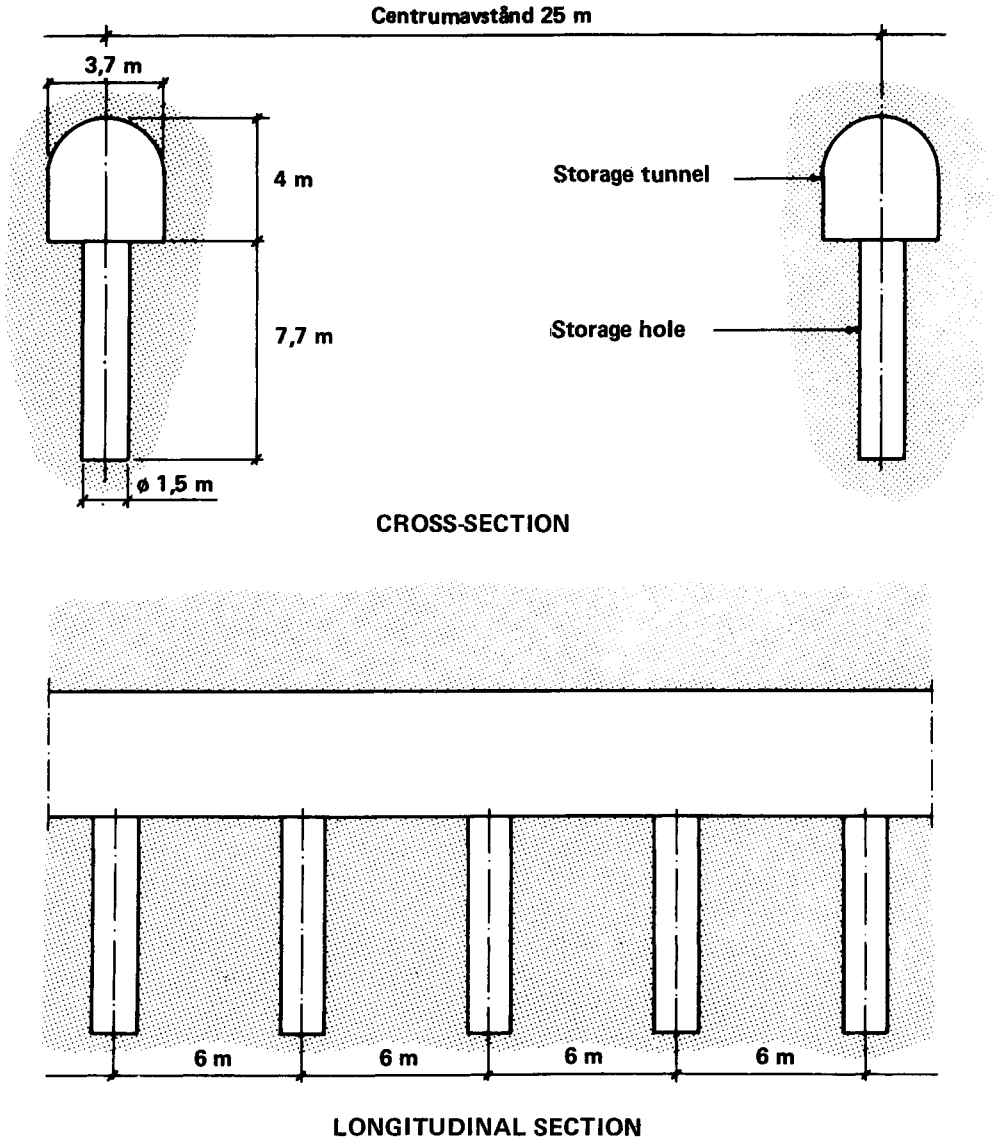

Figure 2-17. Cross-section and longitudinal section of storage tunnels in the final repository. Each storage hole is designed for one canister.

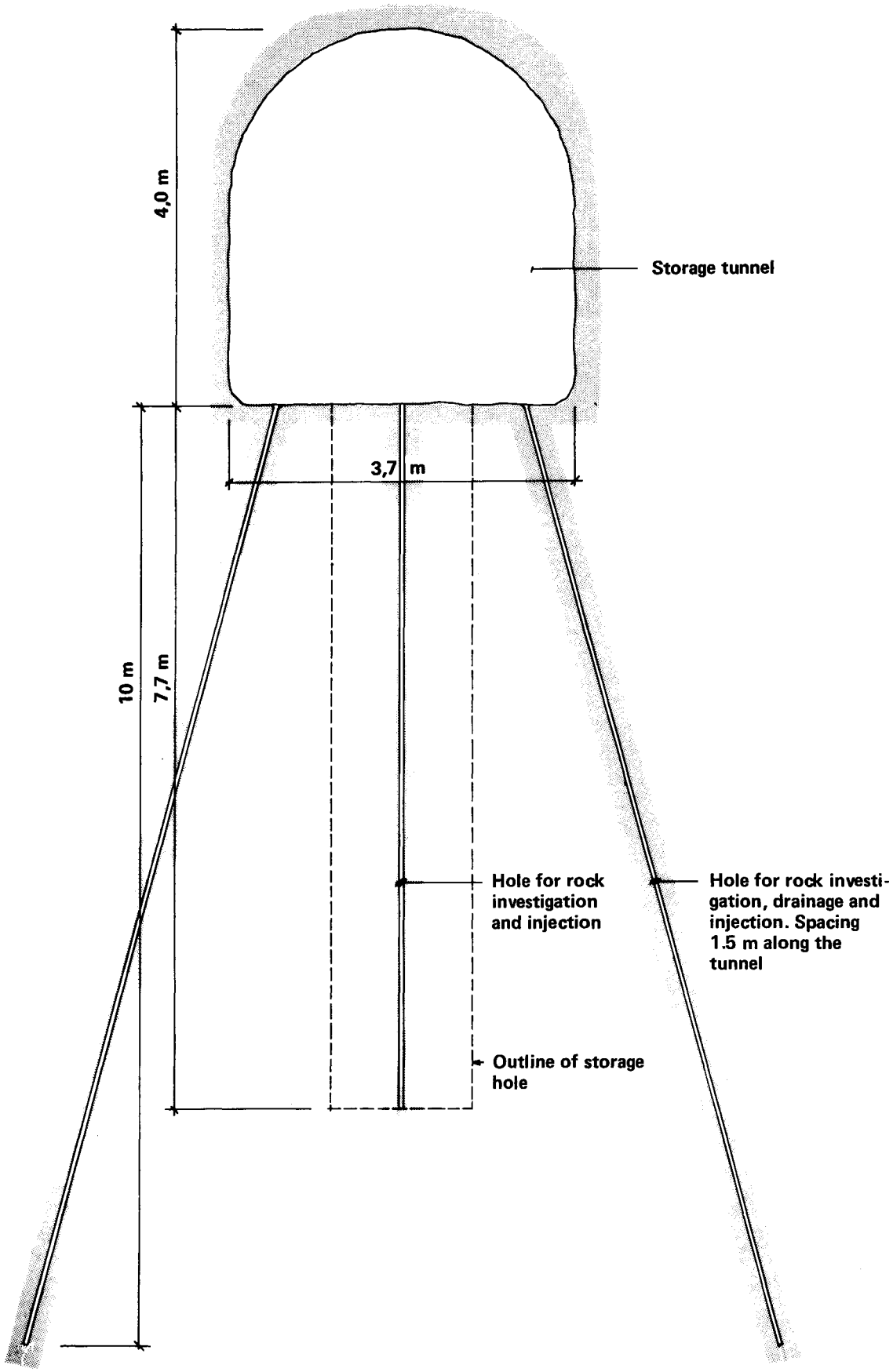

Figure 2-18. Boreholes for investigation, grouting and drainage of the rock around a storage hole.

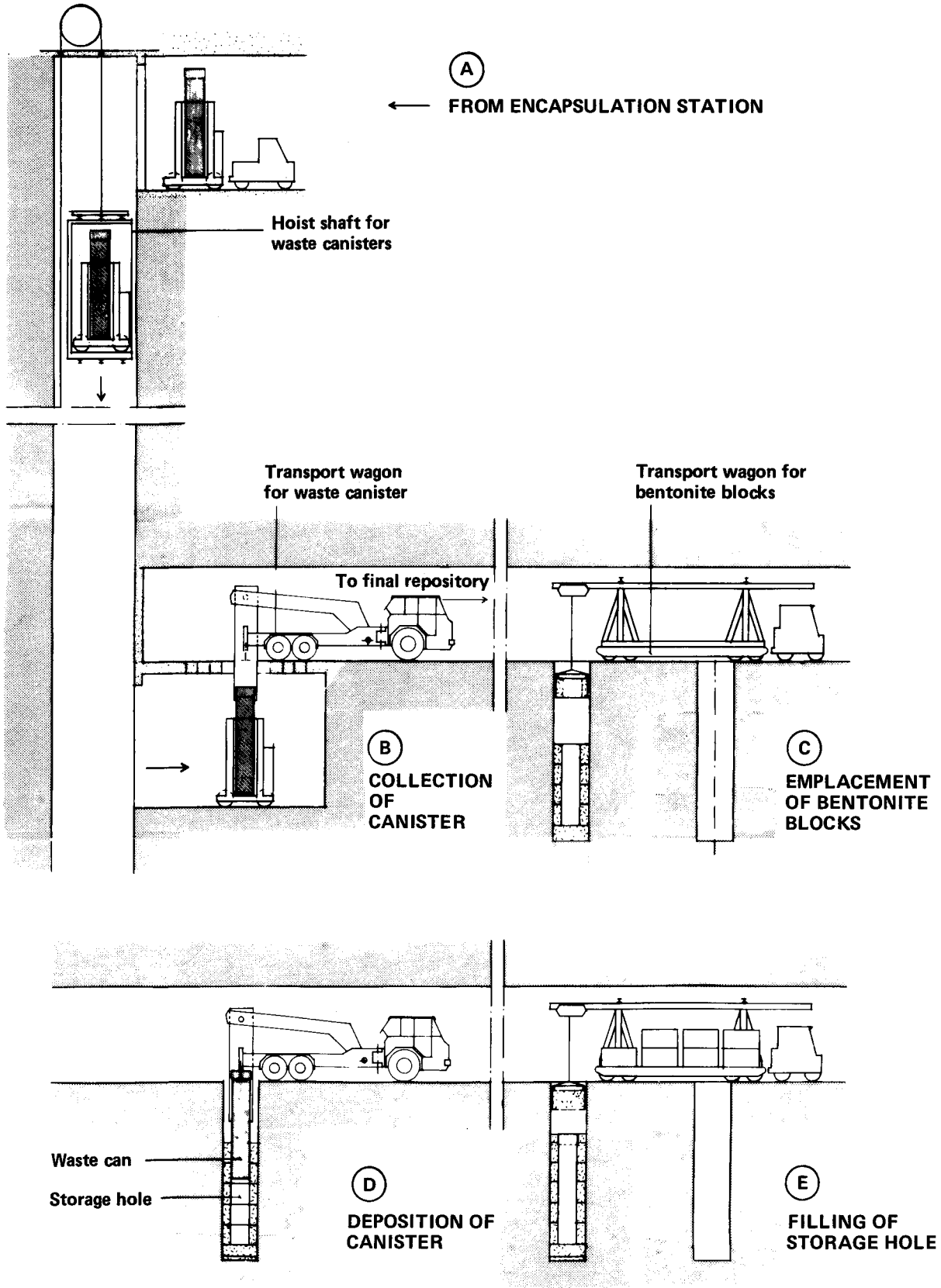

Figure 2-19. Handling of waste canister in final repository.

The storage holes have a diameter of 1.5 metres and a depth of 7.7 metres. Each hole is intended for one canister. They are drilled with full-hole machines. The depth of the holes is such that the canisters will be located well below the zone around the storage tunnels which has been disturbed by the blasting work, where the permeability of the rock can be expected to be higher.

At the site for each storage hole, a smaller pilot hole is first drilled in which the permeability of the surrounding rock is determined by means of water injection. If the permeability of the rock is found to be sufficiently low and the properties of the rock are otherwise suitable for a storage hole, drainage holes are then drilled along the tunnel walls on both sides of the pilot hole at intervals of 1.5 metres, see fig. 2-18. The rock is then grouted by filling the pilot hole with bentonite slurry under pressure at the same time as a vacuum is applied in the outer holes. Tests show that very good sealing of the rock is obtained with such a procedure. An additional sealing effect can be obtained if this procedure is supplemented with electrokinetic grouting /2-7 and 2-8/.

As regards the design of the rock facility in other respects and its auxiliary systems, the reader is referred to the account in the KBS report on vitrified reprocessing waste, Volume III, chapter 6, and to reference /2-9/.

The fuel canister is transferred from the encapsulation station to the final repository in a transport wagon which is taken down to the level of the storage tunnels via an elevator, see fig. 2-19, operation A. The elevator, which runs in a vertical hoist shaft, is designed as a conventional mine elevator with guides and a winding sheave with a number of independent brake systems. The elevator cage is suspended from a number of cables which are strong enough so that a few cables alone can support the load with a good (10-fold) margin of safety. As an additional safety precaution, there is a water pool at the bottom of the hoist shaft which dampens the impact of a falling elevator and prevents canister breakage /2-10/.

When the elevator has reached (the level of the repository, the wagon is moved via remote control out of the elevator into a radiation-shielded handling station, see fig. 2-19 operation B. From here, the canister is lifted up from the wagon into a radiation-shielded transfer cask which is mounted on a special vehicle. After the transfer cask with the canister has been laid down in a horizontal position on the vehicle, the canister is transported to a position above the hole into which it is to be deposited. Positioning of the canister above the hole is effected with the aid of an optical plumb.

Before the vehicle is moved into position, the storage hole is drained of any water which may have entered the hole. The hole is then lined with blocks of highly-compacted bentonite, see fig. 2-19 operation C. The space between the blocks and the rock is filled with bentonite powder. A wagon with a telpher is used to mount the blocks.

The canister is lowered into the hole by equipment mounted on the vehicle, see fig. 2-19 operation D, after which the space between the canister and the surrounding blocks is filled with bentonite

powder. The hole is then filled with additional bentonite blocks, operation E. Finally, a temporary concrete lid is placed over the hole as protection, see fig. 2-20. The lid can be propped up against the tunnel roof in case swelling pressure should build up in the hole before the tunnel is back-filled. For a more detailed account of the handling of the copper canister and the bentonite blocks, see references /2-10 and 2-11/.

The transfer cask on the vehicle provides radiation shielding when the canister is lowered into the hole. The upward-directed radiation from the canister is insignificant (approx. 1 mrem/h), so that the final work of filling the hole can be carried out without any special radiation-shielding precautions.

Bentonite is a naturally occurring clay of volcanic origin which is characterized by a high swelling capacity when it absorbs water. It also possesses a high ion exchange capacity.

The bentonite blocks are produced by compression (isostatic compaction) under very high pressure. ASEA-QUINTUS equipment, which has long been used for the manufacture of e.g. insulators, graphite blocks etc., is used for this purpose. Manufacture of the blocks is described in greater detail in reference /2-11/. Compaction gives the bentonite a high density and thereby good bearing capacity and such a low permeability ($<10^{-13}$ m/s) that it is virtually impenetrable for water. Because the swelling of the bentonite in the hole is restrained, a swelling pressure builds up when the bentonite absorbs water. As a result, water-bearing fissures cannot open in the material, and any fissures which may exist in the walls of the hole at the time of deposition or which may be created at a later time are sealed. For a more detailed account of the properties and function of the highly-compacted bentonite, see chapter 4.

2.4.3 Operation of facility

Canister deposition begins when approximately one-quarter of the total number of storage tunnels have been completed. The facility is designed in such a manner that the construction work can continue without interfering with the transport and deposition of canisters. At the central transport tunnel, the storage tunnels are closed off by a concrete wall with a door and with dampers for regulating the ventilation flow in the storage tunnel.

The storage tunnels in which the canisters have been deposited can be inspected and measurements of rock stresses, temperatures inflow of groundwater etc. can be carried out all the way up to the time when the final repository is to be sealed. During this time, the inflow of water into the storage holes is so small that the bentonite never becomes water-saturated. Among the factors which contribute towards keeping the inflow of water low are the low water flow in the rock, the grouting around the storage holes, the drainage holes along the walls of the storage tunnels and the low permeability of the bentonite in the storage hole.

Owing to the fact that the highly-compacted bentonite is not water-saturated, high swelling pressures cannot build up in the hole before the repository is sealed. The bentonite powder which fills the space between the rock and the bentonite blocks could,

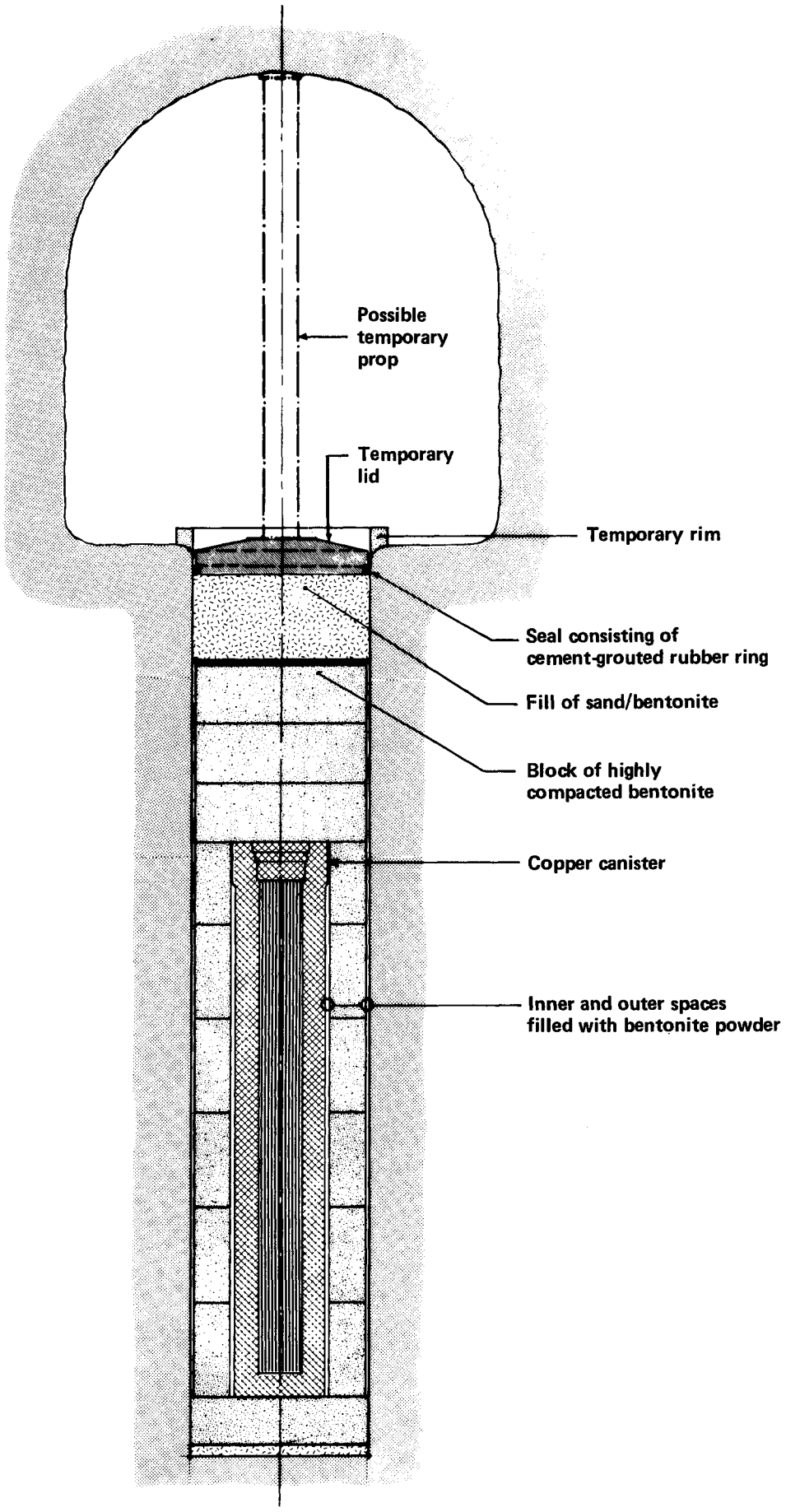

Figure 2-20. After deposition, the storage hole is sealed with a concrete lid. The lid can be propped against the rock roof to counteract any swelling of the bentonite.

however, conceivably absorb sufficient water to give rise to a small swelling pressure. The swelling pressure can, however, easily be absorbed by the temporarily lid, possibly with the aid of a temporary prop against the tunnel roof.

In addition to the inspection of the rock and of the groundwater which is carried out during the construction and operating period, quality control of the final repository will be aimed primarily at verifying the properties of the buffer material. Necessary measures in this respect are described in section 4.4.

The design and operation of the facility will be examined and inspected by authorities such as the Swedish Nuclear Power Inspectorate and the National Institute of Radiation Protection in the same way as a nuclear power station. It will be designed in accordance with regulations issued by these authorities and in consultation with concerned personnel organizations.

With regard to working environment and protection, see 2.5.

2.4.4 Sealing of facility

When the final repository has been filled with canisters to design capacity, the facility can be kept open and inspected as long as surveillance is considered desirable. The facility can then be sealed and finally abandoned.

Prior to sealing, the temporary lids on the deposition holes and the concrete rims are taken away. A copper plate can then be placed on top of the fill in the hole to serve as a diffusion barrier. Even if the temporary lid is affected by the swelling pressure from the fill in the storage hole, the fill will not swell up when the lid is removed. In order to swell in this manner, the bentonite would have to absorb additional water, which is a very slow process.

When the repository is sealed, storage and transport tunnels are filled with a mixture of quartz sand (80-90%) and bentonite (10-20%).

When the sand/bentonite mixture used as a tunnel fill is being prepared, 0.5% ferrophosphate is added to serve as a so-called "oxygen-getter" (see chapter 5).

The lower part of the tunnel fill is deposited in layers which are compacted using a vibrating roller, see fig. 2-21. The upper part is applied using a spray technique which has long been used for spraying concrete. Trials /2-12/ have shown that this technique is well-suited for the spraying of sand/bentonite. The spraying technique and the swelling capacity of the bentonite permit the tunnel section to be filled completely with a high degree of compaction, fig. 2-22.

When the repository is sealed, most of the vertical shafts are filled with a sand/bentonite mixture. In order to provided extra security against water flow in the rock which immediately surrounds the shafts and which may have been disturbed during the shaft-driving work, one or more sections are filled with "plugs" of pure highly compacted bentonite in the manner shown on the

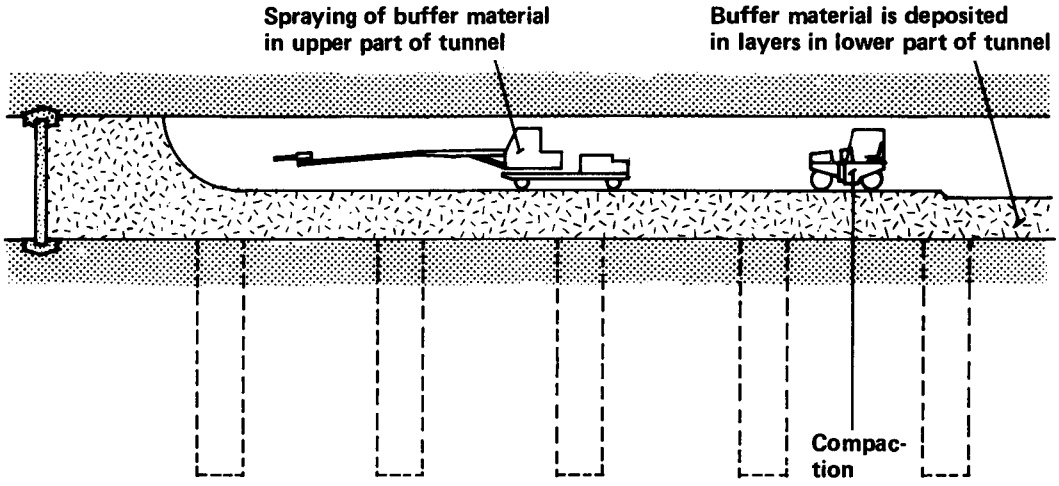

Figure 2-21. When the final repository is sealed, the tunnels are filled with a mixture of quartz sand and bentonite. The lower part of the fill is deposited by tractors and vibrorolled. The upper part of the tunnel is filled by spraying.

appended drawing No. 16. When the bentonite absorbs water and swells, it will penetrate out into fissures which open into the shafts and, together with a previous grouting of the cracks by injection of a bentonite suspension, will block any water pathways around the shafts. Sealing with two "plugs" can be used to isolate local fracture zones in the tunnels, see drawing No. 16.

Boreholes, including those drilled during the preliminary study of the rock formation, are also filled with highly compacted bentonite.

For an account of the properties of the sand/bentonite mixture, see section 6.3, Volume III of the KBS report on vitrified reprocessing waste.

In this way, all cavities in the rock are filled with material which possesses at least as low permeability as the surrounding rock.

It is presumed that observations and measurements of the groundwater system, rock stresses, temperatures etc. will be performed for a certain period of time following the closure of the final repository. A programme for such activities will be prepared in co-operation with the concerned authorities.

2.4.5 Final storage of radioactive metal components etc

The concrete moulds with radioactive metal components and other components from the fuel assemblies are also intended to be deposited in final storage in rock caverns. However, since the radioactivity of this type of waste is considerably lower than that of the fuel, demands on the encapsulation and the buffer material are lower, and the material does not have to be stored at as great a depth below the surface. Furthermore, owing to the limited quantities involved and the negligibly low heat flux of the material, the final repository requires a relatively small volume.

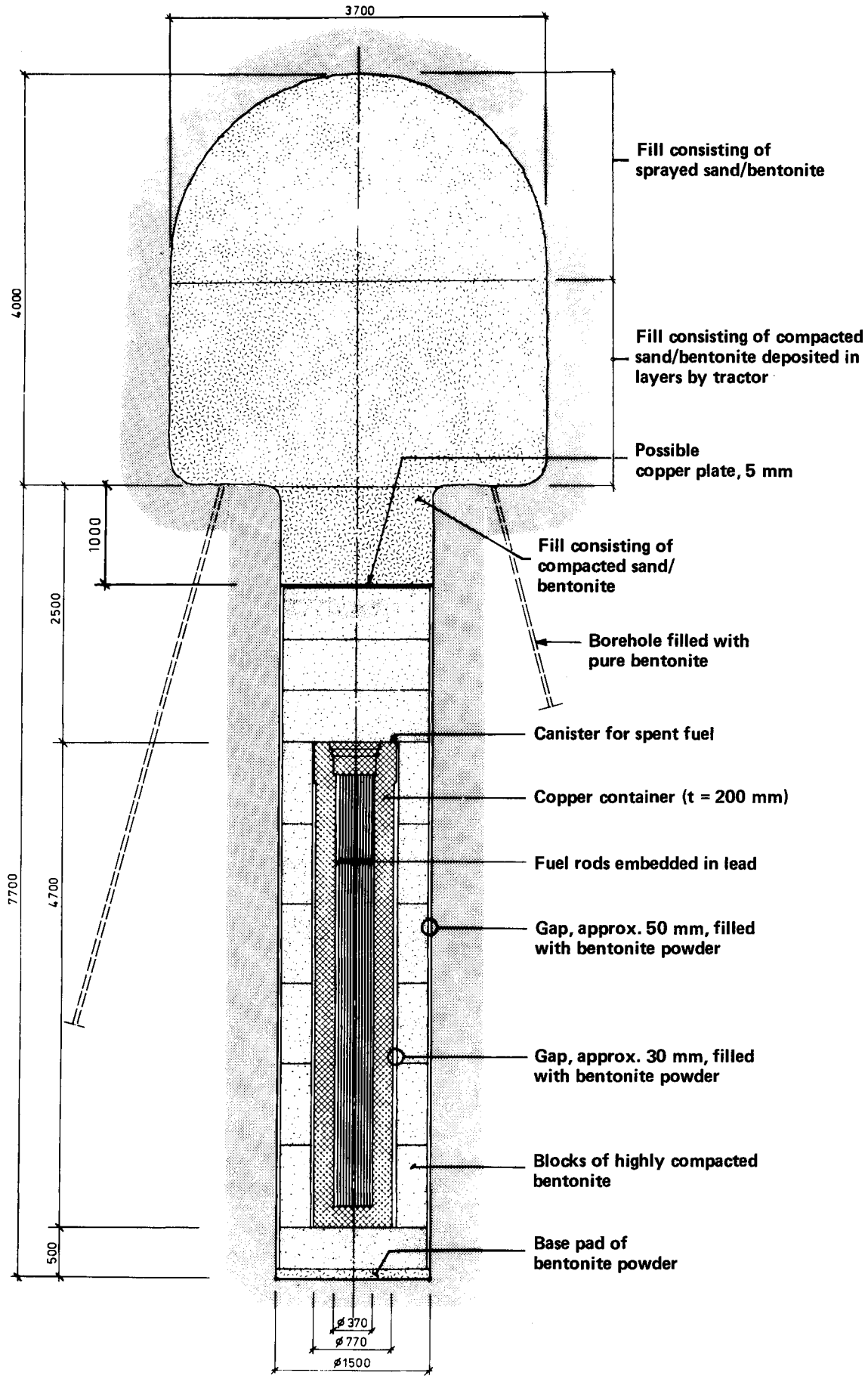

Figure 2-22. The sealed final repository. The canister is surrounded in the storage hole by highly compacted bentonite. The gaps are filled with bentonite powder. The tunnel is filled with a mixture of quartz-sand and bentonite. A copper plate can, if desired, be placed on top of the bentonite block to serve as a diffusion barrier.

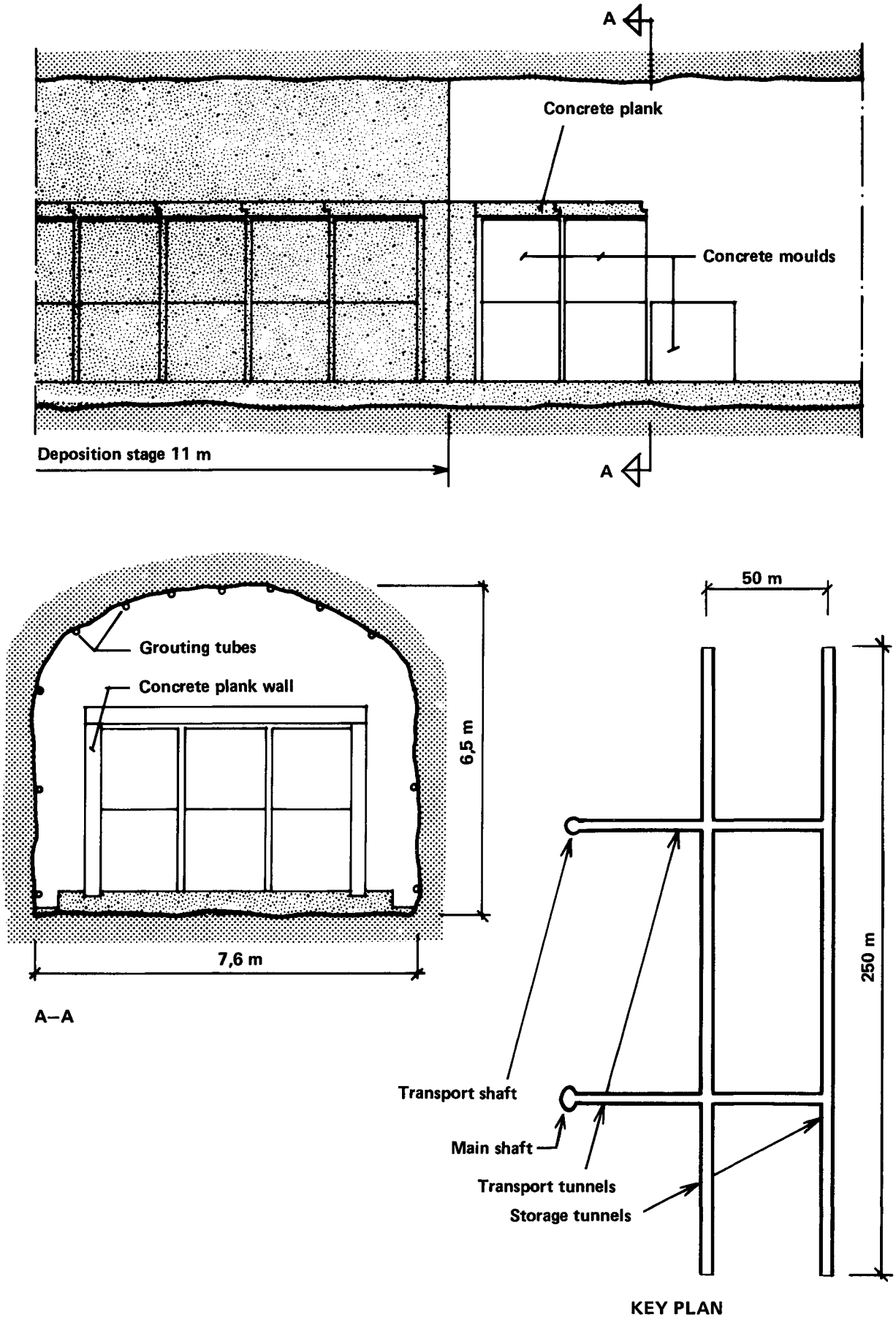

Figure 2-23. Final repository for concrete moulds containing radioactive metal components from the fuel assemblies. The repository is sealed in stages of 11 metres by filling of the tunnel with concrete. In order to guarantee good contact between the concrete and the rock concrete is grouted through tubes along the rock wall.

It is proposed that the facility be designed with two parallel tunnels approximately 250 metres in length and approximately 50 metres from each other. These tunnels are connected with the surface via a hoist shaft and a main shaft, see fig. 2-23. The tunnels have a cross-sectional area of about 50 m^2. The repository is situated approximately 300 metres below the surface.

The final repository for concrete moulds is shown here as a separate facility, but it can also be situated in connection with the final repository for the fuel canisters. Such an arrangement has the advantage that the same shaft systems etc. can be utilized for both repositories. In addition, transport of the moulds from the encapsulation station to the site for the final repository is avoided. A disadvantage of such a joint siting is, however, the negative effects which the final repository for the moulds could possibly have on the chemical environment around the final repository for the fuel canisters. These questions have not yet been studied to a sufficient extent to permit a joint siting of the facility to be proposed.

Another possible siting is in connection with the planned facility for final storage of medium-active waste.

The moulds are transferred to the final repository in a radiation-shielded transport wagon /2-5/, which is brought down to the level of the repository in an elevator. They are stacked two-high and three abreast in the storage tunnels on a concrete floor by the lifting equipment on the wagon. They are then covered with concrete planks on top and on the sides. The planks constitute supplementary radiation shielding which facilitates the work with the sealing of the storage tunnel. Prior to sealing, groundwater entering the tunnels is drained off via floor gutters to pump sumps, from which the water is pumped up to a recipient on the surface.

The storage tunnels are sealed in stages by filling of all spaces between and around the moulds with concrete after deposition has been completed along a length of about 11 metres. The tunnel section is thereby sealed by means of moveable shuttering. During the time the sealing work is underway, deposition of moulds can continue in another part of the tunnel system.

When the entire final repository is full, the transport tunnels and shafts are sealed with sand/bentonite in the same manner as the final repository for fuel canisters.

With the above-described design, the radioactive material in the concrete moulds is isolated from the biosphere by the location of the final repository in rock, which in principle shall meet the same requirements as those which apply to the final repository for the fuel canisters, and by the fact that the rate of dissolution of the radioactive elements in the material is very low.

Concrete provides poorer protection against the penetration of the groundwater to the waste than bentonite or sand/bentonite, since some cracking must be expected, which will locally increase the water flow which can act on the waste. Concrete can also be subjected to chemical action by substances in the groundwater, which will in the long run reduce its impermeability /2-13/. But because the concrete raises the pH of the groundwater and thereby

reduces the rate of dissolution of Ni-59, which is the most important isotope in the metal components of the fuel assemblies from the viewpoint of safety, it contributes towards the adequate safety of the final repository /2-14/.

Quality control of the concrete work shall be carried out in compliance with the directives of applicable concrete regulations.

For a more detailed account of the handling and final storage of radioactive metal components, see reference /2-5/.

2.5 PROTECTION

The word "protection" is used as a collective term to cover working environment, rescue service, radiation protection, physical protection and wartime protection. These matters have been dealt with in the KBS report on the handling and final storage of vitrified waste from reprocessing (Volume III, chapter 7). That report also applies in principle to the final storage of unreprocessed spent fuel. The differences which exist and which affect the question of protection are mainly:

- that the dry intermediate storage of the vitrified waste from reprocessing has been replaced by an extended period of storage in pools in an expanded central storage facility,
- that the receiving section and a large portion of the auxiliary systems for the central fuel storage facility plus the entire encapsulation station have been placed on the surface,
- that the encapsulation procedure involves the handling of spent fuel instead of vitrified waste, entailing relatively complicated work operations, of which, however, some experience has been gained from the operation of nuclear power plants.

Working environment questions during the construction phase are of a similar nature as those described in the KBS report on vitrified reprocessing waste. The encapsulation station, located above the final repository, is commissioned at the same time as the final repository, so that a separation of operative facilities from ongoing construction activities in the direct disposal alternative is only required in the rock cavern section of the final repository and between expansion stages for the storage section of the central storage facility.

The encapsulation procedure involves, among other things, the dismantling of fuel assemblies, pouring lead into the canisters filled with fuel rods and sealing of the canisters. The procedure is based on known technique, but involves relatively complex work operations in connection with the handling of spent fuel. Protection matters must therefore be accorded special attention in the design of the encapsulation station.

The manufacture and handling of the highly-compacted bentonite blocks is not expected to entail any difficult working environment problems. Bentonite is tasteless, odourless and completely harmless.

Radiological safety along the entire handling chain for spent fuel is described in chapter 8.

2.6 DRAWINGS

Drawing	01	Encapsulation station. Building layout. Plan +6.500
	02	Encapsulation station. Building layout. Plan ± 0.000
	03	Encapsulation station. Building layout. Section A-A, B-B, C-C, D-D
	04	General layout
	05	Perspective
	06	Siting example
	07	Construction stages
	08	Transport routes
	09	Ventilation
	10	Storage tunnels
	11	Sealed repository
	12	Transport of waste canister to final repository
	13	Transport and deposition of waste canister in final repository
	14	Emplacement of bentonite blocks in storage holes
	15	Sealing of tunnels
	16	Impervious zone around shafts and tunnels

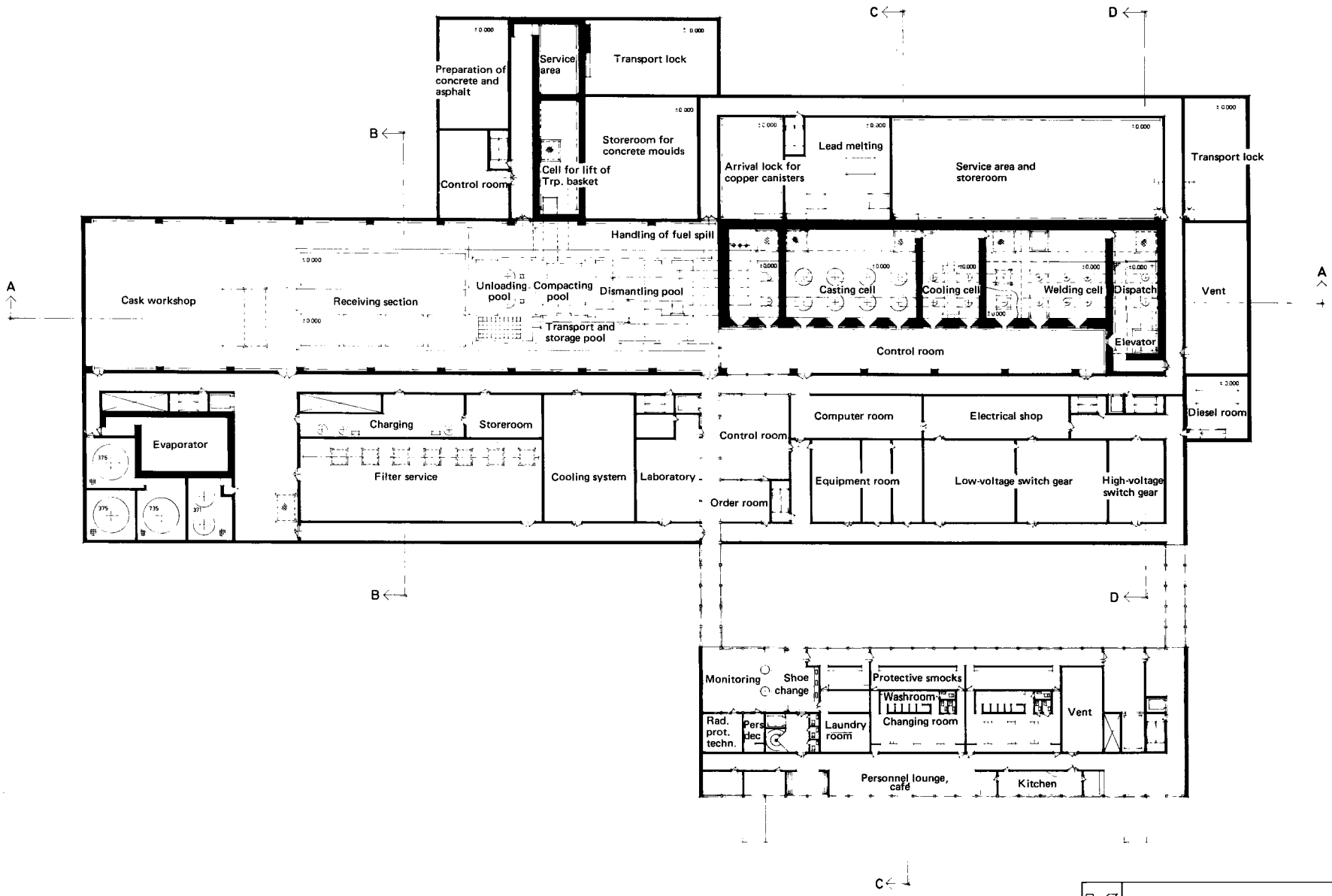

KBS	**ASEA-ATOM**
	ENCAPSULATION STATION BUILDING LAYOUT
	Plan 6500
	DRAWING 01

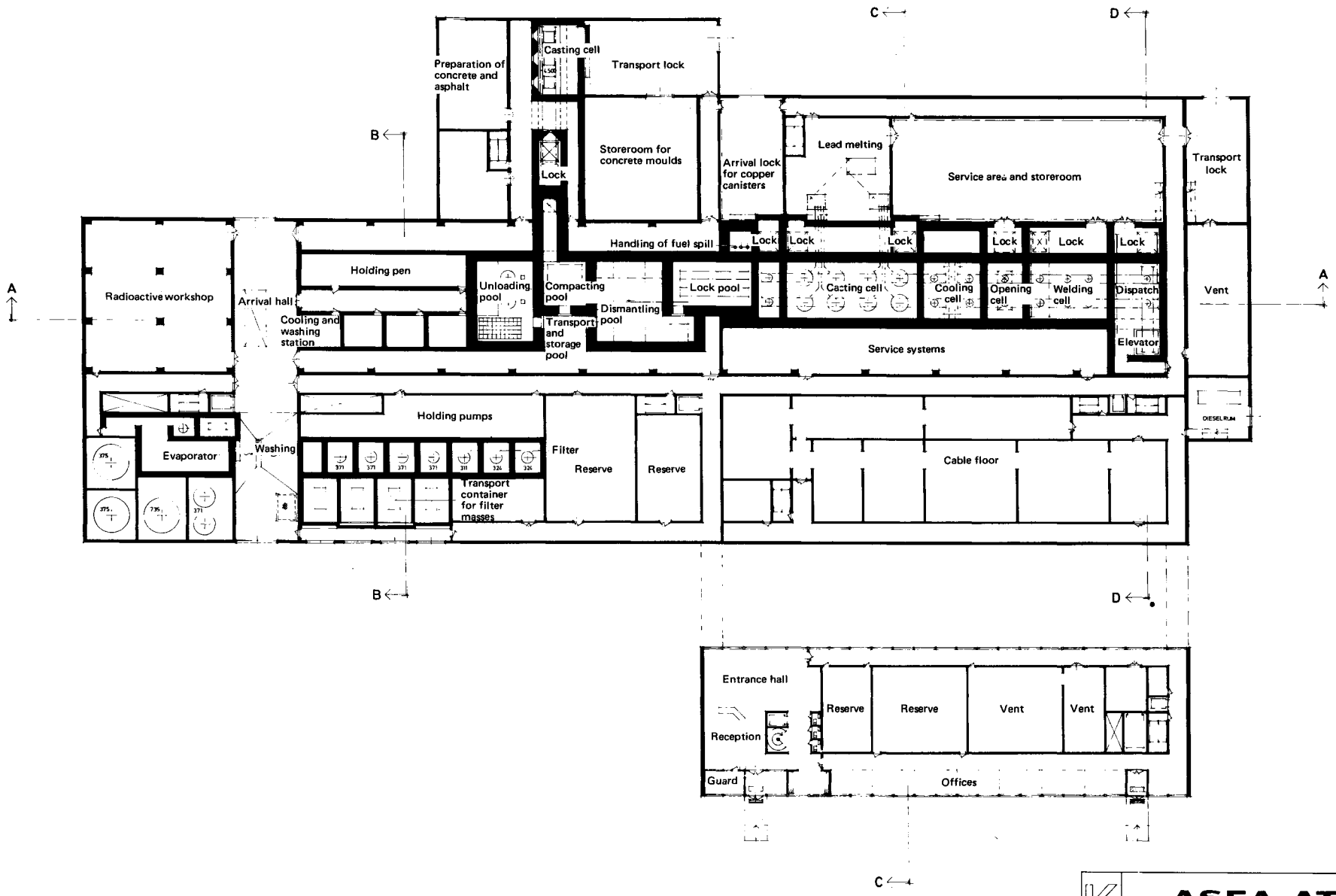

K B S	**ASEA-ATOM**
	ENCAPSULATION STATION BUILDING LAYOUT
	Plan ±0.000
	DRAWING 02

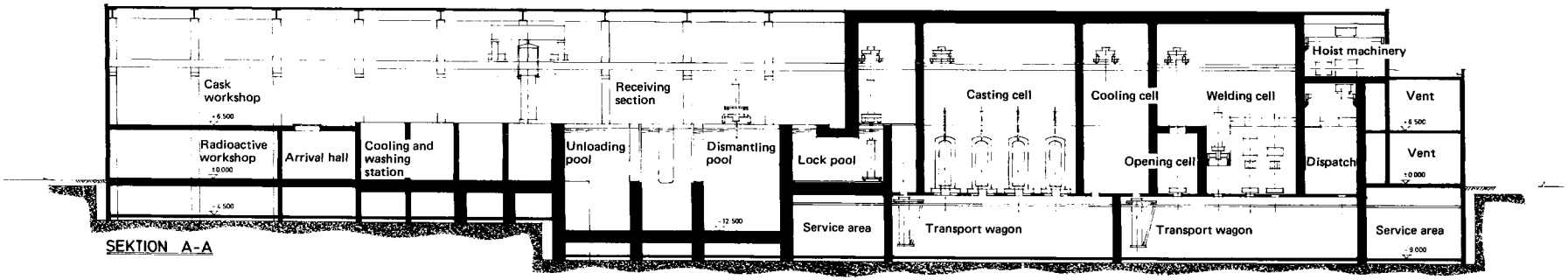

SEKTION A-A

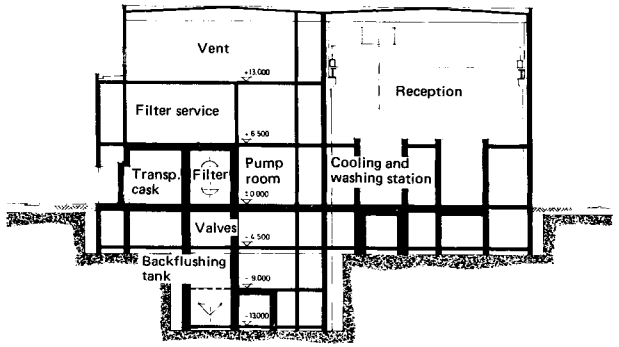

SEKTION B-B

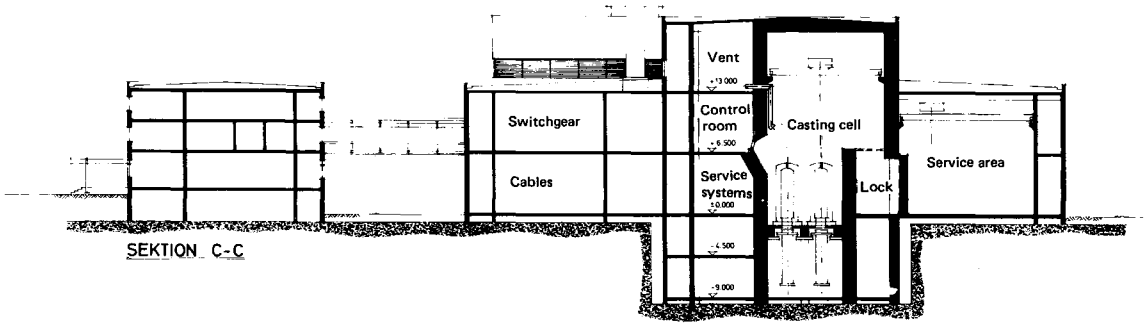

SEKTION C-C

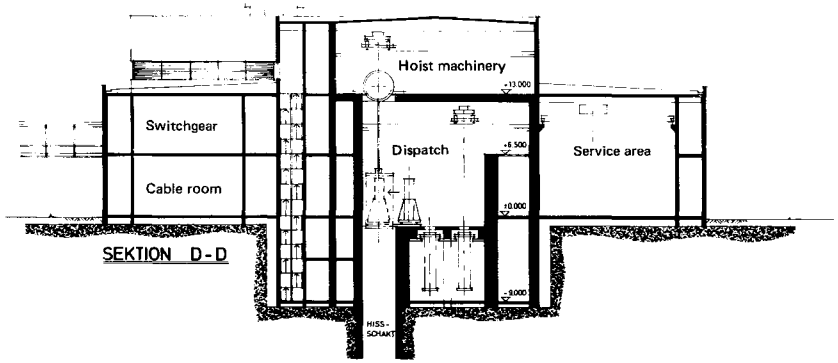

SEKTION D-D

K B S	**ASEA-ATOM**
	ENCAPSULATION STATION BUILDING LAYOUT
	Section A–A, B–B, C–C, D–D
	DRAWING 03

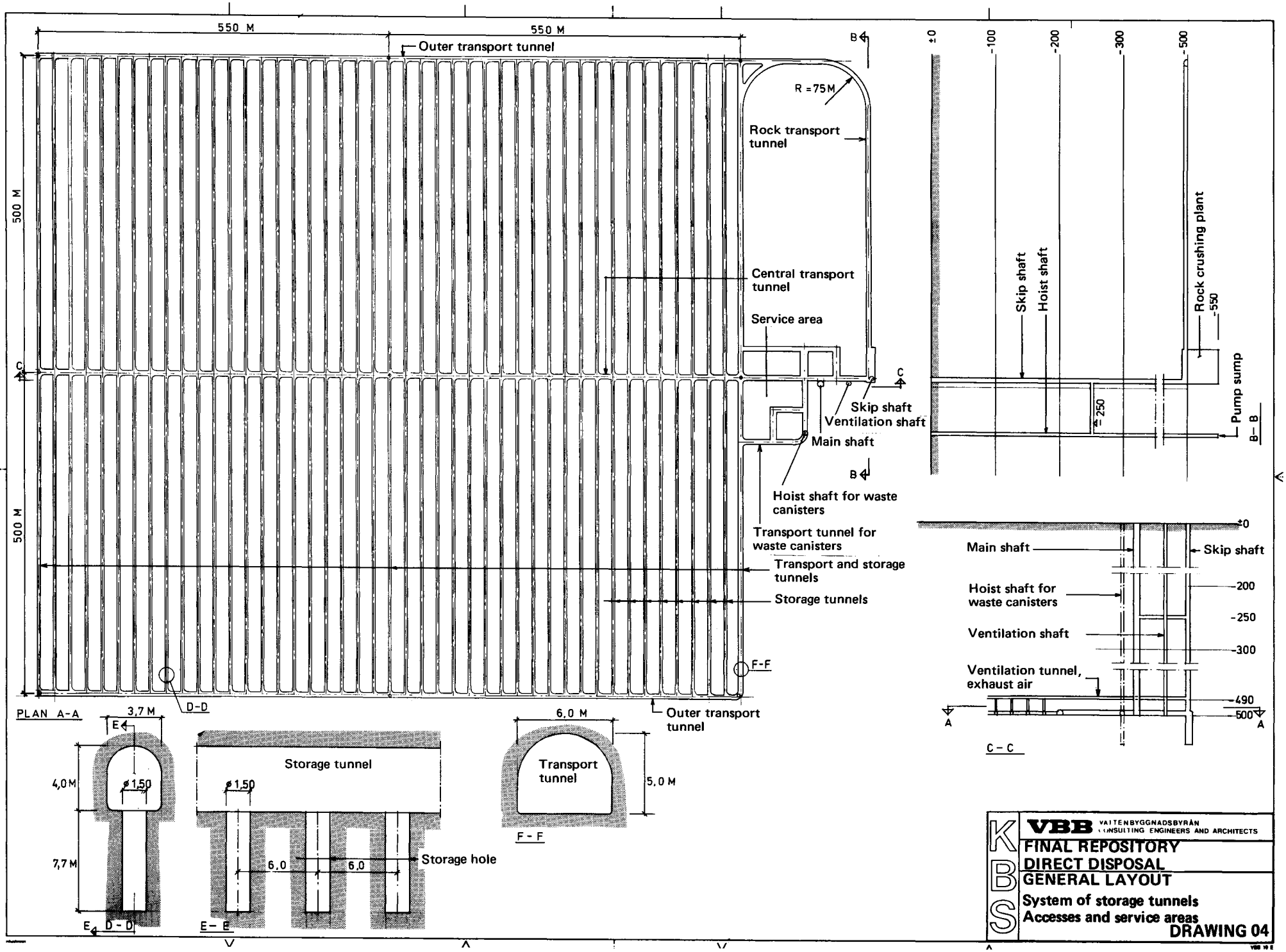

KBS

VBB VATTENBYGGNADSBYRÅN CONSULTING ENGINEERS AND ARCHITECTS

FINAL REPOSITORY
DIRECT DISPOSAL
GENERAL LAYOUT
System of storage tunnels
Accesses and service areas
DRAWING 04

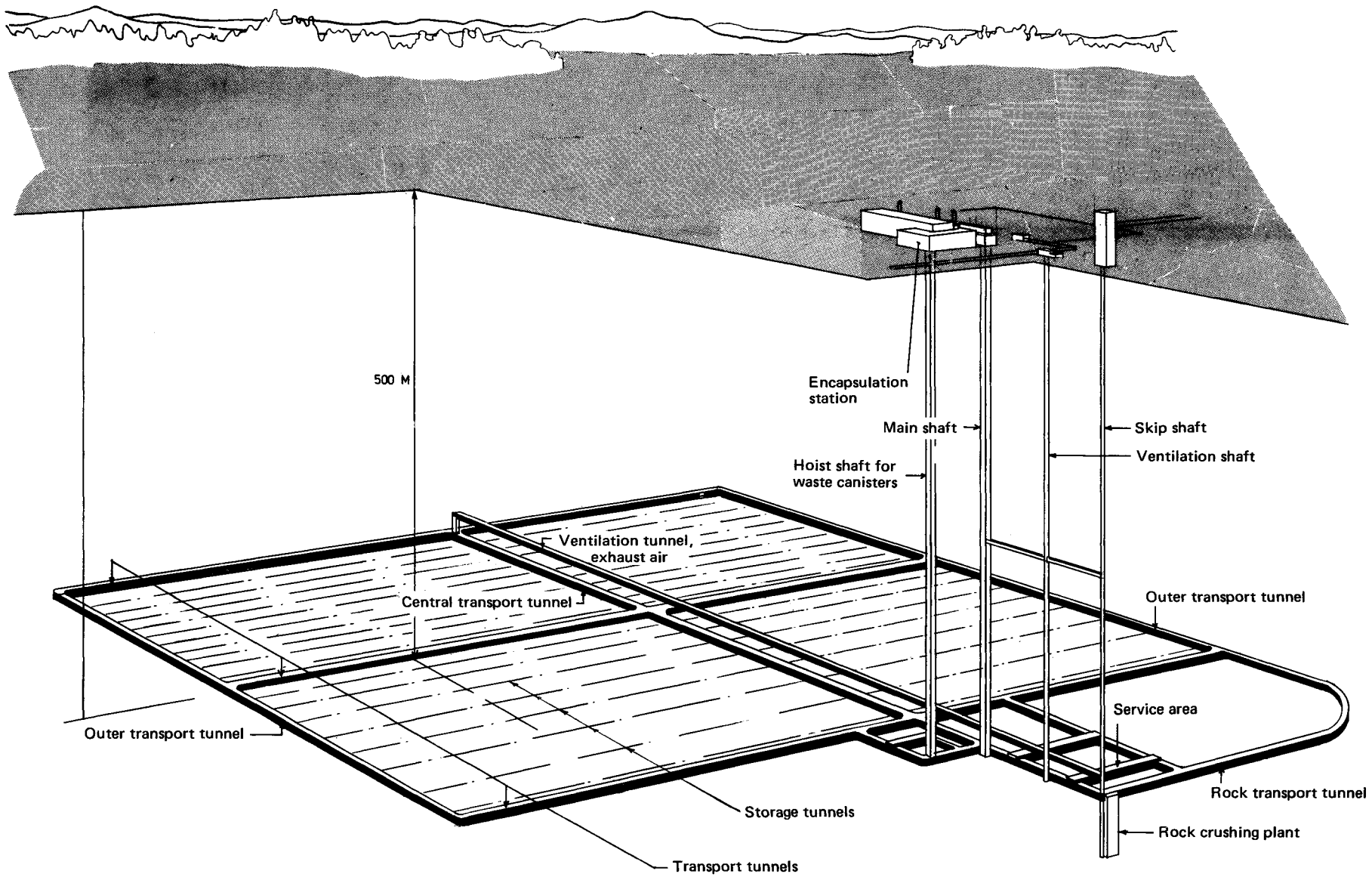

KBS

VBB VATTENBYGGNADSBYRÅN CONSULTING ENGINEERS AND ARCHITECTS

FINAL REPOSITORY DIRECT DISPOSAL

Perspective

DRAWING 05

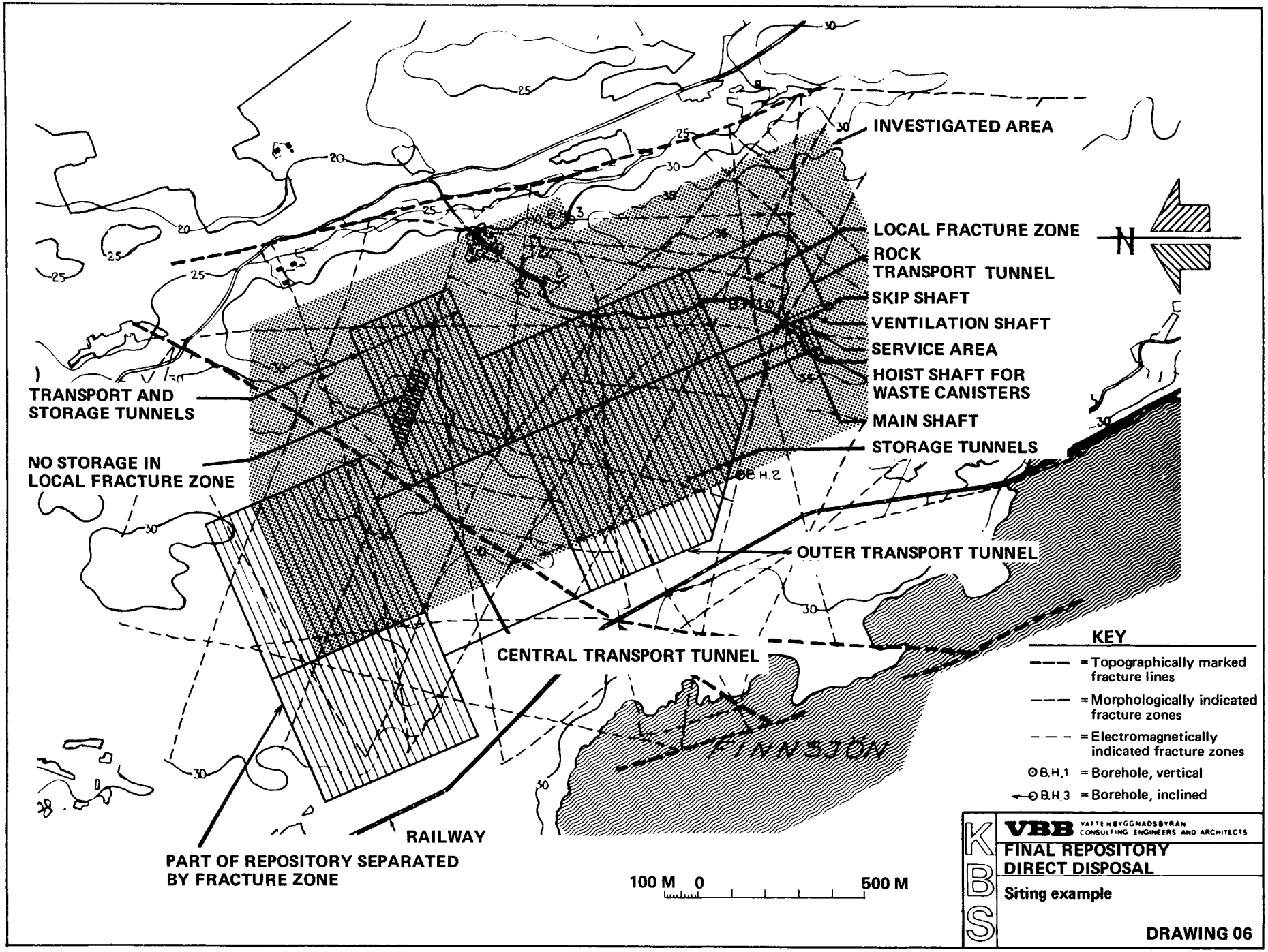
INVESTIGATED AREA
LOCAL FRACTURE ZONE
ROCK
TRANSPORT TUNNEL
SKIP SHAFT
VENTILATION SHAFT
SERVICE AREA
HOIST SHAFT FOR
WASTE CANISTERS
MAIN SHAFT
STORAGE TUNNELS
TRANSPORT AND
STORAGE TUNNELS
NO STORAGE IN
LOCAL FRACTURE ZONE
OUTER TRANSPORT TUNNEL
CENTRAL TRANSPORT TUNNEL
RAILWAY
PART OF REPOSITORY SEPARATED
BY FRACTURE ZONE
N
ÄLVSJÖN
B.H.2
KEY
= Topographically marked fracture lines
= Morphologically indicated fracture zones
= Electromagnetically indicated fracture zones
B.H.1 = Borehole, vertical
B.H.3 = Borehole, inclined
100 M 0 500 M
KBS
VBB VATTENBYGGNADSBYRAN CONSULTING ENGINEERS AND ARCHITECTS
FINAL REPOSITORY
DIRECT DISPOSAL
Siting example
DRAWING 06

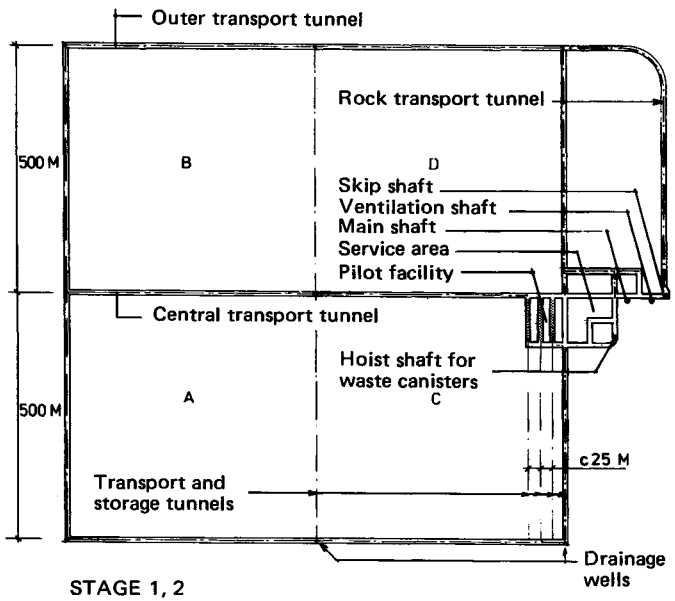

STAGE 1, 2

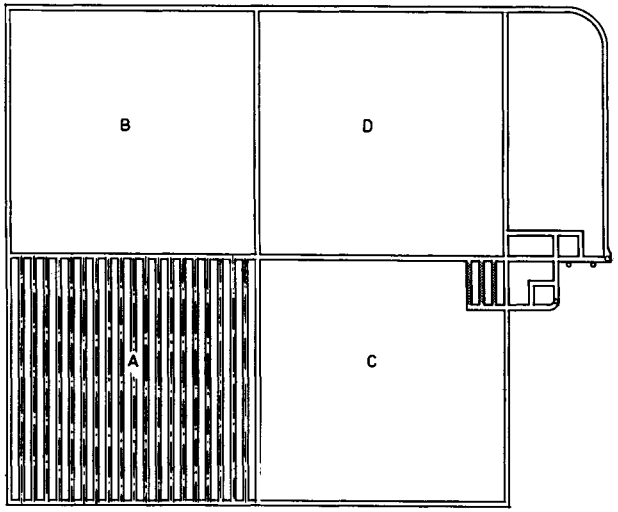

STAGE 3

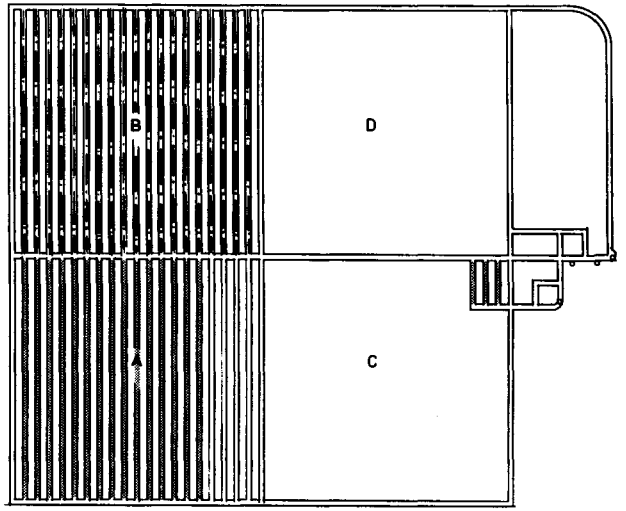

STAGE 4

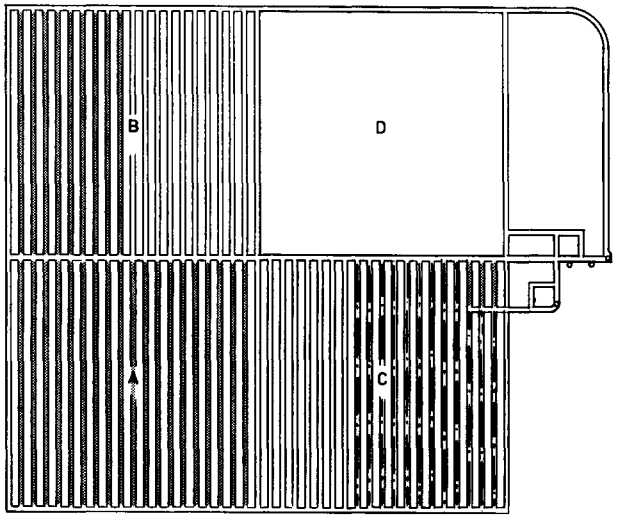

STAGE 6

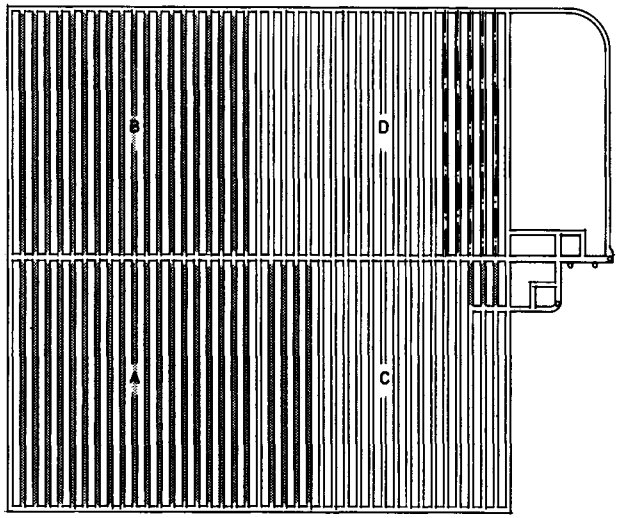

STAGE 8

Tunnel work in progress

Finished tunnel (Deposition in progress)

Sealed tunnel

Stage	Years	Blasting	Deposition
1	1-4	Shafts, pilot facility	Pilot facility
2	4-5	Transport tunnels	
3	5-10,5	Area A finished	
4	10,5-16	Area B finished	Area A 75 %
5	16-18	Area C 35 %	Area A finished
6	18-21,5	Area C finished	Area B 45 %
7	21,5-25,5	Area D 70 %	Area B finished
8	25,5-27	Area D finished	Area C 20 %
9	27-32,5		Area C finished
10	32,5-40		Area D finished

VBB VATTENBYGGNADSBYRÅN CONSULTING ENGINEERS AND ARCHITECTS

KBS

FINAL REPOSITORY DIRECT DISPOSAL

Construction stages

DRAWING 07

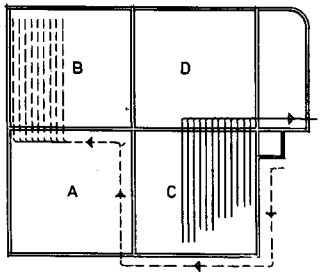

STAGE 6

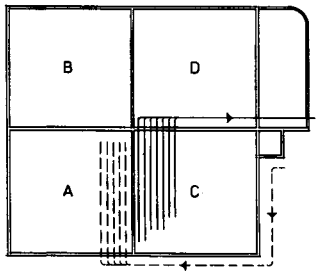

STAGE 5

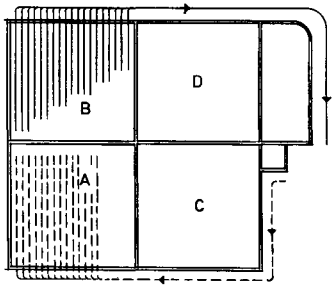

STAGE 4

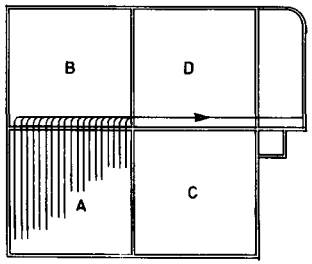

STAGE 3

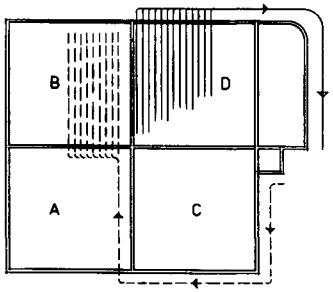

STAGE 7

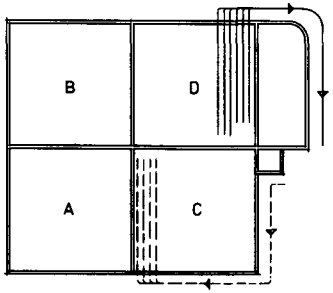

STAGE 8

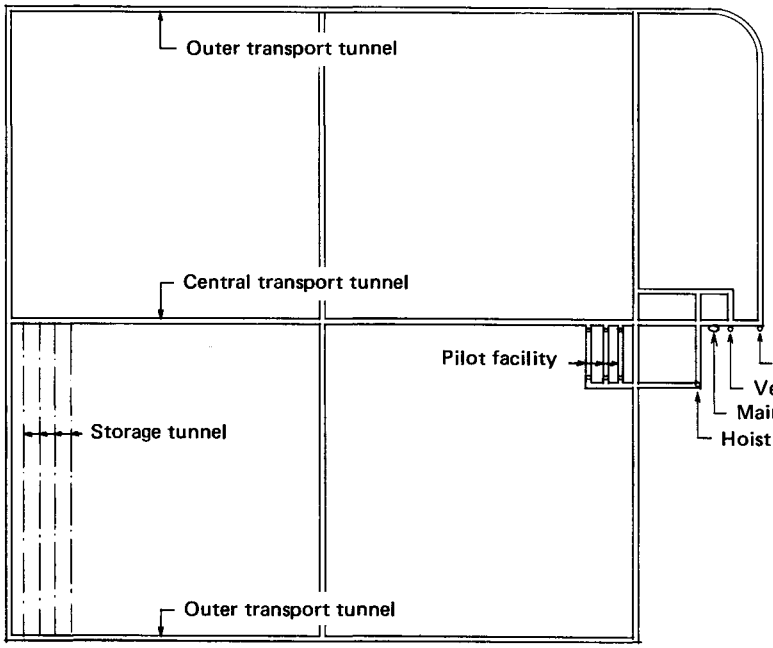

STAGE 2

Transport route for rock

Transport route for waste canisters and buffer materia

Note: Construction stages as per drawing 07

KBS

VBB VATTENBYGGNADSBYRAN CONSULTING ENGINEERS AND ARCHITECTS

FINAL REPOSITORY DIRECT DISPOSAL

Transport routes

DRAWING 08

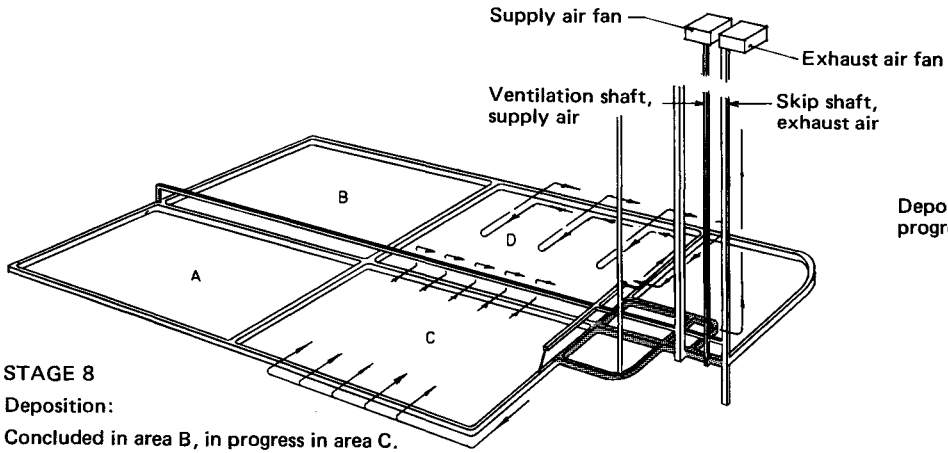

STAGE 8

Deposition:

Concluded in area B, in progress in area C.

Blasting:

Concluded in area C, in progress in area D

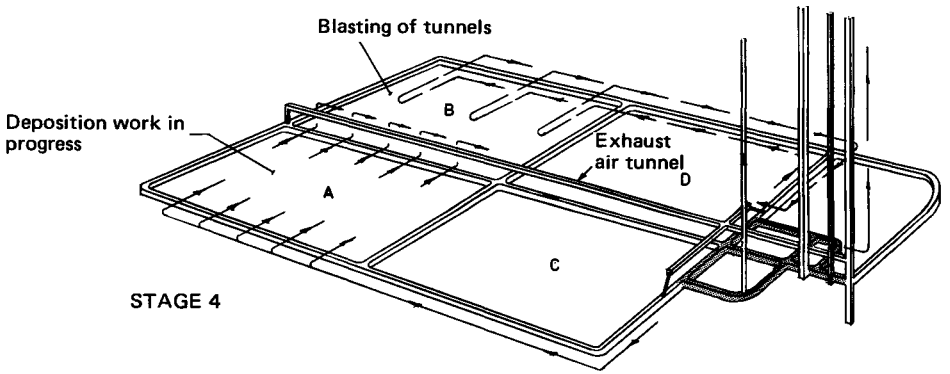

STAGE 4

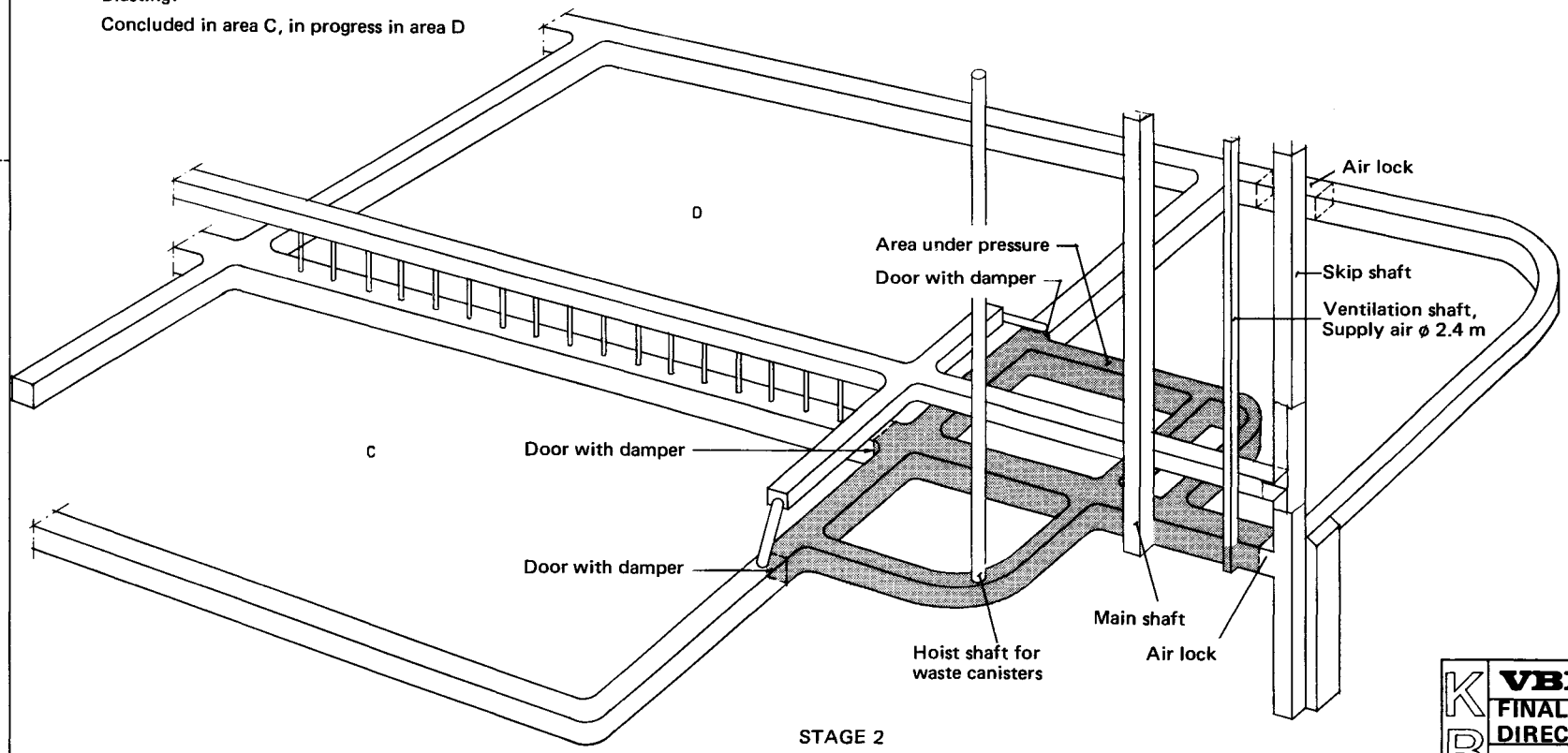

STAGE 2

VBB VÄTTENBYGGNADSBYRÅN CONSULTING ENGINEERS AND ARCHITECTS

KBS

FINAL REPOSITORY
DIRECT DISPOSAL

Ventilation

DRAWING 09

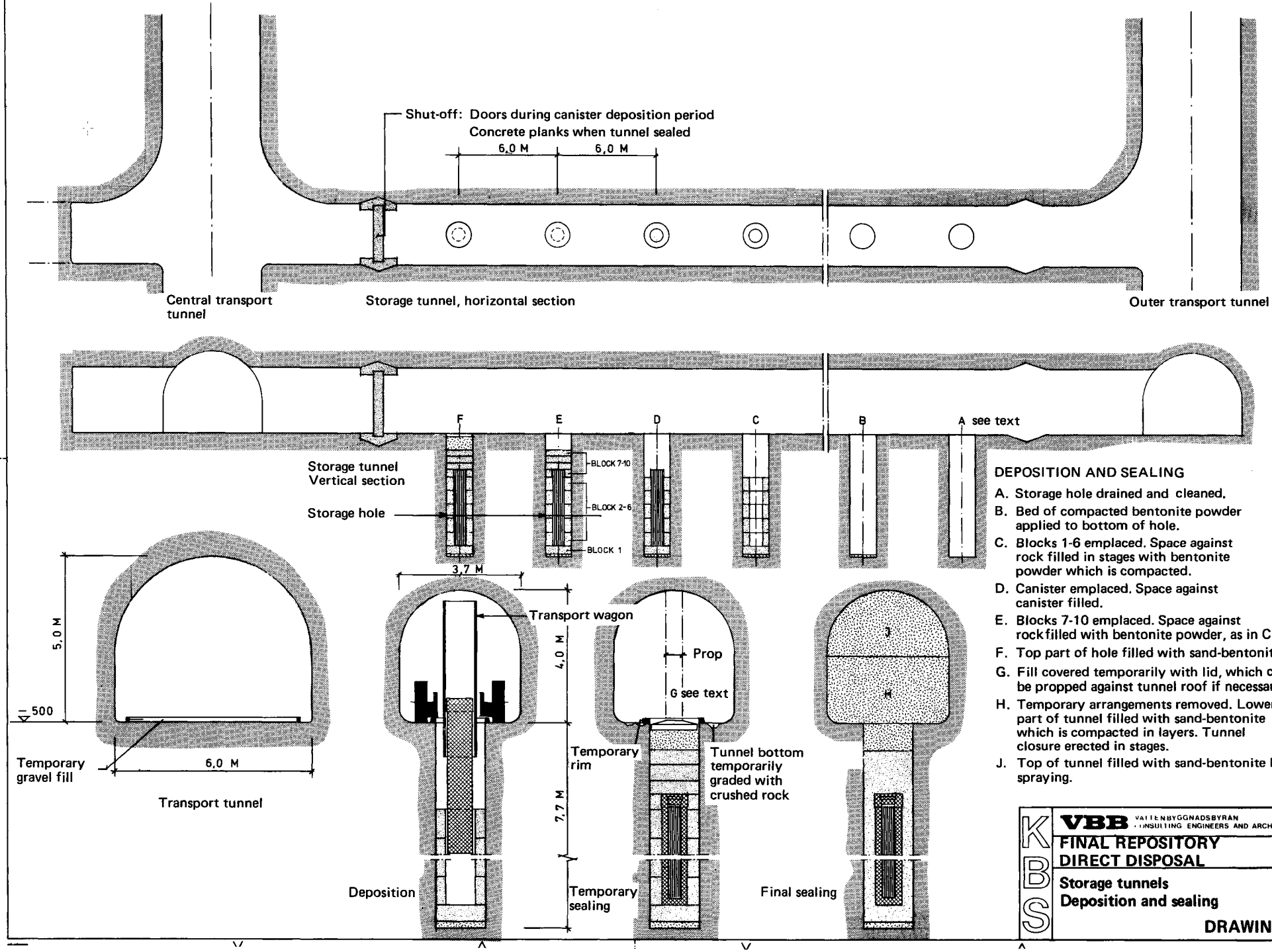

DEPOSITION AND SEALING

A. Storage hole drained and cleaned.
B. Bed of compacted bentonite powder applied to bottom of hole.
C. Blocks 1-6 emplaced. Space against rock filled in stages with bentonite powder which is compacted.
D. Canister emplaced. Space against canister filled.
E. Blocks 7-10 emplaced. Space against rock filled with bentonite powder, as in C.
F. Top part of hole filled with sand-bentonite.
G. Fill covered temporarily with lid, which can be propped against tunnel roof if necessary.
H. Temporary arrangements removed. Lower part of tunnel filled with sand-bentonite which is compacted in layers. Tunnel closure erected in stages.
J. Top of tunnel filled with sand-bentonite by spraying.

KBS

VBB VATTENBYGGNADSBYRAN CONSULTING ENGINEERS AND ARCHITECTS

FINAL REPOSITORY DIRECT DISPOSAL

Storage tunnels
Deposition and sealing

DRAWING 10

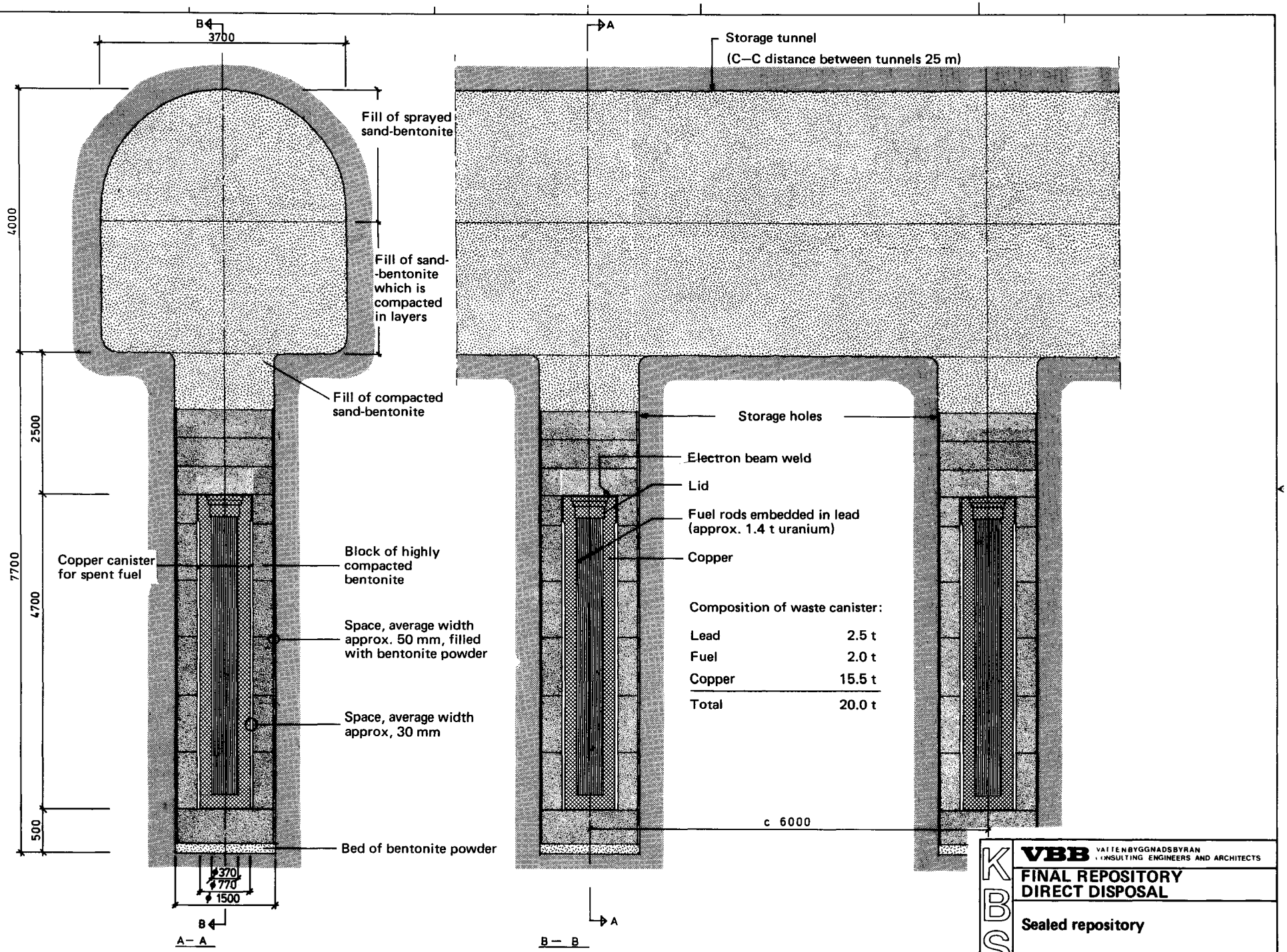
B
3700
A
Storage tunnel
(C—C distance between tunnels 25 m)
Fill of sprayed sand-bentonite
Fill of sand--bentonite which is compacted in layers
Fill of compacted sand-bentonite
4000
2500
7700
4700
500
Storage holes
Electron beam weld
Lid
Fuel rods embedded in lead (approx. 1.4 t uranium)
Copper
Copper canister for spent fuel
Block of highly compacted bentonite
Space, average width approx. 50 mm, filled with bentonite powder
Space, average width approx, 30 mm
Bed of bentonite powder
c 6000
ø370
ø770
ø 1500
B
A
A— A
B— B
Composition of waste canister:
Lead 2.5 t
Fuel 2.0 t
Copper 15.5 t
Total 20.0 t
VBB VATTENBYGGNADSBYRAN CONSULTING ENGINEERS AND ARCHITECTS
KBS
FINAL REPOSITORY
DIRECT DISPOSAL
Sealed repository
DRAWING 11

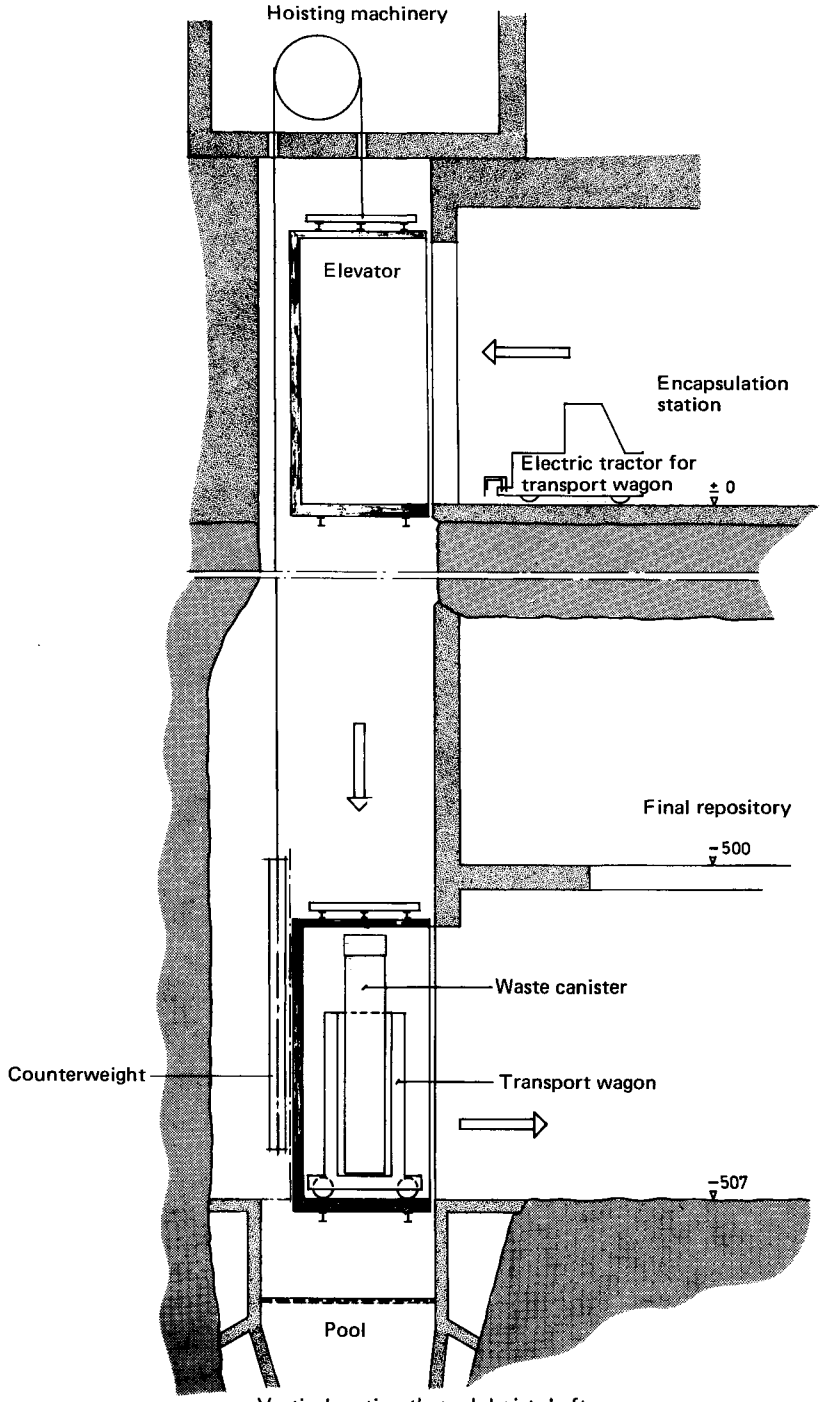

Vertical section through hoist shaft

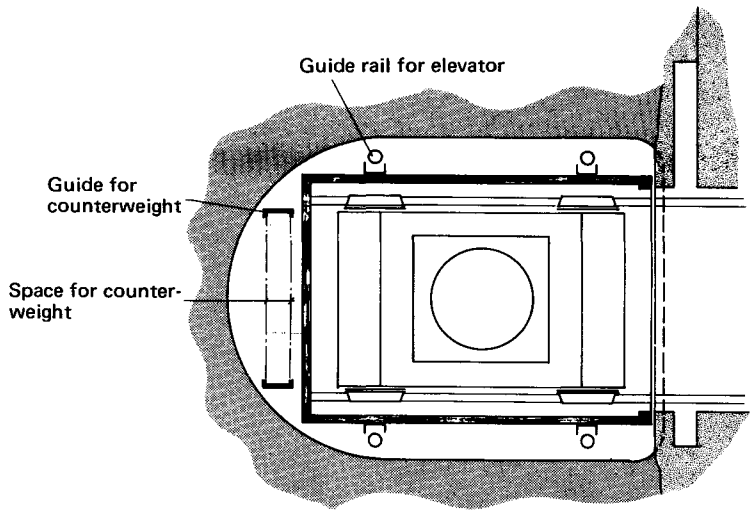

CROSS-SECTION THROUGH HOIST SHAFT

VBB VATTENBYGGNADSBYRÅN CONSULTING ENGINEERS AND ARCHITECTS

KBS

FINAL REPOSITORY
DIRECT DISPOSAL

Transport of waste canister to final repository

DRAWING 12

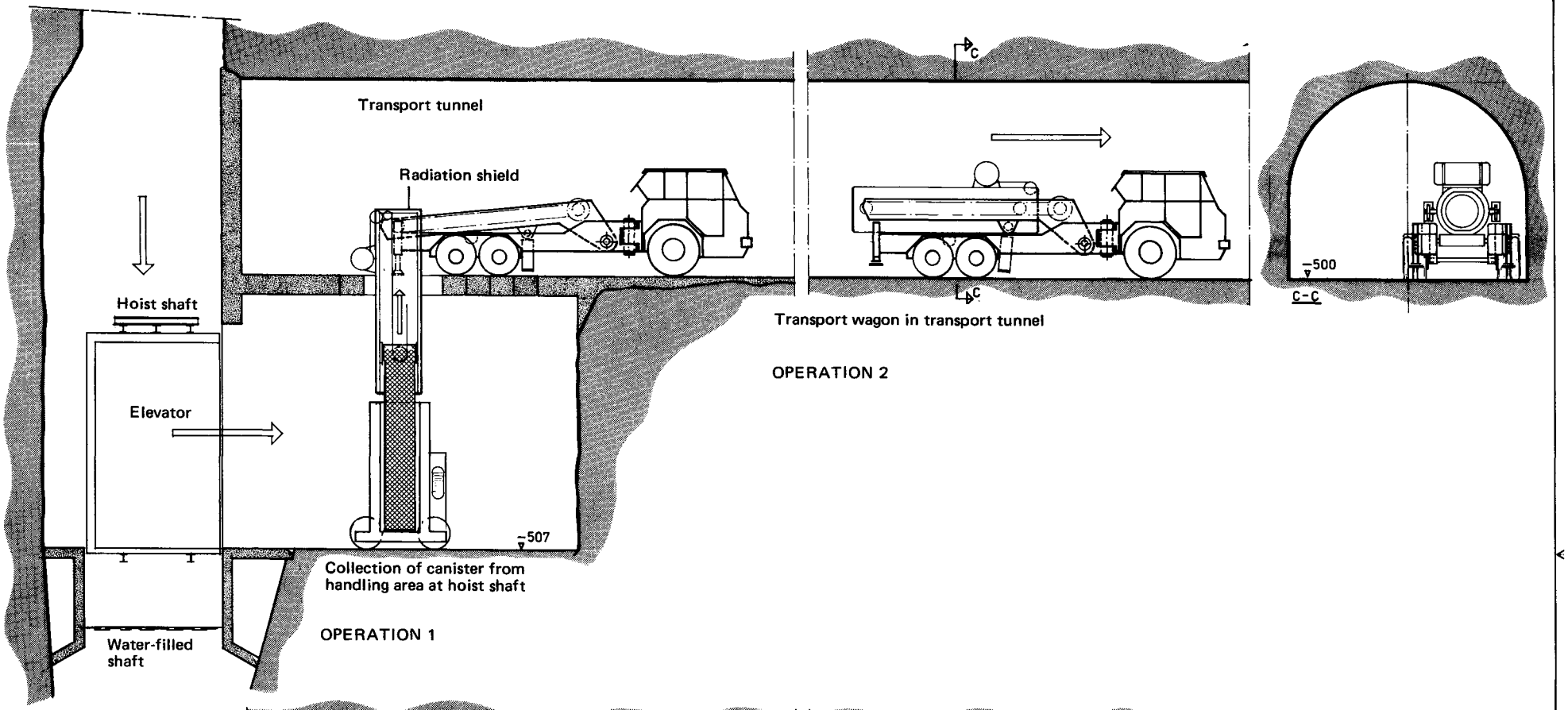

VBB VATTENBYGGNADSBYRÅN CONSULTING ENGINEERS AND ARCHITECTS

KBS

FINAL REPOSITORY
DIRECT DISPOSAL

Transport and deposition of waste canister in final repository

DRAWING 13

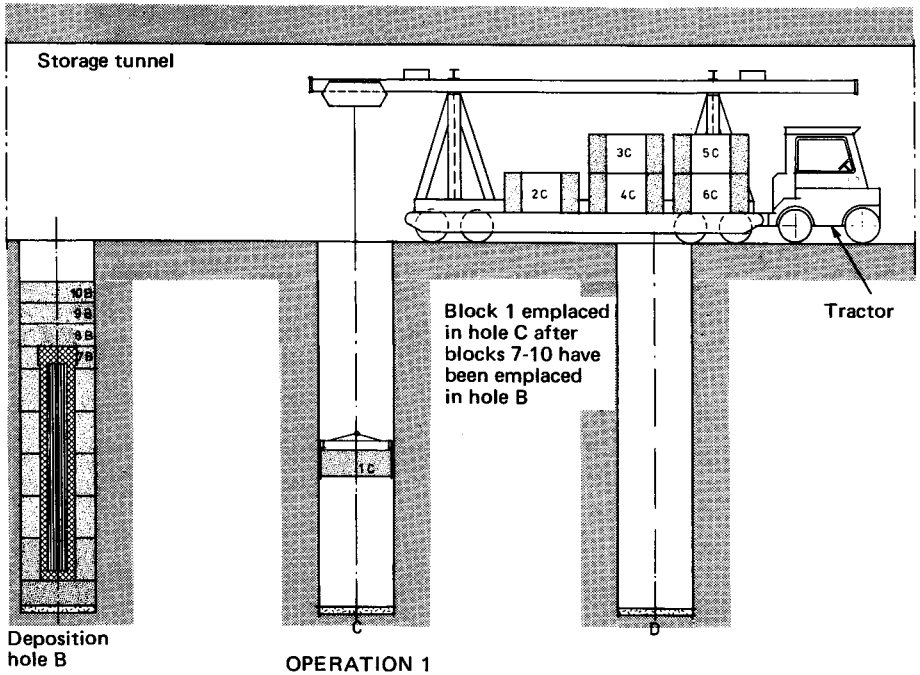

OPERATION 1

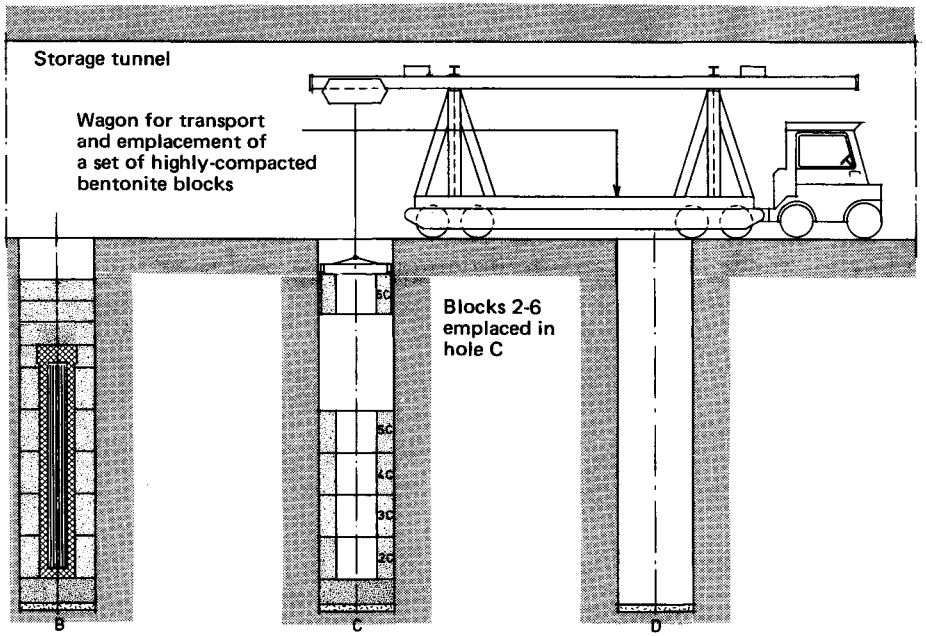

OPERATION 2

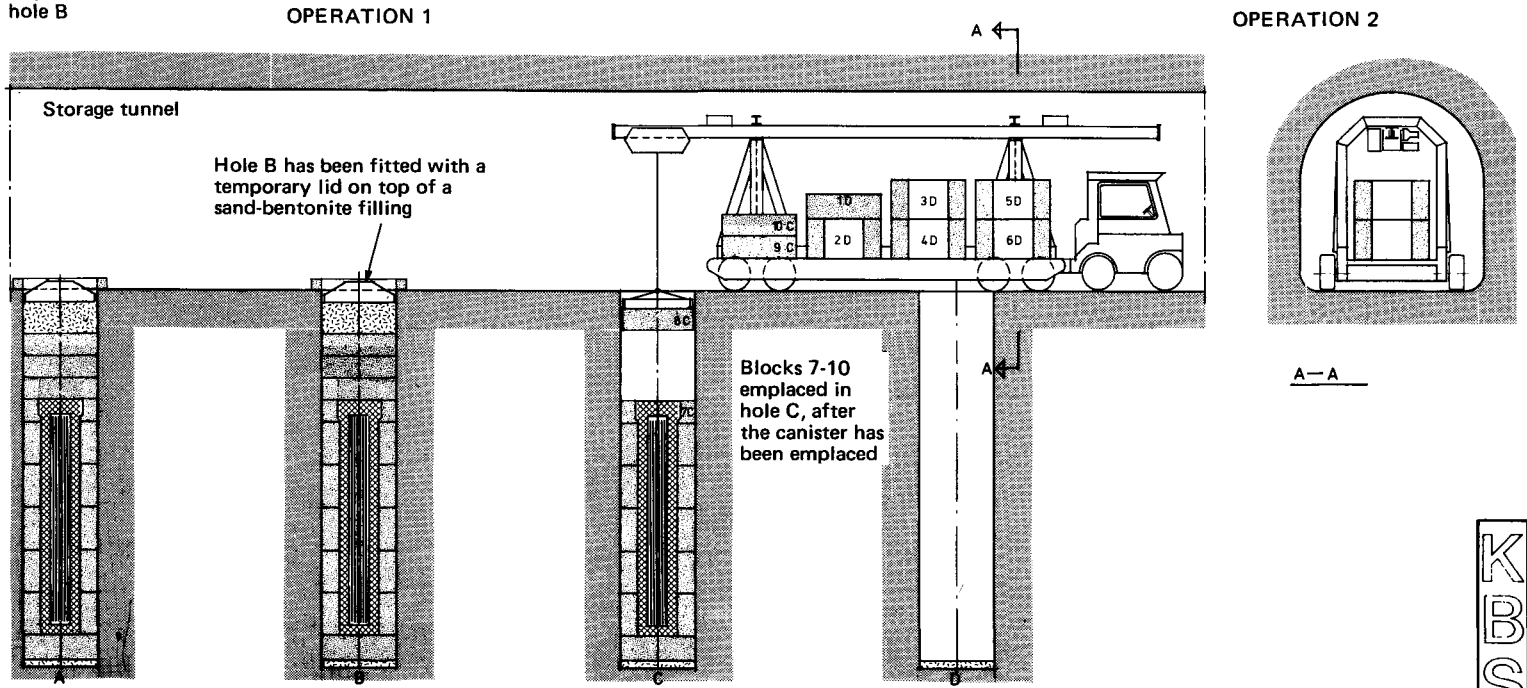

OPERATION 3

A—A

KBS

VBB VIAK AB STOCKHOLM
VATTENBYGGNADSBYRAN
CONSULTING ENGINEERS AND ARCHITECTS

FINAL REPOSITORY
DIRECT DISPOSAL

Emplacement of bentonite blocks in storage holes

DRAWING 14

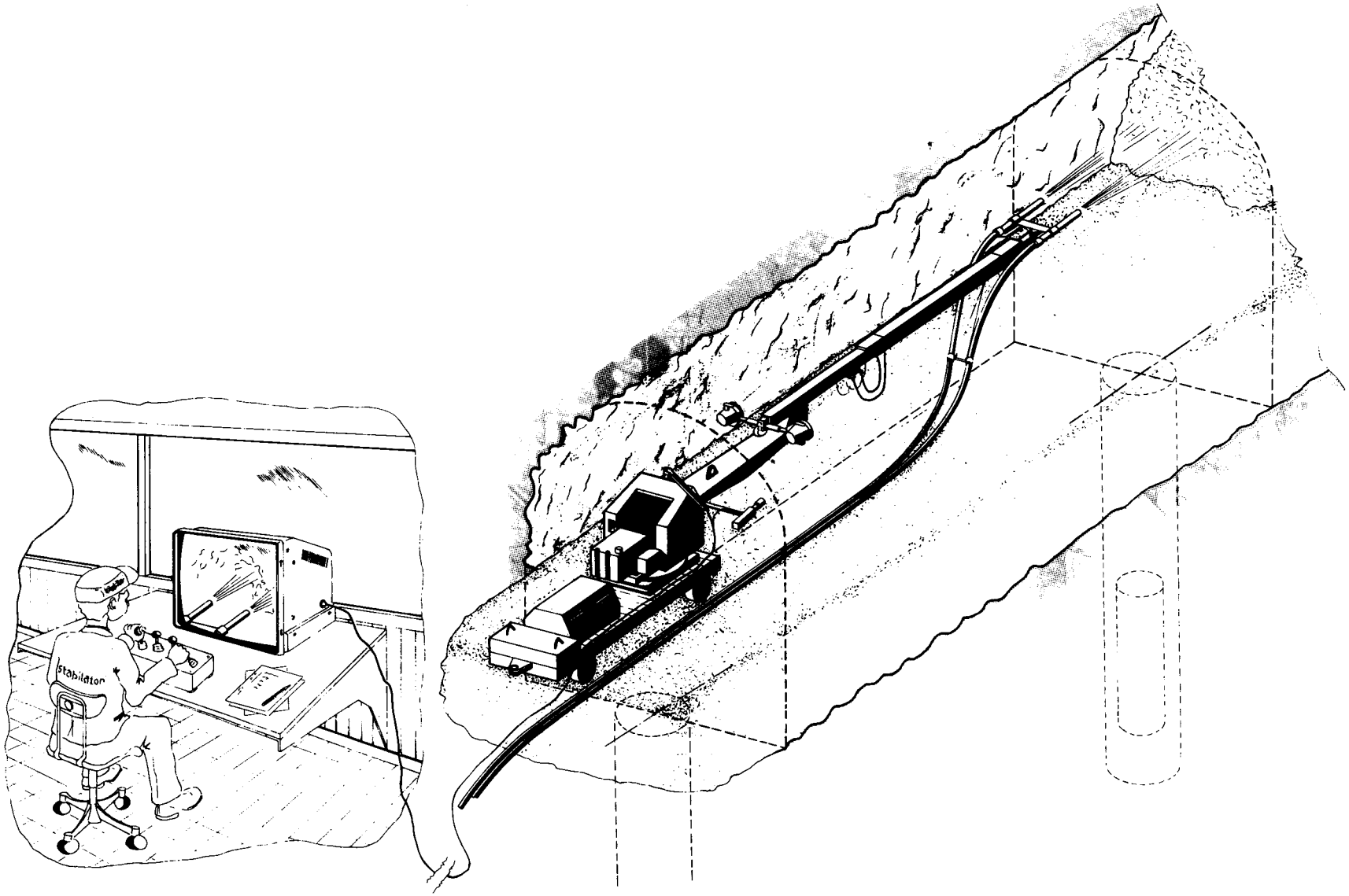

Spraying of buffer material

KBS

VBB VATTENBYGGNADSBYRÅN CONSULTING ENGINEERS AND ARCHITECTS

FINAL REPOSITORY
DIRECT DISPOSAL

Sealing of tunnels

DRAWING 15

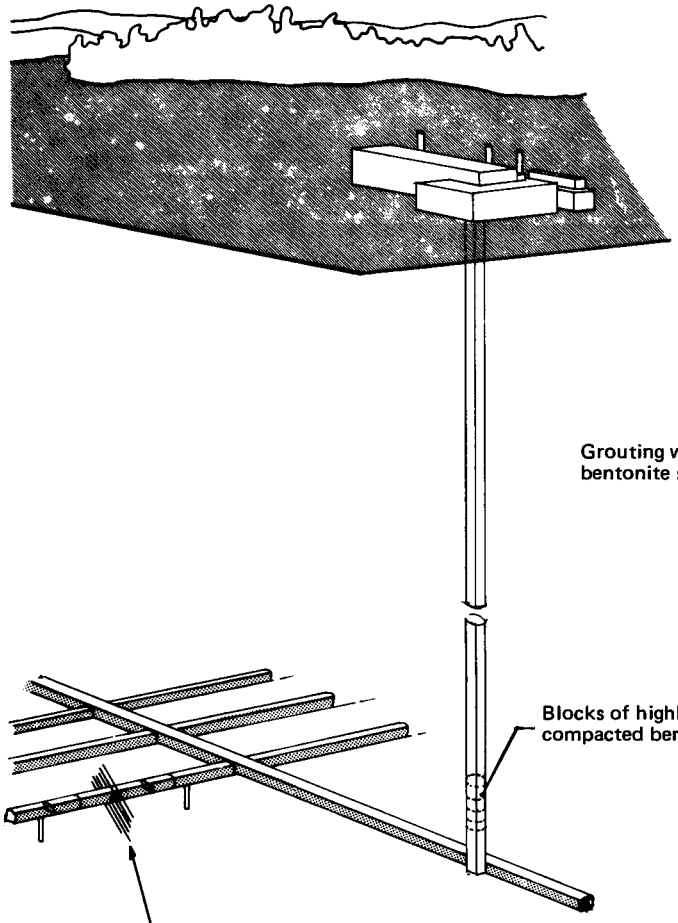

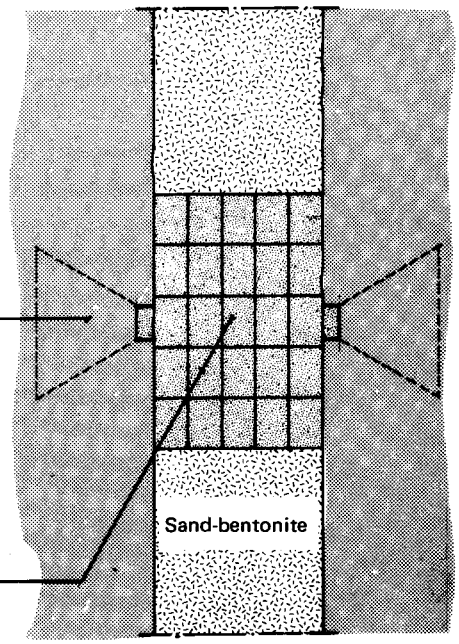

SHAFT

Blocks of highly
compacted bentonite

Local fracture-zone

Grouting with
bentonite suspension

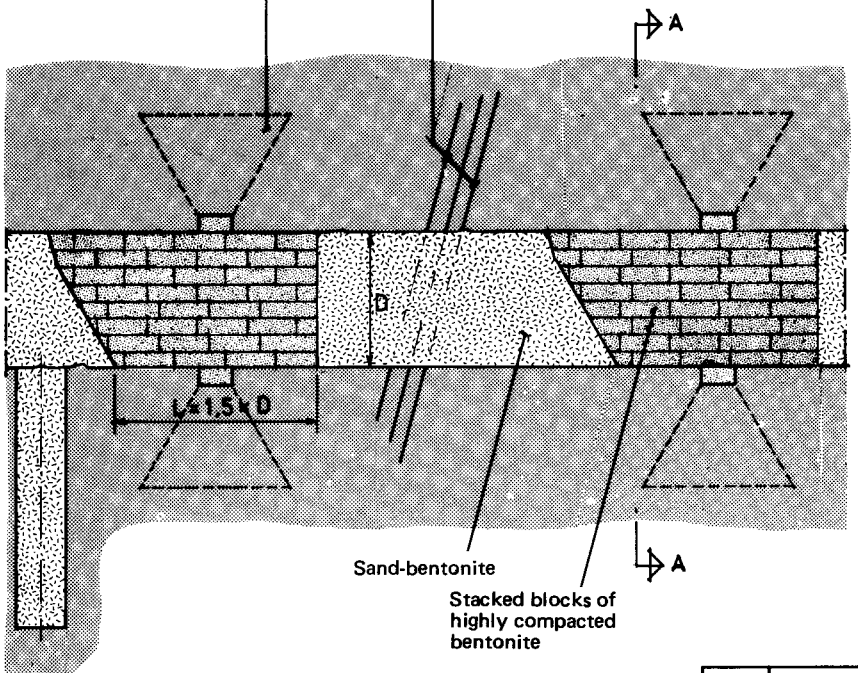

Storage tunnel

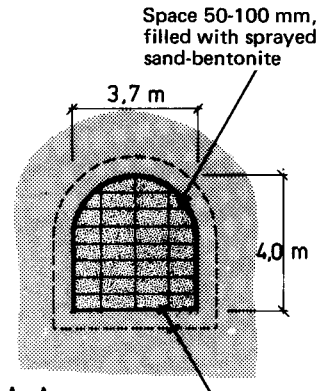

A-A

Slit, depth 0.5-1.0 m and
width about 1 m, made by
seam drilling and rock
splitting or jet burning for
minimal disturbance of
surrounding rock.

KBS

VBB VATTENBYGGNADSBYRÅN
CONSULTING ENGINEERS AND ARCHITECTS

**FINAL REPOSITORY
DIRECT DISPOSAL**

**Sealing of zone around
shafts and tunnels**

DRAWING 16

3 GEOLOGY

3.1 BACKGROUND

The general background for the geological and hydrogeological studies presented in the KBS report for vitrified waste from reprocessing applies in all essential respects to the alternative method of final storage of unreprocessed spent nuclear fuel as well. Since the first report was compiled, the Geological Survey of Sweden, SGU, has concluded the work programme for which is was commissioned by KBS. The present report is therefore based on a more comprehensive body of background material than the previous one.

The locations of the sites where the field work has been done are shown in fig. 3-1.

Certain results concerning rock stresses, permeability and thermal conductivity of the rock and groundwater data are available from tests conducted in the abandoned mine at Stripa. Preparations for the large-scale heating tests, carried out in collaboration with the Lawrence Berkeley Laboratory, are largely completed and heating was commenced on June 1, 1978. The results will be reported as they come in up to the latter part of 1979.

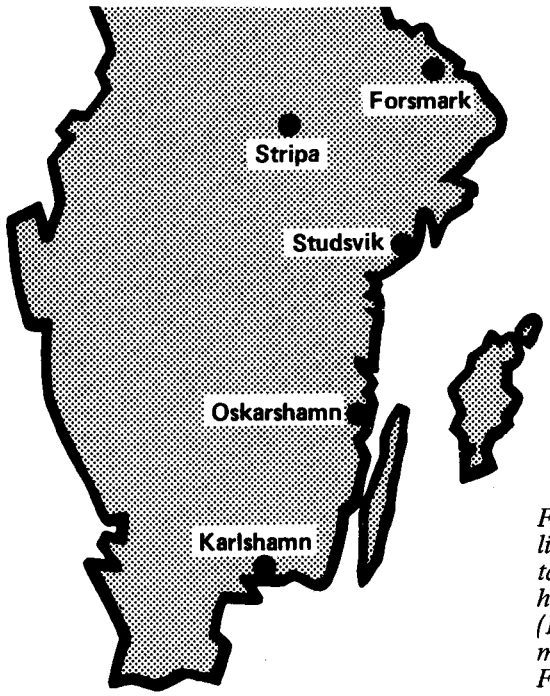

Figure 3-1. Map showing study areas. Test drillings to a depth of about 500 metres were undertaken at Karlshamn (Sternö), north of Oskarshamn (Kråkemåla and Ävrö), and at Forsmark (Finnsjö Lake and Forsmark). The KBS experimental station is located in the Stripa mine. Field studies were carried out at Studsvik.

Tracer tests in fractured rock at Studsvik have been completed and a second stage has been ordered by PRAV (the National Council for Radioactive Waste Management).

Mathematical analysis of groundwater movements has continued and a three-dimensional model has been developed.

The geochemical conditions which may be of importance for the long-term safety of a rock repository for spent nuclear fuel have been further studied, and the results are presented in a following section.

3.2 BEDROCK CONDITIONS

3.2.1 Review of geological evolution

Most of the Swedish bedrock is a part of the so-called Baltic Shield and is composed of crystalline rock which acquired its essential characteristics and structural features a very long time ago. This took place over a period of evolution which lasted more than thousand million years and which included the deposition of sedimentary rocks, widespread volcanism, profound orogeny, regional emplacement of granitic rocks and extensive fracturing. Numerous age determinations of the bedrock in southeastern Sweden are reported by Åberg /3-1/.

The final stage in the formation of the Swedish part of the shield is usually set at the time for the crystallization of the Bohus granite, about 900 million years ago. The mountain belts of the shield were completely eroded more than 600 million years ago. At about this time, the land subsided below sea level, and new sedimentary rocks were deposited on a nearly level surface. The new deposits are preserved today as paleozooic strata in various parts of Sweden. Their undeformed stratification and the large extent of the still-preserved peneplain upon which they were deposited shows that the precambrian crystalline basement has remained almost unchanged over the past 600 million years and has only been subjected to local disturbances.

While conditions in the crystalline shield of Sweden and Finland have been almost unchanged for the past 600 million years, this has not been the case in surrounding areas. The rocks of the Caledonian mountain belt of Scandinavia west of the Precambrian shield were formed or transformed up to around 380 million years ago and an intensive orogeny of somewhat different nature occurred in central Europe up to around 200 million years ago. The formation of the Alps reached a peak about 30 million years ago, and bedrock movements and volcanism in the North Atlantic culminated somewhat earlier. In the Mediterranean area, south of the Alps, this evolution is still continuing today, and is expressed by areas of uplift and subsidence as well as volcanism and earthquakes. Europe north of the Alps, however, obviously exhibits progressing stabilization after the formation of the Alps, as marked by reduced earthquake frequency and extinct volcanism. The North Atlantic area also exhibits such stabilization and its volcanic activity, which previously extended from Ireland to Jan Mayen, Spitzbergen and Greenland, is today limited to Iceland.

Thus, northern Europe has been undergoing a geological development over the past 25 million years characterized by increasing stability. Reports on various features of the geological development of northern Europe have recently been published /3-2/.

The Precambrian Baltic Shield has comprised a stable area even during the most violent phases in the evolution of the surrounding areas. This is far from unique. On the contrary, similar core areas of resistant crystalline rock comprise a basic and recurrent feature in the structure of the continents. Their almost undisturbed cover of stratified deposits and low earthquake activity show that they reached a sort of equilibrium a long time ago, while surrounding regions were still subjected to severe deformations. The latter applies in particular to the mobile border zones and marked rift valleys of the continents, where severe earthquakes, recent volcanism and large active fault lines are conspicuous signs of long-term and profound instability. California and the Central African Rift Valley are good examples of such conditions. Obviously, the outlook for future stability is quite different in such mobile zones than in the crystalline core areas.

Rock movements in the Swedish Precambrian shield can thus be shown to have been of a very limited extent over the past 600 million years, and have consisted for the most part of local fault movements. In addition, more regional movements have also occurred at certain times, changing the elevation of the land. This has occurred repeatedly over the past 2 million years in response to the loading of on earth's crust by thick continental glaciers during a series of glaciations. Similar level changes occurred for other reasons some 30 million years ago, at roughly the same time as the formation of the Alps and major bedrock movements in the North Atlantic.

The above review shows that the Swedish Precambrian bedrock has constituted a markedly stable area for a very long period of time. The possibility of profound deformation which could lead to deep weathering and erosion of the bedrock or regional changes in the slope of the land can therefore be excluded for the next few million years. The possibility of local fault movements, and more extensive level changes in connection with a future ice age cannot, however, be excluded. How such deformations could affect a rock repository is therefore dealt with in greater detail in the following section.

3.2.2 Fracture movements in the bedrock

The fractures in the crystalline bedrock are responsible for the permeability of the rock and fault movements might, at least theoretically, cause damage to the waste canisters. The degree of fracturing of the rock, and its relationship to permeability has therefore been studied in the test areas investigated by KBS /3-3 and 3-4/. The strength of the rock has also been determined /3-5/. Furthermore, general regional surveys of major fracture lines have been carried out for the Swedish parts of the Baltic Shield and on the bottom of the sea off southeastern Sweden /3-6, 3-7 and 3-8/. A rock mechanical analysis of the deformation in fractured bedrock has been carried out /3-9/, as have geotechnical studies of the effects of possible future rock movements on

a rock repository /3-10/. A review and evaluation of available measurements of rock stresses in Scandinavia and Finland has been carried out /3-11/. The distribution of the fracture movements in time and their geological background has also been illuminated /3-12/.

The rock stress measurements which have been reported from Fennoscandia show that strong regional and local variations exist. Aside from isolated exceptions, however, adequate safety margins exist against rock failure caused by the internal stresses in the rock at the depths in question /3-11/. This conclusion is also in full agreement with practical experience from extensive mining operations /3-13/.

Probability calculations have been carried out of the risk that a rock repository will be hit by a fault during a given period of time /3-14/. The probability that a circular rock repository with a surface area of 1 km^2 will be hit by a new fault is reported to be $5 \cdot 10^{-6}$ in 10 000 years. This is based on the assumption that the length-distribution of linear structures observed in satellite pictures of Sweden /3-15/ corresponds to the length-distribution of existing faults. It is further assumed that the formation of new faults has taken place at a constant rate over the past 1 500 million years, and that newly-formed faults appear randomly, i.e. independently of regional differences and the zones of weakness which already exist in the bedrock. It is, however, uncertain whether these assumptions are valid.

Recently, de Marsily et al. /3-16/ pointed out that the fault movements in the bedrock cannot be treated as merely random processes. They have instead indicated that it is possible to make forecasts, based on historical and geological information, for areas in which movements are taking place. The same principle can also be applied to areas where present movements are so small or infrequent that they are normally not noted. This is based on the fact that the present fractures now present in the bedrock at any given site comprise a local record of all earlier events of fracturing.

A study of the fracturing of the bedrock shows that both the fractures and the size of the fault movements are systematically distributed in time and space. An example of the geographic distribution is given in figure 3-2 (cf. also /3-17/), which shows the regular pattern of fracture-lines in the bedrock around Oskarshamn. Here, faults and fracture zones, where the rock is crushed and weakened by closely set fissures, form valleys several miles in length. These valleys enclose, in a network-like pattern, less fractured bedrock blocks which can reach a size of one or more square kilometres. Similar fracture patterns are common in the Swedish part of the Baltic Shield.

There is a close association between the fracture content of the bedrock and its hydraulic conductivity. The conductivity of a given volume of rock formation constitutes the sum of the conductivities of all the interconnected fractures present there. Since these fissures in the shield are the results of fracturing over some one thousand million years, the hydraulic conductivity of the rock at each point would increase over one million years by approximately one-thousandth of its present value if fracturing is proceeding at an unchanged pace. Even if fracturing were

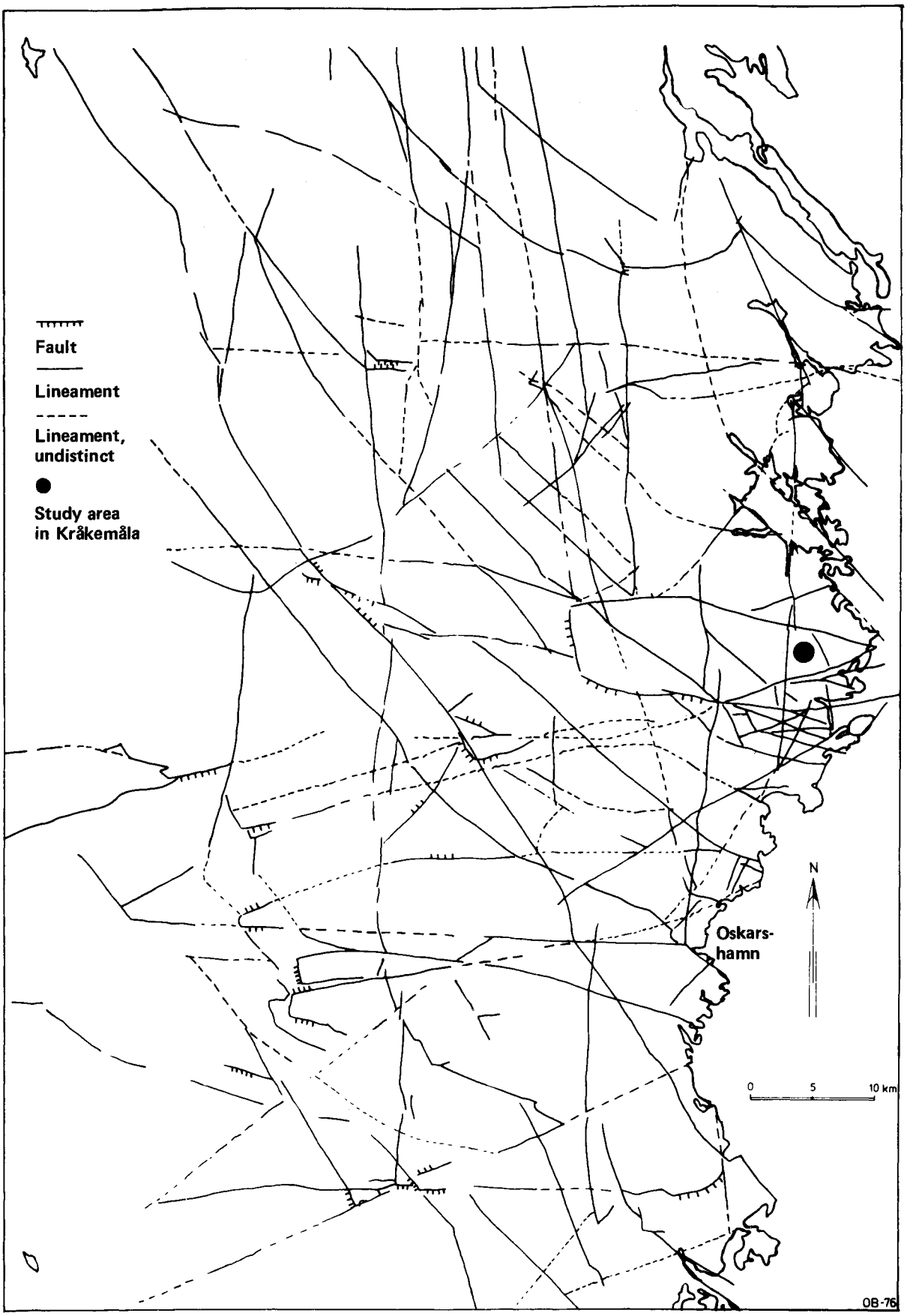

Figure 3-2. Map of the fracture pattern in the Oskarshamn region. (Bedrock Bureau, Geological Survey of Sweden).

one hundred times faster than the average up to the present, the permeability of the rock at each site would only increase by one-tenth of its present value in one million years. In actuality, the zones of weakness in different directions already present in the shield enable new stresses to be released without the formation of new fractures. This is confirmed both by a rock mechanical analysis /3-9/ and by independent field studies, which show that later movements have largely followed older lines of weakness /3-6, 2-7, 3-18 and 3-19/. Already existing planes of weakness in the bedrock therefore comprise a mechanical protection against fracturing in the intervening, less fractured blocks. This leads to the conclusion that future fracture movements over a very long period of time will not appreciably alter the hydraulic conductivity of the rock around a rock repository.

A similar line of reasoning can be applied to the magnitude of the fault movements. Observations in this respect are generally limited to the total sum of the resultant displacement. Often, only one component in a given direction can be measured. Individual steps in such movements and changes in direction can only be studied in special cases. Despite this, it can be shown that the displacements are also clearly regular in their distribution, and that they do not comprise a risk factor for terminal waste storage. The situation is illustrated by figure 3-3, which is based on the following observations.

The largest fault movement which was documented in the KBS survey was at the Svedala fault in Skåne in Southern Sweden /3-7/. The vertical displacement over the past 570 million years there amounts to a total of about 2 000 m. In this connection the province of Skåne marks the movement-prone zone of transition between the Baltic Shield and the younger bedrock of Europe. Within the shield the displacements are generally considerably smaller.

This applies particularly to nearly flat and horizontal areas, where the land has escaped deformation and erosion for a very long period of time, so-called "peneplains", cf. /3-20/. In a fault at Gåvastbo, east of Finnsjö Lake, west of Forsmark, the total vertical displacement during the same period of time has amounted to about 15 m. In a fault at Lake Götemaren, north of Oskarshamn, it amounts to about 30 m.

In Skåne, it has been found that the large displacements there are the result of repeated rock movements which, with some interruptions, have taken place over the past 570 million years /3-7/. The fault movements in the bedrock have consequently displayed a uniform systematic distribution over this long period of time, so that the large displacements have consistently occurred at the same fault lines, while most faults in the shield during the same period of time have been characterized by very small displacements.

It is, however, the fracture movements within the bedrock blocks between the faults which are decisive for a waste storage. During the same span of time, these movements have been extremely small. In the KBS study area at Finnsjö Lake, for example, a maximum displacement of 30 cm was found, and at Karlshamn 2 cm. These figures represent the total displacement at individual fractures over a period of more than 1 400 million years, which gives aver-

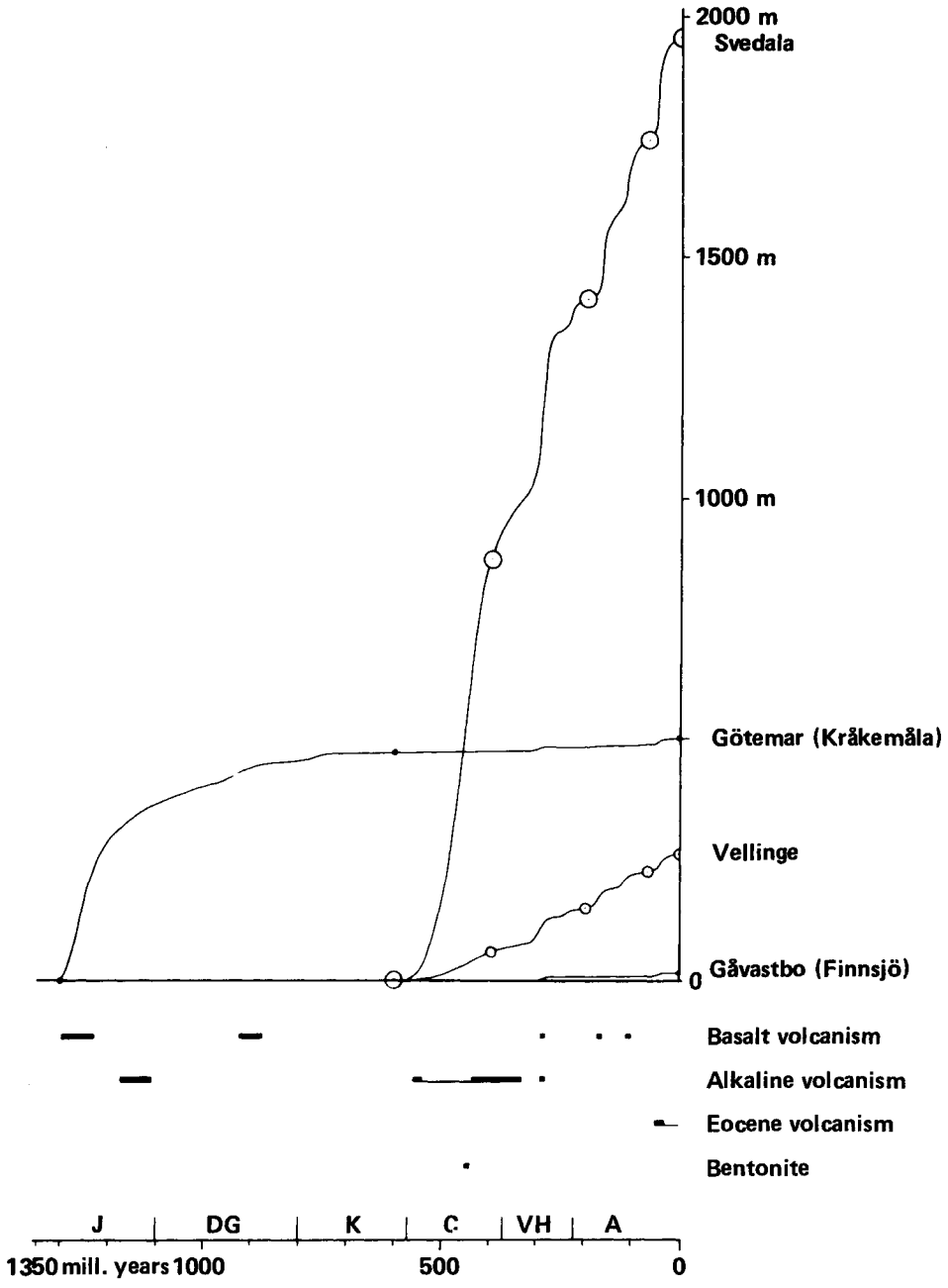

Figure 3-3. Diagram of fault movements, deformation periods and volcanism over the past 1 350 million years. The diagram shows the elevation in metres of the upthrown rock block in relation to the subsided block at four studied faults. The curves connecting the points were drawn on the basis of the peneplain formation of the Precambrian rock (flat portions), volcanism (deep portions) and the character and thickness of the sedimentary bedrock. The values on the flatter portions of the curves for the elevations of the faults in Svedala and Vellinge are approximate between the measured points. The large movements between 400 and 600 million years ago in Skåne (Svedala and Vellinge) have only insignificant counterparts within the Precambrian rock area. Only the Götemar fault can be followed back farther than 600 million years. Bentonite indicates extensive volcanism in the area of the Scandinavian mountain chain (the Caledonians). Eocene volcanism took place outside of Scandinavia. The thickness of the vertical axis corresponds to the next 4 million years.

The following deformation periods are marked on the time axis:

J	*= Jotnian*	*C*	*= Caledonian*
DG	*= Dalsland–Grenville*	*VH*	*= Variscan–Hercynian*
K	*= Katanga*	*A*	*= Alpine*

age displacements of 0.3 and 0.02 mm per million years, respectively. This can be taken as a measure of the tendency towards shearing movements within these blocks, and may as such be compared to the average displacement of around 3.5 m per million years at Svedala.

The fissure at Finnsjö Lake with a displacement of 30 cm was so large and obvious that it would unquestionably be observed, and thereby avoided, prior to drilling a storage hole for high-level waste. The smaller crack at Karlshamn would also undoubtedly be defected by routine mapping of rock fractures in a repository.

A discussion of the probability of a fracture movement of a given magnitude occurring may nevertheless be of interest. It can be based on the conservative assumption that fractures of the size studied at Karlshamn would not be avoided, in which case the site distribution of the displacements observed there applies. It is further conservatively assumed that each displacement has taken place in its entirety in a single movement, even though many observations indicate that displacements are generally the result of repeated smaller movements.

The probability P_d that a displacement larger than d mm will occur within a bedrock section 1 metre in length in a million years is:

$$P_d = \frac{p}{S \times t}, \text{ where}$$

- p is the portion of the total number of observed fractures where the displacement exceeded d mm;
- S is the average distance between fractures;
- t is the age (millions of years) of the rock element which has been subjected to displacement.

Fracture studies at Karlshamn /3-12, p. 47/ show that the probability of a displacement diminishes radpidly with the size of the displacement. Total displacements of more than 1 mm exhibit a nearly lognormal probability distribution, see figure 3-4. For example, if d = 30 mm, p $\sim$ 0.1%. For t = 1 400, which is the age of the pegmatite bodies which have been subjected to fracture movements at Karlshamn, and S = 1 m, $P_{30\ mm} = 10^{-3} : 1\ 400$. With a waste canister length of 5 metres, and a rock repository which can hold 10 000 canisters, an average of one canister every 28 million years would therefore be expected to be hit by a fracture movement in excess of 3 cm. This presumes that each fracture movement only hits one canister. This is a reasonable assumption with regard to the small fracture lengths observed at Karlshamn. With larger total displacements, however, fracture length can also be expected to increase, so that the same fracture could strike several canisters. At the same time, however, as was mentioned above, the probability that such a displacement will occur at all declines very sharply.

So far, it has been assumed that fracture activity has remained unchanged through the ages, but this is not the case. A number of studies have established that the fracture pattern in the shield was formed at a very early stage, for the most part more than 900 million years ago /3-19, 3-21 and 3-22/. This is linked to the fact that deformation of the bedrock was much more extensive in earlier phases. For example, approximately 95% of the total

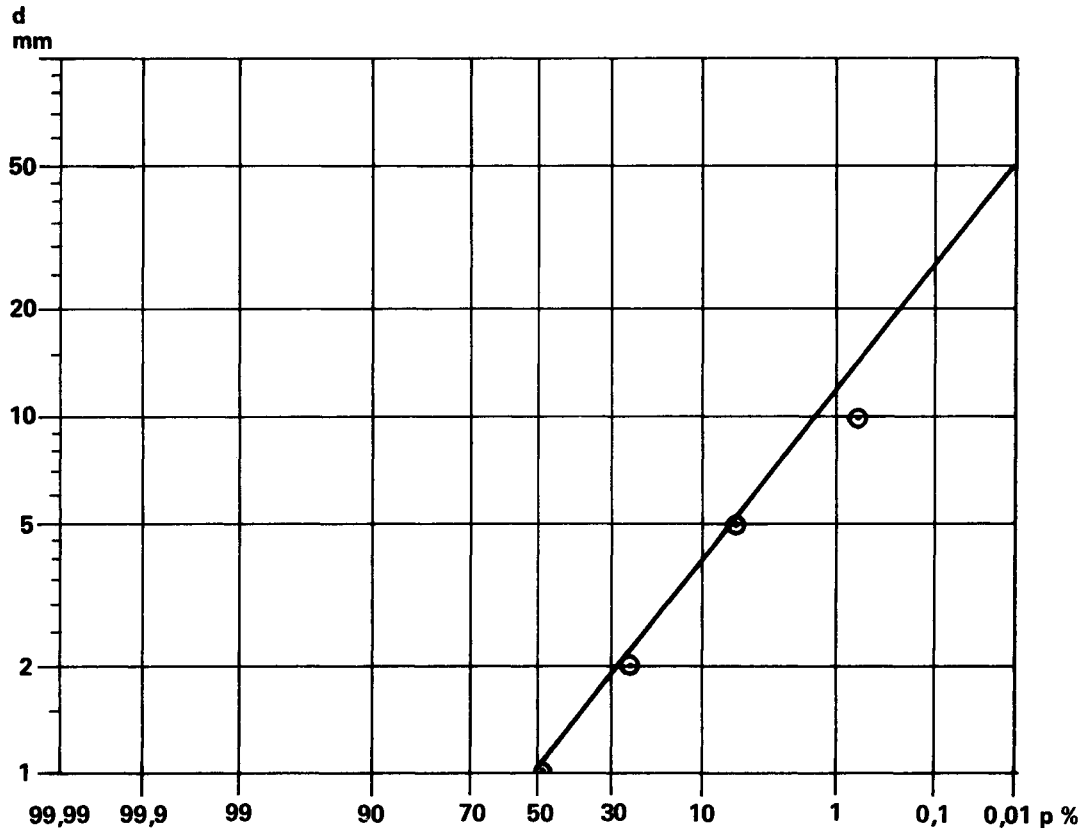

Figure 3-4. Plot of measured displacements, d, on lognormal probability paper. Based on 114 observations exhibiting displacements ⩾1 mm within the study area at Karlshamn.

displacement at the Götemar fault occurred more than 600 million years ago. Geological factors also seem to indicate that the fracture movements which have occurred over the past 300 million years mainly took place in connection with volcanic activity around 290, 170 and 110 million years ago, and in connection with extensive rock movements in Northern Europe and the North Atlantic 40-25 million years ago. Since this time, geological activity in these areas has clearly been abating. Signs of fracture movements during and after the ice age are rare or insignificant in Sweden, and major movements have only been detected locally in the provinces of Norrbotten, Västerbotten, Dalarna and possibly Skåne. The Baltic Shield is thus currently in a very tranquil period, from a geological point of view.

The high age of the fracture pattern, its multi-directional development and the marked decrease in deformation with time all indicate that both the formation of new faults and the actual fracture movements have greatly decreased with time. As a result, their effects on a rock repository should be considerably less than has been indicated above.

The above discussion deals only with the natural fracture movement in the bedrock. Questions concerning the stresses which arise in connection with the construction of the repository and the heat generated by the waste are dealt with in /3-23 and -24/. It is shown there that the low stresses inherent in the KBS design would not lead to serious fracturing. The extent of any new-

ly-formed fractures will be greatly limited by the existing fractures in the rock and the rock reacting elastically.

3.2.3 Uplift and glaciation

The current uplift in Sweden has been studied on the basis of field observations /3-18/ and on the basis of gravitational data /3-25/. Despite differences in basic data and analytical technique, quite similar results have been obtained.

The uplift which followed the ice age reached its maximum on the coast of Ångermanland, where it reached a peak value of more than 800 metres. It mainly represents a rebound of the crust following its depression by the weight of the continental glacier. According to /3-25/, the land is still rebounding from the depression caused by the ice cap. According to /3-18/, this rebound ceased 2 000 - 3 000 years ago, and the current uplift has other causes. A return from an earlier uplift of Western Scandinavia and the concurrent subsidence of the Baltic Sea, which is discussed below could possibly explain this process.

The effects of fracturing and movements in the bedrock in connection with the uplift and a future ice age can be assessed on the basis of the present situation. The hydraulic conductivity in the test boreholes shows that hydraulically continuous fracturing is limited for the most part to the uppermost 100 or 200 m of the bedrock. Below this level, the rock consists of low-permeability blocks situated between larger fracture zones whose minerals, directions and depths show that they were not created in connection with the Pleistocene glaciations. The borehole at Karlshamn showed that the shallow, hydraulically continous fracturing at this site did not even reach a depth of 23 m. Deeper sections of the bedrock which have undergone the same depression and uplift have been found to possess very low hydraulic conductivity. This indicates that the uplift and the preceding depression did not affect the permeability of the bedrock other than at shallow depths. Furthermore, there have been a total of 10 to 20 Quaternary glaciations /3-26/, and the present state of the bedrock reflects the cumulative effects of all of these. This leads to the conclusion that one more glaciation would not appreciably increase the permeability of the bedrock at the depth of a repository. On the other hand, as has been particularly emphasized by Mörner /3-18/, there have been numerous observations of displacements and fracture movement in connection with the ice age which apparently are unrelated to the actual pattern of faults in the bedrock. Their depth is limited, especially in the flat areas which will be sought out for a final repository.

Owing to its weight, an ice cap will increase the load on a rock repository. An ice cap which is 3 km thick is equivalent in this respect to a rock cover about 1 000 m thick. A rock repository at a depth of 500 m will be loaded under such an ice cap as if it had instead been at a depth of 1 500 m. There is a large body of international experience from mining at this depth, and it has been found that extensive fracturing is prevented if the rock caverns are backfilled with a suitable load-bearing material. In the KBS proposal, the tunnels in the repository are filled with a mixture of bentonite and quartz sand, where the sand grains provide the necessary load-bearing structure. The storage holes are

filled with compacted bentonite. A special geotechnical study shows that the waste canisters will be situated in rock of virtually unchanged imperviousness /3-27/. In this context, it is worth bearing in mind that the rocks of the Baltic Shield have previously been subjected to much higher pressures and temperatures for millions of years than those which could occur over the next few million years.

Some 30 million years ago, crustal movements occurred which gave rise to more lasting deformations than those of the Pleistocene. In connection with large bedrock movements in the Alps and the North Atlantic, western Scandinavia was uplifted, giving rise to the steep Atlantic coast of Norway. The Baltic Sea basin subsided. The uplift of the land surface which extends from the West coast of Sweden towards Gävle and further northward along the northern Baltic coast probably occurred at the same time. This uplift marks the western border of the Subcambrian peneplain. Deep weathering in some of the fracture zones in the shield, as well as fossile finds from this period, show that a considerably warmer and more humid climate prevailed then than now. Weathering, erosion and groundwater circulation at this time seem to have reached their greatest depths in the shield. This has given us examples of what can happen in extreme cases in our type of crystalline bedrock. However, these fracture movements and the weathering of these fracture zones are entirely local features /3-28 and 3-29/ and no traces of them have been detected in most of the volumes of bedrock which have thus far been investigated in mines, tunnels and drill cores.

3.2.4 Earthquakes

The effects of the types of earthquakes which occur in Japan on rock tunnels have recently been studied by Dowding /3-30/ and Yamahara et al. /3-31/. Even in the case of very large earthquakes, the maximum temporary additional stress locally in the rock is calculated to be only 3.0 MPa. The risk of damage to a backfilled rock repository under Swedish conditions is therefore negligible.

Earthquakes are rare and of low magnitude in Sweden. Since 1891, systematic records have been kept on earthquakes /3-32/. Since 1951, earthquakes are recorded by means of sensitive instruments which can detect quakes at sea and in uninhabited regions as well. A review of known observations up to 1972 was published in a study by Kulhanek and Wahlström /3-33/. A map of Swedish earthquakes during the period 1951-1976, with comments and other material, was obtained from Båth /3-34/.

Earthquake frequency exhibits wide variation during the observation period. The geographical distribution of earthquakes in Sweden and adjoining areas has, however, remained relatively unchanged.

Southeastern Sweden exhibits extremely few earthquakes. On the map provided by Båth, only two earthquakes, both near the Roxen - Motala fault zone, are shown. Most of the quakes are instead located in a belt extending from the southwest coast of Sweden, across the Lake Vänern region - where they are relatively numerous - towards Gävle and then along the coast of the Gulf of

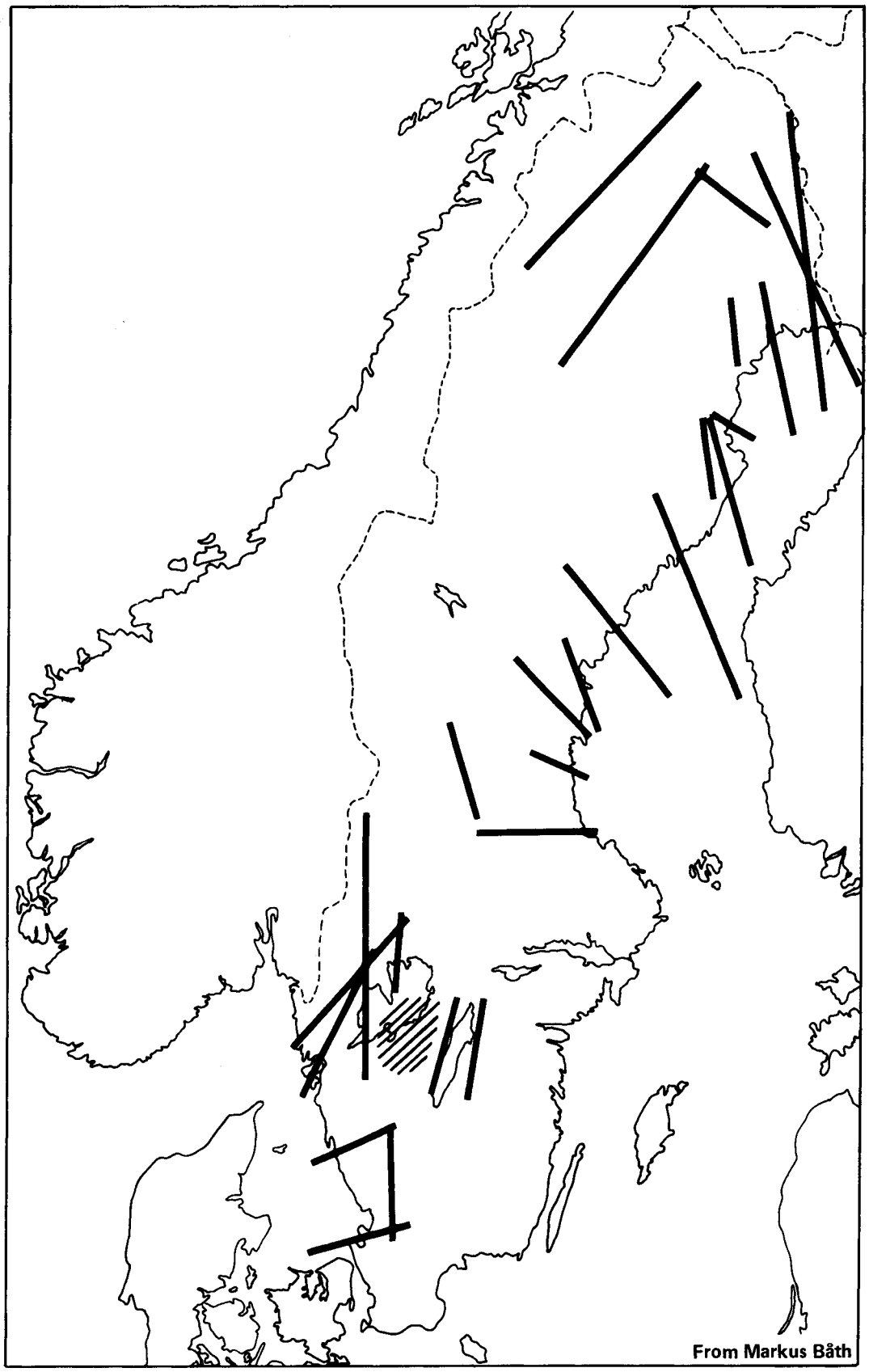

Figure 3-5. 95 % of all quakes which were recorded in Sweden during the period 1951–1976 are located within 26 linear zones plus a nearly circular area in the province of Västergötland.

Bothnia. From the northernmost part of the Gulf of Bothnia, the belt swings towards the northwest and then turns towards the southwest in the Norwegian sea and runs along the coast of Norway, thereby encircling central Scandinavia /3-14/. The distribution of quakes is thus related to bedrock movements on and off the Norwegian coast, and in Sweden a connection can be seen with the fault lines in the Vänern-Vättern region, the western boundary of the Subcambrian peneplain and the areas of recent rock movement in Skåne, Västerbotten and Norrbotten. This would indicate - as was maintained by Kvale /3-35/ - that the Scandinavian earthquakes are related to bedrock movements which are independent of the ice age. From this, it follows that the current distribution of quakes is the manifestation of more far-reaching geological processes and will probably persist for a very long period of time.

The local limitation of the effects of earthquakes has been confirmed in a striking manner by new findings concerning the distribution of earthquakes in Sweden. Professor M Båth has shown (Deep-seated fracture zones in the Swedish crust, manuscript 1978) that 95% of all quakes which were recorded during the period 1951-1976 are located within 26 distinct linear zones, plus a nearly circular area in the province of Västergötland, while intervening areas are virtually completely quake-free. See figure 3-5. The quakes occur at an average depth of 15-16 km. Many of the seismically active zones coincide roughly with present river valleys. Concerning these, it is known through other studies that they largely follow fractured zones in the bedrock, and that the valleys were eroded in many cases around 25 million years ago. These observations thus support the conclusion that recent fracture movements in the Swedish bedrock, as well as earlier ones and movements which could conceivably occur during the waste storage period, are closely associated with pronounced zones of movement. Future rock movements therefore present no threat to an absolutely safe storage outside such zones.

3.3 TEST AREAS

3.3.1 Scope of the work

The work in the different test areas has included the following main pursuits:

- Geophysical measurements, mapping of outcrops and fractures drilling, evaluation of drill cores, borehole logging and TV examination of boreholes.
- Water injection tests and calculations, water sampling for chemical analysis and age determination.
- Field tests with tracers in fissured rock before and after grouting, mainly at Studsvik.

The total length of cored boreholes is more than 5 000 m, distributed among five test areas, three of which have been selected for closer study, namely Sternö near Karlshamn, Kråkemåla near Oskarshamn and Finnsjö Lake near Forsmark. The Precambrian bedrock at these sites is of different types, and the choice of the study areas reflects the wish to elucidate the characteristics of different geological settings.

The results from the field studies have been presented in a number of technical reports /3-3, 3-4, 3-36, 3-37 and 3-38/.

Only brief summaries with an emphasis on results which complement the previous report /3-12/ are provided in the following sections. Additional data have been obtained from similar studies at Stripa. The results from these studies are presented in a special series of reports, as well as in /3-5, 3-38 and 3-39/.

3.3.2 Results

Karlshamn area

Studies in the Karlshamn area have been conducted on the Sternö peninsula, within the grounds of the oil-fired power plant there. Of the different test areas, this is the geologically best known. It is located in that part of Western Blekinge where the regional relationships between bedrock structures and groundwater conditions have been studied most thoroughly in Sweden, and it is the only one of the KBS test areas where data are also available from existing rock caverns, see figure 3-6. The results of the geolocical surveys have been reported in /3-41/.

The study area is composed of a grey gneiss, Blekinge coastal gneiss. It has a low fracture and groundwater content. The directions of the fractures vary and exhibit no pronounced main directions. These factors are also reflected in the statistics for the rock caverns in the gneiss which are used for oil storage. Reported data on water leakage into the rock caverns exhibit low values. The need for reinforcement following blasting has been remarkably low. The hydraulic conductivity of the surrounding rock can be calculated from the leakage data. Values around or lower than 10^{-9} m/s are obtained, which is lower than normal for rock caverns at a depth of 30-50 m.

A core drilling within the area to a depth of 500 m reveals unchanged good rock conditions at greater depth.

Water injection testing in the borehole with a single packer revealed a conductivity for the section 23-500 m equal to or less than 2×10^{-12} m/s, which was the measuring limit for the equipment which was used. Measurements over two-metre sections between two packers revealed values for most of the hole equal to or less than 4×10^{-10} m/s, which was the measuring limit for this method. In the deepest part of the hole, however, somewhat higher values were obtained, between 10^{-9} and 10^{-8} m/s. These values are not consistent with the results of the much more reliable single-packer test and probably stem from the fact that small quantities of water leaked past the seals.

A special study within the test area /3-12/ has shown that dis placements along existing fractures have been small for a very long period of time. Existing fractures are largely mineralfilled. One fracture zone filled with swelling clay minerals has been found north of the test area. No significant crush zones have been found. Rock mechanical tests /3-5/ show that the rock possesses high strength.

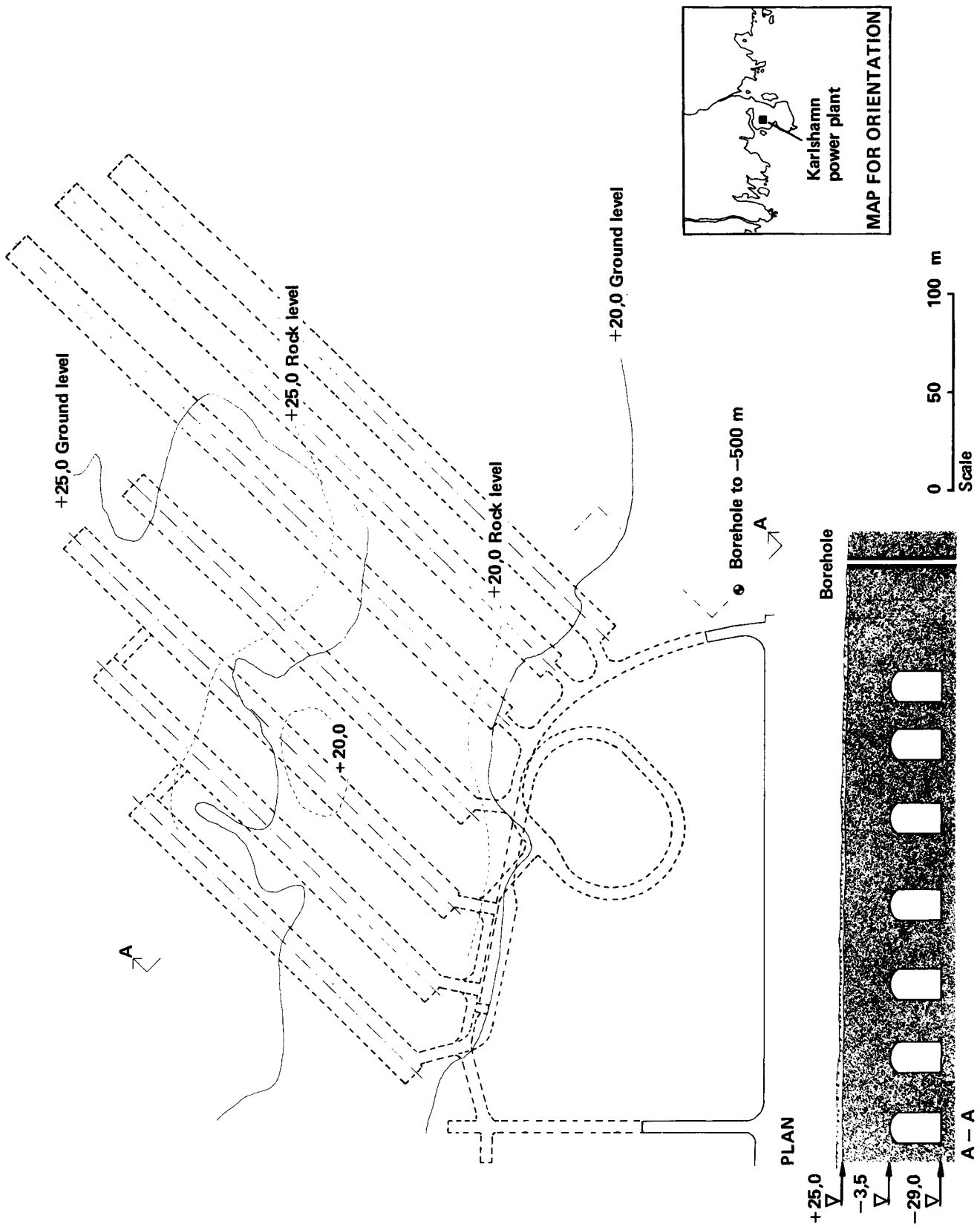

Figure 3-6. Rock caverns for storage of oil at the Karlshamn power plant.

In summary, the study area at Karlshamn is composed of a type of rock which is poor in groundwater and fractures regionally. Within the test area and in its immediate vicinity, there are a number of rock caverns which show that the bedrock, even at relatively shallow depths, is distinguished by low permeability and good stability. Their combined volume is more than one million m^3, i.e. closely comparable to the total volume of the rock repository proposed by KBS, which is estimated to be one million m^3. Many of these rock caverns are used for the storage of heavy oil and are heated to a temperature which is roughly equal to the estimated temperature of the final repository, without their stability or imperviousness being reduced. Finally, test drilling shows that these good rock conditions extend down to a depth of 500 m and that the drilled section is free in its entirety from water-bearing fracture zones and is characterized by extremely low water conductivity.

Finnsjö area

The Finnsjö area is located 16 km west-southwest of the Forsmark nuclear power station in Northern Uppland county. Geological and geophysical studies have been carried out here. The rock conditions have been studied at depth in three cored boreholes, one vertical to 500 m and two at 50^{o} inclination to between 500 and 550 m vertical depth. The area is composed of Early granite, which is a relatively uniform, weakly gneissic rock of granodioritic composition. In the test area, no remnants of leptite have been found in this rock, and a survey on the ground did not reveal any magnetic anomalies which means that the presence of magnetic iron ores can be excluded. The granodiorite is rather strongly fractured. However, the fractures are for the most part irregular, with varying directions, and largely mineral-filled. Low contents of swelling clay minerals are sometimes found. Towards the east, the area is bounded by a fault which is accompanied by a 300 m wide belt with heavier fracturing. In a borehole here, substantial sections of an evenly-grained granite have been found. The central parts of the area, on the other hand, are characterized by large blocks of little fractured bedrock with surface areas of up to 100 000 m^2. Fracture zones, some filled with crushed material, are found between these blocks. Sections several hundred metres in length with conductivities of less than 10^{-9} m/s, interrupted by a few zones with higher values, are found in the boreholes. The groundwater flow in large volumes of rock at a depth of 500 m can be calculated from the obtained data to be about 0.1 $1/m^2$ and year or less. Fracture zones with larger flows exist. Rock mechanical tests on borehole cores show very high strength /3-5/. The Finnsjö area represents a common type of bedrock in Sweden and has been selected as a reference area in some of the KBS studies.

Kråkemåla area

The Kråkemåla area is located 7.5 km north-northwest of the Oskarshamn nuclear power station at Simpevarp, between the Baltic Sea and Lake Götemaren. Geological and geophysical studies have been carried out here. Three cored boreholes have been drilled here, of which two are vertical to 500 and 600 m, respectively, and one is inclined at 50^{o} and drilled to a vertical depth of 550

m. The area is made up of a very uniform, undeformed granite, with a widely spaced but regular network of perpendicular, horizontal, straight and long fractures. The fractures are lined with the granite minerals and special fracture-filling minerals (quartz and chlorite). Pyrite also occurs in the fractures, sometimes abundantly, along with fluorspar. Smectite, i.e. swelling clay with a high capacity for cationexchange, which would retard the dispersal of certain waste elements, occurs in minor amounts. Drill cores from Kråkemåla show high strength, although considerably lower than that shown by the cores from Finnsjö Lake /3-5/.

Long sections with a water conductivity of less than 10^{-9} m/s are found in the boreholes between 300 and 500 metres depth. These sections are, however, surrounded by zones with higher conductivities and water contents. The groundwater flow in the less pervious sections is calculated to be about 0.15 $1/m^2$ and year or less. Much larger flows are found in existing fracture zones, which explains the fact that rock wells in this granite often produce plenty of water. The Götemar granite is characterized by a higher gamma activity than the preceding areas, and exhibits, according to G. Åkerblom of the Geological Survey of Sweden, average contents of 15 g uranium and 55 g thorium per tonne, as well as 4.8% potassium /3-42/, which may lead to certain radon problems during the construction phase.

Other areas

The two other areas in which drilling has been carried out are Ävrö, just north of Simpevarp, and Forsmark, approximately 3.5 km west of the Forsmark power station. Following pilot studies, both of these areas were judged to have less favourable rock conditions than the three preceding areas, so the studies were discontinued.

3.4 GROUNDWATER CONDITIONS

3.4.1 General

Radioactive waste which is stored deep down in the bedrock can in practice be dispersed only via the groundwater. The magnitude of the groundwater flow in the areas under consideration, as well as its velocity, retention time and pattern of movement, are therefore of great interest.

The movements of the groundwater and the dispersal of waste substances with the groundwater are dealt with in a number of technical reports /3-43 to -52/. These reports show that there are a number of different methods available today for modelling these processes. The properties of the bedrock are of fundamental importance for these calculations. Measurement data from the selected test areas were, however, not obtained until a late stage, when the boreholes had already been completed, the measurements had been carried out and the results had been obtained. A number of possible assumptions have therefore been considered in the models, and the calculations were evaluated as the measurement data became available.

3.4.2 Hydraulic conductivity of the bedrock

The hydraulic conductivity of the bedrock has been measured in a number of boreholes in 2 m (in some cases 3 m) long sections from the water table down. The results can be summarized as follows.

The upper part of the bedrock, which may extend down to a depth of anywhere between ten and a several hundred metres is often characterized by relatively high conductivity, owing to an extensive and coherent network of fissures. The upper sections of the bedrock correspond most closely to the model for fractured rock developed by Snow /3-53/ on the basis of a large number of drillings and permeability determinations down to a depth of 100 m. With increasing depth, the abundance of sections of very low conductivity increases, and there is a transition to conditions characterized by large volumes of predominantly impervious rock, interrupted by narrow water-bearing fracture zones. The lower sections therefore exhibit the conditions for crystalline rock at great depth described by Webster et al. /3-54 and 3-57/. It is shown in the cited studies that the groundwater movements in the network of fissures which exists in the upper part of the bedrock, as well as in the narrower fracture zones in the deeper parts, can be calculated with the use of well-known formulae for the movement of liquids in porous materials.

Most of the groundwater flow in the bedrock takes place in the upper part of the rock, where hydraulic conductivity is often between 10^{-5} and 10^{-7} m/s. Hydraulic communication in this section is generally good, which gives rise to a continuous and flat water table /see Larsson et al., 3-55/.

A smaller portion of the groundwater flows through the deeper part of the bedrock, where its movement is for the most part restricted to certain water-bearing zones. (Highly water-bearing zones have been found in Swedish mines down to a depth of 900 m.) Intervening sections of rock have a conductivity of less than 10^{-9} m/s. In gneiss at Karlshamn, a value of 2×10^{-12} m/s or less has been obtained /3-36/. 5×10^{-11} m/s has been measured in granite at Stripa /3-56/. Hydraulic connection between the individual fractures at great depths appears to be greatly limited, as is evidenced by the fact that no measurable water flow was found in sections where both the drill core and TV examination indicate the existence of fractures. Obviously, in order for water to actually flow, the fractures must be in hydraulic contact with each other, as is the case in the above-mentioned fracture zones. Differences in the chemical composition and age of the water, however, also indicate that hydraulic connection even between the water-bearing zones in the same boreholes can be limited at these depths.

In the deeper parts of the Kråkemåla 1, 2 and 3, Ävrö 1 and Finnsjö 1 and 2 boreholes, the frequency distribution of conductivity values is clearly divided in this manner into two parts. The values lie either around and above 10^{-7} m/s, or below the measurement limit at $2\text{-}10^{-9}$ or 4×10^{-10} m/s, respectively. The few sections which give values between 10^{-8} and 10^{-9} m/s are probably mixed cases, where one part of the section has the higher value and the remainder has the lower value. Below 400 m, leakage around the packers appears to have given rise in some cases to a more uniform distribution of the measurement values. A more homo-

geneous distribution of the permeability values is exhibited by the Finnsjö 3 borehole, which goes for the most part through more highly fissured rock, owing to the fact that it is situated near the Gåvastbo fault.

More than 1 500 conductivity determinations in 2- and 3-metre sections in all boreholes except for Finnsjö 3 appear therefore to confirm the postulate that the rock deep down in the Swedish bedrock is often divided into transmissive and non-transmissive rock /3-54,3-57/. The non-transmissive rock has conductivities below $4 \cdot 10^{-10}$ m/s, and probably also below $5 \cdot 10^{-11}$ m/s (Stripa) and $2 \cdot 10^{-12}$ m/s (Karlshamn). Transmissive rock possesses conductivities of more than 10^{-8} m/s, calculated over the length of the measured section. Most of the deep groundwater moves in the zones of transmissive rock.

3.4.3 Groundwater flow volumes

The groundwater flow in the three test areas have been determined with the aid of models based on potential theory as developed by Stokes /3-45/. Here, flows and flow lines for various topographical and hydrological conditions and a starting hydraulic conductivity of 10^{-6} m/s are derived. An adjustment for measured conductivity values can easily be done. For Karlshamn, a flow of 0.2 l/m^2 and year has previously been reported. This was based on information available at the time, namely a conductivity at shallow depth of 10^{-9} m/s or less combined with good rock conditions in the existing borehole, a water table slope of 0.05 and an island-like topography. The model used here is represented by Fig. 15 in /3-45/ and assumes radial symmetry, an impenetrable bottom surface at a depth of 1 000 m, above which conductivity decreases with depth according to $K = K(z) = 10^{0.0013\ z-6}$ m/s where z is the depth in m (negative). Measurements have since shown that the conductivity in the borehole at Karlshamn from 23 to 500 m is equal to or less than $2 \cdot 10^{-12}$ m/s, this value can instead be applied to the model as per Fig. 14 in /3-45/. Here, constant conductivity and no bottom surface at finite depth is assumed. A flow equal to or less than 0.0015 l/m^2 and year is then obtained.

In the same way, a corresponding model with a two-dimensional flow pattern perpendicular to a valley slope - Fig. 8 in /3-45/ - can be applied to Finnsjö Lake and Kråkemåla. Here, the slope of the water table can be set equal to 0.008 and 0.0012, respectively, which, for rock with a conductivity of 10^{-9} m/s, gives flow volumes of 0.1 and 0.15 l/m^2 and year, respectively. These small water volumes probably represent an overestimate of the actual flows, since they have been calculated on the basis of a measuring limit of 10^{-9} m/s, while the actual conductivity around the waste canisters is much lower. Thus, the cited measured values from Karlshamn and Stripa would give flows which are 500 and 20 times smaller, respectively, than those used in the safety analysis. The small flow volumes greatly restrict the amount of substances which the groundwater can carry to or from a rock repository.

3.4.4 The pattern of groundwater flow

The flow of the groundwater is determined by an area's precipitation and topography as well as the nature of the ground and the bedrock. Computer programmes have been developed which can be used to calculate the three-dimensional flow pattern for an area /3-45/.

The results show, as expected, that the groundwater seeps down into the bedrock in elevated areas, after which it turns upwards again towards large adjoining valley floors, where it may reach the surface. This takes place at points of groundwater discharge into lakes, streams and springs. The influence of topography often extends down to a depth of several thousand metres. The longer the slopes are, the deeper their influence reaches. The surface areas where groundwater from great depths issues are small, and the upflow is accompanied by a very heavy dilution of the groundwater by water from higher levels.

One consequence of these general conditions is that the groundwater movements in an area of crystalline rocks are divided into smaller flow cells, and that the groundwater transport is predominantly of a local character. This pattern becomes more pronounced when the valleys follow fracture zones in the bedrock, where vertical permeability is high. The potential for upward flow which was formerly assumed to exist in the Gåvastbo zone east of the Finnsjö area has now been verified by means of piezometric measurements in a percussion hole drilled through this zone /3-3/.

Calculations have been carried out of the upward flow over a rock repository which is caused by the heat generated by the waste during the introductory phase of the storage period /3-46/. In agreement with previous American estimates, it is reported that this heating gives rise to only an insignificant perturbation of the prevailing flow pattern. The effects of drainage of the rock around the final repository during the construction and deposition phase have also been investigated /3-45/.

The calculations of the flow volumes and the flow pattern are based on the present topographical contours of the land. These contours, however, manifest underlying differences in the structure of the bedrock and its resistance to destructive forces. The terrain at Finnsjö Lake and Kråkemåla is, in its main features, approximately 600 million years old and lacks potential for renewed erosion, while future erosion in the Karlshamn area would reduce the present elevation differences and thereby also the slope of the water table.

Our present-day climate is characterized by large quantities of precipitation in relation to evaporation. As a result, the water table generally follows the topographical contours of the land near the surface of the ground. In the calculations, it has generally been assumed that the water table and the terrain coincide, which constitutes a limiting case with maximum possible slopes of the water table. In a more arid climate, the water table would be deeper and its gradients would decrease. In a more humid climate, low-lying areas would be flooded and the regional hydraulic gradient would also decrease.

The same factors also control the conditions for a transport of dissolved substances with the groundwater. The lower the water table, the less the transport. Consequently, placing of the water table at the surface of the ground constitutes a conservative limiting case. Finally, since both topography and the hydraulic conductivity of the bedrock are largely determined by the existing bedrock structure, the paths of flow in the investigated areas will persist for a very long period of time.

3.4.5 Groundwater flow time

Calculations of groundwater flow time are based on Darcy's Law, which can be written:

$$t = \frac{s \times \varepsilon}{3.2 \times 10^{7} \times K_p i}$$

where

t = time (years)
s = length of flow path (m)
K_p = permeability (m/s)
i = hydraulic gradient (m/m)
ε = effective porosity of the rock, i.e. the volume of the water-conducting pores as a fraction of the total volume (m^3/m^3).

Of the quantities in the equation, values for K_p are available from measurements in KBS boreholes, and the hydraulic gradient at various depths can be calculated on the basis of the elevation of the free water table (ground surface). As is mentioned under 3.6.1, the actual gradients are roughly half of those on which the following calculations are based, which means that the actual flow times are approximately twice as long as those which are calculated.

A value for the effective porosity has been calculated to be nearly 0.001 on the basis of long-term tracer tests between two boreholes in a permeable zone of fissured rock at a depth of around 500 m, with conductivities of around 10^{-6} m/s /3-57/. Only laboratory determinations and indirect field measurements appear to be available for less pervious rock. For crystalline rocks from Norway with conductivities of between 10^{-10} and 10^{-13} m/s, effective porosities of between 0.001 and 0.028 have been measured, and most tested samples exhibit values of between 0.005 and 0.015, Heimli /3-58/. The same porosity range has also been given for crystalline rock species from North America /3-59 and 3-60/.

A somewhat lower range, 0.001 - 0.004, is obtained from measurements of Swedish crystalline rocks, namely six non-fractured samples from the drill core from Forsmark /3-61/ and some 50 rock samples from Norrland /3-62/. All of these determinations have been carried out by means of water saturation and water-loss measurements, respectively.

An indirect method to measure the porosity of the bedrock in boreholes is to determine its electrical resistivity, provided that no electrically conductive minerals are present. Brace /3-59/

has shown that, for crystalline rock with low porosity:

$$\varepsilon^m = \frac{r}{R}; \text{ where}$$

ε = porosity
r = resistivity of the pore liquid
R = resistivity of the bedrock
m = an exponent with values near 2 in normal rock. In fracture zones with predominantely parallel fractures, m = 1.

Measurements carried out in KBS boreholes show that R in non-transmissive rock lies around 10^5 ohmmeters, while 10^4 ohmmeters has been measured in many intensively fractured zones. The resistivity of the pore liquid can be assigned a value of around 3 ohmmeters /3-63/, which gives porosities of around 0.005 for rock sections with hydraulic conductivities of less than 10^{-9} m/s. In the fracture zones, the resistivity of the water is around 40 ohmmeters, which gives similar porosity values for zones with hydraulic conductivities around 10^{-7} m/s as well.

The cited data indicate that ε is between 0.001 and 0.01 for non-transmissive rock as well, and confirm Heimli's conclusion that there is no direct connection between effective porosity and hydraulic conductivity in this type of low-porosity rock. This is because the water moves in pores and small fissures with short length, uneven walls and poor hydraulic connection, so that the actual flow channels are tortuous and, at points, constricted. Often used relationships between permeability and porosity, which have been worked out for grouting operations in heavily fractured rock, are, on the other hand, based on the assumption that the water-bearing fractures represent openings between infinitely long, plane-parallel and smooth-walled plates /3-53/. This leads to a gross underestimate of the porosity, and therefore also of the flow time, in sound rock.

The time it takes for the groundwater to move from a rock repository to the surface has been calculated with data from the Finnsjö area and different distributions of K_p and ε. On the basis of data obtained from the Finnsjö 3 borehole, a three-dimensional calculation with $K_p = 10^{0.003\ z-6}$ m/s (z is the depth in m, negative) and $\varepsilon = 0.001$ is considered to correspond most closely to the actual flow times. K_p varies in this model from 10^{-6} m/s at the surface to $10^{-7.5}$ m/s at a depth of 500 m. A number of large fracture zones with permeabilities hundreds of times higher have also been incorporated in the calculation model.

This model shows that a rock repository at a depth of 500 m and with a surface area of 1 km^2 would fit within an area where the groundwater takes around 3 000 years or more to reach the surface, see figure 3-7. This does not take into account the time during which there is only an inflow of groundwater to the repository, and no outflow.

The effects of crush zones may be somewhat underestimated by this model, since the lowering of the water table above these zones has been neglected.

However, this model, with its predominantly regular permeability distribution, represents a great simplification of reality. A re-

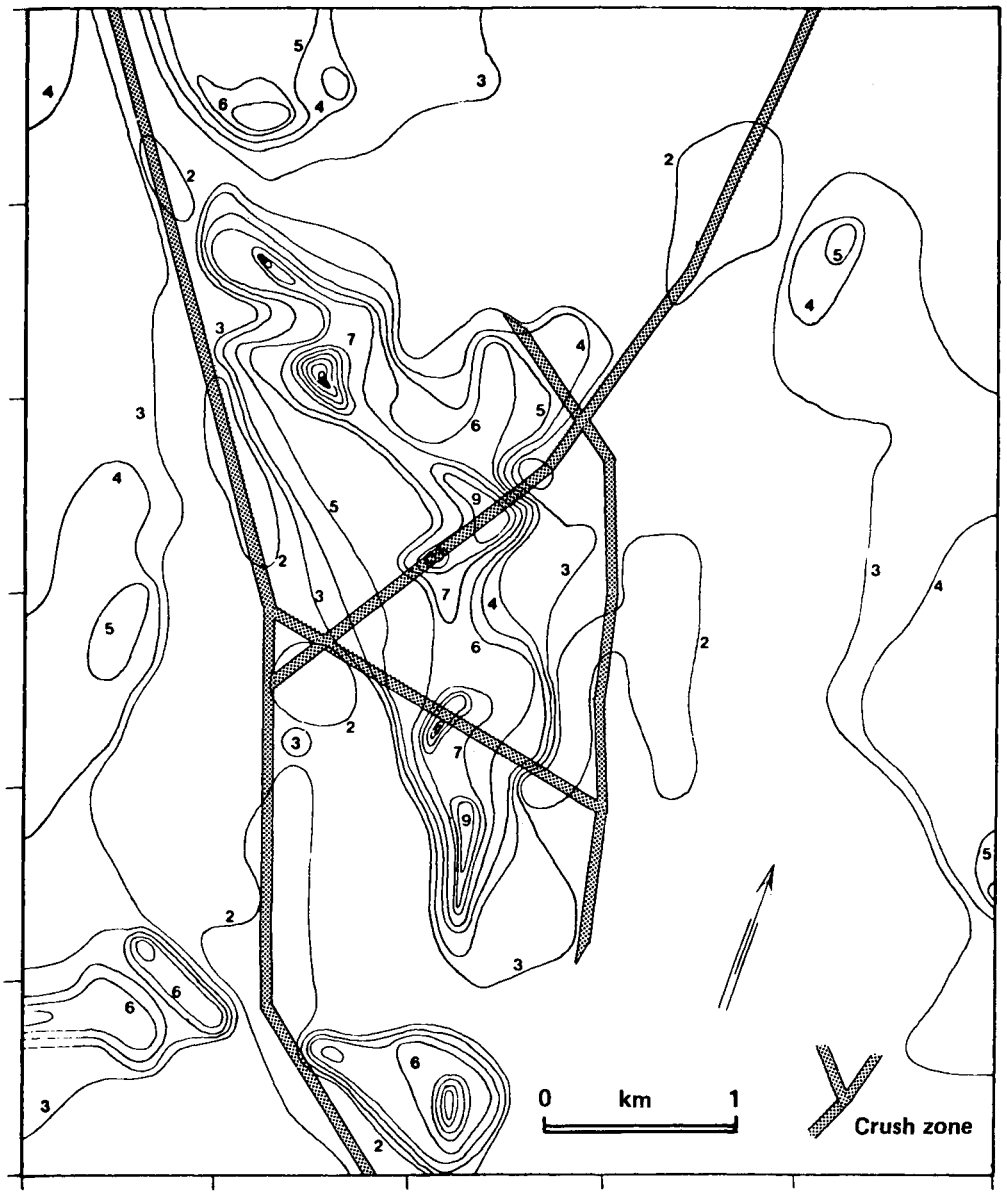

Figure 3-7. Flow times for the groundwater from a rock repository at a depth of 500 metres to the surface according to a three-dimensional model for the Finnsjö area. The water table is assumed to conform to the surface of the ground. The conductivity of the bedrock is taken to vary according to

$$K_p = 10^{0.000\,003\,z-6}\ m/s,$$ *(corresponding to measurement in the bore hole Finnsjön 3)*

where z is the depth below the surface in metres (negative). A number of 50-metre wide vertical crush zones have been incorporated in the model. For these, it is assumed that

$$K_p = 10^{0.0003\,z-4}\ m/s.$$

The curves encompass areas within which the flow times are equal to or longer than the given number of years in powers of 10. For example, the flow time to the surface is more than 10 000 years from all points which lie within the curve marked with 4. The area inside this curve is approximately 2 km^2. (According to Stokes and Thunvik/3–45/).

The effects of crush zones may be somewhat underestimated by this model, since the lowering of the water table above these zones has been neglected.

liable assessment of actual flow times can nevertheless be based on these calculations, since an overview of the effects of the local variations between water-bearing fracture zones and less pervious rock masses can be obtained from an application of Darcy's Law.

For example, let us take a general case where the hydraulic gradient is 0.01 and the porosity of the bedrock is 0.003. For a fracture zone with a conductivity of 10^{-7} m/s, it is found that it takes 0.1 years for the groundwater to move 1 metre in the direction of the gradient. In a less pervious rock section with a conductivity of 10^{-11} m/s, the water takes a thousand years to travel the same distance. This can also be expressed by saying that it takes just as long for the groundwater to move 1 metre through the less pervious rock as through a fracture zone 10 kilometres in length. This demonstrates that it is the presence of impervious rock around the individual waste canister which is decisive in determining the flow time of the groundwater from this canister up to the surface.

In the borehole in Karlshamn, where the hydraulic conductivity over a section of 477 m has been measured to be $2 \cdot 10^{-12}$ m/s or lower, the total section length of rock with a permeability of 10^{-7} m/s cannot exceed 1 centimetre. It is therefore absolutely certain that each waste canister here would be surrounded by extremely low-permeable rock many metres thick. Consequently, it would take many thousands of years for groundwater which has been in contact with such a canister to flow through the rock and up to the surface. Furthermore, the flow of the water in such impervious material does not follow Darcy's Law, but is rather slower. It is therefore probable that the water will take hundreds of thousands of years or even longer to flow from a depth of 500 m up to the surface through such rock.

At Kråkemåla and Finnsjö Lake, drillings show that the volumes with low-permeable rock are considerably smaller, but can still reach a size of hundreds of thousands and even up to a million cubic metres. Thus, there is room at these sites as well to locate the waste so that it is surrounded by many metres of non-transmissive rock, so that flow times of several thousand years can be counted upon.

However, the bedrock blocks in question are surrounded by fracture zones with conductivities of around 10^{-7} m/s. The boreholes show that their volume is only one-fifth to one-tenth that of the non-transmissive blocks. With the given values for K_p (10^{-7} and 10^{-11} m/s) it can therefore be calculated that around 99.9% of the groundwater flow through the bedrock goes through the fracture zones. This means that the flow time for most of the groundwater is determined by the conductivity of the transmissive rock, which corresponds to the three-dimensional calculations presented in figure 3-7. But, as has already been noted above, the flow time for the water which has been in contact with a waste canister in non-transmissive rock is several thousand years longer than that calculated for the fracture zones.

The boreholes, together with field observations on the surface, show that the fracture zones intersect the bedrock in different directions and are generally of limited length. They normally consist of several long fractures which succeed one another, or

of systems of more closely spaced small fractures. The water which follows the fracture zones can therefore not flow without interruption in the direction of the hydraulic gradient, but is rather governed by the course of the fractures. The actual flow paths are therefore longer than in the flow calculations and probably include sections of lower conductivity. This gives rise to the so-called "tortuosity" of the flow paths, which lengthens the flow time.

The magnitude of the lengthening factor is, however, difficult to specify. If a contiguous flow route runs parallel with and perpendicular to the gradient in equal proportions, this would entail a doubling of the flow time. Small sections of less pervious rock along the flow path would also lead to a lengthening of the flow time. As was shown above, however, the water's long flow times in the less transmissive rock surrounding the individual waste canisters are most important.

The conclusion of this analysis is that most of the groundwater moves in the fracture zones in the bedrock. Calculations of groundwater flow time show that a rock repository at a depth of 500 m with an area of 1 km^2 at Finnsjö Lake could be contained completely within an area from which the flow time of the groundwater to the surface exceeds three thousand years. Water which has been in contact with an individual waste canister surrounded by low-permeable bentonite and several metres of low-permeable rock would require an additional several thousand years in order to reach a fracture zone. Conditions are similar at Kråkemåla. At Karlshamn, the flow time of the groundwater to the surface from a rock repository at a depth of 500 m would probably exceed hundreds of thousands of years.

3.4.6 Groundwater age

Information on flow times can also be obtained from age determinations made on groundwater. A number of such determinations has therefore been carried out using the carbon-14 method. This method is based on the fact that the element carbon has two stable isotopes, carbon-12 and carbon-13, and one radioactive isotope, carbon 14, which decays at a known rate. Carbon-14 is constantly being formed in the atmosphere, where it is incorporated in the carbon dioxide in the air. When this carbon dioxide is assimilated by plants or dissolved in the water, the carbon-14 isotope goes along with it.

However, when the water becomes groundwater, it can no longer absorb carbon-14. The carbon-14 radioactivity of the water thereupon diminishes regularly with time, according to the formula

$$t \text{ (years)} = 1.85 \cdot 10^4 \log_{10} m/x;$$

Where m is the original carbon-14 content of the carbon dioxide and x is the content when the measurements are made. It is assumed in the calculations that the carbon dioxide in the air has always had a constant level of carbon-14, but that some fractionation of the carbon isotopes has taken place. A correction is therefore made for this fractionation on the basis of the carbon-

Tabell 3-1. Age determinations of deep groundwater using the carbon-14 method.

Sample	K 1	K 1	K 2	K 2	Fi 2	Fi 2	Fo 1	Fo 1
Depth, m	407	493	291	510	360[1)]	360[1)]	458	458
Analysis No., St	6229	6246	6221	6203	6388	6387	6263	6319
pH	8.45	7.95	7.3	7.25	7.65	7.75	7.9	7.85
x/m, %	25.75	36.63	58.84	59.76	64.14	64.44	69.15	69.52
d ^{13}C o/oo	-15.35	-16.3	-16.2	-16.6	-11.9	-12.95	-15.4	-15.2
Age, conv., years	10980	8140	4330	4200	3680	3630	3040	3000
Age, m = 80 %, years	9190	6350	2550	2410	1880	1840	1250	1210

Sample	Fo 1	C_n5	A 8	Ave. value	Correction 1	Correction 2
Depth, m	355	300	300	380	Half-life 5 730 yrs(+3%)	Time variation of ^{14}C
Analysis No., St	6389	6033	6032			
pH	-	8.05	7.55	7.72		
x/m, %	69.63	42.80	50.46			
d ^{13}C, o/oo	-15.4	-17.9	-18.3	-15.6		
Age, conv., years	2990	6870	5550	5150		
Age, m = 80 %, years	1190	5080	3760	3350 ± 850	+ 100	+ 200
					Corrected ave. value	3 650 ± 850

Note: 1) = Vertical depth
K = Kråkemåla
Fi = Finnsjön
Fo = Forsmark
Cn and A = Storjuktan

m = carbon dioxide's original carbon-14 content
x = sample's measured carbon-14 content
d ^{13}C = sample's measured carbon-13 content

See tables 1 and 2, KBS Technical Report No. 62.

13 content of the sample. In this manner, a so-called conventional carbon-14 age is obtained.

Conventional carbon-14 ages for 15 groundwater samples, determined at the laboratory for isotope geology in Stockholm, are reported along with conventional chemical analyses in /3-37/. In addition, determinations have been made on water from the Stripa mine, giving ages of up to 30 000 years. If water from mines, where groundwater conditions have been disturbed for a long time, is disregarded, 11 age determinations on deep groundwater are reported. These give ages of between 3 000 and 11 000 years. The average is 5 300 years, the average depth 380 m.

However, the level of carbon-14 in the air's carbon dioxide has varied with time. It has been possible to follow this variation 6 000 years back in time by the analysis of wood specimens whose age has been determined by counting their annual rings. A curve for the correction of conventional carbon-14 ages in reference to this is provided by Faure /3-64/, who also presents an up-to-date review of the background and principles of the carbon-14 method.

The age determinations have been carried out on the carbon dioxide (CO_2) and hydrogen carbonate (HCO_3^-) in the water samples. However, a portion of these substances can derive from the dissolution of inactive calcite in the ground through reaction with the carbon dioxide in the air in the ground according to

$$CaCO_3 + CO_2 + H_2O = Ca^{2+} + 2HCO_3^-;$$

or with the sulphur oxides in the air according to

$$CaCO_3 + H_2SO_4 = Ca^{2+} + SO_4^{2-} + CO_2 + H_2O;$$

Such contributions of inactive carbon dioxide and hydrogen carbonate would result in excessively high ages.

The low level of sulphate in the water samples shows that contributions from sulphuric acid can be ignored. A maximum contribution of inactive carbon from the dissolution of calcite can therefore be calculated according to Mook /3-65/ on the basis of the original carbon-14 activity (100%) and carbon-13 deviation (-25 o/oo) of the carbon dioxide, the activity and carbon-13 deviation (0%, 0 o/oo) of the calcite and the carbon-13 deviation (15.6 o/oo), pH (7.7) and temperature (5-15°C) of the water. The values given in parantheses are those which were used in the calculation. The values for the carbon-13 deviation and pH of the water are the averages of the 11 determinations. The pH of the groundwater shows that the calcite reaction has taken place primarily in the intermediary zone and not in the deep bedrock (3-66). This is confirmed by the fact that calcite-filled fissures generally occur in the rock near the surface as well. The main source of the calcite in the ground is marine limestone, which is now a part of the soil cover. Its carbon-13 deviation is 0 $\pm$2 o/oo, according to /3-67/. According to determinations carried out on three samples of Paleozoic limestone from the Baltic area and one sample of crystalline Precambrian limestone from the Finnsjö district, the carbon-13 deviation is less than 1 promille. These data show that the contribution from calcite dissolution is at most 20% of the water's content of carbon

dioxide and hydrogen carbonate. This is because some of the carbon dioxide in the soil air has reacted with silicate minerals instead of calcite. According to Vogel /3-68/, the contribution from calcite dissolution in modern groundwater is, on the average, around 15%. The 11 conventional carbon-14 ages have each been corrected for a contribution of 20% inactive carbon. This gives a new average value of 3 350 ± 850 years. Correction for changes in carbon-14 activity with time and for a half-life of 5 730 years give a final result of 3 650 ± 850 years, see table 3-1.

This age is an average value of the time it has taken for the water to reach the sampling points after isolation from the atmosphere. The sampling points can be conservatively regarded as being randomly distributed with regard to the areas of groundwater recharge and discharge, although no sampling has taken place at depth in typical discharge areas. From this, it can be concluded that this average age gives approximately half of the flow time for groundwater along flow paths at a depth of approximately 380 m. The flow time from a rock repository at a depth of 500 m, which extends half-way from the inflow area out towards the outflow area, is consequently around 3 650 years or longer. The water samples which were studied, however, were all taken from water-bearing zones in the rock. As was shown above, these zones are responsible for most of the groundwater transport. Attemps to sample less pervious sections have not yielded adequate amounts of groundwater. It has therefore not been possible to ascertain the longer flow times which pertain to such sections.

The chemical complications associated with groundwater formation can be eliminated if two groundwater samples from the same inflow area are available and if the samples exhibit comparable carbon-13 deviations. The transit time between the sampling points is obtained by taking x/m for the sample nearest the groundwater divide as m and x/m for the other sample as x in the decay equation. This can be applied to samples from Kråkemåla and the Finnsjö area, see table 3-2.

The correction for the time variation in the original carbon-14 activity gives in these cases an increment of about 600 years. The standard deviations indicated represent random errors of measurement. In reality, the Finnsjö value must be regarded as a substantial underestimation, since the Gåvastbo sample from approximately 55 m vertical depth contains a large portion of young groundwater which does not derive from near the groundwater divide, but was infiltrated near the sampling site. All dated samples also have a certain portion of young water resulting from contamination in connection with sampling. This is indicated by the tritium content of the samples. Admixture of young water makes the quoted carbon-14 ages too low. In other words, the unmixed groundwater is older, and the flow times are longer than indicated here, but it is not now possible to give reliable corrections for these sources of error. In summary, it can be concluded that carbon-14 determinations carried out to date indicate a transit time of more than 3 000 years. The actual transit times, however, can only be determined by additional studies.

Table 3-2. Carbon-14 determinations of transit times.

Borehole	Kråkemåla K 2	Kråkemåla K 1	Finnsjön Fi 2, I	Gåvastbo
Depth (vertical)	291 m	493 m	360 m	55 m
Analysis No.	6221	St 6246	St 6387	St 6430
x/m %	58.84	36.63	64.44	47.83
d ^{13}C o/oo	-16.2	-16.32	-12.95	-13.1
t, years		3 800 ± 150	2 400 ± 120	
Correction for half-life and time variation of ^{14}C		+ 600	+ 600	
Corrected transit time		4 400 years	3 000 years	

3.4.7 Short-term variation of the groundwater level

The depth of the free water table varies in connection with seasonal variations and variations between dry periods and times of precipitation. Additional short-term variations are caused by such factors as the gravitational effects of the sun and the moon on the bedrock (tidal effects), atmospheric pressure variations and earthquakes in other parts of the world. A special study of these effects has been carried out /3-49/. No disturbances of a rock repository have been demonstrated.

3.5 CHEMICAL ENVIRONMENT

3.5.1 Groundwater composition

The chemical environment in and around a rock repository for high-level waste is important for the durability of the canisters and the buffer material and for the possibilities of dispersal of the waste substances. These questions can be illuminated with the aid of chemical equilibrium calculations based on the composition of the groundwater and knowledge of the natural occurrence of the materials in question. In some cases, it can be shown that the natural form of occurrence of the material has remained unchanged for many millions of years, thereby providing answers to questions concerning its durability.

An survey of the composition of Swedish groundwater has recently been published by Wenner et al. /3-69/. A large body of data from rockwells in Finland,giving average levels and ranges of variation

Table 3-3. Probable composition of groundwater in crystalline rock at great depth, according to Rennerfelt and Jacks /3-76/.

Analysis	Units	Probable interval	Min. value x)	Max. value x)
Conductivity	µS/cm	400 - 600		1100
pH		7.2 - 8.5		9.0
$KMnO_4$ cons.	mg/l	20 - 40		50
COD_{Mn}	"	5 - 10		12.5
Ca^{2+}	"	25 - 50	10	60
Mg^{2+}	"	5 - 20		30
Na^{+}	"	10 - 100		100
K^{+}	"	1 - 5		10
Fe-tot	"	1 - 20		30
Fe^{2+}	"	0.5 - 15		30
Mn^{2+}	"	0.1 - 0.5		3
HCO_3^-	"	60 - 400		500
CO_2	"	0 - 25		35
Cl^-	"	5 - 50		100 xx)
SO_4^{2-}	"	1 - 15		50
NO_3^-	"	0.1 - 0.5		2
PO_4^{3-}	"	0.01 - 0.1		0.5
F^-	"	0.5 - 2		8
SiO_2	"	5 - 30		40
HS^-	"	<0.1 - 1		5
NH_4	"	0.1 - 0.4		2
NO_2	"	<0.01 - 0.1		0.5
O_2	"	<0.01 - 0.07		0.1

x) The estimated probability that a value will fall between the min. value and max. value is 95 %. Higher values occur locally, see /3-77/ and /3-75, p. 13-17/.

for many components, has been presented by Laakso /3-70/ and other valuable data are supplied by Lahermo /3-71/. Feth et al. /3-72/ present analyses of groundwater from dioritic rocks in California and Nevada. Data from Böhmen are presented by Paces /3-73/, who also presents groundwater analyses from similar bedrocks from other areas. In this way a good review of conditions in different climates and environments is obtained. The work which has preceded this present report includes analyses of groundwater from Swedish bedrock compiled by Gidlund /3-37/, Rennerfelt /3-74/ and Jacks /3-75/, see table 3-3. Jacks also provides a survey of pertinent chemical equilibria and relevant literature.

3.5.2 Chemistry of groundwater in contact with uranium ores

Like the uranium minerals in most uranium ores, spent fuel is composed of more than 95% uranium dioxide. Knowledge of how the uranium minerals are affected by groundwater can therefore shed light upon the long-range situation in a rock repository. The ores have normally been exposed to the action of the groundwater for many millions of years.

Groundwater which moves through a stratum of permeable sandstone and, on its way, passes a uranium ore which has been formed in the pores of the sandstone has been studied by Germanov and Panteleyev /3-78/. The groundwater flow is slow, the ore has a large specific surface area and the process has been going on for several million years. The groundwater has been studied in seven sections on its path, see figure 3-8. For each section, the range

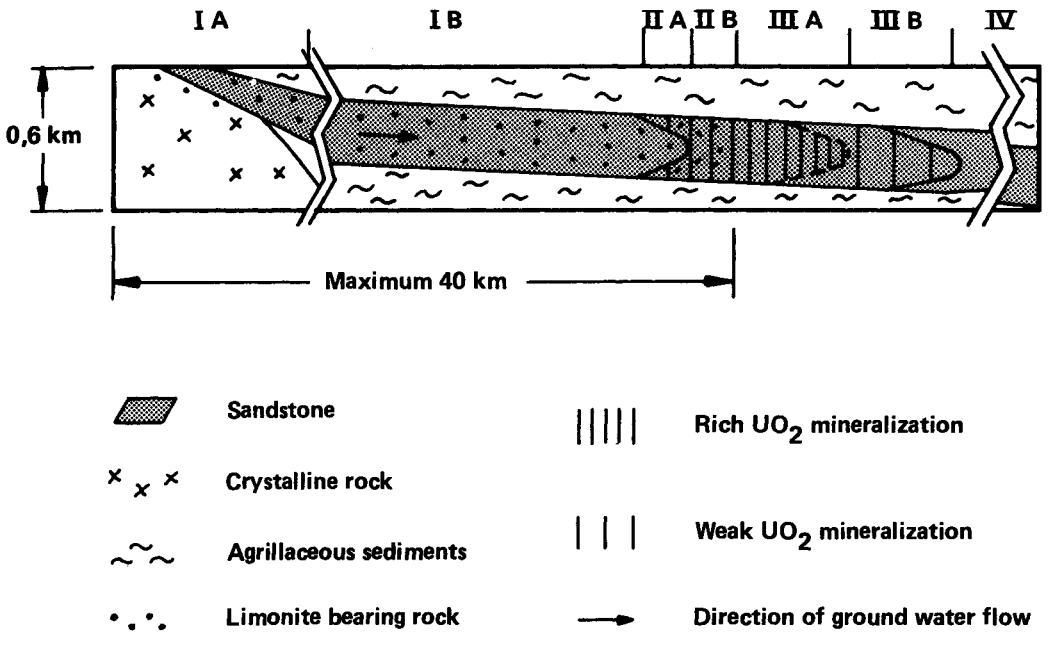

Figure 3-8. Schematic illustration of the geological situation and the different zones around a uranium ore exposed to ground water. (According to Germanov and Panteleyev /3-78/).

of variation of the obtained data is given. An extract is provided in the following table, 3-4. E_h is the groundwater's electrical potential in relation to a hydrogen electrode, i.e. the water's redox potential, given here in millivolts.

Table 3-4. Chemical groundwater data according to Germanov and Panteleyev /3-78/.

Section zone	Number of samples	Eh mV	pH	Organic carbon mg/l	Uranium µg/l
IA	6	450 - 250	7.0-7.4	1.4 - 1.8	5 - 300
IB	12	300 - 212	7.1-7.7	3.9 - 6.0	21 - 150
IIA	23	250 - 147	6.7-7.7	7.3 -10.4	40 - 720
IIB	9	220 - 57	6.7-7.5	10.4 -16.0	125 - 5000
IIIA	8	-72 --195	7.2-7.7	9.9 - 8.0	3100 - 34
IIIB	12	-165 --212	7.5-7.8	8.0 - 6.9	32 - 3
IV	12	-7 --186	7.6-8.0	6.4 - 5.4	3.0 - 1.6

As is seen in the table, the concentration of uranium in the groundwater increases towards the ore, which shows that uranium is first dissolved from the bedrock. According to the same study, this takes place primarily through the formation of uranyl-carbonate complexes. In the actual ore zone, zone III A, the uranium content of the water decreases sharply, which means that most of the dissolved uranium has precipitated. The existence of the ore deposit in itself shows that the chemical environment leads to precipitation. In the sections downstream of the ore, the uranium levels are very low. The table also shows that the precipitation of uranium takes place in connection with a transition from positive to negative Eh values in the transitional zone between oxidizing and reducing conditions in the groundwater. In the case cited here,this transition takes place at a depth of around 400 m.

Lisitsyn and Kuznetzova /3-79/ have further shown that the groundwater upstream of such an ore area is oxygen-bearing while oxygen is lacking in the water downstream, and that the sandstone upstream is rust-coloured by limonite /$Fe(OH^3)$ and FeO(OH)/, while the sandstone downstream is grey and lacks these compounds of trivalent iron. It is also interesting to note that various microorganisms are found mainly in the actual zone of transition and to some extent also in the rust-coloured limonitic part, but that they are not found, with the exception of nitrogen bacteria, in the unaffected, oxygen-free part of the sandstone located downstream of the uranium ore.

These relationships between the groundwater's uranium content, redox potential and oxygen content are not accidental, but rather determined by chemical laws. They conform to a more general model for the formation of uranium ores in sedimentary rock. In this model, oxygen-bearing water leaches out the low concentrations of uranium in the upper parts of the bedrock by converting it to a hexavalent, easily soluble form. When the water later becomes reducing as a result of reactions with organic material and compounds of bivalent iron, it is no longer able to transport the uranium, which is then precipitated in tetravalent, poorly soluble form. These precipitations can be concentrated to mineable deposits /3-80/. An analysis of transport and precipitation conditions with respect to the stability fields of the various uranium compounds in relation to the pH and Eh of the groundwater has been carried out by Hostetler and Garrels /3-81/. Other contributions have been made by Batulin et al. /3-82/ and Dahl and Hagmaier /3-83/.

In the KBS studies, this has been expanded to analysis of the hydrolysis and redox chemistry of the actinides in water /3-84 and 3-85/ in the laboratory as well as theoretically. This work shows that neptunium and plutonium are reduced to insoluble tetravalent (in the case of plutonium, possibly also trivalent) compounds at higher Eh values than uranium. This means that their occurrence in nature is similar to that of uranium and that their dispersal with the groundwater is prevented by reducing conditions in the same manner, but more easily than in the case of uranium. That such is really the case on a geological time scale is illustrated by the natural reactor at the uranium deposit at Oklo, where transuranium elements, including plutonium, have remained undispersed until complete natural decay /3-86 and 3-87/.

3.5.3 Swedish conditions

The principles and reactions discussed above apply generally. However, the composition of the Swedish groundwater at depth differs in some respects from the Russian groundwater. The sulphate content is generally lower while the pH is somewhat higher. However, these differences do not affect the retention of the uranium and other actinides in the bedrock.

A more fundamental difference lies in the fact that the Swedish bedrock, as well as the prevailing soil strata, possess lower permeability than the sandstones which were studied in the Russian examples, and that the Swedish groundwater systems are less extensive and exhibit lower flow volumes. In addition, the continental glaciation removed older weathering products, which, together with the climatic trend following the ice age, results in the fact that the water under Swedish conditions meets fresh, little-weathered and unoxidized material only a few dm below the surface. The main limonite formation therefore takes place above a depth of one metre, and even at this slight depth, oxidation is severly limited. Such an easily-oxidized material as pyrite has, for example, been found in the form of 0.2-0.6 mm large particles with thin weathering layers of limonite in moraine where the particles have been accessible for weathering for more than 6 000 years /3-88/. Similarly, apparently fresh pyrite is often found in rock fractures near the surface. This means that the transition between oxidizing and reducing conditions which occurred at

a depth of about 400 metres in the Russian example in general occurs right near the water table under Swedish conditions.

Eh values which are positive, but which fall rapidly with increasing depth, have been measured in the groundwater in an esker /3-89/, while Eriksson and Khunakasem /3-90/analyzing some 70 groundwater samples from an esker formation in the Piteå area, showed that conditions there correspond to a reducing environment.

The redox potential in deep groundwater has been studied in water samples from Stripa and the Finnsjö area /3-91/, see table 3-5.

Table 3-5. The redox potential in deep groundwater from Precambrian Swedish bedrock, according to Grenthe /3-91/.

Sample No.	Site	Eh, mV
7	Stripa	-152
8	Stripa	- 31
18	Stripa	-173
19	Finnsjö area	-191
21	Stripa	-210
14	Stripa	- 26
20	Finnsjö area	-157
24	Stripa	-140

In the samples from Stripa, the pH was around 8.2, and in those from Finnsjö, 7.7. The slight deviations exhibited by the values for samples 8 and 14 were probably caused by contamination by small quantities of air. Otherwise, the obtained values show that the redox potential of the Swedish water samples very nearly corresponds to the above-cited Russian values for the nearly uranium-free groundwater which passed through the uranium ore zone. Chemical analysis has also shown that samples of Swedish groundwater from great depth in the KBS test areas have a very low oxygen content /3-74/.

3.5.4 Redox systems in the bedrock

Up to now, only a few determinations of redox potential or oxygen content have been carried out on deeper groundwater in Sweden. However, these results can be accorded wider applicability by considering the redox systems in the bedrock with which the water can react. These are composed primarily of different iron compounds, mainly chloride and similar iron-bearing silicate mine-

rals with layer lattices, generally containing both bivalent and trivalent iron. The redox reaction can be written

$$2FeO_{sil} + H_2O_{sil} = Fe_2O_{3\ sil} + 2H^+ + 2\ e^- ;$$

(sil indicates that the component is part of the silicate structure.) Following /3-92/, Gibbs' free energy for this reaction can be calculated to be 9.7 kcal, which gives

$$Eh(V) = 0.21 + 0.03 \log (Fe_2O_3)/(FeO)^2 - 0.06\ pH;$$

where (Fe_2O_3) and (FeO) stand for the chemical activity of the respective component in the mineral. Mineral analyses show that both FeO and Fe_2O_3 in these minerals can vary between 0.1 and approx. 40% by weight, where the higher value approximately indicates a saturated, solid solution. It is then possible to write

$$Eh(V) = 0.21 + 0.03\ (\log 40 + \log \overline{Fe_2O_3}/\overline{FeO}^2) - 0.06\ pH =$$

$$= 0.26 + 0.03 \log \overline{Fe_2O_3}/\overline{FeO}^2 - 0.06\ pH;$$

where $\overline{Fe_2O_3}$ and $\overline{FeO}$ indicate the concentration of these components in the mineral, expressed as percent by weight. With these concentration limits, the following approximation is obtained:

$$Eh(V) = 0.26 \pm 0.1 - 0.06\ pH;$$

which for pH = 7.7 gives Eh $= -0.2 \pm 0.1$ V, i.e. -200 ± 100 mV.

Iron-bearing chlorite characterizes the rock fractures in all of the KBS test areas. The mineral is, alone or together with other layer-silicates such as biotite, illite and smectite, a normal constituent of the bedrock, and especially its fissures. The deep groundwater, within a pH interval of 7-9, should therefore exhibit an Eh interval between -60 and -380 mV. In limonite-/$Fe(OH)_3$ and FeO(OH)/-bearing fracture zones, however, positive Eh values can be expected. As an example of the prevailing conditions, 18 analyzed samples of fissure-filling layer-silicates from relatively shallow tunnels in Gothenburg /3-93/ can be cited. Their Eh values, calculated for a pH of 7.5 to permit comparisons with previously cited data, fall between -120 and -230 mV. Two samples from borehole 2 at Finnsjö both indicate Eh values near -200 mV.

Other minerals, such as magnetite, pyrite (FeS_2) and pyrrhotite (FeS), which contain bivalent iron, are less common than chlorite, but nevertheless occur, generally in small quantities, in the Swedish bedrock. The sulphides particularly weather easily in oxidizing environments. As a result, they constitute Eh indicators, whose general occurrence also shows that negative Eh values prevail in the bedrock.

Mineralogical and mineral-chemical observations thus show, along with the cited Eh and oxygen determinations, that the groundwater at depth in the Swedish bedrock, aside from locally occurring limonite-bearing fracture zones, is characterized by negative Eh values. In this respect, it is very similar to previously discussed Russian groundwater.

According to the Russian analyses, the uranium content of the water in equilibrium with uranium dioxide lies between 1.6 and 3

micrograms per litre. These values agree well with maximum uranium contents in groundwater calculated from equilibrium constants /3-85/. The average concentration of uranium in Swedish springs and wells is also around 3 micrograms per litre. On the other hand, levels of up to and over 2 milligrammes per litre have been found in shallow rock fractures and under oxidizing conditions, for example in mines with uranium mineralization /3-94/. The groundwater in the Swedish bedrock is therefore not able to dissolve and leach out uranium at great depths. That this is really the case is demonstrated by the fact that the continental glaciation has exposed uranium mineralizations in the Precambrian bedrock which have not been carried away by the groundwater, despite the fact that they were formed more than 1 000 million years ago /3-95 and 3-96/.

3.5.5 Extreme climatic changes

As was mentioned earlier, the climate in Sweden around 30 million years ago was much warmer and more humid than it is today. Plant remains from that time show that nearly tropical conditions prevailed. Changes in the level of the land also led to an intensive and deep groundwater circulation. This has given rise locally to deep weathering, which shows what can happen in extreme cases in our type of crystalline bedrock. The best-studied cases have been found in certain mines /3-28, 3-29/ and represent limonitic alterations which may reach depths of several hundred metres. This represents a transition from magnetite to hematite together with a locally strong development of limonite in connection with severe crush zones in the rock, all of which is a sign of deep and intense oxidation. Without exception, however, it is always found that the oxidation is limited to near the surface, or to the immediate vicinity of such crush zones. At a distance of some metres from the limonite formation, completely intact sulphides are often found, for example PbS and ZnS, which show that the oxidation never reached far out into the surrounding rock. This also indicates that extreme changes in climate, topography and groundwater circulation, which appear extremely unlikely today, would not lead to oxidizing conditions for a waste repository. In such limonite-bearing crush zones, as well as in less extreme cases of limonite-stained fractures, the transitional zone between positive and negative Eh values is situated at the border of the unaltered rock. In general, however, the fracture zones in the bedrock, even at shallow depth, have not become oxidized in this manner, but instead exhibit varying contents of bivalent iron in the layer silicate minerals.

3.5.6 Impact of construction and drainage

So far, we have been discussing the natural, undisturbed chemical environment around a rock repository. However, the actual process of constructing and draining a rock repository causes the groundwater to flow towards the repository and lowers the water table in the form of a funnel-shaped depression, Thunvik /3-45/. As a result, the natural chemical conditions around the repository are altered so that oxidation above the water table reaches greater depth and horizontal extent. At the same time, the rock walls of the repository are aerated. A valuable analysis of such a situation is provided by Paces /3-97/, who has studied the chemical

conditions at the Svornost uranium mine at Jachymov in Czechoslovakia. Mining operations have been pursued here for several hundred years. The groundwater table is now 300 m below the surface. At the time of the study, the mining operations had reached a depth of about 500 m. From the surface to this depth, the following variations were measured in the groundwater (average values of 9 samples at surface and 5 samples from 480 m):

	At surface	At depth of 480 m
Temperature, ^{o}C	7.1	21
pH	6.5	7.6
Na content mg/l	3.6	95
Eh, mV	+473	-53

Despite the presence of air in nearby mining chambers, the Eh in the inflowing groundwater at the deepest level in the mine is clearly negative. The sulphate concentration (average) at this level is 280 mg/l, which is related to the fact that the surrounding crystalline bedrock is composed of metamorphic rocks, in some cases with considerable purite concentrations. 5 groundwater samples from granite in the same mine at depths of 520-720 m give instead 14 mg/l as an average value for the sulphate content. Despite the fact that the sulphate content at higher levels of the mine is very high, the groundwater remains nearly neutral or weakly alkaline owing to reactions with surrounding silicate minerals.

Of special interest is the fact that the uranium content of the groundwater is given for four samples. Some chemical data on these samples are presented in table 3-6.

Table 3-6. Groundwater data from Svornost uranium mine /3-97/.

No.	Depth	T	Cl^-	HCO_3^-	SO_4^{2-}	H_2SiO_3	pH	Eh	U
	m	C^o	mg/l	mg/l	mg/l	mg/l		mV	μg/l
20	445	17,6	16,7	143,4	394,6	20,3	6,55	-5	471
21	445	20,0	10,6	183,1	862,9	23,9	7,15	+57	9 000
23	486	23,9	5,3	367,9	54,3	70,2	7,80	-89	76
31	636	29,8	12,4	441,8	15,6	56,2	6,75	-62	17

The two deepest samples, 23 and 31, show how rapidly the Eh and the uranium and sulphate concentrations decrease in the deeper part of the mine. They also provide some idea of the chemical environment in the immediate vicinity of a rock repository which has been dewatered for a very long period of time and of the solubility of uranium dioxide which can be expected in corresponding situations in groundwater of a similarly bicarbonate-rich type as in the Swedish bedrock. The high sulphate contents are

however, not to be expected in areas with sulphide-poor bedrock of the type which occurs within the areas studied by KBS.

This study shows that the effects of the construction and drainage of a rock repository on the groundwater's redox potential and its capacity to disperse uranium in solution are limited to the vicinity of the rock caverns. Immediately outside the disturbed area, the natural equilibria are restored, and the groundwater cannot cause any substantial dispersal of the uranium. When a rock repository is backfilled and the water table resumes its natural level, the local perturbations also gradually disappear.

3.5.7 Application to a waste repository

In the previous KBS study on the storage of vitrified high-level waste, it was concluded that most of the fission products are retarded so long by sorption in the bedrock that they decay before they reach the biosphere. However, spent fuel contains considerably higher levels of uranium and other actinides, many of which have very long half-lives. It has been shown above that the actinides, even if they are partially present in higher valence states at deposition, would, owing to the natural redox conditions in the bedrock, be precipitated and retained in tetravalent form for millions of years.

In a rock repository, the temperature will be elevated for a limited period of time, whereas the specified chemical equilibria apply at 25°C and atmospheric pressure. It can be shown thermodynamically that the equilibria between the concerned solid phases would not be appreciably shifted if the temperature were increased to 200°C. However, precipitation takes place more rapidly at higher temperatures, as has been demonstrated experimentally /3-98, 3-99 and 3-100/.

The cited examples show that precipitation occurs at the depth and at the pressures which are suggested for a Swedish rock repository. The disturbance of the natural redox conditions caused by the aeration and drainage of the repository have been shown to be of a local nature and negative Eh values have been found immediately outside of similarly aerated mine chambers. Extreme geological disturbances of the natural redox conditions, represented by the limonitic alteration discussed above, are also of a local nature and have remained local for a very long period of time, probably around 25 million years.

In order for it to be possible to apply conditions, observed in nature and explained theoretically and on the basis of experimental data, to a waste repository, the water must be in direct contact with the spent fuel in the same manner as it is with the uranium dioxide in the studied uranium ores. Cited data show that uranium, plutonium and other actinides will not be dispersed to the biosphere with the groundwater despite such direct contact.

However, KBS' storage proposal provides two additional barriers between the fuel and the groundwater, namely a canister and a buffer substance between the canister and the surrounding rock. The copper canister will, among other things, reduce external radiation so that the effects of radiolysis will be virtually negligible. The function and durability of these barriers are dealt

with in chapters II:4 to 6. From a geological point of view, it can be added that metallic copper is a material which is stable in natural groundwater and which has been found in small quantities at various locations in Sweden. A natural deposit of metallic copper together with uranium dioxide has been noted by Welin /3-96/. An interesting observation is that metallic copper proved to be chemically stable over geological periods of time in water with an extremely high salt content, containing, among other solutes, 176 g/l Cl^- and 110 mg/l SO_4^{2-} /3-40/.

With regard to the proposed buffer material (Na-bentonite), an abovecited study of fracture-filling materials from the Gothenburg district and the analytical data given there show that bentonite of the relevant Na-dominant type is a natural constituent of the Swedish bedrock. Groundwater chemistry studies /3-75/ cited above show that this material is also generally in chemical equilibrium with the groundwater in a crystalline bedrock of roughly granitic composition.

3.6 EVALUATION AND SUMMARY

3.6.1 Evaluation

Within the framework of KBS's geological study programme, the natural conditions for a deep rock repository for vitrified high-level waste or spent nuclear fuel have been studied in three separate areas. The obtained data are summarized and evaluated in the following sections.

The borehole at Karlshamn shows that the local rock type, Blekinge coastal gneiss, which is observed on the surface extends down to a depth of at least 500 m. The borehole also shows that this rock possesses extremely low permeability and that the vertical distance between water-bearing zones in the rock exceeds several hundred metres. Rock caverns within the area and in its vicinity show, over large areas and volumes, that the infiltration from existing fissures, even at shallow depths, is unusually low. In addition, water-bearing zones within this area are so widely spaced horizontally that a number of large rock caverns could be built without any problems with water infiltration. The stability and low reinforcement costs reported for these caverns show that the Blekinge gneiss is favourable from the constructional point of view, that any existing rock stresses here do not give rise to any engineering problems and that the effects of previous ice ages on the bedrock in the area has been limited to surface features and the uppermost surface layer of the rock. Existing rock caverns for the storage of heavy oil at elevated temperature serve as a large-scale, long-range experiment which demonstrates in actual practice that the bedrock here can withstand the heat load arising from a waste storage programme in accordance with the concept proposed by KBS.

These observations prove that a deep-lying rock repository could be constructed here. The natural rock conditions are such that each individual waste canister in such a repository can be surrounded by many metres of rock of extremely low permeability. As is shown in section 3.4 concerning the volume and velocity of the

groundwater, this means that the quantities of water which can come into contact with the canisters are very small, and that the flow time to the surface is very long. As is examined in greater detail elsewhere (chapters 6 and 7), this, along with the retardation of the waste substances in the rock, means that most of the waste elements will decay before they reach the biosphere. This means that even if there were no encapsulation and the groundwater came into direct contact with the waste, the chemical and mineralogical composition of the bedrock would ensure that long-lived elements such as uranium, plutonium and other actinides would remain virtually insoluble in the water.

The geological history of the Precambrian bedrock, as well as local fracture studies, show that the bedrock conditions and the local permeability of the rock will not change appreciably over the next few million years, and that the probability of fracture movements in the rock which can cause canister damage is extremely small. On the basis of the results, it is maintained that the geological prerequisites for satisfying the Swedish Stipulation Law have been demonstrated to exist.

It must be emphasized that no crush zones have been encountered in the rock in the deep borehole at Karlshamn. Nor have any significant crush zones been found in rock caverns here, which have a total combined volume of more than 1 million m^3.

This shows that such zones are widely spaced and probably few in number within the area. Even if crush zones should occur, they would not in themselves pose a threat to an absolutely safe storage of high-level waste, as long as no waste is emplaced directly in such zones. The decisive condition is instead that each individual waste canister can locally be surrounded by a rock volume of low permeability.

Naturally, knowledge of the location and extent of local crush zones is of vital importance in determining the final configuration of a rock repository. For this reason, the rock repository proposed by KBS has been designed as a modular system which can be adapted to local rock conditions. In this way, the question of the location and extent of any crush zones is reduced to an economic question on which the Stipulation Law has no bearing. However, the aforementioned low costs of rock reinforcement encountered in the Karlshamn area indicate favourable conditions in this respect as well. The results of the regional study of the Blekinge coastal gneiss show, moreover, that many other areas should also possess the same favourable character.

The boreholes at Kråkemåla, as well as the Finnsjö 1 and 2 boreholes (near Forsmark) show that the bedrock in these two areas consists of blocks of low permeability which are, however, bounded by water-bearing zones.

The latter comprise between 5 and 20 percent of the deeper bedrock, and their spacing varies in general from 10 up to a 100 metres or so. Moreover, some indications of high permeability in isolated measuring sections may have been caused by leakage around the packer seals, which would mean that the length of the impervious sections is actually greater than is indicated by the measurements.

Since the boreholes are not located in the same plane, the results show that there are also large volumes of rock at Finnsjö Lake and Kråkemåla with low permeability. Both of these sites therefore offer good opportunities for surrounding the individual waste canisters with several metres of such rock.

The length distribution of the low-permeability sections in the deeper parts of these boreholes is fairly similar in these two areas. This shows that the two areas are roughly equivalent in this respect, and that each of the boreholes is sufficient in itself to provide a representative picture of these conditions at this stage.

The permeability of the water-bearing zones at Kråkemåla is, however, sometimes clearly higher than at Finnsjö. Owing to this factor, along with the pronounced fracture system and elevated natural radioactivity at Kråkemåla, this area must be regarded as less suitable than the Finnsjö area for a rock repository.

The boreholes show that the water-bearing zones in the bedrock consist predominantly of multiple fracture zones, whose width often extends over several measuring sections. The most marked fracture structures in the Finnsjö area, namely the Gåvastbo fault and the fracture zone which is intersected by the Finnsjö 2 borehole and which passes Finnsjö 1, are of this type. They are also characterized by fairly moderate permeability (between 10^{-6} and 10^{-5} m/s).

The minerals in the fracture zones show that these zones were initiated at a very early stage when these parts of the bedrock were located at greater depth and not at their present shallow location.

Sampling of the groundwater in the boreholes, as well as the number of age determinations and other special analyses carried out on the groundwater samples, have been expanded considerably compared to the situation at the time of the previous KBS report. The results are presented in greater detail in section 3.4.

The boreholes have permitted a determination of the actual elevation of the groundwater table above sea level at points in the study areas. As expected, they show that the groundwater table is considerably flatter than the surface of the land, whose slope has been used in all calculations of groundwater volumes and flow times as a measure of the hydraulic gradient. The hydraulic gradient determined in this manner is only about half of that used in the calculations. This means that the stated groundwater flows should be reduced by half and the flow times doubled.

In calculating the flow times, it has generally been assumed that the permeable zones of the bedrock possess complete continuity with each other and that the water can move constantly in the direction of the theoretical potential field. The borehole results and fracture studies of outcrops show that the latter is not the case. The boreholes do not definitively demonstrate the three-dimensional continuity of the deeper fracture zones, and do not even show that such a continuity actually exists. If the continuity of the deep water-bearing zones is incomplete, then the true flow times would be longer, but no allowance for this has been made in the safety analysis.

As was emphasized above, however, the question of the location and extent of water-bearing zones is not of decisive importance for the safety of the final repository, as long as each individual waste canister can be surrounded by a rock volume of low permeability. In this context, it may also be recalled that KBS' geology programme is not aimed at selecting the final site for a future rock repository, but rather at demonstrating how and where an absolutely safe final storage of high-level waste can be effected. The selected areas therefore comprise examples of sites where a final repository could conceivably be located. Before a final decision is made concerning the location and detailed design of the final repository, extensive studies and tests over many years within possible areas are required.

3.6.2 Summary

- A survey of the history and evolution of the bedrock in Sweden shows that the bedrock in the Baltic Shield has constituted a markedly stable unit in the geology of Europe for more than 600 million years. During the past 25 million years, Europe north of the Alps, as well as adjacent areas of the north Atlantic, have been developing towards increasing stability. There is therefore virtually no possibility of such widespread rock movements occurring that could bring about such deep weathering or erosion that the integrity or safety of a rock repository located at a depth of several hundred metres in the bedrock could be jeopardized.

- Local fracture movements in the bedrock cannot be excluded, but a closer analysis shows that they will not lead to any appreciable changes in the permeability of the bedrock or to any canister damages when the canisters are emplaced in sound rock.

- Over the past two million years, Sweden has been subjected to between ten and twenty different glaciations. These, and the changes in the level of the land associated with the deglaciation stages, have not lead to any hydraulically coherent fracturing of the bedrock at depth.

  A future ice age cannot differ radically from previous ice ages. Consequently, a future ice age cannot in these respects affect the safety of a deep rock repository.

- Previous land level changes, with accompanying deep groundwater circulation and heavily climate-dependent weathering, have had only a local effect on the bedrock. This confirms that not even extreme changes in ground levels and climate can have any decisive impact on a suitably located rock repository in the Precambrian bedrock.

- Experiences abroad have shown that even severe earthquakes have very limited effects on tunnels and rock caverns. Only weak earth tremours occur in Sweden. Their effect on a deeplying rock repository would be completely negligible. Southeastern Sweden is, moreover, an area with an extremely low earthquake frequency.

- The KBS study area at Karlshamn is made up of a gneiss which is regionally characterized by weak fissuring and low groundwater content. A total of more than one million m^3 of rock caverns are located in the area and its immediate vicinity, which is roughly equal to the calculated volume of a final repository. Data is available for 700 000 m^3 of these rock caverns, which exhibit remarkably low water infiltration and good rock stability. Many of the rock caverns are heated to temperatures which correspond to the temperatures which have been calculated for a final repository for high-level waste without any adverse effects. A borehole in the area reveals consistently good bedrock conditions down to a depth of 500 m and an extremely low water permeability has been measured for the entire borehole between 23 and 498 m. No water-bearing fracture zones have been encountered in the borehole. It can be safely assumed that the bedrock here consists for the most part of rock with extremely low water permeability, which ensures that each waste canister can be surrounded by large volumes of good rock.

- The study areas at Finnsjö Lake, west of Forsmark, and Kråkemåla, north of Oskarshamn, also exhibit large volumes of good rock. This guarantees that each waste canister there can be surrounded by several metres of rock with low permeability. There are, however, water-bearing fracture zones in both areas, which must be carefully considered in the design of a rock repository.

- The results of the work done since the previous report have confirmed the ranking assigned to the study areas in the previous report, namely Karlshamn, Finnsjö and Kråkemåla, in that order.

- The permeability of good rock has been determined to be equal to or less than $5 \cdot 10^{-11}$ m/s at Stripa and $2 \cdot 10^{-12}$ m/s at Karlshamn. Similar values probably apply to the rock in the other study areas as well, although technical limitations have prevented the measurement of values below $4 \cdot 10^{-10}$ m/s.

  Water-bearing fracture zones within the study areas generally have permeabilities of around 10^{-7} m/s. Higher values were found, however, and values up to 10^{-3} m/s have been measured in isolated zones at Kråkemåla.

- The groundwater flow in good rock in the study areas has been calculated to be 0.2 l/m^2 and year, based on the permeability value $K = 10^{-9}$ m/s. If the permeability values for good rock at Stripa and Karlshamn are applied, ten to one hundred times lower water flows are obtained in the impervious rock sections around the waste canisters.

- The groundwater flow pattern is characterized by local flow cells, with downward flow at groundwater divides and upward flow under more pronounced valleys. In between, the groundwater flow is predominantly horizontal. Since both topography and bedrock permeability are largely determined by the structure of the bedrock, the flow pattern of the groundwater in the study areas will persist for a very long time.

- The flow time of the groundwater has been calculated by means of a three-dimensional model over an area of 30 km^2 around the study area at Finnsjö Lake for a water permeability which decreases from 10^{-6} m/s at the surface to $10^{-7.5}$ m/s at a depth of 500 m. Porosity is set at 0.001. A number of 50-metre-wide crush zones with a hundred times higher permeability have been included in the model. The calculations show that a rock repository at a depth of 500 m and with a surface area of 1 km^2 can be located in this area in such a manner that the flow time of the groundwater from the peripheral parts of the repository to the surface of the ground is more than three thousand years. These calculations apply primarily to the water which flows in the fracture zones in the rock. Supplementary calculations show that a few metres of good rock around each waste canister increases the flow time by several thousand years. The flow time for the study area at Karlshamn for groundwater from a depth of 500 m to the surface is probably hundreds of thousands of years.

- On the basis of eleven age determinations carried out on groundwater by means of the carbon-14 method, the flow time of the groundwater from a repository at a depth of 500 m has been estimated to be around 3 000 years or more.

- Studies of uranium ores and laboratory experiments show that the dispersal of uranium and other actinides by the groundwater is prevented by the reducing conditions which prevail at the depths in question.

- Measurements of the redox potential and oxygen content of Swedish groundwater from great depths, as well as mineralogical and mineral-chemical observations, show that reducing conditions generally prevail in Swedish bedrock. The groundwater at great depths therefore lacks the ability to dissolve and disperse uranium (and other actinides) to any appreciable extent, even if it should come into direct contact with spent fuel in a rock repository.

- Extreme climatic changes give rise to only local changes in the redox potential of groundwater in crystalline rock and cannot hereby affect the safety of a suitably located rock repository.

- The construction and drainage pumping of a rock repository produces only local disturbances of the redox conditions in the immediate vicinity of the rock caverns. Just outside of the affected area, the natural equilibria are restored. The groundwater can therefore cause only a very limited and local dispersal of uranium and other actinides. When a rock repository has been backfilled, such local disturbances will gradually disappear.

4 BUFFER MATERIAL

4.1 GENERAL

Two types of buffer material are used in the final repository: first, a mixture of sand and bentonite similar to that used in the final repository for vitrified waste from reprocessing; and second, highly-compacted pure bentonite.

As was noted under 2.4 above, the sand/bentonite mixture is used to backfill tunnels and shafts. 0.5% ferrophosphate (vivianite) is added to the tunnel fill as a so-called "oxygen-getter" (see chapter 5). For a description of the properties and function of the sand/bentonite mixture, see section 6.3, Volume III of the KBS report on vitrified waste from reprocessing and chapter II:4. The following description deals exclusively with the buffer material of highly-compacted pure bentonite which surrounds the canister in the storage hole and which is used in certain places to seal tunnels and shafts.

The reason why pure bentonite is used in the storage hole instead of a mixture of sand/bentonite as in the vitrified waste alternative is that the demands on the service life of the canister are considerably higher for direct disposal than for vitrified waste from reprocessing. By using pure bentonite of high density, we obtain a buffer material which possesses very low water permeability and the other properties which a good buffer material should have, namely:

- good bearing capacity, so that the canister is held in its position in the storage hole,
- good thermal conductivity, so that the heat generated by the fuel in the canister is transmitted to the rock without the canister being heated to an excessively high temperature,
- good ion exchange capacity, so that the migration of radioactive elements which may leak out from the canister is retarded,
- long-term stability, so that the material retains its properties over the very long period of time during which the function of the final repository is to be maintained.

Another condition is that the buffer material shall not contain components which can decisively reduce the resistance of the copper canister to corrosion.

Besides the above-mentioned properties, bentonite of high density is characterized by the fact that it gives rise to a very high

swelling pressure when the bentonite absorbs water, if swelling is restrained. This provides a guarantee that water-bearing fissures cannot open up in the buffer material. Owing to this swelling pressure, the bentonite also penetrates into and seals fissures which may exist (or which may open up at a later time) in the walls of the storage holes.

Because many of the properties of the buffer material which are fundamental to its function are dependent upon a sufficiently high density being obtained in the storage hole, the bentonite is applied in the hole in the form of highly-compacted blocks of very high density. Under the influence of penetrating groundwater, the bentonite swells and fills out the spaces and cavities resulting from the application procedure. The swelling is restrained by the surrounding rock and the fill in the overlying tunnel so that a very high density is maintained. (The bentonite absorbs water so slowly and groundwater seaps into the storage holes at such a low rate that high swelling pressures cannot arise during the period of time for which the tunnel is kept open.)

Even though many of the most important properties of the bentonite in relation to its function as a buffer material improve with increasing density, there is an upper limit which is dependent upon the fact that exceedingly high swelling pressures can give rise to undesirable stress concentrations in the surrounding rock.

4.2 PROPERTIES

Bentonite is a naturally occuring clay which is characterized by the fact that it swells upon absorbing water. As a reference material, KBS has chosen a bentonite of the type Volclay MX-80, which is mined in Wyoming and South Dakota in the United States. (Other types of natural or synthetic bentonite can probably also be used.) MX-80 is a so-called sodium bentonite whose main constituent (90%) is montmorillonite. It has a large number of uses, for example within foundry and oil-drilling technology. The annual quantities required in the final repository comprise a very small portion of the current annual production and adequate reserves exist.

The chemical composition of bentonite is as follows:

	%		%
SiO_2	approx. 63.0	CaO	0.7
Al_2O_3	approx. 21.0	MgO	2.7
Fe_2O_3	3.2	Na_2O	2.2
FeO	0.3	K_2O	0.4
TiO_2	0.1	Water of crystallisation	5.6
		Misc.	0.8

The grain size of the granulate is approx. 0.07-0.8 mm, compact

density 2.7 t/m^3. For a more detailed account of the properties and structure of bentonite, see /4-1/.

The bentonite is applied in the storage hole both in the form of blocks (fig. 4-1), which are compacted under 100 MPa of pressure, and in the form of bentonite powder, which is used to fill the spaces between the blocks and the rock and between the blocks and the canister. The bulk density of water-saturated bentonite is about 2.30 t/m^3 for the blocks and about 1.75 t/m^3 for the powder in the spaces. The mean density, when all bentonite in the storage hole has been water-saturated and swelling has ceased, is 2.1 t/m^3. It is determined by the increase in volume which results from the fact that the joints between the blocks are filled up, the bentonite in the spaces (see fig. 2-22) is compressed and bentonite from the storage hole displaces and compresses the sand/bentonite fill in the overlying tunnel to some extent.

Stability

Natural deposits of bentonite which have been exposed to the temperatures, groundwater conditions and pressures which prevail in the final repository show that the bentonite can be counted on to remain stable for the period of time during which the buffer material must retain those of its properties which are vital to the function of the final repository /4-1/.

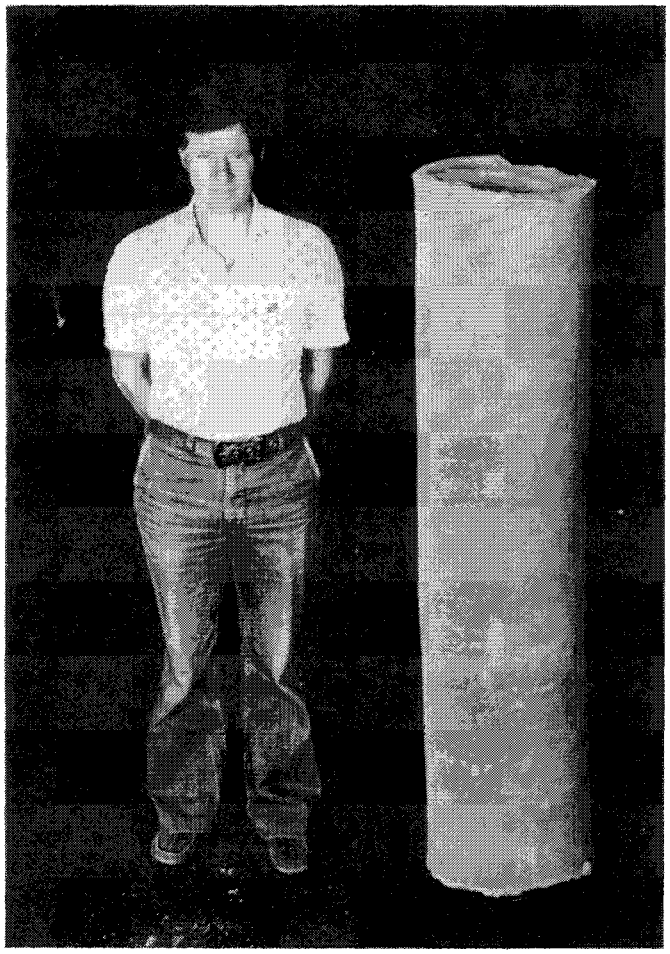

Figure 4-1. Bentonite can be compressed by means of isostatic compaction into large blocks. The photograph shows a test block.

Permeability and diffusivity

The permeability of bentonite as a function of dencity is well-known from the literature /4-2/. The general relationship is illustrated by the graph in fig 4-2. At a density of 2.1 t/m^3, the permeability coefficient of bentonite is about 2 x 10^{-14} m/s. This means that the material is virtually impenetrable by water.

Thanks to its low permeability, diffusion is the controlling mechanism for transports of ions through the buffer material. The diffusion constant for bentonite in the storage hole is about 4 x 10^{-11} m^2/s for metal ions and 8 x 10^{-11} m^2/s for oxygen and small ions, at 50°C. At 25°C, these values are halved. The diffusion constant for bentonite with a degree of compaction corresponding to highly-compacted bentonite blocks has been determined by means of laboratory tests /4-3/.

Bearing capacity

The blocks of highly-compacted bentonite which are placed in the storage hole possess very high bearing capacity. In appearance and to the touch, the material resembles soap-stone. Its shear strength is comparable to that of sedimentary rocks. Its water content, i.e. the ratio between the weight of the water and the weight of the solid material, is approximately 10% in the blocks.

Bearing capacity is a function of the material's density. The final average density of the material in the storage hole when it

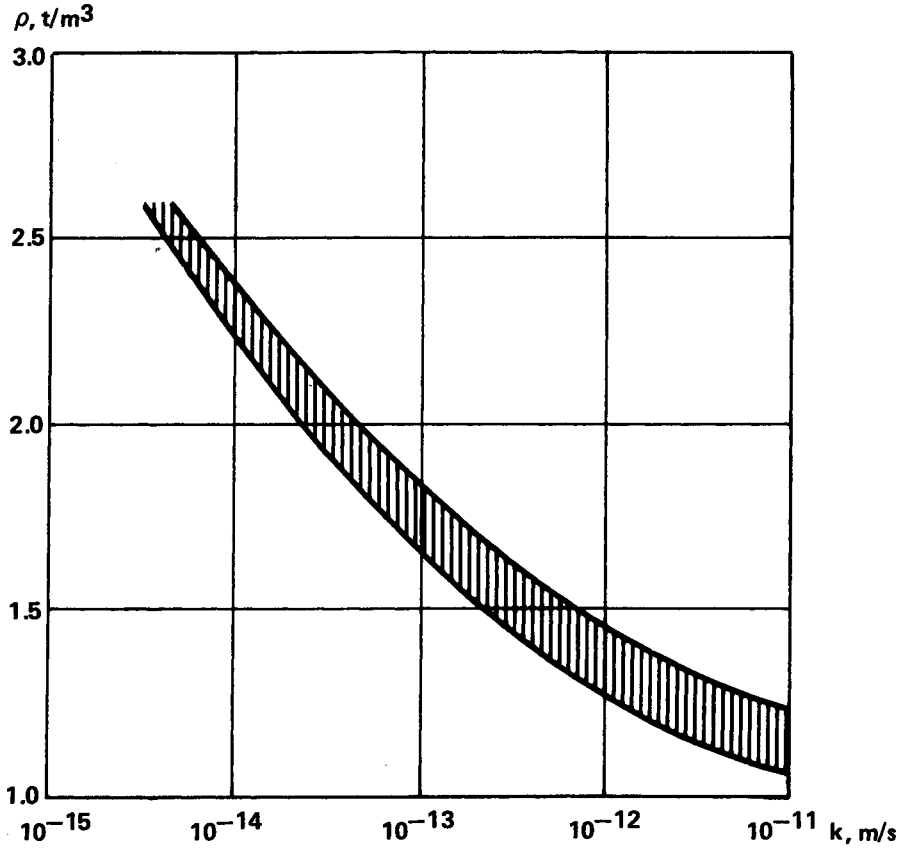

Figure 4-2. The graph illustrates the relationship between permeability (k) and bulk density (ρ) for sodium bentonite. The shaded area between the curves shows the range of variation due to the effects of varying salt content in the pore water and the scatter of experimental measurement data.

is fully water-saturated (water content about 20%) is, however, so high that the subsidence caused by gravity, even after one million years, is negligible /4-2/. Even at a bulk density of 1.4 - 1.5 t/m^3, when the consistency of the bentonite is comparable to that of solid modelling clay, its bearing capacity is sufficient to prevent the canister from sinking through the underlying bentonite, even over a very long period of time. This means that, even assuming improbably high material losses through fissures and the like, the bentonite still possesses sufficient bearing capacity.

Swelling pressure

Bentonite, which absorbs water under restrained swelling exerts a swelling pressure which is a function of the density of the material. The ratio between swelling pressure and density has been determined by tests for MX-80 and verified by means of theoretical calculations /4-4/. At a bulk density of 2.1 t/m^3, the swelling pressure is on the order of 5 MPa, see fig 4-3.

Its high swelling capacity in connection with water absorption gives bentonite a "self-sealing" capacity in that it is forced into fissures in the walls of the storage holes and prevents the opening of water-bearing fissures or cavities in the buffer material.

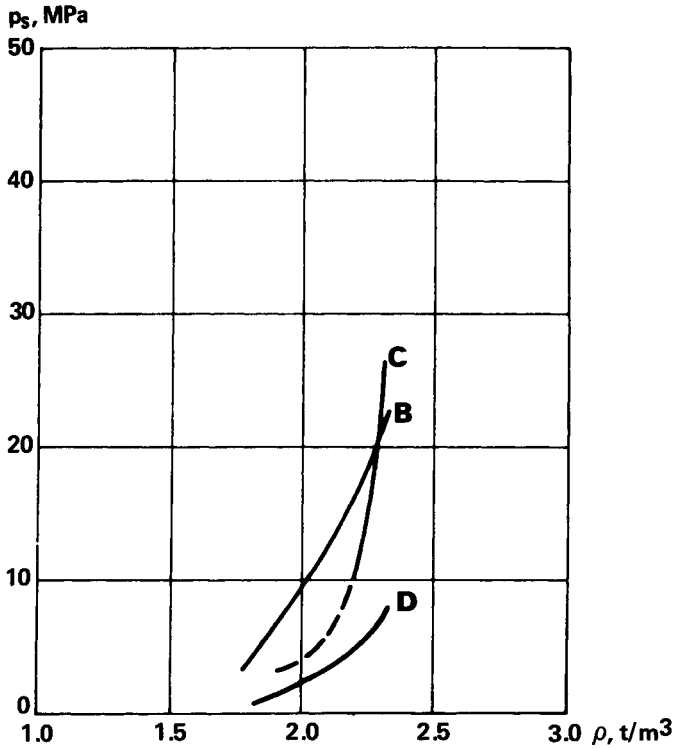

Figure 4-3. The graph illustrates the relationship between swelling pressure (p_s) and bulk density (ρ) for sodium bentonite. Curves B and D pertain to bentonite with 100 % sodium montmorillonite, curve B with all particles oriented in parallel (anisotropically), curve D with the particles oriented in parallel in the three main directions (isotropically). Curve C illustrates swelling pressure with highly compacted Volclay-type bentonite.

Thermal conductivity

The thermal conductivity of blocks of highly-compacted bentonite with a bulk density of 2.0 t/m^3 and a water content of about 10% has been determined to be about 0.75 W/m^oC /4-5/. The highest temperature at the surface of the canister has thereby been calculated to be 77^oC, /4-6/.

Effect on the resistance of the canister to corrosion

Bentonite can contain sulphides and organic material which can directly or indirectly contribute towards a greater corrosion attack on the canister - see chapter 5. The concentration of these materials should not exceed 200 mg/kg bentonite. If this level is exceeded, the bentonite should be purified by heating in air to 425^oC for 15 hours. Tests have shown that such a heat treatment does not affect the swelling properties of the bentonite /4-1/.

Ion exchange capacity

Owing to its high content of the clay mineral montmorillonite, bentonite possesses a considerable capacity to retard certain nuclides through ion exchange, see chapter 6.

4.3 FUNCTION

Following deposition and during the period of time during which the storage tunnels are kept open and the boreholes on both sides of the storage holes drained, it is probable that no water will be able to penetrate into the storage holes. But even if this should occur, the bentonite powder which fills the spaces between the highly-compacted blocks and the rock will absorb most of the water, since the permeability of this layer is higher than that of the blocks. But it is sufficiently low to greatly restrict further penetration of water after the layer has become water-saturated.

When the final repository has been sealed, the original groundwater conditions are gradually restored. Water then seeps slowly into the hole and is absorbed by the highly-compacted bentonite. This will probably occur most rapidly in the joints between the bentonite blocks and the water will therefore first migrate into the inner space next to the canister, which will therefore be water-saturated earlier than the highly-compacted bentonite blocks. As the bentonite absorbs more and more water, its permeability decreases, so that water absorption takes place at an increasingly slow rate. Considering the very low groundwater flow rate and the low permeability of the buffer material and the surrounding impervious (grouted) rock, it will take a very long time (probably hundreds of years) before all of the bentonite becomes water-saturated.

The swelling pressure forces the bentonite into fissures in the walls of the storage holes, sealing them. This includes fissures which may arise following deposition. When the bentonite penetrates into a fissure, the swelling pressure of the bentonite

declines rapidly as the density of the swelling bentonite in the fissure declines. In the tiny fissures (width < 1 mm) which may occur adjacent to a storage hole, the transit time for the water through the bentonite which fills the fissure, and the friction against the fissure walls, will cause the penetration to cease after a few decimetres /4-4/. The outer part of the penetrating bentonite forms a stable gel under the influence of the calcium ions in the groundwater, which means that the transport of bentonite from fissures will be negligibly small /4-7/.

The swelling pressure created by the highly compacted bentonite will compress the sand/bentonite fill in the tunnel above. As a result, the bentonite will be able to swell a few decimetres upwards. The specified final density of 2.1 t/m^3 takes this volume increase into consideration, however. This density may be slightly lower in the top part of the storage hole and higher in the bottom part, but this will not have any appreciable effect on the function of the buffer material. The bentonite cannot penetrate into the pores in the sand/bentonite fill in the same manner as it penetrates into fissures, since the pores are too small.

If the original distribution of stresses and orientation of fissures in the rock are unfavourable, the swelling pressure can open new fissures. But it can be shown that such fissures will not exceed a few metres in length and a millimetres or so in width. The amount of bentonite which can penetrate into such fissures is so small that it will not affect the density of the buffer material and thereby its function. In order to avoid such fissuring, the storage tunnels should be situated so that the primary rock stresses perpendicular and parallel to the tunnel axis are as equal as possible and so that the tunnels are oriented in relation to the prevailing fissure direction /4-8/.

4.4 QUALITY CONTROL

Bentonite which is to be used as a buffer material shall possess the following properties:

Clay content (percent by weight of particles less than 2 μm) shall be at least approx. 80%. This is checked by means of suspension analysis.

Montmorillonite shall constitute at least 70% of the mineral substance. Checked by means of X-ray diffraction analysis.

The content of sulphides and organic material shall each be lower than 200 mg/kg. Checked by means of chemical analysis.

The swelling pressure for bentonite with a water content of 10% which has been compacted under a pressure of 50 MPa shall, upon absorbing water and at constant volume, be 10 MPa ± 20%. This is checked in a cylindrical cell by means of a technique developed by Asea-Atom /4-1/.

The bentonite of type Volclay MX-80 which has been tested within the KBS Project meets these requirements but heat treatment has been necessary to reduce the content of sulphides and organic material to the above-specified value.

5 CANISTER MATERIAL

5.1 GENERAL

The primary function of the canister is to constitute a long-term durable barrier against the escape and dispersal of radioactive elements from the fuel. Such a dispersal can only take place via the groundwater. As long as the canister has not been penetrated, it therefore comprises an absolute barrier, in contrast to the other barriers in the final repository, which are based on very slow processes of dissolution and transport.

A secondary function of the canister is to afford radiation shielding to reduce radiolysis of the groundwater to a level which is low from the viewpoint of corrosion. This radiation shielding also facilitates handling when the canister is transported down to the final repository and when it is placed in the storage hole.

Penetration of the canister can be caused either by corrosion attack or mechanical stresses leading to failure.

5.2 CHOICE OF MATERIAL AND CANISTER DESIGN

In the final repository, the waste canisters will be subjected to the action of groundwater. In view of the high demands on the service life of the canister, it is therefore necessary that the canister material have a very low reaction rate with water. The supply of small quantities of substances dissolved in the groundwater which can cause corrosion can be limited by surrounding the canister with a buffer material - see chapter 4.

The best guarantee for a low reaction rate with water is thermodynamic stability, which means that no demonstrable reaction at all takes place, not even over an unlimited period of contact. If such a material is chosen, data on reaction kinetics are unnecessary.

Copper is a material which is practical to use and thermodynamically stable in pure water. Other metallic materials with this property are silver, gold and the platinum metals, but these are out of the question for economic reasons.

Pure metallic copper, so-called Oxygen Free High Conductivity Copper (SIS 5011), has therefore been chosen as the canister material. The design of the canister is illustrated in fig. 5-1.

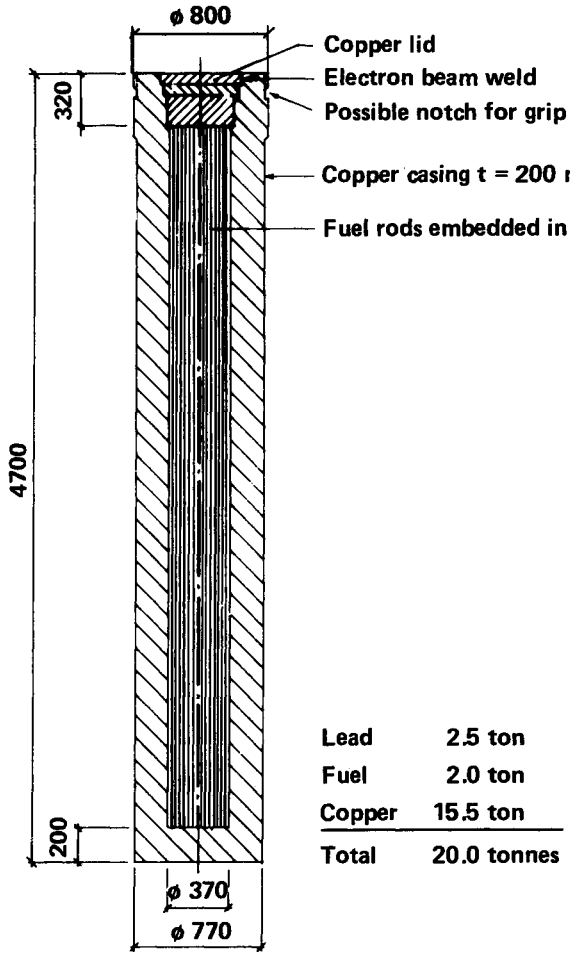

Figure 5-1. Longitudinal section of copper canister with fuel rods embedded in lead.

Its minimum wall thickness is 200 mm, its outer diameter is 770 mm (upper end 800 mm to provide a grip for lifting). Its length is 4 700 mm and its weight is about 16 tonnes. The three lids are joined to the canister by means of electron beam welding. The fuel in the canister is embedded in lead, preventing deformation of the canister due to external overpressure.

Copper also possesses the strength properties required for the canister to be able to withstand the mechanical stresses to which it will be subjected.

Ceramic materials may also be considered as canister materials. Although they are not thermodynamically stable in the same sense as copper, they can exhibit a very low reaction rate with water in some cases. Asea has, for example, with the cooperation of KBS, developed a canister made of alpha-aluminium oxide by means of a method based on high-pressure isostatic compaction at high temperature. This type of canister is described in Appendix 1 to this report.

5.3 THE CORROSION ENVIRONMENT OF THE CANISTER

Since copper is thermodynamically stable in pure water, corrosion reactions can only take place with certain substances which are dissolved in the groundwater. The corrosion environment of the canister is defined by the temperature, pressure and chemical composition of the groundwater which comes into contact with the

canister. Undissolved substances in surrounding materials are of importance only to the extent that they affect the composition of the groundwater.

The heat which is generated by the waste gives rise to an elevated temperature next to the canister. The maximum temperature of 77°C is reached 10-20 years following deposition. After 1 000 years, the temperature has dropped to 50°C, after 100 000 years to 22°C (2°C above the starting temperature), see fig. 5-2 and /5-1/.

The hydrostatic pressure corresponding to the depth of the groundwater is 5 MPa. The swelling pressure of the surrounding buffer mass is 5-10 MPa.

The chemical composition of the water which is in contact with the surface of the canister depends on the composition of the groundwater in the regional groundwater system around the final repository and on the composition of the buffer material as well as on the rate of reaction between the canister material and constituents of the surrounding water for which a reaction is thermodynamically possible. In evaluating canister corrosion, it is primarily the latter which shall be taken into consideration.

A detailed report on the thermodynamic prerequisites for copper corrosion is provided in /5-2/.

In order for copper to corrode, it must give off electrons and become ionized. In ionic form, it can then react with other ions

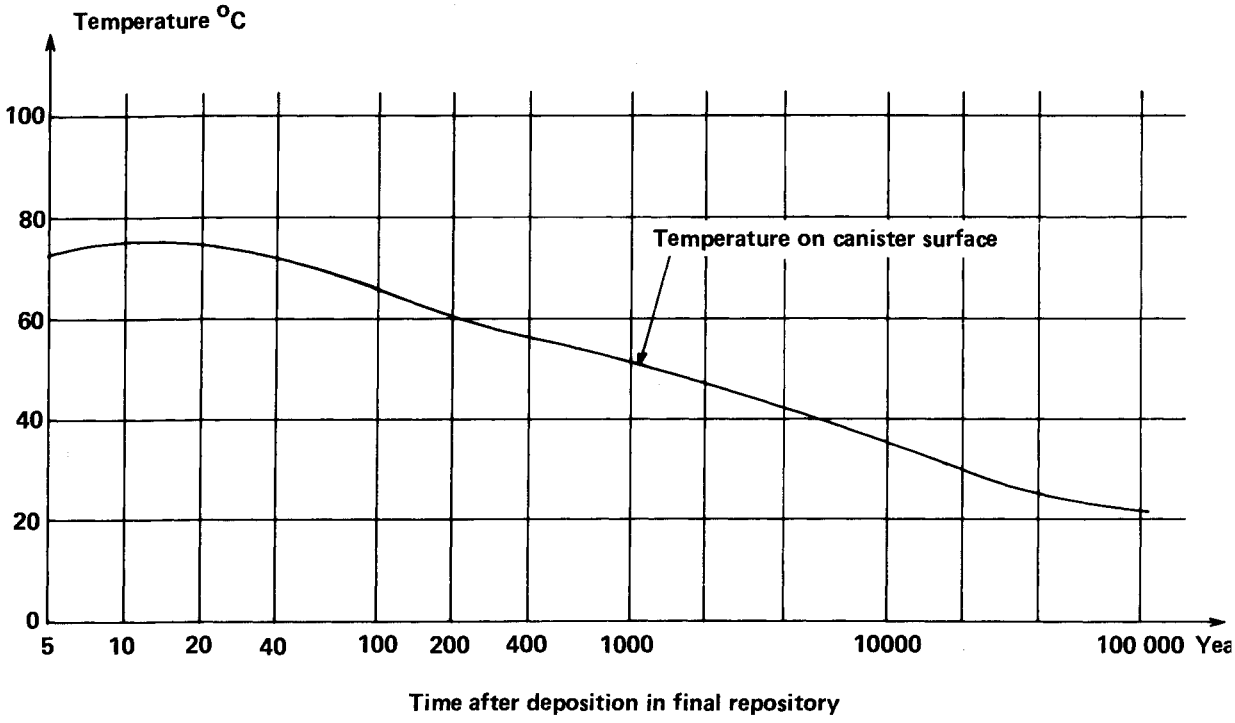

Figure 5-2. The graph shows how the surface temperature of the canister varies with time following deposition in the final repository.

in the solution. The electrons must be accepted by another substance, a so-called electron acceptor or oxidant. In order for the reaction to take place, there must be a reduction of the so-called "free energy" in the system. This reduction depends on how effective the oxidant binds the electrons and to what extent copper ions are bound in poorly soluble compounds with low free energy or remain in free form.

In the case of the reaction of copper with pure water, hydrogen ions are the potential oxidant and copper is bound as an oxide. The contribution towards a reduction of the free energy is too small, and no reaction takes place. In other words, copper is thermodynamically stable in pure water.

If, however, free oxygen is present in the water, it binds the electrons so much more effectively than hydrogen ions that the reaction becomes possible. The conversion of copper to an oxide is thermodynamically favoured in this case.

However, hydrogen ions can serve as oxidants provided that the copper ions which are formed are bound in a compound with very low free energy (lower than that of the copper oxide). Such a compound is copper sulphide. If sulphide ions are present, copper corrosion can therefore occur to an extent which is determined by the supply of sulphide.

The review of the thermodynamic prerequisites for corrosion reactions at the copper surface which is presented in /5-2/ shows that the above-mentioned substances free oxygen and sulphide are the only substances which can cause corrosion in practice. Purely thermodynamically, sulphate can also act as an oxidant with the formation of copper sulphide, if the reaction is coupled to an oxidation of e.g. bivalent iron to trivalent iron. However, geological evidence indicates that this reaction does not take place at all in practice (it is kinetically inhibited). The latter also applies to another thermodynamically possible oxidant, namely nitrate, which, moreover, is not likely to be present at all in groundwater at great depth.

Other dissolved constituents of the water which is in contact with the canister are of no importance for corrosion. After a very long time, they can be assumed to be present at a concentration which corresponds to the composition of the groundwater (see section 3.5). In an introductory phase, however, the composition of the water corresponds to the equilibrium provided by the buffer material (bentonite). The pH is then slightly more than 9, but gradually drops to about 8.5. Attainment of equilibrium with the groundwater takes place relatively quickly as regards anions, but more slowly when it comes to cations, owing to the ion-exchanging properties of the bentonite. Attainment of complete equilibrium for cations takes millions of years, according to calculations /5-3/. Since the flow of water through the very impervious buffer material is negligible, material transport takes place solely by means of diffusion.

5.4 EXTENT OF CORROSION

5.4.1 General

As we have seen above, sulphide and free oxygen are the only constituents of groundwater which can potentially cause corrosion of metallic copper. The maximum possible extent of this corrosion can be calculated if it is assumed that these substances react immediately upon contact with the canister.

Since their concentration at the canister surface then becomes zero, the force of diffusion acting on the substances to drive them towards the canister from the environment is maximum. The maximum corrosion rate thereby corresponds to this diffusion rate. The actual corrosion rate can be less if a protective layer of corrosion products is formed at the surface.

The transport of dissolved substances in the buffer material to and from the canister and to and from the groundwater system in the rock is dealt with in greater detail in section 6-5. With the methods described there, the supply of corrosive substances (free oxygen and sulphide) to the canister has been calculated /5-4/.

5.4.2 Corrosion caused by free oxygen

As is evident from section 3.5, free oxygen is virtually absent from the groundwater in rock at great depth, which is related to the presence of minerals containing bivalent iron in the fissure walls. This is also backed up by the analysis results for groundwater from boreholes at a depth of about 500 metres. However, in view of the fact that analysis accuracy is 0.1 ppm, this value is conservatively assumed. It gives a total maximum corrosion attack on a copper canister after one million years of only about 1.5 kg.

In addition, however, relatively large quantities of atmospheric oxygen become entrapped in the pores in the buffer material when the final repository is sealed. By far most of this oxygen is present in the bentonite-sand mixture in the tunnel above the storage hole. This oxygen is removed, however, by the addition to this mixture of 0.5% ferrophosphate (in mineral form known as vivianite), which is stable in contact with bentonite. Practical tests /5-7/ have shown that this mineral reacts at a suitable rate with oxygen under the conditions which prevail in the final repository. The oxygen is therefore consumed long before it can diffuse into the canister. Ferrophosphate is not added to the storage hole, but the oxygen volume entrapped in the storage hole is relatively small and corresponds to the corrosion of only about 2.5 kg copper per canister.

Another conceivable contribution towards the oxygen supply is radiolytic disintegration of water caused by the gamma radiation coming from the waste. But because the copper canister has a wall thickness of 200 mm, the radiant energy which penetrates through and is absorbed by the water-containing buffer material is relatively insignificant, see fig. 8-6. The maximum yield at which radiant energy can cause disintegration of water is known from radiation chemistry /5-5/. By assuming this yield, and that all

formed oxygen and hydrogen peroxide is able to diffuse to the canister surface and react completely there, an upper limit for the copper corrosion which could be caused by radiolysis can be calculated. It corresponds to only 0.4 kg per canister in a million years /5-4/.

When the corrosion caused by free oxygen is added to that caused by oxygen formed by radiolysis, a total maximum copper consumption per canister of approximately 4.5 kg after one million years is obtained.

5.4.3 Corrosion caused by sulphide

As in the case of oxygen, the corrosion caused by sulphide can be divided into two components, namely one from the groundwater and one from material which is initially present in the buffer material.

Sulphide in the groundwater generally derives from sulphate in the surface water, which, when it penetrates down into the fissures in the rock, becomes microbiologically reduced to sulphide. Locally, at the depth at which the reaction takes place, this can give rise to relatively high sulphide concentrations. As in the case of free oxygen, however, the level of free sulphide in the groundwater at great depth is limited by the presense of iron, which binds the sulphide in the form of pyrite. Even though this reaction is slow, the solubility of the iron sulphide will always limit the concentration of sulphide, see section 3.5.

In calculating the corrosion contribution from sulphide, it has been assumed that the level of free sulphide in the groundwater is 5 mg/l, which has been measured in one case (Forsmark) /5-6/. In view of what has been said above, this value is much too high, and the analysis result is probably due to the presence of colloidal or suspended iron sulphide (FeS). Since its diffusion through the bentonite buffer is very slow, the corrosion it causes will be negligible. Furthermore, free sulphide would be consumed more or less completely upon its passage through the buffer material by reaction with the iron oxide present there. However, in order to be on the safe side, it has been assumed that none of these obstacles exist, and the calculation has been carried out as if 5 mg/l free sulphide were actually present in the groundwater and could diffuse to the canister without being consumed on the way.

Additional sulphide in the groundwater can theoretically be formed by microbiological sulphate reduction owing to the presence of dissolved organic material (max. 12.5 mg/l) /5-8/. This could then give rise to an additional 2 mg/l free sulphide in the groundwater. In practice, however, it is doubtful whether this organic material (humus substances and so-called fulvic acids) can be used for sulphate reduction. If this were the case, it would most likely already have been consumed in this manner. Nevertheless, it is assumed here that a corresponding quantity of sulphide is formed.

A level of free sulphide in the groundwater of 5 + 2 = 7 mg/l gives a theoretically calculated corrosion attack of 50 kg copper per canister and million years. This is probably a considerable

overestimation of the actual corrosion attack, possibly by several orders of magnitude.

The buffer material (after oxidizing heat treatment, if necessary) contains very small quantities of sulphide. The remaining quantity, about 200 mg/kg, derives almost entirely from pyrite, FeS_2. It is very poorly soluble. The sulphide content of a solution in equilibrium with pyrite is so low that the corrosion it could cause by diffusion to the canister surface is negligible.

Bentonite can contain organic material which could theoretically give rise to sulphide through a microbiological sulphate reduction. But an oxidizing heat treatment, see 4.2, burns away all such material which could serve as a substrate for the sulphate-reducing bacteria. Analyses show that the total level of organic material after heat treatment can be assumed to be less than 200 ppm. If it is conservatively assumed that this entire quantity can be used as a bacteria substrate for the production of free sulphide, a maximum calculated corrosion attack corresponding to 5.4 kg copper per canister and million years is obtained. All organic material in the bentonite, both in the storage hole and in the adjacent tunnel volume, is hereby included. Since the tunnel fill contains a surplus of bivalent iron, the sulphide which is formed there will probably not be available for reaction with copper. The actual corrosion attack would therefore be, at the most, only half of that specified above.

The total calculated maximum corrosion contribution from sulphide in one million years amounts to a maximum of about 55 kg. However, actual corrosion would be considerably less.

5.4.4 Total corrosion

If the contributions from oxygen and sulphide are added together a total maximum corrosion of about 60 kg copper after one million years is obtained. (However, addition is not justified in this case, since the copper oxide formed by oxygen corrosion will consume sulphide without metal corrosion.) This quantity of corroded material corresponds to an average corrosion depth of about 0.5 mm, compared to the canister thickness of 200 mm. The top part of the canister could conceivably be more heavily attacked than the bottom part, due to the fact that sulphide from the tunnel would react preferentially with this part. If it is assumed that this sulphide attack is concentrated to the top 10% of the canister surface, the mean corrosion depth there would be about 2.4 mm. This, however, represents a substantial overestimation, since, as was already mentioned, the iron content of the tunnel fill should prevent sulphide from diffusing down into the storage holes.

The above-mentioned corrosion rates pertain to conditions with an intact copper canister. What would happen following a penetration of the canister is more difficult to foresee, and the corrosion rate could conceivably increase due to the presence of e.g. free oxygen formed by the radiolysis of water in direct contact with the fuel.

This oxygen could also conceivably affect the corrosion rate for nearby canisters. However, the diffusion resistance offered by the buffer material will render such effects insignificant.

5.5 CHARACTER OF THE CORROSION ATTACK

It can be concluded from the above that corrosion penetration of the canister within one million years is only possible if the corrosion attack becomes concentrated to a very small part of the surface in the form of a spot attack, known as pitting. There is no risk for cracking due to stress corrosion in the case of pure copper.

Pure copper is a material which possesses very little tendency towards pitting. But pitting can occur in some cases, e.g. in water pipes and in material buried in certain soils.

The relationship between pit depth (p) and time (t) is usually expressed empirically in such cases by means of the equation

$$P = A\, t^{n} \qquad (1)$$

where A and n are constants. n has a value of between 0 and 1.

A statistical analysis /5-9/ of the results of a long-term study of copper corrosion in different types of soils in the USA involving exposure over a period of many years has shown that the relationship between pit depth and time can better be expressed by means of the equation:

$$P = A(t - t_o)^{n} \qquad (2)$$

where t_o is the incubation time before pitting starts.

The results of the aforementioned study show that n decreases with time.

In agreement with equation (1), the life of, for example, a water pipe of copper increases sharply with wall thickness. If the wall is sufficiently thick, the growth of the pit in depth virtually ceases altogether with time. The continued attack then takes the form of a widening of existing pits and initiation of new pits. With extremely thick walls - as in this case 200 mm - the attack, after a very long period of time, assume the character of an eroded surface zone with local variations in depth.

A conservative value for the maximum corrosion depth is obtained by disregarding this evening-out of the attack with time and instead using the maximum value (approx. 25) for the pitting factor which was observed in the aforementioned study. The maximum attack depth after one million years obtained in this manner is 60 mm (30% of the wall thickness).

5.6 CANISTER LIFE

5.6.1 Life in view of mechanical stresses

The mechanical reliability of the copper canister has been studied in relation to the stress which can arise in connection with fabrication, handling and final storage /5-14/. Fabrication of the copper canister and handling in connection with the encapsulation of the spent fuel are discussed in section 2.3.

The mechanical stresses which can affect the service life of the canister in the final repository are of three types:

a) External overpressure (hydrostatic pressure and swelling pressure of buffer mass).

b) Shear forces due to possible movements in the rock.

c) Internal overpressure due to helium formation in the fuel, caused by alpha decay of heavy nuclides.

A uniform external overpressure will not give rise to stresses in the canister wall, since the inside of the canister is completely filled with lead and fuel rods. The cladding on the fuel rods will not undergo creep deformation under prevailing conditions.

Cracks in the canister wall or in the welds could possibly grow as in result of an unfavourable distribution of thermal stresses /5-14/. Both the parent metal and the welds are inspected by means of special ultrasonic technique to make sure that they are free of cracks.

If water absorption or swelling in the buffer material takes place unevenly at the beginning, certain stresses may arise in the canister material, but not of such a magnitude that they could lead to failure. The stresses gradually disappear due to creep relaxation so that the material eventually becomes stress-free.

As is shown in section 3.2, the probability of even small rock movements is very low. The pliancy of the buffer material and the ductility of the copper would prevent any failure due to the small rock displacements which are possible. Here again, any stresses eventually disappear due to creep relaxation.

The internal overpressure in the fuel rods depends on how quickly helium formed by radioactive decay is released from the uranium dioxide matrix. This process is not yet entirely understood. Even if the most unfavourable assumption is made, namely that the helium is liberated immediately upon formation, it can be shown that the cladding tubes on completely spent PWR fuel do not undergo any creep deformation due to overpressure within a period of one million years /5-10/ and /5-11/. No internal overpressure is created in BWR fuel within this period of time.

In summary, there are no mechanical stresses which can limit canister life to less than one million years.

5.6.2 Service life

It was concluded above that the mean attack depth on certain parts of the canister could possibly amount to a maximum of 2.4 mm after one million years. Variations in attack depth are, however, possible, but are not judged to be great. A very conservative assessment of the maximum attack after one million years is, as argued above, 60 mm. The conclusion is that service life should not be less than one million years.

It should be emphasized particularly that the above conclusion concerning service life is not critically dependent upon assumptions of an absence of rock movement with accompanying fracturing or an increase in the groundwater flow owing to a change in the hydraulic gradient. The compacted bentonite as a buffer material functions as an elastic defense which, by virtue of its swelling capacity, guarantees that no water-bearing fracture which would greatly increase material transport can reach the canister - even in the event of substantial rock movements. In the unlikely case that large fractures were to form in the rock, the compacted bentonite will penetrate into these fractures, swell up and effectively prevent material transport to the canister. The bentonite can swell to several times its own volume without losing its protective capacity. A heavy increase in the groundwater flow would only give rise to a limited increase in the corrosion rate.

5.6.3 Summary evaluation of canister life

From the above, it can be concluded that neither mechanical stresses nor corrosion attack can be expected to give rise to canister penetration within one million years, i.e. the minimum expected canister life. This estimate of canister life is based on extremely unfavourable assumptions concerning groundwater chemistry and conservative assumptions concerning rock fissure content and groundwater flow. Reasonable assumptions of higher values for the latter factors do not have an appreciable effect on the estimate of canister life.

A group of specialist, mainly from the field of corrosion and materials, has, under the auspices of the Swedish Corrosion Research Institute, carried out an evaluation of the corrosion life of the canister for KBS /5-12/. This evaluation arrives at the following conclusion:

"Copper is a relatively noble (electro-positive) metal and is therefore thermodynamically stable in oxygen-free pure water. In the case in question, however, some corrosion can occur due to the presence of oxygen or sulphide in the water which comes into contact with the canister. It is assumed that the oxygen in the buffer material in the tunnels can be eliminated by the addition of the deoxidizers. However, oxygen is present in the buffer material which is applied to the deposition holes, and sulphide is supplied with the groundwater.

Even when these reactants are taken into consideration, however, it is considered realistic to anticipate a serive life of hundreds of thousands of years for a copper canister with a wall thickness of 200 mm."

Eight of the group's nine members stand behind this statement, while one has made a reservation.

The objections of the dissenting member /5-13/ are based on, among other things, the opinion that a future ice age could cause considerable fracturing of the rock, which would lead to a dramatic increase of the groundwater flow and thereby of the corrosion rate on the copper canister. This postulated effect of an ice age on the Swedish bedrock at a depth of 500 m does not agree with the geological interpretation of the pattern of fractures which can be observed today - see section 3.2. In the hypothetical case that a glaciation would result in extensive fracturing of the rock around the canisters, the buffer material, with its great potential swelling capacity, will seal new or widened fissures and the reported conclusion concerning the service life of the canister will not be affected.

6 LEACHING AND MATERIAL TRANSPORT

6.1 GENERAL

Assessments of the leaching of radioactive elements from radioactive waste are normally based on laboratory measurements of the leaching rate. Such measurements are made with a free supply of water of varying composition and at different temperatures. A large body of experimental data of this type is available for vitrified high-level waste. Corresponding data for spent uranium dioxide fuel are much scarcer. Assessments of the leaching of radioactive elements from such fuel must therefore be based primarily on other types of information.

This chapter starts with a report of the results from various experimental studies of the leaching rate of spent uranium dioxide fuel. It then continues with a discussion of various possible scenarios following contact between uranium dioxide and groundwater which has penetrated the outer barriers (copper, lead, zircaloy cladding). Limitations on the leaching rate for certain nuclides related to their solubility in water are then discussed.

The transport of various water-soluble substances through the buffer material and in nearby thin rock fissures is explored. This transport is of importance both for corrosion of the copper canister and for the migration of radioactive elements. Calculations of the supply of oxidants (oxygen and sulphide) to the copper canister constitute the basis for the evaluation of canister life. This has been reported in chapter 5. The rate of dissolution of the uranium dioxide matrix and the calculated outward transport of radioactive elements comprise the basis for the dispersal calculations and consequence analysis in chapter 8.

In connection with the final storage of spent fuel in the manner described in this report. The rate of corrosion of the canister and the rate of dissolution of the fuel will be governed by the transport velocity for soluble species. This is limited by the low water turnover rate stemming from the low water flow through the rock and by the very low permeability of the buffer material. See chapters 3 and 4. In the following, it is shown that material transport is controlled by diffusion through the buffer mass and by the "film resistance" in the phase interface between the clay and the slowly flowing water in the thin rock fissures. Under these conditions, with virtually stagnant groundwater in the buffer material, the possible rate of dissolution of

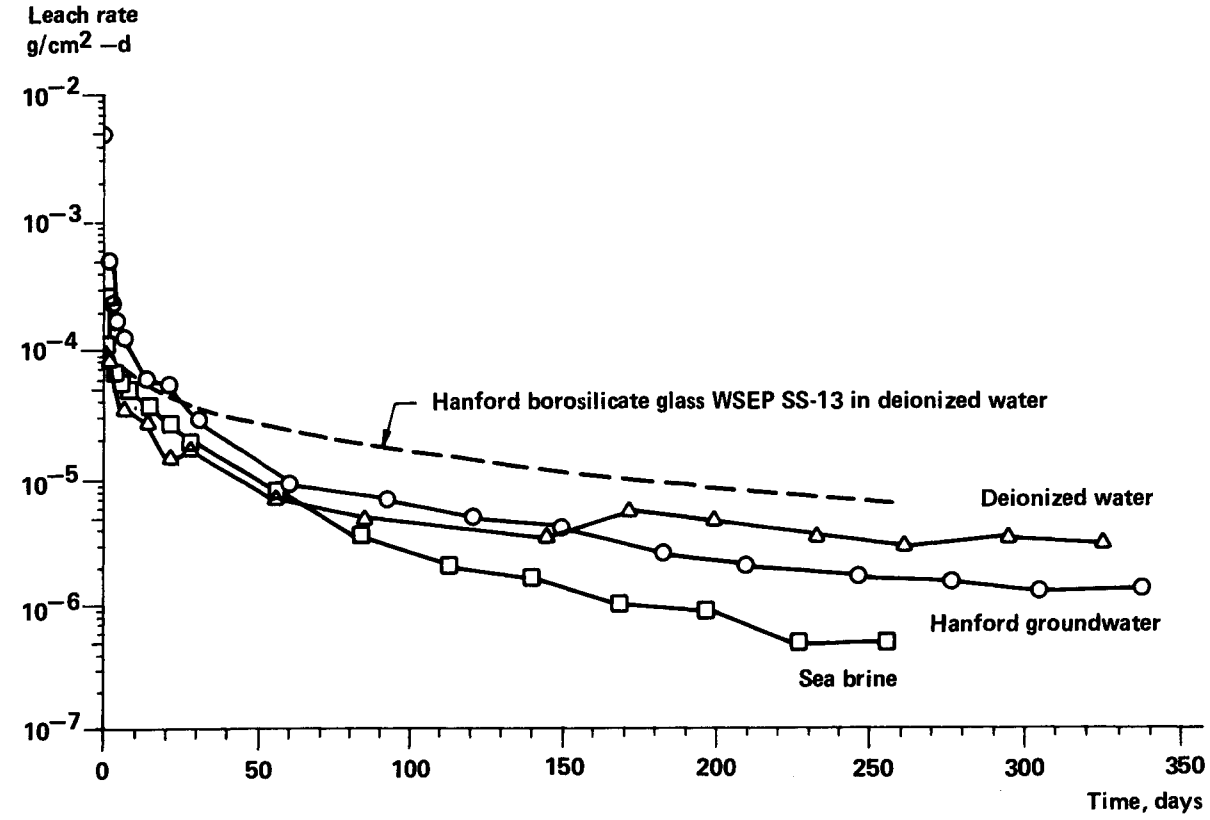

Figure 6-1. The graph shows the leach rate of irradiated LWR fuel, 54 400 MWD/MTU, based on release of cesium-137. The dashed curve illustrates the leaching of cesium-137 from borosilicate glass from Hanford as a comparison.

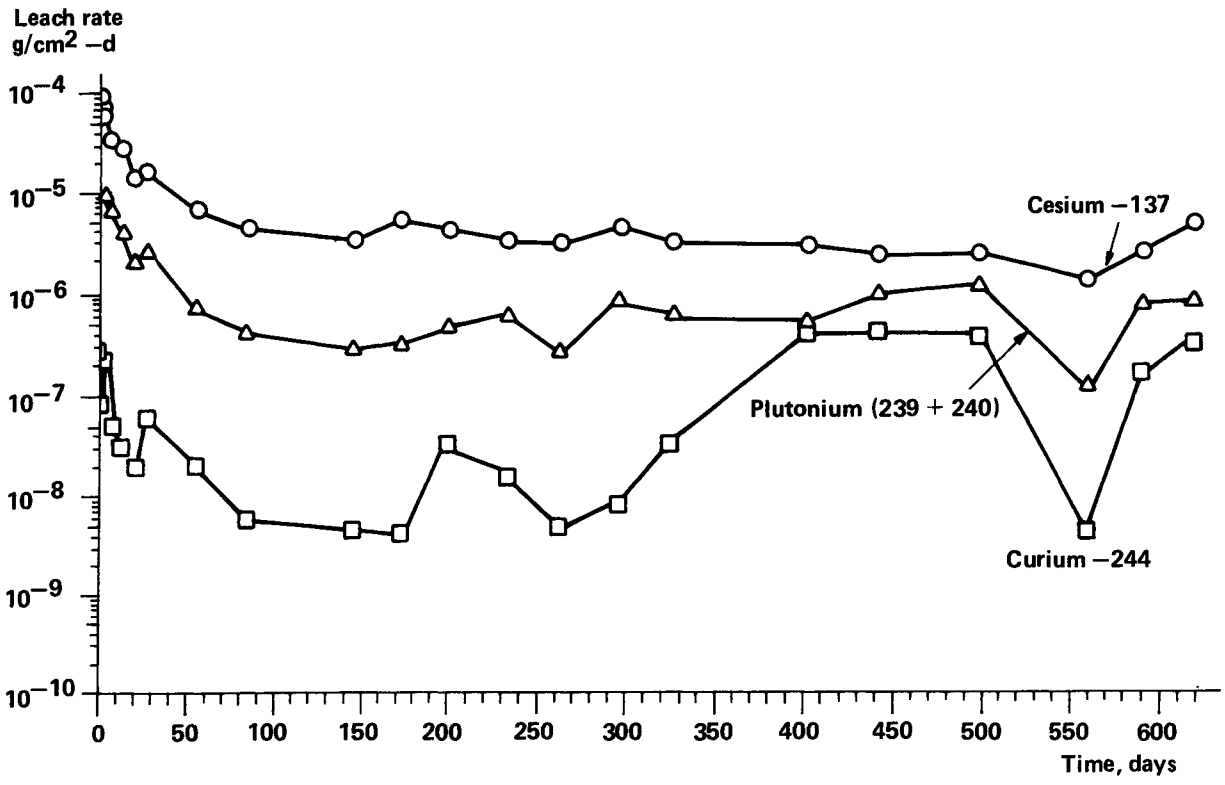

Figure 6-2. The graph shows the leach rate of irradiated LWR fuel, 54 400 MWD/MTU, based on radionuclides indicated.

the spent fuel is several orders of magnitude lower than the rate obtained from dynamic leaching trials with a "free" supply of water.

6.2 LEACHING OF FUEL

6.2.1 Experimental studies, general

During the 1950s, certain studies were conducted on the dissolution of irradiated uranium dioxide in carbonate solutions /6-1, 6-2/. These tests were related to the extraction of uranium from ores by carbonate leaching. The results are of only limited interest for the direct disposal of spent nuclear fuel. This is also true of more recent studies of the dissolution rate in water of samples of the mineral uraninite /6-3/.

In 1975, tests with irradiated uranium dioxide fuel were begun at Battelle Pacific Northwest Laboratories, Richland, USA (BNWL) in order to measure the leaching rate for directly deposited spent nuclear fuel /6-4, 6-5/.

KBS has also sponsored leaching tests at Studsvik on spent nuclear fuel from a Swedish power reactor /6-6/.

6.2.2 Studies at Battelle, Pacific Northwest Laboratories

The American tests were carried out on pellet fragments from light water reactor fuel which had been irradiated to an average burnup of 54 450 MWd/MTU. The uranium was enriched from the start to 5.81% uranium-235 and the pellets had 93.6% theoretical density. The total irradiation time was 32 800 hours, of which 27 800 at full power.

The leaching tests were carried out at 25°C. Three different types of water was used: groundwater from the Hanford area, deionized water and building distilled water.

In figure 6-1, the leaching rate for cesium-137 has been plotted as a function of time. For the purposes of comparison, the results of a test carried out at BNWL with borosilicate glass containing high-level waste have also been plotted (curve WSEP SS-13). According to the curves, dissolution from irradiated LWR fuel is greater than dissolution from vitrified high-level waste to start with, but after a month or so, it drops down to the same level and then falls somewhat lower. It should be noted in this connection, however, that the borosilicate glass which was used as a comparison was vitrified in 1970 and that current glass compositions exhibit leaching rates which are up to a factor of 10 lower.

The analyzed nuclides exhibit extremely different leaching rates. The values for the dissolution of cesium are about 1 000 times higher than those for curium to start with. The value for plutonium is between these two. This is shown by figure 6-2, which depicts leaching in deionized water for slightly more than 600 days. (The test series with deionized water was continued after other tests had been interrupted). The curves show a relatively

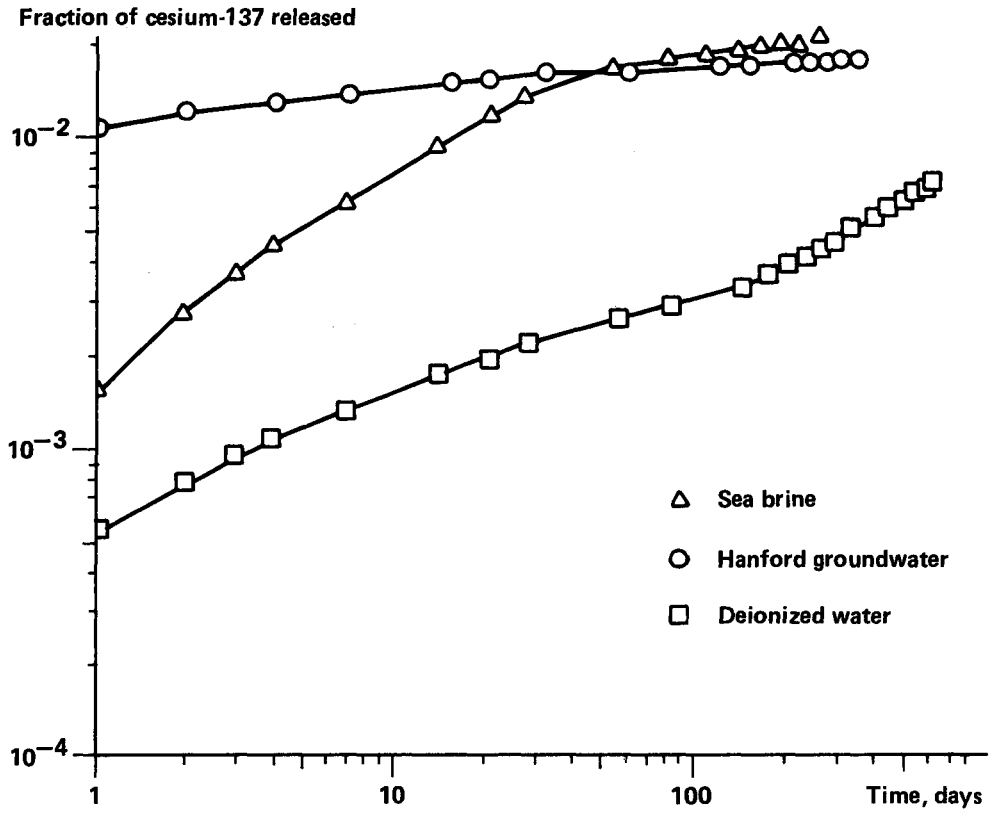

Figure 6-3. The graph shows the fraction of cesium-137 released to leachant.

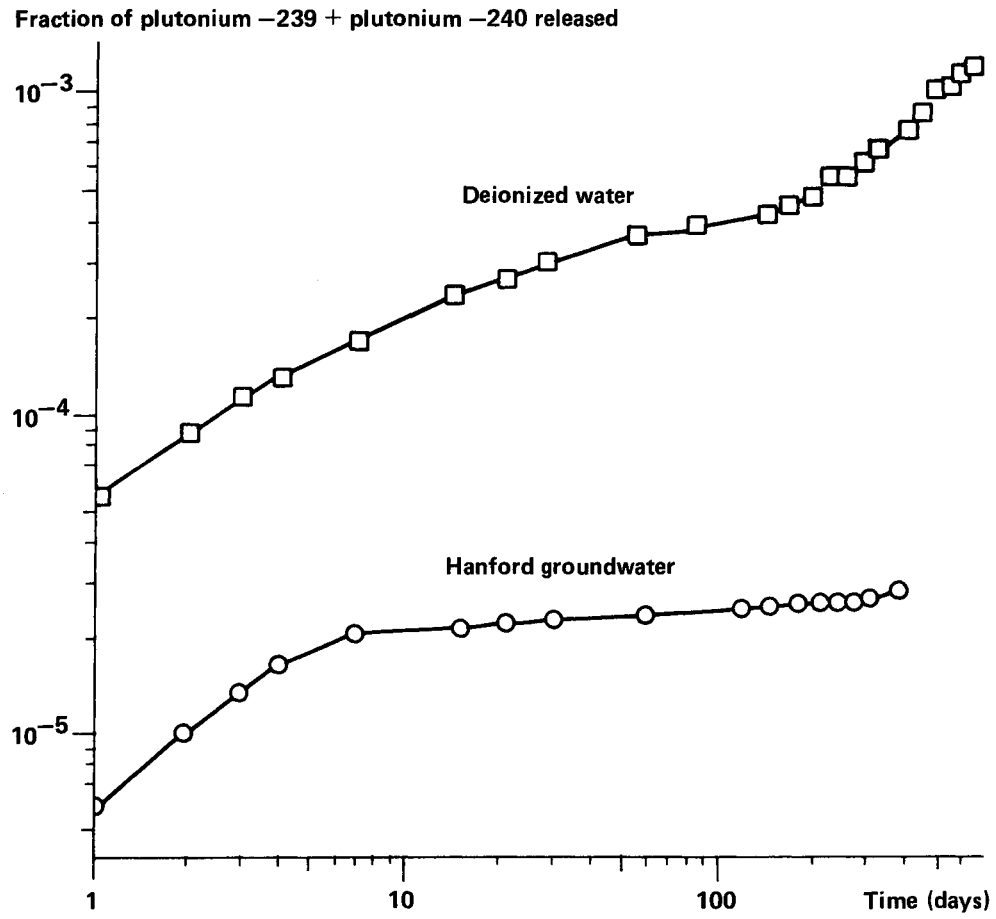

Figure 6-4. The graph shows the fraction of plutonium released to leachant.

slight increase of the leaching rate for cesium towards the end of the period. But the leaching rate is lower than during the first weeks. The same applies for plutonium, while the leaching rate for curium according to the curve is very irregular.

Another way to illustrate leaching schematically is to plot the fractional release of various nuclides as a function of time. The leaching of cesium and of plutonium is depicted in this manner in figures 6-3 and 6-4. As these figures show, approximately 1% of the cesium content is rapidly dissolved in groundwater. After 150 days, some 1.5% has been released. The portion of the plutonium which has been dissolved in the groundwater after 150 days is $3 \cdot 10^{-5}$. Leaching in deionized water differs considerably from leaching in groundwater; it is lower for cesium, higher for plutonium.

6.2.3 Studies at Studsvik

The leaching tests /6-6/ were carried out on 20 mm long sections of an irradiated fuel rod from reactor 1 at Oskarshamn. The sections-fuel with clad - were selected from axial locasions along the rod corresponding to average linear heat ratings of approx. 11 kW/m and 24 kW/m. The irradiation period was 902 days and the decay period two years. Of these specimens, one highly-rated and one output low-rated specimen were leached in distilled water and the other two specimens in groundwater, in all cases in a volume of 500 cm^3. The temperature was kept constant at $60^{o}C$ throughout the tests.

All the leached species which were measured showed relatively large initial leach rates - expressed as fractions leached per day of the total inventory - but towards the end of the leaching period, values of approximately 10^{-6}/d were obtained for uranium, strontium-90 and cesium-137 and approximately 10^{-7}/d for total alpha activity (fig. 6-5).

A comparison between the accumulated quantities which were leached out in 105 days from highly-rated and low-rated specimens revealed the greatest difference for cesium-137, where values of approx. 0.7% and 0.03%, respectively, of the total cesium-137 inventory were obtained (fig. 6-6). These values demonstrate the high load-dependence during reactor operation of the migration of cesium-137 to the gap between the pellet and the cladding and to peripheral cracks in the fuel.

6.2.4 Limitations of experimental studies

The studies at BNWL and at Studsvik differ in many respects, such as the fuel's burnup (and probably also the linear heat rating, the extraction of specimens (the cladding is included in the tests at Studsvik, so that radioactivity in the gap between the pellet and the cladding can be leached out), leaching temperature and circulation of the solution. Direct comparisons of the results are therefore impossible. With regard to the previous history of the fuel, specimen extraction and, to some extent, leaching temperature, the experimental programme at Studsvik can be considered to be more relevant to the penetration of groundwater into directly deposited fuel from light water reactors. In other

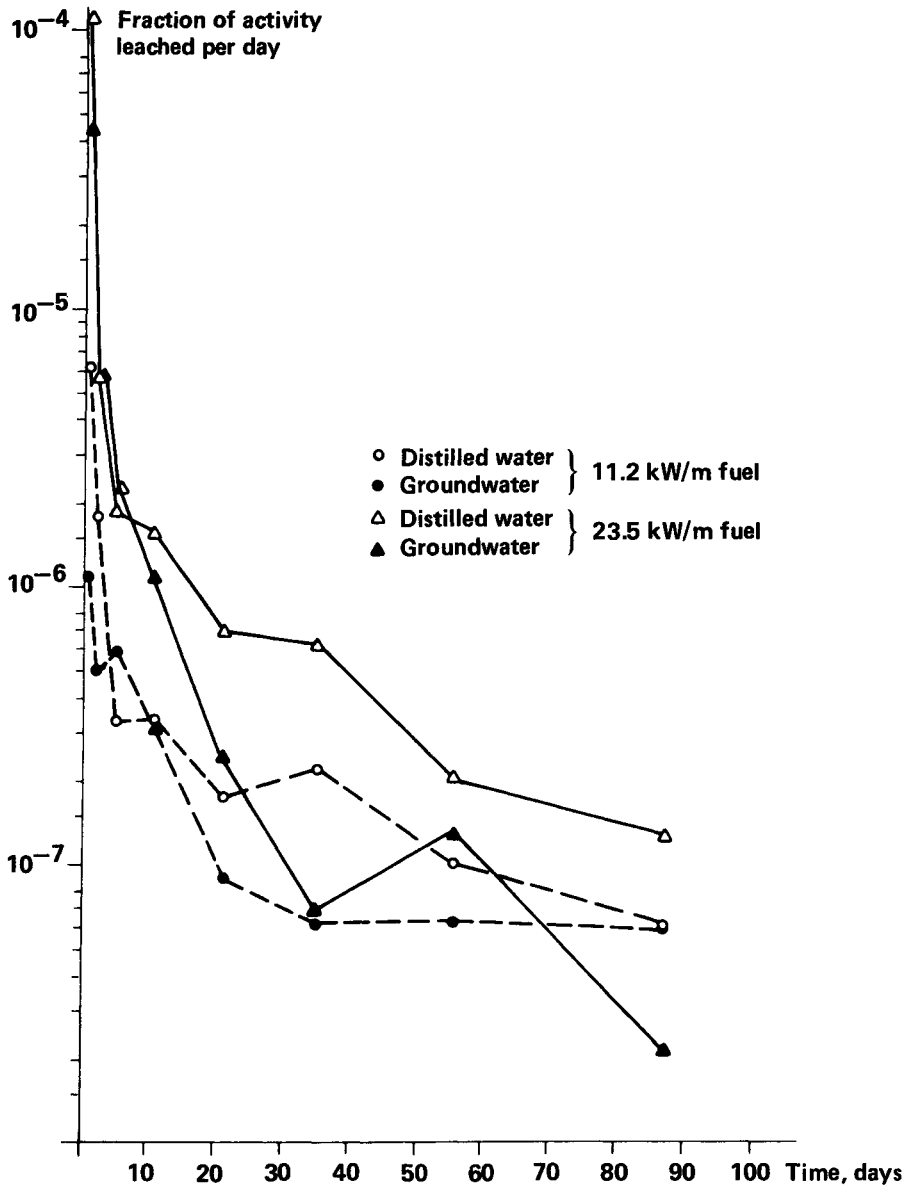

Figure 6-5. The graph shows the leach rate for alpha activity in distilled water and groundwater.

respects, especially the ratio water: fuel and the flow of the solution, it has not been possible in a short-term experiment to simulate the conditions which can be expected to exist in a repository when groundwater has penetrated all of the other barriers and has come into direct contact with the fuel.

The results of the few tests which have been conducted thus far must therefore be used with caution. Above all, it is of questionable validity to extrapolate the results over the long periods of time which are of interest in this context.

6.3 SOME POSSIBLE SEQUENCES OF EVENTS UPON WATER PENETRATING THE CANISTER

A repository for the direct disposal of spent nuclear fuel must be situated in bedrock where the groundwater flow is very slow. If the external barriers (copper, lead and zircaloy cladding) are

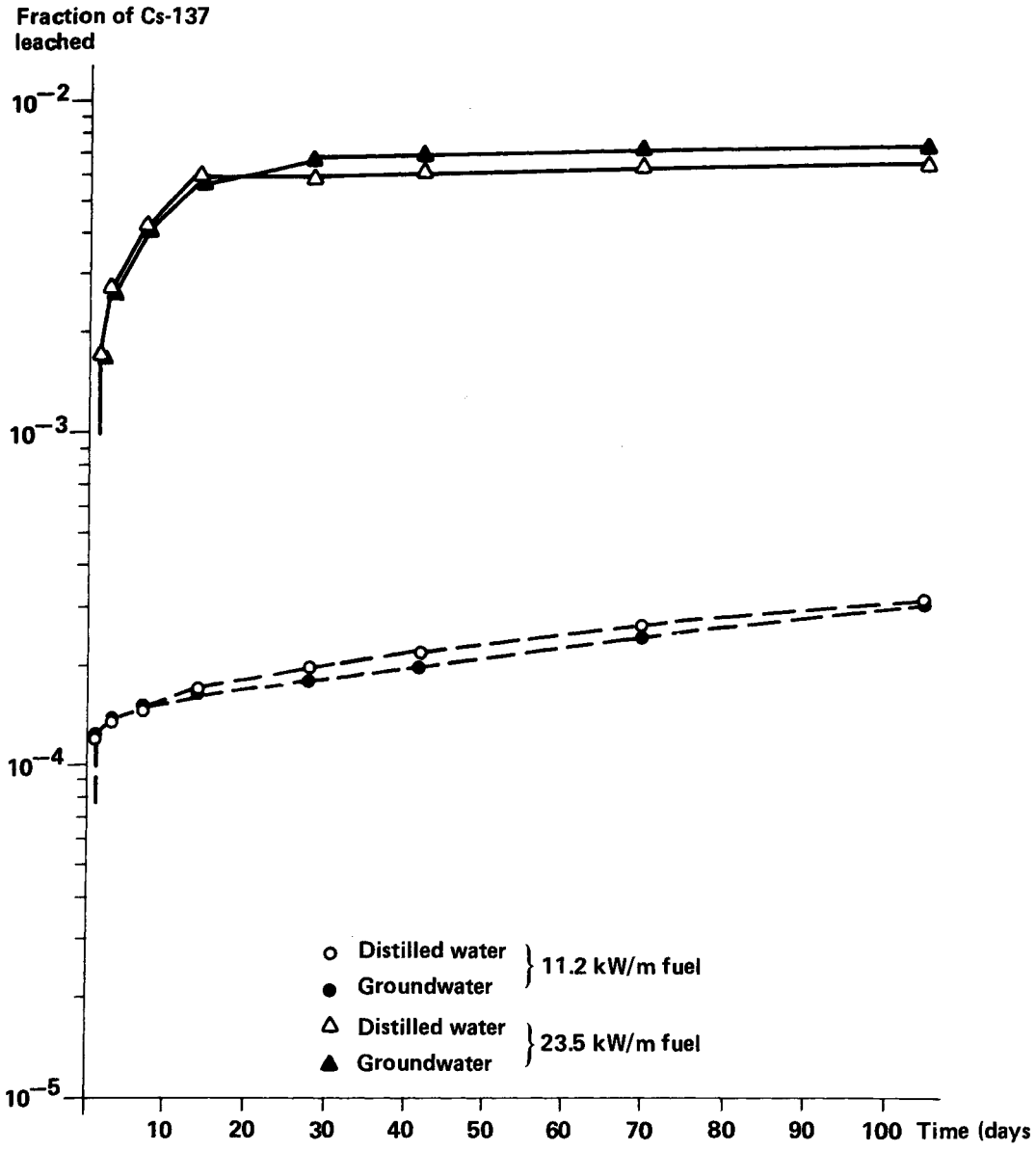

Figure 6-6. The graph shows the cumulative leaching of cesium-137 in distilled water and groundwater.

penetrated, water will come into contact with the uranium dioxide fuel. Water will penetrate into the space between the fuel and the zircaloy cladding and into cracks in the pellets. Oxidizing products formed by the radiolysis of water could then oxidize the uranium dioxide. The extent of this oxidation depends upon:

- the type and amount of radiation in nearby layers of water
- absorption in these layers
- the type and amount of radiolysis products which are formed
- how great a portion of the radiolysis products reach the uranium dioxide surfaces without having lost their reactivity on the way as a result of recombination or reaction with redox systems other than uranium
- how great the yield for the reaction between uranium oxide and (especially the oxidizing) radiolysis products will be.

The type and amount of radiation coming from the spent fuel changes greatly with time. The intensive gamma and beta radiation

declines relatively quickly. After 500 - 1 000 years, the alpha radiation will therefore dominate. The alpha radiation has a short range. In a relatively intact uranium dioxide pellet, only a very small portion of the alpha radiation will reach the water. On the other hand, the radiolysis caused by the alpha radiation will occur in a thin layer adjacent to the surface of the uranium dioxide. Oxidizing radiolysis products are therefore only a short distance away from their attack target. They may oxidize the uranium dioxide surface to some extent. Surface layers which have been oxidized to hexavalent uranium can be dissolved in the form of carbonate complexes in the groundwater. New uranium dioxide surfaces are thereby exposed for attack by the oxidizing radiolysis products. These oxidizing attacks can lead to a widening and lengthening of existing cracks and the formation of new cracks. This leads to increased radiolysis of the water, increased oxidation of the uranium, widening of cracks etc. This could conceivably result in disintegration of the uranium dioxide fuel, resulting in the exposure of a large surface area to inflowing water.

In the long run, the alpha decay in the fuel, with its accompanying helium formation, may also contribute towards the formation of cracks in the uranium dioxide matrix.

Each alpha particle collides with a limited number of uranium and oxygen atoms in the uranium oxide. If these atoms are close enough to the interface between the uranium oxide and the water, some atoms may go over to the aqueous phase ("sputtering"). Other nuclides could be affected to approximately the extent to which they are present in the matrix. The zone around the alpha track is chemically reactive. The water can therefore corrode the uranium dioxide at those points where the alpha particles have penetrated the surface. This can especially be the case if the water contains free radicals resulting from radiolysis /6-7/.

When water is radiolysed, reducing products can also be formed, which can counteract the above-sketched course of events.

The grain size of the irradiated uranium dioxide can vary, especially in the radial direction. This probably also causes a variation of the oxidation rate and of the tendency for the fuel to crack.

As long as most of the zircaloy cladding is left, it has some impeding effect on water penetration and water turnover and on the increase in volume which heavy oxidation would lead to.

On the basis of present knowledge, it is not possible to estimate the rates for all of these processes at different points in time. However, preliminary calculations indicate that the effects of "sputtering" will be insignificant within the time period of interest /6-7/. The oxidation resulting from the radiolysis of water caused by the alpha radiation is more difficult to assess /6-8, 6-9/.

6.4 LIMITATIONS ON LEACHING OF CERTAIN NUCLIDES BY GROUNDWATER

6.4.1 Uranium

The reactions and courses of events sketched in the preceding section are, as was mentioned above, very difficult to quantify. It may then be asked whether there are not any limitations on leaching of another nature - limitations which are easier to calculate. As was stated above, the leaching of oxidized uranium by groundwater is determined by the composition of the water. The carbonate content of the water would seem to be the dominating factor, since hexavalent uranium forms strong carbonate complexes /6-1, 6-2, 6-3/.

Carbonate contents of 150-300 mg/l are normal for groundwater at great depth in granitic bedrock /6-10/. But if the carbonate content of the groundwater is as high as 550 mg HCO_3/l and uranium goes into solution primarily in the form of the bicarbonate complex of hexavalent uranium, $UO_2(CO_3)^{2-}_2$, a maximum of 1 070 mg uranium/l can be maintained in solution. Each copper canister contains 1.1-1.4 tonnes of uranium. The leaching-out and carrying-away of this amount of uranium would require 1.4-1.8 million years, if the flow rate for the groundwater in the surrounding rock is 0.2 litres per m^2 and year /6-24/.

6.4.2 Radium

Uranium-234 (half-life 247 000 years) decays to thorium-230 (half-life 80 000 years), which in turn decays to radium-226 (half-life 1 600 years). The radioactivity from radium-226 is low upon discharge from the reactor, $1.1 \cdot 10^{-8}$ Ci per tonne uranium. It then rises, reaches a maximum of about 1 Ci per tonne after about 300 000 years and then declines, but levels out at a relatively high level, 0.3 Ci per tonne /6-11/.

If water comes into contact with spent fuel, it can dissolve radium-226 directly as well as thorium-230 or uranium-234 (and uranium-238), which eventually decay to radium-226. However, most of the radium which is dissolved directly decays before dissolved uranium or thorium have had time to build up radium-226 to any appreciable extent.

Radium forms sulphate of low solubility. The solubility product of $RaSO_4$ is $4 \cdot 10^{-11}$ /6-12/. Sulphate concentrations of a few mg/l up to approx. 50 mg/l have been measured in groundwater at great depth in granitic bedrock /6-10/. Assume that the sulphate content is as low as 1 mg/l. The radium content will then be about 1 mg/l, which corresponds to 1 m Ci/l. The sulphate content of the groundwater thereby sets an upper limit for the leaching of radium directly from the spent fuel.

6.4.3 Iodine

The only iodine isotope which is of interest in this context is iodine-129 (half-life 17 million years). Its radioactivity amounts to 0.038 Ci per tonne uranium in the fuel. It is virtu-

ally constant for the first few million years, after which it starts to decline very slowly /6-11/.

If iodine were to go into solution only to the extent that the uranium dioxide matrix of the fuel is oxidized and dissolved by the carbonate in the water, then leaching would be slow. However, iodine compounds tend to accumulate in the space between the fuel and the cladding as well as in the peripheral parts of the fuel, which are at lower temperature during reactor operation. A more rapid leaching of iodine by the water must therefore be expected during an initial phase. The leaching rate after this initial period can then be expected to drop to a level determined by the uranium leaching; but only under the assumption that the matrix of uranium dioxide does not disintegrate rapidly due to oxidation so that a large surface area is exposed to water.

As far as iodine is concerned, it cannot be assumed that any component in the groundwater which may leak into the fuel will set a reasonable upper limit on leaching from the spent nuclear fuel.

6.4.4 Plutonium

The total plutonium content of PWR fuel upon discharge from the reactor is approximately 11 kg per tonne, with the following breakdown /6-11/:

Plutonium isotope	g/t
238	150
239	6 390
240	2 340
241	1 550
242	440
	10 870

Thus, plutonium-239 dominates quantitatively. If plutonium were released to the same extent as the uranium dioxide matrix is oxidized and dissolved by a carbonate level of 550 mg/l in the groundwater (1 070 mg uranium/l maximum), the maximum plutonium level would amount to about 10 mg plutonium per litre.

This presumes that plutonium is evenly distributed in the fuel, which is not quite true /6-14/.

The total level of soluble plutonium has been estimated to be about $2 \cdot 10^{-3}$ mg/l /6-13/. Thus, the composition of the groundwater limits the concentration of plutonium in actual solution to low levels. However, plutonium could also cenceivably come out into the groundwater in colloidal or particulate form. But all of these different forms of plutonium have a great tendency to adhere to mineral surfaces /6-15/.

6.5 MASS TRANSPORT IN THE BUFFER MATERIAL

6.5.1 Transport mechanisms, general

Some material transport will take place to or from the canister through the clay which constitutes the buffer material around the copper canisters in the final repository. Oxidizing substance in the form of dissolved gases or ions as well as other components in the groundwater can be transported into the outer surface of the canister. In the event of canister failure, the radioactive nuclides in the waste can be transported away from the canister.

In order to be able to estimate the magnitude of this mass transport, the borehole with surrounding fissures has been assumed to conform to the model illustrated in fig. 6-7. In the calculations, the fissures have been assumed to run perpendicular to the axis of the borehole and to be of infinite length. Other orientations have also been studied. The width of the fissures and their internal spacing have been assigned different values on the basis of measurements of the permeability of the undisturbed rock. Clay from the borehole is assumed to have penetrated out into the fissures to a certain distance.

6.5.2 Flow

Beyond the clay in the fissures, the groundwater flows at a velocity which is determined by the hydraulic gradient (i m/m), the

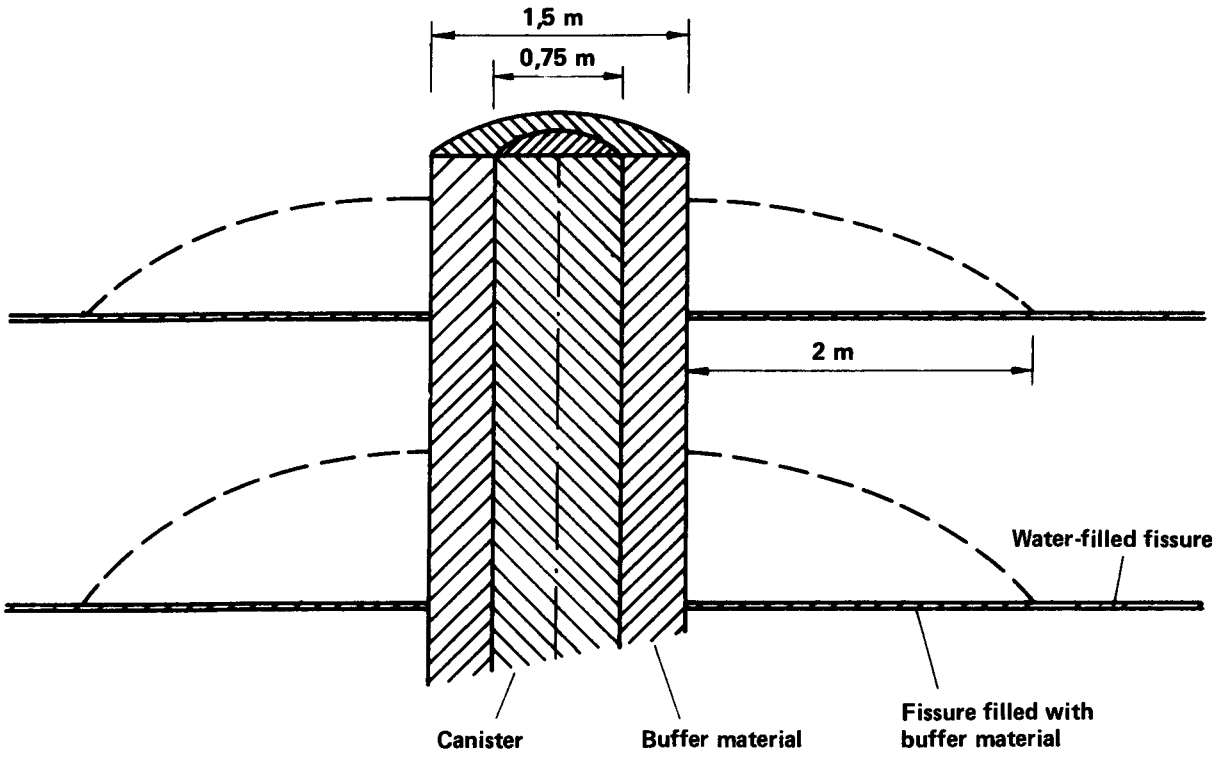

Figure 6-7. Model for calculations of mass transport between canister and water in rock fissures.

permeability of the rock (K_p m/s) and the porosity of the rock (ε m^3 fissures/m^3 rock) in accordance with Darcy's equation:

$$U_p = K_p \cdot i/\varepsilon \text{ m/s}$$

The permeability of the clay is much lower than of the host rock:

$$K_p < 10^{-13} \text{ m/s /6-18/.}$$

Besides the hydraulic gradient in the clay, a thermally induced hydraulic gradient i_{th} can also arise as a result of the heat generation which takes place in the canister. The magnitude of this gradient has been estimated /6-19/. At the highest temperature gradient which will occur and the highest temperature at the canister wall, 80°C, $i_{th} = 1.5 \cdot 10^{-3}$ m/m. This value is of the same order of magnitude as the hydraulic gradient in the rock ($i \approx 3 \cdot 10^{-3}$ m/m). If the permeability of the clay is of such an order of magnitude that groundwater flow stemming from the hydraulic gradient can be neglected, then the thermally induced flow is also negligible.

6.5.3 Diffusion

Besides flow, when the entire mass of liquid moves, mass transport can take place by the diffusion of individual substances under the influence of a concentration gradient. The diffusion rate depends on the nature of the substances (and in the case of ions, on the presence of other ions as well) /6-20/ and on the temperature /6-16/.

Diffusion can take place in the water absorbed in the clay. The diffusion rate at a given concentration gradient - the diffusivity is much lower here than in water alone, owing to a reduction of the available area, the tortuosity of the channels and retardation due to sorption of the diffusing substance.

Measurements of diffusivity for methane, cesium and strontium in compacted bentonite /6-21, 6-22/ have shown that the value in the clay is approximately 1/100th of the value in water. The diffusivity in the clay in the fissures has been set at 1/5th of the diffusivity in water, since the clay there is not so compact.

It follows from these data that mass transport by diffusion is considerably greater than transport by flow over distances of a few meters.

6.5.4 Ion exchange and other sorption mechanisms

Some of the substances which diffuse through the clay are retarded owing to various sorption mechanisms. These include ion exchange, where it is mainly the Na ions in the clay which are exchanged for other cations in the groundwater, or adsorption on the clay. Since sorption is a reversible process, the sorbed substances will be desorbed again if their concentration in the aqueous phase decreases. At the low concentrations with which we are dealing here, the ion exchange and adsorption equilibria can be considered to be linear, i.e.

$$q_A = K_d \cdot C_A$$

where q_A is the concentration of the substance sorbed on the solid material, C_A is the concentration of the substance in the aqueous phase and K_d is a constant /6-23/.

The substance which diffuses through the clay will be retarded in transit owing to sorption until equilibrium is established. Only then will the substance migrate further. Retardation increases as the value of K_d increases.

The solubility of certain substances is so low that the solubility product is reached. These substances cannot be transported in water in higher concentrations than their solubility permits. They are greatly retarded at high total concentrations and less at low concentrations. At concentrations below the solubility limit, they are retarded by means of the same mechanism as other sorbing substances.

The concentration profile in the clay is described by either curve 2 or curve 3 in figure 6-8 /6-23/. Curve 1 illustrates the ideal case, where neither dispersion nor diffusion occur, flow alone is transporting the nuclides. Which of the curves 2 or 3 gives the truest picture of the situation depends on whether mass transport is due solely to diffusion or whether flow must also be taken into consideration. In this case, when diffusion can be regarded as being dominant, curve 3 will describe the situation most accurately.

6.5.5 "Film resistance"

When a substance is transported over a phase interface, in this case between the water in the clay and the flowing water in the fissures, there is a certain resistance to this mass transfer across the interface. This is due to the fact that the substance only has time to diffuse a limited distance out into the water during the time it takes for the water to pass. The concentration profile at the phase interface is shown in figure 6-9. The mass transfer resistance is localized to an imaginary "film" next to the phase interface. In this "film", the concentration of the substance changes from that which prevails in the phase interface to the concentration in the free aqeous phase. At the retention times which are possible in this case, the liquid within a metre or so of the clay will absorb (or be depleted of) the substance in question /6-24/.

6.5.6 Relative importance of the different barriers

Diffusivity in the compacted clay in the storage hole is low, limiting the rate at which a substance can be transported per unit surface area. Diffusivity in the clay in the fissures is higher due to the fact that the clay there has swelled compared with the clay in the hole. In the fissures the available area for diffusion is, however, many times less. This more than compensates for the higher diffusivity, provided that the depth of the clay in the fissures is of the same order of magnitude as in the hole. The "film resistance" at the retention times in question offers greater resistance than the clay in the hole. This is

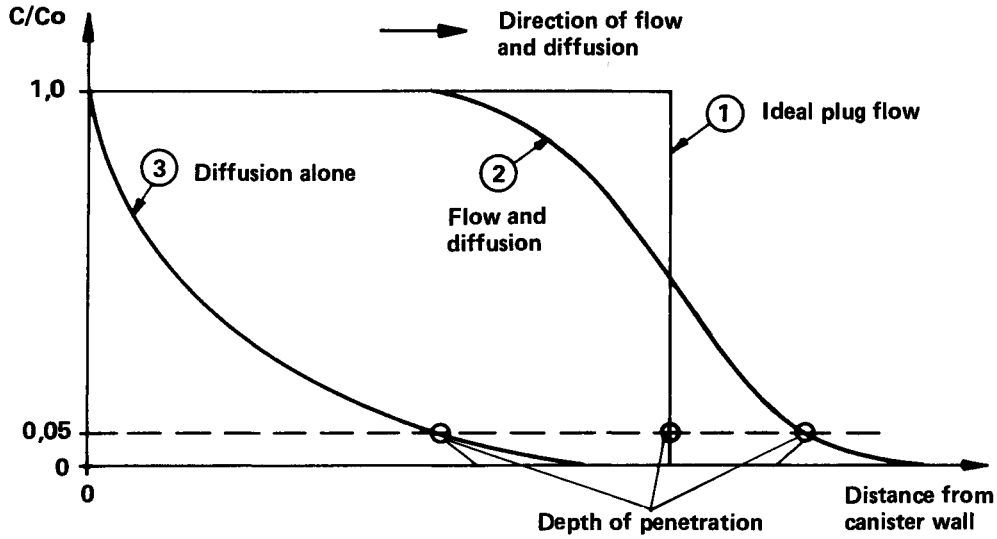

Figure 6-8. The concentration profile in the clay for »plug flow» diffusion alone and a combination of flow and diffusion.

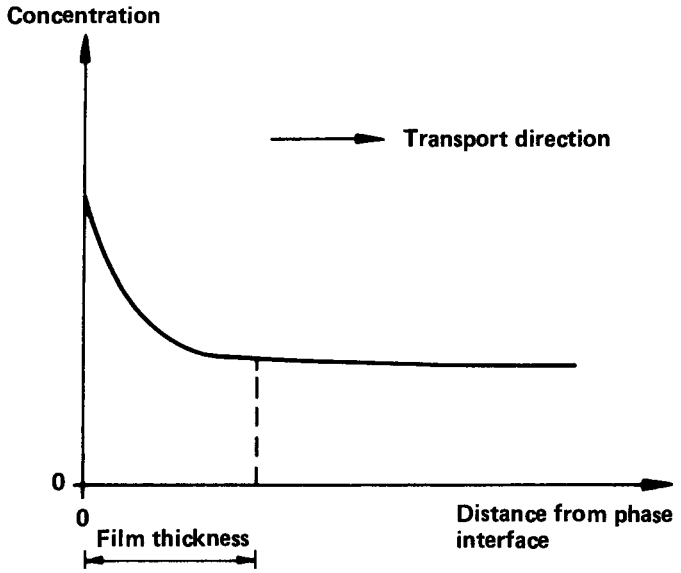

Figure 6-9. The concentration profile in the aqueous phase at a phase interface. Outward transport of the substance.

shown in table 6-1, which shows the relative importance of the various resistances in columns 7-9. For the central case - 5 - the resistance in the film is about 7 times more important than the resistance in the clay in the hole. No resistance at all is accredited to the clay in the fissures in the following calculations, since it cannot be guaranteed at the present time that all fissures will always be filled with clay.

6.6 DISSOLUTION OF THE URANIUM OXIDE MATRIX FOLLOWING CANISTER PENETRATION

6.6.1 General

The spent fuel rods consist mainly - 95% - of uranium dioxide, UO_2. In the event of canister penetration, water will penetrate into the UO_2 matrix and gradually dissolve it.

6.6.2 Dissolution of UO_2 in groundwater

The solubility of uranium in groundwater is determined by the composition of the water, especially as regards salt content, pH and redox potential /6-12, 6-13/.

The uranium is quadravalent in the uranium oxide. Quadravalent uranium has very low solubility in the types of groundwater in question, where the redox potential is such that the quadravalent state is maintained. This solubility has been calculated to be about 2 µg/l at pH 8. Uranium could conceivably be oxidized from a quadravalent to a hexavalent state due to radiolysis. Hexavalent uranium has a much higher solubility in the waters in question here.

6.6.3 Dissolution related to carbonate level

A limiting factor for the amount of uranium which can be dissolved is the water's carbonate content. Hexavalent uranium forms strong complexes with carbonates /6-12, 6-13/.

Solubility is based on measured carbonate levels in groundwater /6-10/ and the assumption that each uranium atom binds two carbonate ions. With a carbonate content of 550 mg/l, a solubility corresponding to 1 070 mg U/l is obtained.

This approaches the level of cations in the Gulf of Bothnia.

In a study of the uranium level in groundwater in uranium mines in Czechoslovakia, Paces /6-25/ has measured less than 0.1 mg U/l under reducing conditions (Eh < 0) and 9 mg U/l under oxidizing conditions and a carbonate level of the same order of magnitude as in Swedish groundwater.

Russian studies (section 3.5) reveal similar conditions. The water in these studies has migrated from areas with oxidizing conditions where the water has a high uranium content, through a zone where uranium is precipitated out and into an area with reducing conditions. The level of uranium in the water decreases there to very low values, less than 0.05 mg U/l. At the depth at which the repository is to be located, the water is reducing and uranium solubility should then be less than 0.05 mg U/l. These observations are in good agreement with calculated solubilities /6-13/.

The dissolution time for uranium has been calculated for various combinations of fissure width, water velocity, fissure spacing and clay depth in fissures, table 6.1.

In calculating the uranium dissolution, it has been assumed that there is nothing left of the canister wall, i.e. that the entire surface of the canister is accessible for mass transfer. It has also been assumed that there is no mass transfer resistance in the degraded canister wall. These assumptions lead to an overestimation of the dissolution rate, since the canister's corrosion products constitute a diffusion barrier. Furthermore, it is very improbable that the copper will corrode within the time span under consideration. If a hole were created in the canister, it

Table 6-1. Uranium diffusion from the repository.

Case	U_o	2b	S	Z_c	N/LΔC	Relative mass transfer resistance			Time to carry off all uranium, years	Time for concentration of easily soluble nuclides in canister to decline to half
	m/year	mm	m	m	g/year,m,g/m^3	Clay in borehole	Clay in fissures	Film resistance		t_a years
1	$1 \cdot 10^{-3}$	0.1	1	0	$30 \cdot 10^{-5}$	1	0	3.2	$0.90 \cdot 10^{6}$	1 000
2	$1 \cdot 10^{-3}$	0.1	1	2	$0.6 \cdot 10^{-5}$	1	204	1.7	$44 \cdot 10^{6}$	30 000
3	$1 \cdot 10^{-3}$	0.2	0.4	0	$55 \cdot 10^{-5}$	1	0	1.7	$0.49 \cdot 10^{6}$	500
4	$1 \cdot 10^{-3}$	0.2	0.4	2	$2.9 \cdot 10^{-5}$	1	49	0.9	$9.1 \cdot 10^{6}$	6 000
5	$2 \cdot 10^{-4}$	0.1	1	0	$15 \cdot 10^{-5}$	1	0	7.1	$1.8 \cdot 10^{6}$	2 000
6	$2 \cdot 10^{-4}$	0.1	1	2	$0.6 \cdot 10^{-5}$	1	204	3.7	$45 \cdot 10^{6}$	30 000
7	$2 \cdot 10^{-4}$	0.2	0.4	0	$31 \cdot 10^{-5}$	1	0	3.9	$0.86 \cdot 10^{6}$	1 000
8	$2 \cdot 10^{-4}$	0.2	0.4	2	$2.9 \cdot 10^{-5}$	1	49	2.0	$9.3 \cdot 10^{6}$	6 000

U_o = bulk flow velocity for groundwater in rock, m^3/m^2, year

2b = fissure width mm

S = spacing between fissures m

Z_c = length of fissure which is filled with clay m

N/LΔC = amount of component transferred per m canister at concentration difference 1 g/m^3

would certainly be very small in relation to the total surface area of the canister.

The results of these calculations are presented in table 6-1. The time required to carry off 1.4 tonnes of uranium is 1.8 million years under oxidizing conditions. This time will be at least 5 000 times longer under reducing conditions.

The table also shows that the greatest mass transfer resistance is in the clay in the fissures, in those cases where the clay has penetrated out into the fissures. This is largely due to the fact that the cross-sectional area is very small in the fissures as compared to in the borehole.

6.6.4 Leaching of other nuclides

During the irradiation of the fuel in the reactor, some of the fission products have become concentrated in the outer parts of the fuel pellets and in the space between the pellets and the zircaloy cladding, the cladding gap. This applies especially to volatile elements and elements which are formed through the decay of volatile elements, such as iodine and cesium. The nuclide quantities in question here are so small (a kilogramme or less per tonne uranium) that the solubility product for their salts will hardly be reached, so that it is assumed that 100% of these nuclides dissolve immediately when the water enters.

Other nuclides which are embedded in the uranium oxide matrix are dissolved along with this matrix, since diffusion in the solid material is very slow at the prevailing temperature. This has been established by a study of uraninite crystals from a natural reactor in Oklo /6-26/.

Despite the fact that a formal oxidation of the uranium can take place while it is still in the solid lattice, the lattice structure will probably be retained. Regardless of the increase in the solubility of the uranium in carbonate-bearing water upon its transformation from the quadravalent to the hexavalent state, the kinetics for the breakdown of the crystal lattice probably also control the dissolution of the solid mixed oxide. A dissolution rate for uranium and plutonium which is proportionate to their concentration in the oxide matrix would appear to be reasonable, if lattice breakdown is assumed to be rate-determining. However, it is probable that uranium will be transported away from the immediate vicinity of the fuel more rapidly than plutonium, owing to possible oxidation of uranium and carbonate complex formation.

6.7 TRANSPORT OF NUCLIDES THROUGH THE BUFFER BARRIER

The buffer material will retard nuclide transport to a different degree for different nuclides owing to the fact that sorption effects for the different nuclides vary in magnitude. The influence of sorption can be expressed by means of the retention factor K_i /6-23/. This factor is the ratio between the velocity of a noninteracting species and the velocity of the nuclide in question. The retention factors for some nuclides of interest are presented in table 6-2 /6-24/. All data apply under oxidizing conditions.

Table 6-2. Retention time in the clay barrier for interesting nuclides.

Nuclide	Half-life years	Retention factor 1)	Retention time in clay in borehole, years 2)
Sr^{90}	28	1 000[4]	1 800
Tc^{99}	$2 \cdot 10^5$	1	2
I^{129}	$2 \cdot 10^7$	1	2
Cs^{137}	30	400[4]	700
Ra^{226}	$1.6 \cdot 10^3$	1 000[3]	1 800
Th^{229}	$7.3 \cdot 10^3$	4 000[5]	7 000
Np^{237}	$2 \cdot 10^6$	800[5]	1 400
Pu^{239}	$2.4 \cdot 10^4$	4 800[5]	8 400
Pu^{240}	$6.6 \cdot 10^3$	4 800[5]	8 400
Am^{241}	458	12 800[4]	22 400
Am^{243}	$7.4 \cdot 10^3$	12 800[4]	22 400

1) The porosity of the clay has been set at 0.25.

2) Diffusivity in the clay has been assigned a value of $6 \cdot 10^{-11}$ m^2/s for all nuclides /6-22/.

3) Assumed to be the same as for strontium.

4) From measured data for 100 % clay /6-13/.

5) Converted from measured data for clay/quartz mixture. 10/90, where the quartz has been assumed to be inert.

Figure 6-10 shows the dissolution curve for a nuclide with a retention factor of K_i. If t_{clay} is the time it takes for a noninteracting nuclide to diffuse through the barrier, it takes t_{clay} K_i after canister penetration for the nuclide to diffuse out through the clay so that a certain portion of the final maximum concentration is reached outside of the barrier. The concentration then increases for a period of time, after which it either immediately starts to decrease in the case of an easily soluble nuclide or level out in the case of a poorly soluble nuclide. The dissolution time, t_{diss}, is dependent upon the dissolution of the fuel, the mass transport velocity through all the barriers and on how much of the nuclide is originally present in the fuel.

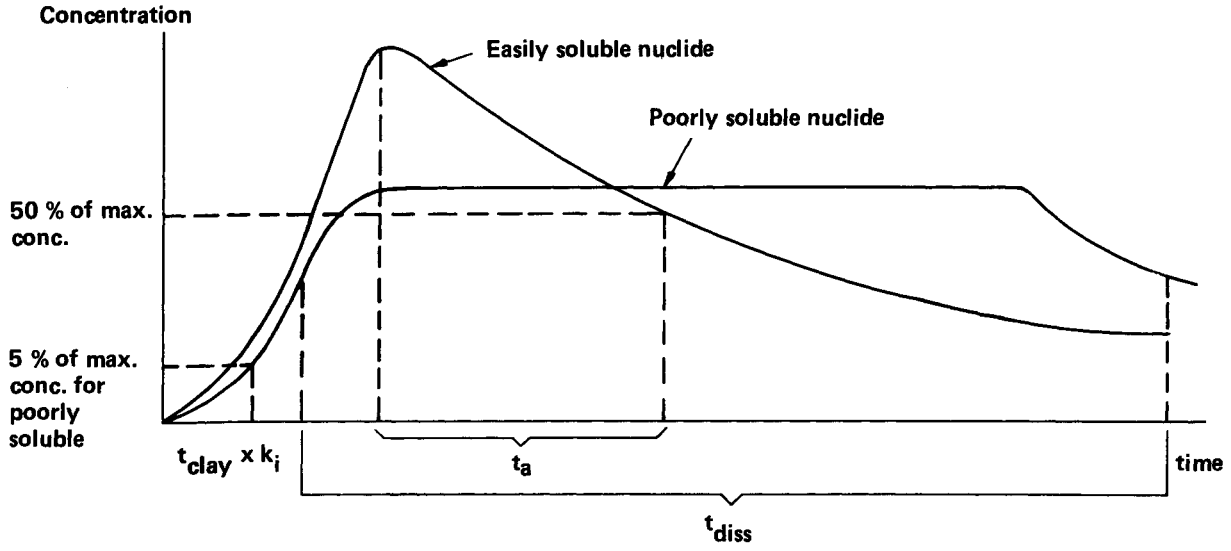

Figure 6-10. The nuclide concentration outside of the clay barrier as a function of time.

The retention time in clay $t_{clay}^{K_i}$ is given in table 6-2 for a number of nuclides of interest. It can be seen in the table that cesium-137, strontium-90 and americium-241 will have a retention time in the clay greater than 25 half-lives and will consequently have time to decay, while other nuclides will not have time to decay to any appreciable extent. They are retarded by the clay, but after a sufficiently long period of time, they will have passed through it.

The easily soluble nuclides which are not sorbed will be present at maximum concentration in the water at the instant when the water has just entered into the canister and dissolved them. Their concentration will then decline as the nuclides diffuse out. The concentration difference and therefore the material flow of these nuclides will therefore decrease with time. After a certain period of time, t_a, their concentration outside of the clay barrier will have decreased to half. This time is given in table 6-1 for small molecules such as iodine.

These times are short compared to the other periods of time involved in these studies and can in many cases be regarded as being equivalent to "instantaneous" dissolution.

6.8 SODIUM-CALCIUM ION EXCHANGE IN BENTONITE

The bentonite which is intended to be used in the buffer material contains a great deal of sodium bentonite. This material swells much more than calcium bentonite upon contact with water and has

a lower permeability and a larger specific surface area than calcium bentonite /6-27/.

When the groundwater contains calcium, the sodium bentonite will be partially converted to calcium bentonite by the exchange of the sodium in the bentonite for the calcium in the water.

The calcium content of the groundwater is not sufficient for any appreciable ion exchange to take place when the clay has just been wetted; most of the calcium must diffuse in from the flowing water.

The time required to exchange all sodium for calcium has been estimated /6-24/. The ion exchange capacity has been taken from the supplier's specifications. It has been assumed in the calculation that all sodium, approximately 0.6 mequiv/g clay, has been replaced by calcium.

The clay in the fissures is converted in roughly 10 000 years, at a clay depth of 2 m. It has also been assumed in the calculations that the only mass transport resistance consists of film and diffusion resistance for Ca^{2+}. The results of these calculations are presented in table 6-3. With these suppositions, a complete

Table 6-3. Time required for sodium-calcium ion exhange in the bentonite.

Case	U_o m/year	2b mm	S m	Z_c m	Time for ion exhange, years in fissures	total
1	$1 \cdot 10^{-3}$	0.1	1	0		$1.6 \cdot 10^6$
2	$1 \cdot 10^{-3}$	0.1	1	2	10 000	$115 \cdot 10^6$
3	$1 \cdot 10^{-3}$	0.2	0.4	0		$0.7 \cdot 10^6$
4	$1 \cdot 10^{-3}$	0.2	0.4	2	12 000	$26 \cdot 10^6$
5	$2 \cdot 10^{-4}$	0.1	1	0		$3.8 \cdot 10^6$
6	$2 \cdot 10^{-4}$	0.1	1	2	12 000	$116 \cdot 10^6$
7	$2 \cdot 10^{-4}$	0.2	0.4	0		$1.6 \cdot 10^6$
8	$2 \cdot 10^{-4}$	0.2	0.4	2	15 000	$26 \cdot 10^6$

Diffusivity in water: $2 \cdot 10^{-9}$ m^2/s
Ion exchange capacity (Na): 60 mequiv/100 g clay
Density of wet clay in pores: 1 750 kg/m^3

ion exchange of all the clay in the storage hole takes 3.8 million years.

6.9 ANALYSIS OF VARIATION

The central case 5 in tables 6-1 and 6-3 has been selected without clay in the fissures, despite the fact that these fissures will be grouted with bentonite, since it is not impossible that new fissures may open in the rock due to thermal and other stresses. The water flow of 0.2 $1/m^2$ and year used in case 5 corresponds to a maximum value in sound rock at the depth in question. The high water flow rate of 1 $1/m^2$ and year in cases 1-4 is only judged to be possible in an extreme case where, for example, a local disturbance increases water passage in to a canister. The fissure frequency of 1 per metre and the fissure width of 0.1 mm in the vicinity of the canister correspond to a permeability in the vicinity of the hole which is approximately 1 000 times greater than the permeability of the undisturbed rock, and a porosity in water-bearing fissures which is approximately 10 times higher than in undisturbed rock. These relatively high values have been chosen in lieu of sufficient measured data so that these factors will not be underestimated. An even greater fissure frequency (2.5 per metre) and width (0.2 mm) have been used in cases 3, 4 and 7, 8. Even these high figures only increase the transport velocity by a factor of approximately 2. Compare, for example, case 7 with case 5.

If the rock should be extremely fractured and its porosity in the vicinity of the storage hole should be considerably greater, "film resistance" could decrease sharply. The greatest increase of the mass transport velocity which is possible is limited by the diffusion resistance in the clay in the storage hole. In the central case, the increase could never be greater than approximately 8 times, even if the film resistance were eliminated completely.

If the clay can be made to fill up any fissures which may open in the rock, mass transport will be greatly reduced. In case 6, where 2 m of clay has been deposited in the fissures, the transport velocity has been decreased to 1/20th of the value in case 5.

6.10 FINAL STORAGE OF THE FUEL'S METAL COMPONENTS

6.10.1 General

The radioactive metal components from the reactor are compacted and placed in concrete moulds, which are placed in a rock repository at great depth. The repository is filled with concrete. The moulds are cubical boxes with 1.6 m sides and 0.8-1.0 m cubic holes. A total of about 720 tonnes of metal - zircaloy-2 and -4, stainless steel and inconel-650 and -718 - will be deposited. In all, there are some 78 tonnes of different nickel isotopes. Nickel-59 above all must be prevented from reaching the biosphere. This nuclide has a half-life of nearly 80 000 years. Compared to nickel-59, other metals are of very little radiological importance.

After the repository has been sealed, groundwater will eventually come into contact with the waste. The metals in the repository will then be able to corrode and go into solution, offer which they will be transported out by the mechanisms described in sections 6.5 and 7.2.

6.10.2 Chemical environment in the repository

The concrete will determine the pH of the water in and around the repository. In an initial phase, the pH will be 13-14 as a result of the dissolution of small quantities of sodium hydroxide and potassium hydroxide. Then, during a second phase, the "free" calcium hydroxide in the cement will be dissolved and the pH will stabilize at 12-13. In a third phase, calcium will be dissolved out of silicate and aluminate. The pH of the groundwater will be around 10 during this phase /6-28/.

6.10.3 Corrosion

Nickel is a relatively noble (electro-positive) metal and may be stable in the environment in the repository /6-29/. Corrosion of the less noble metals is accompanied by hydrogen evolution, which has an inhibitory effect on the oxidation of nickel. It is nonetheless assumed in the following that nickel corrosion is not a limiting factor.

6.10.4 Solubility of nickel

Oxidized nickel will be bivalent in the environment in question. Bivalent nickel forms poorly soluble compounds with hydroxide, phosphate, sulphide and carbonate. Fulvic acids in the groundwater could conceivably form strong complexes with nickel and increase its concentration in the water. Phosphate and sulphide are present in such small quantities that they do not suffice to precipitate all the oxidized nickel. Nickel solubility will therefore be determined by the hydroxide. Within the pH range of 10-13 which prevails in the water in and immediately around the concrete moulds, the solubility of the hydroxide limits the nickel concentration to 0.1 mg/l /6-28/. If all available fulvic acid were to form nickel complex, the solubility of nickel could reach a maximum of 30 mg/l /6-28/.

6.10.5 Transport of nickel

The transport of nickel out through the concrete has been calculated using the same method as that used for the transport calculations in sections 6.5 and the following. It is hereby conservatively assumed that the nickel oxidation is not a limiting factor. If the repository is situated in rock which is of as good quality as that in which the fuel is stored, it will take 20 million years to transport all of the nickel out through the concrete. This applies at water flows in the rock of 0.2 l/m^2 and year and a nickel solubility of 30 mg/l. It is assumed that the concrete does not have through cracks.

When and if the concrete has decomposed or undergone extensive

cracking, the water will have direct access to the metal surfaces. Both diffusion resistance in the concrete and "film resistance" are then irrelevant and it is assumed that all of the water which reaches the tunnel becomes saturated with nickel. It would then take about 2.5 million years for the water to carry away all the nickel if the pH is still kept within the range 10-13. The water in the concrete will retain this pH as long as the concrete contains soluble hydroxide.

The concrete continuously gives off calcium hydroxide to the water in the rock. Transport calculations show that it will take at least 24 million years for the concrete to give up all its calcium hydroxid if the concrete has cracked and the water can flow freely through it.

The conclusion is that it will take at least 2.5 million years to leach out all of the nickel, even if the concrete barrier cracks apart immediately.

7 DISPERSAL MECHANISMS FOR RADIOACTIVE ELEMENTS

7.1 GENERAL

In order to achieve a safe terminal storage of the spent uranium dioxide fuel, the fuel is surrounded in the final repository by a number of consecutive barriers:

- uranium dioxide in itself is poorly soluble and chemically relatively stable. Most of the radioactive elements are bound to the uranium dioxide matrix,
- the uranium dioxide is enclosed in zircaloy cladding tubes,
- the fuel rods are encapsulated in copper cylinders with excellent corrosion resistance in the environment in question. Inside the canisters, the fuel rods are embedded in lead,
- the copper cylinders with the fuel rods are packed in a buffer material of low permeability - highly compacted bentonite,
- the final repository is situated in stable crystalline bedrock with a low groundwater flow at a depth of 500 m.

Metal scrap from the spent fuel is surrounded in its final repository by barriers of concrete and rock.

Each of these barriers provides protection against the dispersal of radioactive substances. The barriers possess different protective properties and thereby protective functions which both reinforce and complement each other. In order for a dispersal of radioactive substances to take place, the barriers must be penetrated and the radioactive substances must come into contact with water.

It is possible to differentiate between slow dispersal processes and events which lead to sudden dispersal. The latter type of events is extremely rare and is analyzed in section 8.7.

In order for the slow dispersal of radioactive elements to be possible at all, the groundwater must come into contact with the waste. Corrosion of the copper canister has been investigated in chapter 5. Leaching of the uranium dioxide and material transport through the buffer mass is analyzed in chapter 6.

The leaching of radioactive elements from metal components embedded in concrete moulds is discussed in section 6.10.

This chapter describes various mechanisms for dispersal in rock and in the biosphere.

Dispersal in rock takes place through water flow and diffusion in rock fissures or in the tunnel fill of quartz/bentonite. Through chemical reactions between the radioactive elements and the rock mass, fissure-fillers or tunnel filler, the radioactive elements are retarded in relation to the water flow. Sections 7.2 and 7.3 discuss various factors which influence dispersal. The results of dispersal calculations are reported in section 8.5.

If the radioactive elements break through the various barriers, they can eventually come into contact with the biosphere. In this case, they will be dispersed via the groundwater to a primary water recipient, which may be a well, a lake or part of the sea. From this primary recipient, the elements can then disperse into the biosphere via a large number of paths. In section 7.4, the model which is used to analyze dispersal in the biosphere is described. The model calculates radiation doses to human beings. The calculation results are given in section 8.6.

7.2 GROUNDWATER FLOW

7.2.1 Background

Groundwater in the rock is the transport medium via which oxidants and salts can be transported to the canister and via which soluble corrosion products and any escaping nuclides can be transported to the biosphere.

The regional water flow is of great importance in determining the transport paths of the water and its residence times in the rock. The local flow rate and residence time of the water in the rock at the repository is of great importance in determining the quantity of substances which can be transported to and from the repository.

Groundwater conditions in the Swedish bedrock have been described in section 3.4. A resumé of the factors which must be taken into consideration in calculating the dispersal of radioactive elements is provided here.

7.2.2 Regional water flow

Near the ground, the rock is often riddled with interconnected fissures. The measurements which have been performed at greater depth /7-1/, however, reveal large areas of sound rock - often 20-50 m or more in depth - in which it has not been possible to measure water losses using available methods. See also chapter 3. Permeability in these areas is less than 10^{-9} m/s. The flow rate in the highly fractured surface rock can be described fairly well by Darcy's equation:

$$q = A \cdot K_p \cdot i \qquad (1)$$

where

q = the water flow rate m^3/s,
A = the cross-sectional area m^2,

K_p = the permeability m/s,
i = the hydraulic gradient m/m.

With the aid of Darcy's Law, the water flow through the repository can be calculated. Such calculations have been carried out /7-2, 7-3/ for a large number of combinations of hydraulic gradients and permeabilities. The permeabilities have thereby been varied in depth and given different values in vertical and horizontal directions. Calculations /7-2/ show that the water flow rate through the repository is approximately 1 litre per m^2 and year (l/m^2 . year) at a permeability of 10^{-8} m/s, while it can be considerably lower at lower and with depth decreasing permeabilities. Calculations have also been carried out /7-2/ for a case where the rock around the tunnels is highly fractured and has a permeability of $3 \cdot 10^{-3}$ m/s. This means in practice that the fractured rock does not offer any resistance to water flow. Despite this, the water flow increases less than 50% through the zone nearest the repository, as compared with the flow in the main body of the rock.

The repository will be situated in an area where the rock is impervious over large areas. The permeability in this rock is less than 10^{-9} m/s. In such areas, the water flow rate will be less than 0.2 l/m^2 . year. The measurements and other evaluations on which these values are based are presented in detail in chapter 3. The flow may be greater in fractured zones, but no canisters will be placed in such zones.

Locally, new fractures in the rock may open around the tunnels as a result of rock stresses and thermal stresses which arise due to the heat generated by the waste. This fracture zone should be limited to a distance of 1.5 - 6 m from the tunnel /7-2/. A local increase of permeability can be expected in this zone. The consequences of this have been dealt with in the calculations of transit times and flows.

7.2.3 Flow in fractured rock

The water flows in the fissures (fractures) in the rock. An average value for the water velocity U_p, can be estimated from the flow and the porosity of the rock, ε_p:

$$U_p = \frac{q}{A \quad \varepsilon} \qquad (2)$$

It has not been possible to measure the porosity of the rock in situ. Even if this were possible, difficulties would arise in determining how large a portion of the fissures are closed and are therefore unable to conduct the water (see chapter 3).

Various evaluations of the porosity accessible to the flowing water have lead to values between $5 \cdot 10^{-5}$ and 10^{-5} /7-2, 7-4/. These evaluations have been carried out with the aid of a model proposed by Snow /7-5/. In this model, the fissures in the rock are described as equidistant channels with parallel walls and of equal width. The values for fracture spacing and fracture widths have been estimated on the basis of water injection measurements /7-1, 7-2/.

Fracture spacing can vary from a metre or so up to tens of metres in sound rock at great depth /7-1/.

An essential part of the difference between the porosity which can be calculated using Snow's model and that which has been measured in laboratories can be explained by the fact that the individual fissures have a width which varies in the flow direction (see section 3.4) and that all fissures are not in hydraulic contact with each other. A local increase of fissure width contributes greatly towards porosity but does not affect permeability much, which is determined primarily by the narrowest sections.

It is very doubtful, however, whether the flow in the rock at great depths can be described by means of such simple models as Darcy's or Snow's. These models cannot describe variations in transport velocity, i.e. the fact that the water flows faster in certain sections than in others. Snow's model does not take into account the fact that the fissures are of varying orientation. The transport path and the fissure area available for adsorption are therefore greater in reality than the model indicates. In lieu of more accurate models, Snow's model has been used here for calculating fissure size.

The average velocity in a plane-parallel fissure can be calculated from the following elementary relationship from flow theory /7-6/:

$$U_p = \frac{g}{12\nu} (2b)^2 \cdot i \qquad \text{(m/s)} \qquad (3)$$

g = gravitational constant 9.81 m/s^2
n = kinematic viscosity of water $\sim 10^{-6}$ m^2/s,
2b = fissure width m.

The fissures in the rock are not plane and of uniform thickness, and the above formula provides only a qualitative description of the influence of the various factors. Because the velocity is proportional to the square of the fissure width, a doubling of the fissure width leads to a quadrupling of the velocity. The flow through the fissure increases with the cube of the fissure width. A large fissure is therefore much more important than a small one, since the transit time is much shorter and the flow is much greater in the large fissure. A similar situation exists in one and the same fissure if the width of the fissure varies across the flow direction.

Landström et al. /7-7/ carried out measurements of the migration of different nuclides with the water along two flow paths in Studsvik. The measurements were performed at a depth of about 70 m. Radioactive bromine-82 was injected virtually instantaneously in one borehole. Bromine-82 migrates with the speed of the water. The average residence time of the water at a hydraulic gradient of 0.11 m/m was 10 h between two boreholes 22 m apart. The average fissure width for this case is then approximately 0.06 mm.

The broadening of the originally very narrow peak is caused by dispersion. In porous media, dispersion is caused by statistical fluctuations in velocity at different points in the material. The different points in the material are interconnected. This type of

dispersion is very similar to that caused by molecular diffusion. For such a case, however, the corresponding curve is more symmetrical and does not have such an extended tail.

The curve shown in figure 7-1 may result if transport takes place in many fissures of varying fissure width /7-4/. With normally distributed fissure widths, as in figure 7-2, good agreement is obtained between observed and theoretical values. The theoretically calculated curve has been adjusted to the same peak height as the measured values, since dispersal perpendicular to the flow direction is not described in the model. The fissures in this model, unlike those in the diffusion model, are not interconnected. The diffusion model gives an increasingly narrow residence time distribution relative to the mean value of the residence time with increasing flow length, while relative residence time distribution in the parallel flow model's does not change. The practical difference is that in the parallel flow case, a certain fraction of the tracer pulse height always emerges at, for example, 25% of the mean residence time, regardless of the flow

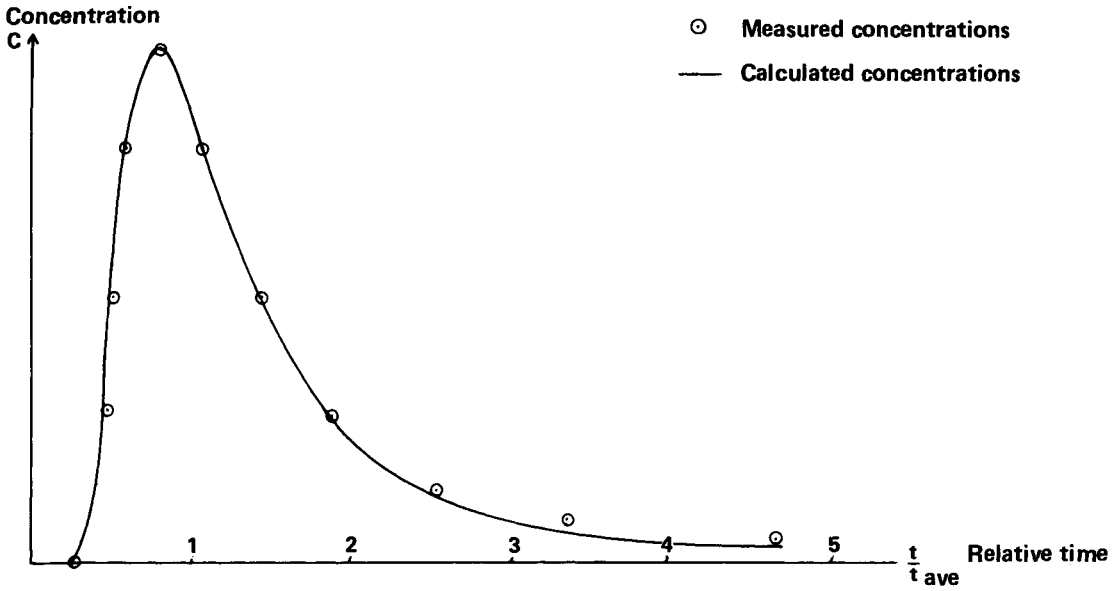

Figure 7-1. Relative concentration of bromine-82 in a borehole as a function of time after injection in another borehole at a distance of 22 metres. Measurements performed at Studsvik /7-7/. The calculated curve is adjusted to the maximum point in the measurement series.

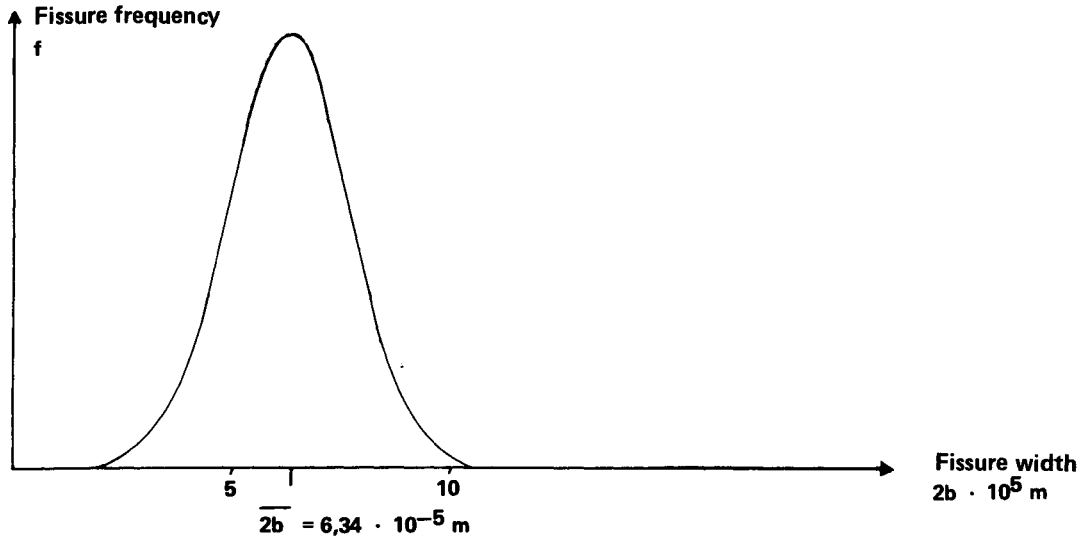

Figure 7-2. Calculated curve for normally distributed fissure width frequency /7-4/.

length, while in the diffusion case, an increasingly smaller portion emerges prior to, for example, 25% of the mean residence time as the flow length increases. Since it is very uncertain as to whether the dispersion model provides a good description of the rock at great depth, the influence of the more conservative parallel flow case on nuclide transports has been taken into consideration. This is described in greater detail in the section on nuclide transport in rock, 7.3.

The fissures in which the water is transported can be very small. Each fissure can have varying width. The water seeks out the large channels in the fissures, and its velocity is limited by the narrowest sections of the large channels. Nominal fissure sizes can be calculated from the relationship between permeability, K_p, fissure width, 2b, and fissure spacing, S /7-4/.

$$2b = 0.01\ (K_p \cdot S)^{1/3}$$

At $K_p = 10^{-9}$ m/s, the nominal fissure width for some average fissure spacings are given in the table below.

S	m	1	8	27
2b	mm	0.01	0.02	0.03

Observed fissures are often much larger. But they may constitute closed cavities or have narrow connections with other fissures. Visually observed fissure sizes are therefore not clearly related to the water-bearing capacity of the fissures.

7.2.4 Water flow around tunnels

Stresses caused by work in the rock, thermal stresses induced by the energy emitted by the radioactive waste and the altered water flow during the construction period will probably alter the water-bearing capacity of the rock in the vicinity of the repository.

A crush zone next to the tunnels will attract water from a large volume of rock. Calculations /7-2/ show in some examples that, at most, twice as much water can flow through the repository if a large crush zone is created than if the rock retains its original imperviousness.

In these sample calculations, the main direction of flow around the repository is largley vertically downwards, whereby the maximum possible water flow passes the repository, since the projected area of the repository will then be greatest. "Fresh" water which has not come close to any other hole flows past each hole with a canister. The projected area of the repository for water flow will be smaller, or at most equally large, for every other flow direction. In /7-8/, it is shown that even if a hole with a canister is surrounded by a crush zone, the water flow in the zone will not increase radically. In the case of flow perpendicular to a tunnel, the water flow per unit tunnel area cannot be more than twice the water flow in the undisturbed rock, even if the tunnel is surrounded by a crush zone of very high permeability. When the water flows parallel to a tunnel, the flow per unit area can increase more. But the flow per unit volume in the

repository does not increase more, owing to the fact that the projected area is correspondingly reduced.

Actually, it is very unlikely that such large zones of high permeability will exist, since the clay which is used as a material in the storage holes will swell and penetrate buffer into the large fissures. The clay forms a dense and stable gel in the groundwater, with its content of calcium and magnesium /7-9 to 7-12/.

Observations made to date demonstrate clearly that the clay is not carried away by the water if the water contains the same levels of bivalent cations as the groundwater does in this case. The clay which surrounds the canister is originally compacted to a density of approximately 2.3 t/m^3 (incl. 10% moisture). When this clay absorbs water, it forms a very dense, impervious structure with a permeability which is so low that water transport through the clay virtually ceases. Permeability is lower than 10^{-13} m/s, even if the density of the material, including absorbed water, decreases to approximately 1.7 t/m^3 /7-12/. See also chapter 4, figure 4.2. The flow of water through the clay is therefore much less than in the rock. In practice, it should be possible to regard the clay as an impervious body as far as flow is concerned. The hydraulic gradient induced by the temperature gradient in the clay is no greater than the hydrostatic gradient /7-13/, so it will not appreciably increase the flow of water.

Dissolved substances are transported more rapidly through the clay barrier by means of diffusion than by means of flow.

7.2.5 Transport capacity of the water

The water flow limits the quantity of substances which can be transported to and from the canister. If there were no transport resistance, all of the water which came near the canister would constitute a perfect transport medium. The various transport resistances have been described and their importance evaluated in chapter 6. It has thereby been shown that a canister has a "capture area" for the water flow which is slightly more than the projected area of the canister at low water flows (0.2 l/m^2 . year) in the undisturbed rock and approximately half the projected area at higher water flows (1 l/m^2 . year). In arriving at these figures, the resistance offered by the clay filler in the fissures has not been taken into account. Since the clay actually does penetrate out into the fissures /7-12/, the transport resistance will be greater - 10 to 200 times - if the clay penetrates 2 metres out into a fissure /7-8/. The transport of substances to and from the canister is reduced accordingly.

If the resistance offered by the clay in the fissures is neglected a canister has a capture area of about 5 m^2 at a water flow of 0.2 l/m^2 . year in undisturbed rock. It can then accept components from approximately 1 litre of water per year. In the same manner, products leaking out of the canister can saturate an equally large water volume. The inward transport of oxidants and outward transport of radionuclides via ordinary dissolution mechanisms have been dealt with in chapter 6. Two additional mechanisms will be dealt with here - the transport of radionuclides by organic complexing agents and in the form of colloids.

Organic complexing agents

Marsily et al. /7-17/ point out that plutonium, in a known case of rapid transport, may have been transported via organic complexing agents.

There is a maximum of 200 mg/kg organic material in the buffer material (see chapter 4). There is about 18 tonnes of bentonite, counted as dry matter in a hole for a canister. This amount contains a maximum of about 3.6 kg organic material. Even if all organic material is assumed to have complex-forming properties and low equivalent weight, it cannot transport more than a kilogramme or so of metal. The larger quantity of clay in the tunnels greatly increases the total quantity of organic material per canister. But this material is much less accessible owing to its greater distance.

The groundwater contains some organic material. Analysis of deep-lying water from the Finnsjö area has revealed a maximum of 0.5 mequiv per litre of fulvic acids /7-39/. This means that metal ions with an equivalent weight of 240 can be dissolved to a concentration of 120 mg/l. However, much of the complex-forming capacity of the groundwater is already utilized by dissolved metals, such as iron.

With a water flow of 1 l/canister and year, a solubility of 120 mg/l means that no more than 120 kg of the metal can be transported out of the repository by complexing agents over a period of 1 million years.

Colloids

Colloidal solutions contain tiny particles > approx. 100 Å with molecular weights > approx.~1 000. They form stable systems.

Radionuclides can be transported by colloids both in the form of true colloids and in the form of pseudocolloids. In the latter case the nuclide is adsorbed onto other colloids in the water. The true colloid can be formed by precipitation. In order for this to occur, the solubility product must be reached. But attainment of the solubility product does not guarantee that colloids will be formed. The true colloid is formed at concentrations greater than approx. 10^{-5} mole/l. Pseudocolloids are formed at considerably lower concentrations of approx.~10^{-9} mole/l /7-14, 7-15/.

Colloidal particles diffuse more slowly than small molecules, but approximately at the same speed as large molecules of the same mass. The smallest colloidal particles have a diffusivity of about 10^{-10} m^2/s. Due to their size and mass, they can be separated by means of, for example, ultrafiltration, but in many cases by means of filtration in ordinary filters as well /7-16/. In this respect, the clay is a very efficient filter, owing to the small size of the clay particles.

The charge of the colloidal particles may be either positive or negative, depending upon concentration and pH. As a result, they can be adsorbed differently on different surfaces.

A large number of experiments with different nuclides and adsorption surfaces are reviewed in /7-15/. The tested colloids include the nuclides uranium, plutonium, americium and europium. The colloids are usually adsorbed very well on glass surfaces and minerals.

But on the basis of current knowledge concerning the adsorption of colloids on rock surfaces, the possibility that some colloidal particles of, for example, plutonium may migrate with the speed of the water cannot be completely excluded.

Three mechanisms for nuclide transport with colloids are dealt with here:

a) the colloid is formed inside the clay barrier and diffuses out through the clay,

b) the colloid is formed after the radionuclide has diffused out through the clay,

c) the nuclide is adsorbed on particles of colloidal size outside of the clay barrier.

Measurements of the diffusion of macromolecules in compacted clay have been carried out for KBS /7-11/. Sodium ligno-sulphonate, with a molar weight of around 50 000 g/mole, has not been detected on the other side of a 3 mm thick layer of clay after more than 850 hours. With the detection methods used, it can be concluded that diffusivity is lower than $3 \cdot 10^{-14}$ m^2/s. This is approximately 1 000 times lower than for nuclides in ionic form. This leakage mechanism can therefore be regarded as being of very little importance in comparison with other mechanisms.

The importance of mechanism b), where the colloid is formed after passage through the clay layer, cannot be evaluated with certainty on the basis of available data. However, dilution effects owing to a widening geometry in the direction of transport and a decrease in concentration upon diffusion through the clay barrier contribute towards a much lower concentration outside of the barrier than inside. There is therefore little probability that the solubility product will be exceeded outside of the barrier, since the nuclide is dissolved inside the barrier.

In the case of mechanism c), two colloid sources have been identified. In the first place, colloidal particles are probably present in the groundwater /7-39/, and in the second place, the finest particles of the clay can, under certain conditions, form colloids. Attempts to make a slurry of the clay in the groundwater have shown that the clay quickly forms a very stable gel over whose surface virtually no clay particles can be observed, the level is lower than 1 mg/l /7-10, 7-11/. Gel formation is caused primarily by the presence of multivalent ions. The levels of calcium (2+) and magnesium (2+) are sufficiently high (> 20 mg/l) in all deep groundwaters for the clay to form a gel.

The capacity of the natural colloid content of the water to adsorb radionuclides is unknown. However, many studies show that radiocolloids form readily as the nuclides are adsorbed on colloidal particles and the resultant radiocolloids are then in turn adsorbed on various surfaces /7-14, 7-15/. Water samples taken

from great depths are very clear. This is an indication that there are few solid particles in the water. Measurements of water from the Finnsjö area show that the particulate level is lower than 0.001 mg/l /7-11/. Jacks /7-39/ states that the colloid content should be very low - on the order of µg/l. The quantity of radionuclides which can be transported by the colloids cannot exceed the quantity of colloids. The transport capacity of the colloidal particles is therefore very small in relation to other transport mechanisms.

7.3 NUCLIDE TRANSPORT IN THE ROCK

7.3.1 The leaching process

Following a hypothetical penetration of the canister, leaching takes place very slowly owing to the limited transport capacity of the water. Uranium constitutes most of the spent fuel - approximately 95%. Other elements (transuranium elements, fission products etc.) each make up no more than about 1% of the fuel, and often much less. Some of these elements have become concentrated at points which are easily accessible to the water. This applies to cesium and iodine, among others /7-18/. These elements can be dissolved from the canister faster than the uranium dioxide matrix can be dissolved. The quantity of all individual radionuclides aside from uranium is relatively very small and will give rise to very low levels in the water. Only uranium could possibly give rise to such high levels in the water outside of the clay barrier that the salt content of the water will be appreciably affected. Owing to dilution, the uranium level and the level of other radioactive elements will decrease at longer distances from the repository.

7.3.2 Non-interacting nuclides

The so-called "non-interacting" nuclides - which include iodine, among others - are transported with the velocity of the water, on the average. Technetium is probably non-interacting under oxidizing conditions, but not under the reducing conditions which exist in the final repository /7-21/. Since the water flows at different speeds in different channels, an originally concentrated front will spread out. The same effect occurs due to molecular diffusion. At very low water velocities, transport over short distances via molecular diffusion can be much faster than via flow. This applies, as was demonstrated above, to transport through the clay barrier /7-4/. Transport in the rock, however, is dominated completely by water flow at distances of more than 10 or so metres /7-4, 7-19/. On its way through the rock, the water is diluted owing to the intersection of different fissure systems. An originally high level at the repository will therefore decrease upon transport through the rock.

The transit time for a nuclide will be determined by the retention time of the water and the distribution of the retention time. The concentration of the nuclide at a given point is determined by the original concentration and the effects of dispersion and diffusion as well as dilution. Figure 7-3a shows how a

pulse release is affected by these factors, and figure 7-3b shows how a prolonged release is affected.

Dilution can be very great. Calculations for the Finnsjö area show that the nuclides released in a year will be diluted in water-volumes between $0.5 \cdot 10^6$ and $25 \cdot 10^6$ m^3 depending upon the point of outflow /7-38/.

7.3.3 Nuclide retardation in the rock, retardation mechanisms

Most nuclides from the spent fuel which are dissolved in the groundwater are affected in some manner by the rock. Metal ions with positive charges are affected to a particularly great extent. As a result, these nuclides will migrate at a much slower velocity than the water. Many nuclides migrate at a velocity which is many thousands of times slower than water transport.

A number of mechanisms are known for the retardation of the nuclides:

- precipitation
- mineralization
- adsorption
- ion exchange

When the solubility product of a compound is exceeded, a solid phase is formed, which often precipitates and is not transported further with the water. Water emerging from a zone in which the solid phase is present contains a concentration which is determined by the solubility product and the other constituents of the water, as long as there is any solid phase left. Irreversible reaction with the rock (mineralization) will completely take away the nuclide from the aqueous phase.

Physical adsorption and ion exchange are two reversible mechanisms which are of great importance for retardation. At low nuclide concentrations, these mechanisms can be described by one and the same simple relationship:

$$q_A = K_d \cdot C_A \qquad (5)$$

where

q_A = concentration of A in the solid phase (quantity of A/kg solid),
C_A = concentration of A in the water (quantity of A/m^3 water),
K_d = equilibrium constant (m^3 water/kg solid).

K_d is constant at low concentrations, but usually decreases at higher concentrations in the water. These reversible mechanisms will retard the nuclides to a lesser degree than precipitation and irreversible reaction. In calculating the retardation of the nuclides, it is therefore cautiously assumed that reversible sorption is the dominant mechanism.

Some sorption reactions take place on the outer surface of the solid material. In this case, it is not the quantity of solid substance which is decisive for its adsorption capacity, but rather the size of its surface area. Equilibrium is described by means of a surface quilibrium constant for this case:

$$s_A = K_a \cdot C_A \qquad (6)$$

where

s_A = quantity of A/m^2 outer surface of the solid material,
K_a = surface equilibrium constant, m^3 water/m^2 surface area.

For a solid material with a known surface area a m^2/m^3, the relationship between the two equilibrium constants is as follows:

$$K_a = \frac{K_d}{a} \cdot \rho$$

where ρ = the density of the solid material, kg/m^3.

7.3.4 Studies of equilibrium values

Some sorption equilibria from previous studies in the literature are reported in /7-20, 7-21/ and /7-4/. These studies report results which are similar to those obtained from the measurements performed within the project. Allard et al. /7-20, 7-21/ have performed measurements for two different water compositions with 14 different elements, including radium and the actinides thorium, uranium, neptunium, plutonium and americium. Besides measurements on clay and finely-crushed granitic rock, adsorption on larger rock surfaces has also been carried out.

The measurements which are reported in /7-20/ were all performed under oxidizing conditions. Later measurements under reducing conditions exhibit appreciably higher equilibrium constants for uranium and technetium /7-21/.

It has not been fully clarified to what extent adsorption on rock is a volume reaction and should thus be able to utilize the entire volume of the rock or a surface reaction, where only the fracture surfaces are utilized. Allard's measurements on crushed rock with particle sizes up to 0.12 mm show that americium and cesium react in depth while strontium shows signs of a surface reaction.

In all calculations of retention factors, it has been assumed that surface reaction is the dominant mechanism. This could lead to a large underestimation of the retention factors if the reaction actually takes place in depth.

If the volume reaction were prevalent and sufficient time were provided for penetration to the rock, the retention factors could be roughly 10 000 to 30 000 times larger than those used in the calculations. For example, cesium would migrate about 30 million times more slowly than water.

7.3.5 Retention factors in rock

When water flows through an adsorbing medium, the nuclide will migrate more slowly than the water. The ratio between the velocity of the water (U_p) and the velocity of the nuclide (U_i) is

called the retention factor, K_i. It can be calculated from the equilibrium constant.

$$K_i = \frac{U_p}{U_i} = 1 + \frac{K_d \cdot \rho}{\varepsilon} (1-\varepsilon) = 1 + \frac{a\, K_a}{\varepsilon} (1-\varepsilon) \qquad (8)$$

ε = the porosity of the solid material.

The retention factors for rock have been calculated from Allard's /7-20, 7-21/ measured equilibrium data and under the assumption of surface reaction. K_a values have primarily been calculated by using the geometric surface area a_{exp} of the crushed rock as the adsorption area a_{exp}. 30 m^2/kg. This value has been modified somewhat as a result of recent measurements where it has been possible to use measurements on rock surfaces of known area as a reference /7-23/. The surface area of the rock fissures, a, has been calculated under the assumption that the surfaces of the rock fissures are plane and parallel.

The transport velocity for a nuclide is not affected by the porosity ε. This can be shown by combining equation 2, which describes the water velocity in the fissures, with equation 8, which describes the retention factor. For the nuclides of interest whose retention factors are considerably greater than 1, the following is obtained for rock with low porosity:

$(\varepsilon << 1)$

$$U_i = \frac{K_p \cdot i}{K_a \cdot a} \qquad (9)$$

The transport velocity of the nuclide, U_i, is thus dependent only upon the measured quantities K_p and K_a and the gradient i as well as the size of the fissure surfaces in relation to the rock volume a (m^2/m^3).

Table 7-1 presents three sets of K_d and K_a values from measurements and theoretical equilibrium analyses /7-20, 7-21/. Two important factors in the determination of the K_d and K_a values are the redox potential of the groundwater and the contact time between the phases. It is shown in chapter 3 that natural groundwaters are reducing and that the groundwater flow is slow. The retention factors which are used in calculations of the nuclide transport through the rock should therefore be based on K_d values which are determined in a reducing environment and with a long contact time between the phases.

The retention factors which are used in the KBS safety analysis for the final disposal of vitrified waste /7-24/ were based on K_d values measured in an aerated system, i.e. under oxidizing conditions, and with a maximum contact time between phases of 7 days. Despite the fact that more recent measurements show that the K_d and K_a values are greatly underestimated, certain calculations have been carried out using the K_a values for an oxidizing environment for the alternative of final storage of unreprocessed nuclear fuel as well /7-23/.

In a reducing environment, it can be expected that uranium and neptunium especially, but possibly also plutonium, will have con-

Table 7-1. K_d and K_a values in different environments.

Element	Oxidizing environment[1]		Reducing environment with[2] cautions concentration values and short contact time		Best estimate for reducing[3] environment and slow groundwater transport	
	K_d (m^3/kg)	K_a (m)	K_d (m^3/kg)	K_a (m)	K_d (m^3/kg)	K_a (m)
Ni	-	-	-	-	0.32	0.032
Sr	0.0079	0.00026	0.0063	0.00063	0.016	0.008
Zr	1.3	0.042	1.3	0.025	3.2	0.32
Tc	0	0	0	0	0.05	0.005
I	0	0	0	0	0	0
Cs	0.13	0.0042	0.032	0.0063	0.064	0.021
Ce	13	0.42	5.0	0.10	10	1.0
Nd	4.0	0.13	1.0	0.02	10	1.0
Eu	7.9	0.26	7.9	0.16	10	1.0
Ra	0.1	0.0033	0.063	0.0063	0.50	0.25
Th	0.79	0.026	0.50	0.01	2.4	0.24
U	0.0063	0.00021	0.50	0.01	1.2	0.12
Np	0.04	0.0013	0.50	0.01	1.2	0.12
Pu	0.16	0.0053	0.72	0.014	0.30	0.03
Am	13	0.42	5.0	0.10	32	3.2

1) See table 11, "low nuclide concentration" and "low salt concentration", in /7-20/.

2) See table 19, in /7-20/.

3) See tables 6, 7 and 9, "low nuclide concentration" and "low salt concentration" in /7-21/, and discussion in /7-23/.

siderably higher K_d values than in an oxidizing environment. The values in the column "Reducing environment with cautious concentration values and short contact time" are based for most of the elements on the lowest measured K_d values from measurements in an oxidizing system with a contact time shorter than 7 days. For uranium, neptunium and plutonium, the values are based on a theoretical analysis of the redox and complex equilibria in the groundwater-granite system for reducing conditions /7-20/. These values have been confirmed experimentally for uranium /7-21/.

In the column "Best estimate for reducing environment and slow groundwater transport", K_d values measured over a contact time of more than six months are presented for most of the elements. The values for technetium and uranium, however, were determined for a contact time of max. 1 and 4-5 days, respectively, which means that the values for these elements may be underestimated by a factor of between 2 and 5.

The retention factors presented in table 7-2 were calculated for rock with a permeability of 10^{-9} m/s and a fissure spacing of 1 m. This gives a nominal fissure width of 0.01 mm and a fissure wall surface area of 2 m^2/m^3 rock.

The use of K_d and K_a values for calculating the retention factors is discussed at length in /7-23/.

7.3.6 Dispersion effects

The retention factors provide only an average measure of retarda-

Table 7-2. Retention factors K_i [1].

Element	Oxidizing environment	Reducing environment with cautious concentration values and short contact time	Best estimate for reducing environment and slow groundwater transport
Ni	-	-	6 100
Sr	51	120	1 500
Zr	8 000	4 800	61 000
Tc	1	1	950
I	1	1	1
Cs	800	1 200	4 000
Ce	80 000	19 000	200 000
Nd	25 000	3 800	200 000
Eu	50 000	30 000	200 000
Ra	670	1 200	48 000
Th	5 100	1 900	46 000
Pa	37	37	11 400
U	41	1 900	23 000
Np	260	1 900	23 000
Pu	1 100	2 800	5 700
Am	80 000	19 000	610 000
Cm	40 000	9 500	305 000

1) See footnote, table 7-1, and /7-23/.

tion. Due to dispersion effects, some of the water will emerge sooner than average. In the case of nuclides which are retarded, this is further accentuated if the transport takes place in fissures with few or no interconnections. The model for residence time distribution described above in connection with water flow has also been used in an extended form to describe nuclide dispersion /7-4/. While the flow velocity of the water increases in proportion to the square of the fissure width, the velocity of the retarded nuclide varies in proportion to the cube of the fissure width. This further accentuates the importance of the large fissures.

On the basis of the measurements at Studsvik /7-7/, where inter alia strontium was used as a tracer nuclide, a broadening of the front was noted in agreement with the model which was used. Approximately 5% of the maximum concentration can emerge after only about 20% of the mean transit time for a pulse if dispersion is due to the described mechanism. At the same time as they are

broadened, pulsed releases will be diluted considerably in the longitudinal direction, whereby the maximum level of the pulse will decrease. The velocity variations in the flow direction will, however, not reduce the maximum level of prolonged releases.

In areas where the fissures have good connections with each other and are closely spaced, the broadening of the front will not be so accentuated. On the other hand, dilution will contribute towards reducing the level.

Figure 7-3 illustrates the effects of dispersion on the concentration profile for the pulsed release (figure 7-3a) and for the prolonged release (figure 7-3b). The solid curves show the effects of dispersion alone, while the dashed curves show the combined effects of dispersion and dilution.

7.3.7 Decay during migration

The radioactive nuclides in the fuel decay with time. Some of the nuclides decay to stable elements. This applies to many of the fission products. Other nuclides form radioactive daughter products when they decay. This applies above all to the heavy nuclides in the fuel, the actinides, but also to some of the fission products (for example, cesium-137 decays to barium-137 m and zirconium-93 to niobium-93 m).

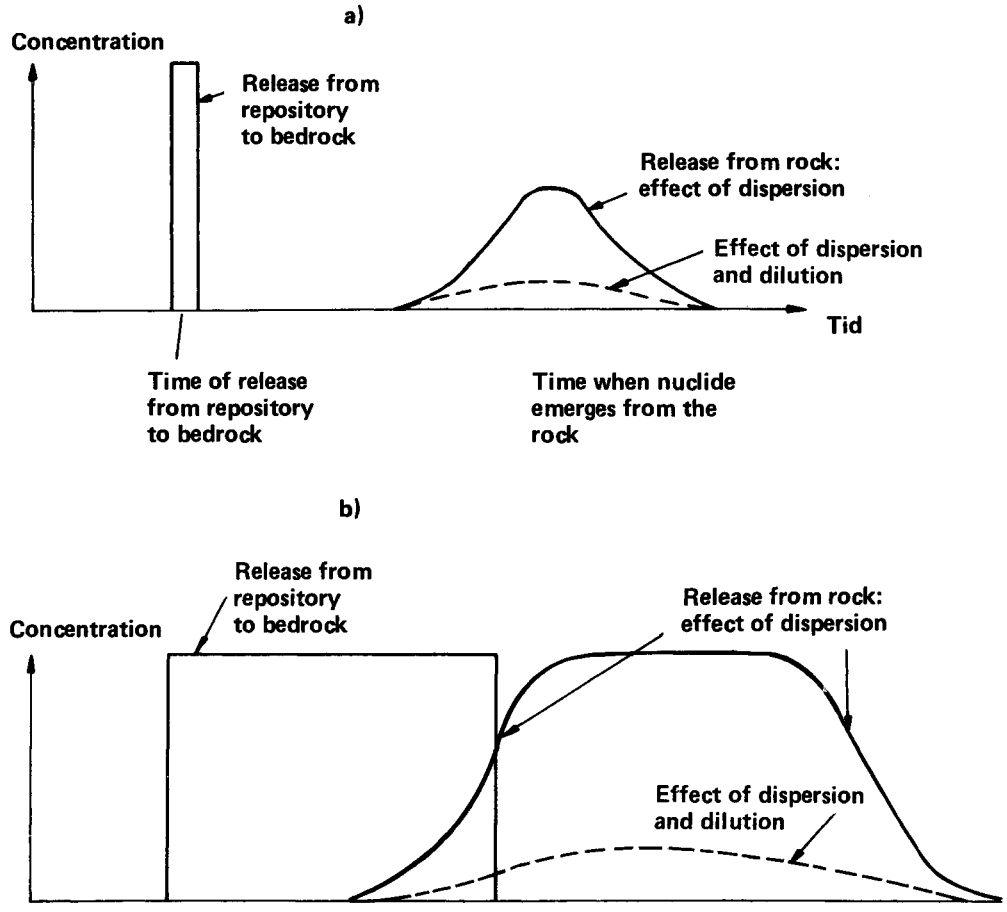

Figure 7-3. Effects of dispersion on pulse release and prolonged release without taking into account the lowering resulting from decay and dilution.

Owing to the fact that the different nuclides in a decay chain usually migrate at different velocities, the entire decay chain must be taken into account in calculating the times for nuclide transport. This is accomplished with the use of the GETOUT computer programme /7-22/.

Radium-226 is an example of a nuclide in the fuel with a relatively short half-life (1 600 years) and a sufficiently long transit time for the radium to decay to a harmless level before it reaches the biosphere. However, radium-226 is formed through the decay chain uranium-238 → uranium-234 → thorium-230 → radium-226 (thorium-234 and protactinium-234 m have very short half-lives and do not therefore affect the time it takes for the formation of radium-226.)

Figure 7-4 shows the maximum inflow of radium-226 to a hypothetical recipient as a function of the transit time for uranium. The following input data are used for the calculations whose results are illustrated in the figure:

Parameter	Values
Time for canister penetration	100 000 years
Duration of leaching period	500 000 years
Groundwater transit time	400 years
Retention factor for radium	1 200
Retention factor for thorium	1 900
Retention factor for uranium	40 - 190 000

The figure also shows the contributions from radium's parent nuclides to the total inflow. The amount of uranium-234 which is present at canister penetration comes primarily from the decay of the plutonium-238 which is in the fuel when it is taken out of the reactor. As is shown by the figure, uranium-234 is responsible for most of the radium-226 inflow to the recipient area in the case of short uranium transit times, while uranium-238 makes the greatest contribution in the case of long uranium transit times.

A point corresponding to what is reported in chapter 8.5 as a pessimistic calculation case has been marked in the figure with a vertical dotted-dashed line. The total radium-226 inflow at this point is $1.6 \cdot 10^{-2}$ Ci/year.

7.4 NUCLIDE TRANSPORT IN THE BIOSPHERE AND RADIATION DOSES

7.4.1 Model for transport in the biosphere

A model system has been developed to simulate the dynamic exchange of radionuclides in the biosphere. The design of the model is basically the same as in previous studies of vitrified waste

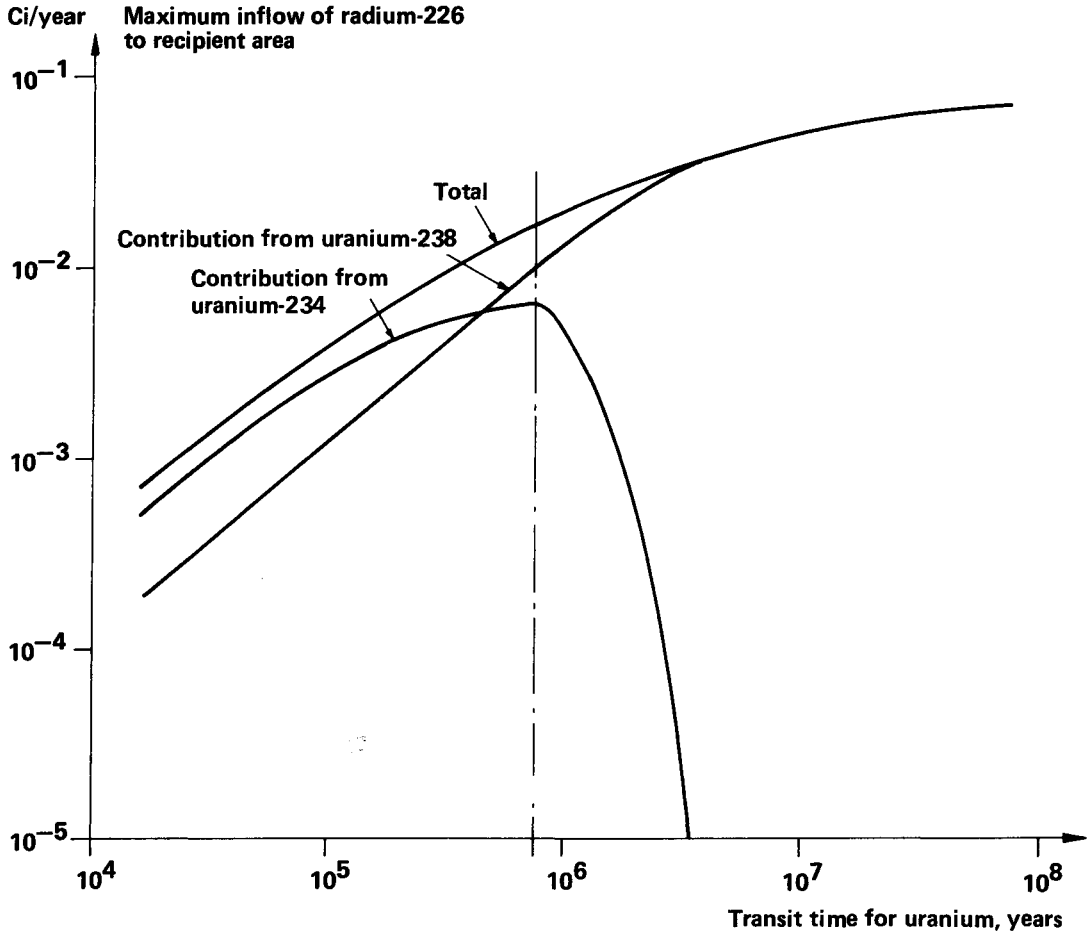

Figure 7-4. Maximum inflow of radium-226 as a function of the transit time of uranium. The pessimistic calculation case (see section 8.5) is marked with a dotted-dashed line. The contribution of other nuclides to the inflow of radium-226 is negligible.

/7-37/. Compartment theory has been utilized, whereby the ecosystem is divided into a number of physically well-defined areas or volumes. These are referred to in the following as reservoirs. The radioactivity concentrations in the reservoirs are described by a system of ordinary differential equations of the first order. The solution of this equation system has been carried out by means of the BIOPATH computer programme /7-25/. The mathematical model takes into account the processes of turnover and transport within and between the different reservoirs and calculates the dose load to man via the predominant paths of exposure. The model has also been developed for calculation of a simple decay chain /7-26/.

The model system (see fig. 7-5) encompasses four interconnected areas within and between which the elements are transferred and where feedbacks take place. These areas are:

- The local area at the point of outflow from the geosphere to the biosphere.
- The regional area in the immediate vicinity of the point of outflow.
- The intermediary area consisting of the Baltic Sea with the surrounding coastal zone.
- The global area.

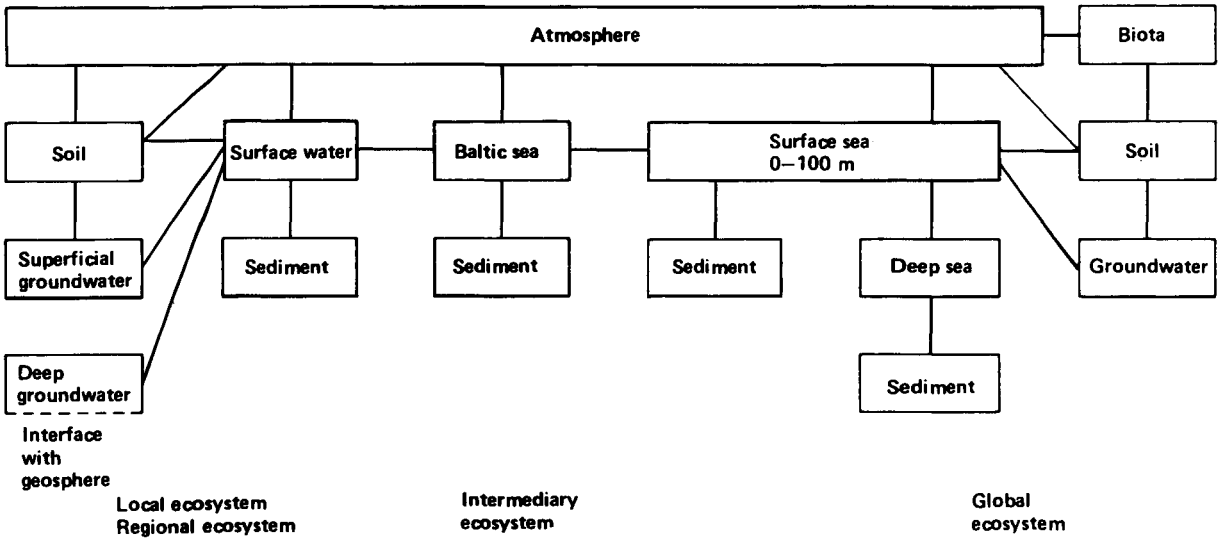

Figure 7-5. Reservoirs for the various ecosystems.

Inflow into the biosphere is defined by the groundwater-borne radioactice flow which reaches the interface between the geosphere and the biosphere.

Three main cases (see fig. 7-6) for inflow into the biosphere model are studied:

Alt. 1 The groundwater-borne material is distributed equally at inflow between a valley in which a well is located and a nearby lake.

Alt. 2 The flow is distributed equally between a nearby lake and the lake system down stream.

Alt. 3 Inflow to the Baltic coastal zone.

The makeup of the intermediary and global systems is the same for the three alternatives. But the makeup of the local and regional systems depends upon whether the outflow to the biosphere takes place in an inland area (alt. 1 and alt. 2) or to the coast (alt. 3).

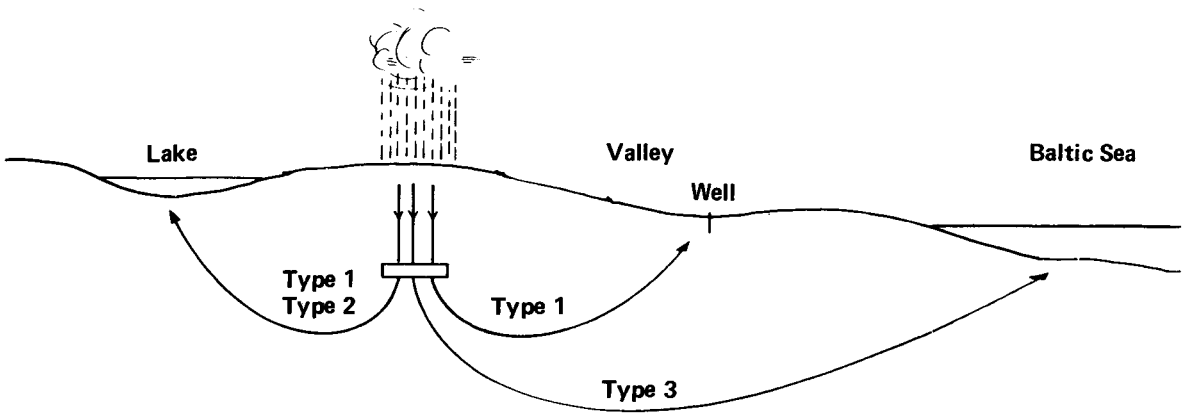

Figure 7-6. The three main paths of transport of radioactive substances to the biosphere.

The local eco system

In the well and lake cases, the local ecosystem consists of a 0.25 km^2 area of farmland, divided into a soil reservoir down to a depth of 0.5 m and a reservoir encompassing the soil-borne groundwater down to the same depth.

In the Baltic Sea alternative, the local ecosystem consists of 1 km^3 of brackish water within a coastal belt 2 km wide and 30 km long with underlying sediment.

The regional eco system

In the well and lake alternatives, the regional ecosystem consists of 900 km^2 of farmland with the same vertical division as in the local ecosystem. A lake (Finnsjö Lake) with a surface area of 5 km^2 is included in the regional model.

In the Baltic Sea alternative, the regional ecosystem is the same as the local system.

The intermediary ecosystem

The intermediary ecosystem consists of the Baltic Sea and its coastal region. This system also includes the Baltic Sea sediment and the volume of air in the atmosphere above the Baltic Sea and the region up to an altitude of 1 km.

The global ecosystem

The global ecosystem encompasses 7 different reservoirs:

- The global atmosphere.
- The surface sea, which comprises the upper 100 m of the pelagic division. It mixes relatively rapidly, but has a relatively slow rate of exchange with the deep sea.
- The deep sea, which includes the global sea volume below a depth of 100 m.
- The sediments below the surface and deep seas.
- Soil, comprising a ground layer down to a depth of 0.5 m.
- Groundwater below the ground.
- The biomass on the global land area.

7.4.2 Exposure situations

When the radioactive elements are exchanged between the different reservoirs, they reach man via different paths of exposure. (Fig. 7-7). Internal exposure via inhalation, food and drinking water and external exposure from material deposited in the ground have been shown by experience to be of importance. Bathing, presence on beaches where radioactive material has accumulated and the handling of fishing tackle which has come into contact with bottom sediments comprise other possible paths of exposure.

Internal exposure from food takes place via a number of ecological transport paths, such as uptake in crops via root uptake, con-

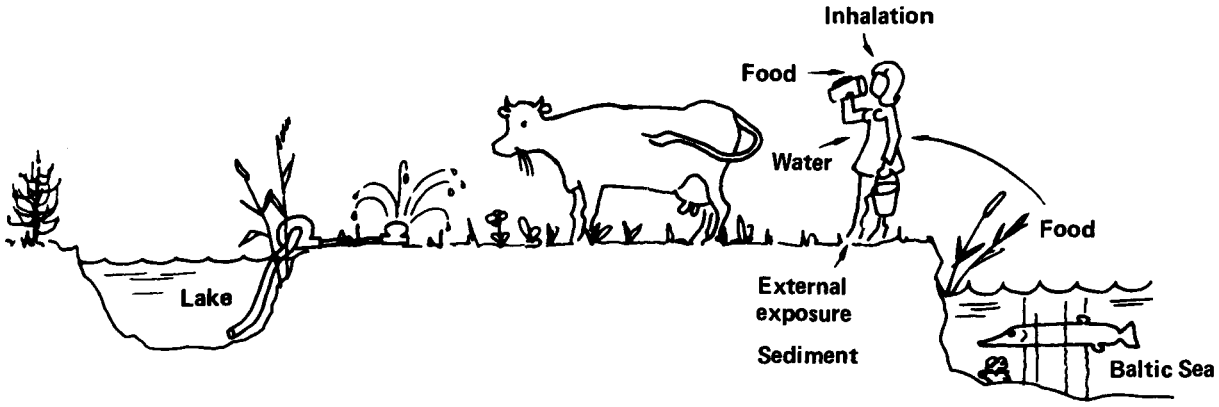

Figure 7-7. Paths of human exposure in the local ecosystem.

centration in fish via surrounding water and uptake via the food chain from plants to man via the meat and milk of grazing animals. A number of feedbacks in the ecosystems reinforce the paths of exposure. In the local area, pasturage and crops are irrigated. In the region, groundwater from irrigated areas is used for drinking water.

Paths of exposure in the local ecosystem

The paths of exposure which are dealt with for the different alternatives well, lake and Baltic Sea are:

Path of exposure	Inflow alternative[a)]
Soil - grain	W, L
Soil - green vegetables	W, L
Soil - root vegetables	W, L
Soil - grass	W, L
Grass - milk	W, L
Grass - meat	W, L
Grain - eggs	W, L
Drinking water	W, L
Water - fish (fresh and salt water fish, respectively)	W, L, B
Land (external exposure)	W, L, B
Beach activities (external exposure)	L, B
Bathing (external exposure)	L, B
Fishing (external exposure)	L, B

a) W (well), L (lake), B (Baltic Sea)

The radioactive elements which enter the local ecosystem in the inland alternative are accumulated in the upper 0.5 m of the ground, after which they are gradually distributed in the environment via groundwater and surface water runoff. Exposure in the terrestrial environment has been calculated on the basis of the activity which reaches the local ecosystem via irrigation and long-term accumulation in the ground. Only doses to individuals are taken into account in the local ecosystem. In the Baltic Sea case, where the outflow takes place in the coastal zone, the critical group is exposed internally through fish consumption and externally via bathing and contact with sediment.

Paths of exposure in the regional ecosystem

The paths of exposure in the regional ecosystem are the same as those in the local ecosystem. The average exposure of the individuals in the region, however, differs quantitatively from the exposure of the critical group in the local system. Exposure within the regional ecosystem is used as a basis for calculating the collective dose load to the population within the area.

Paths of exposure in the Baltic Sea area and globally

The number of people who are exposed in the intermediary area is defined by fish consumption. The total yield of fish from the Baltic Sea is approximately 200 million kg per year. With an average consumption of 20 kg per year and individual, the affected population is 10 million individuals. With regard to external exposure, the situation for the population in the Baltic Sea area is assumed to be qualitatively identical to that in the coastal zone in the local and regional systems. All paths of exposure are included in the global area. Approximately 1% of the world's population lives in coastal regions with an exposure situation similar to that in the Baltic Sea area. For the remaining 99% of the world's population, it is assumed that external exposure occurs through radioactive material in the global model's atmosphere and soil reservoirs.

Relations for uptake in the food chains

The concentration of radioactive elements in meat and milk originates from uptake over the following principal paths of exposure:

- pasturage which has become enriched via the root system
- pasturage which has become enriched via deposition
- drinking water

In the local area, pasturage is irrigated with water from the well and the lake; drinking water is taken from the same sources. Of the radioactivity deposited on the pasturage, either through irrigation or atmospheric fallout, 80% is assumed to remain.

7.4.3 Calculation of uptake of radioactive elements

The uptake of radioactive elements in different foodstuffs via various paths of uptake has been calculated in the following manner.

Symbols:

U_i = uptake of a certain nuclide in foodstuff i. Given in Ci per unit of foodstuff (kg, litre or piece).

F_i = distribution factor for a given nuclide for foodstuff i. Given as day per unit of food stuff (kg, litre or piece).

C_i = concentration of a certain nuclide in reservoar i. Given in Ci per unit (kg or litre).

i =

m	milk (litres)
k	meat (kg)
v	green vegetables (kg)
g	grain (kg)
r	root vegetables (kg)
e	eggs (pcs)
f	fish (kg)
p	pasturage (kg)
w	groundwater (litres)
a	air (kg)
l	lakewater (litres)
s	soil (kg)

E_n = concentration factor for certain nuclide for uptake via n, where

n =

p	soil → pasturage
v	soil → green vegetables
g	soil → grain
f	fishing water
r	soil → root vegetable

Mc_i = daily consumption of foodstuff i.

DEP = deposition (m per day).

COV_i = degree of coverage for foodstuff or pasturage i (kg per m^2).

IRR = irrigation (litre per m^2 and day).

29 = $\int_0^\infty \varepsilon^{-\lambda t} dt$ where $\lambda = \frac{\ln 2}{T_{1/2}}$ and $T_{1/2}$ is the "ecological" half-life of grass (20 days).

Values used for the quantities F_i, E_n, DEP, COV_i, IRR and Mc_i are given in /7-26/.

For each nuclide, the following equations are obtained for uptake in the different foodstuffs:

Uptake in Milk:

U_m (in Ci per litre) =

F_m ($Mc_p \times E_p \times C_s + Mc_w \times C_\ell + 0.8 \times DEP \times C_a \times 29 \times COV_p^{-1} \times$

$\times Mc_p$)

Uptake in Meat:

U_K (in Ci per kg) =

F_K ($Mc_p \times E_p \times C_s + Mc_w \times C_\ell + 0.8 \times DEP \times C_a \times 29 \times COV_p^{-1} \times$

$\times Mc_p$)

The concentration of radioactive elements in green vegetables originates from two sources: the uptake of radioactivity via the root system and deposition directly onto the surfaces of the leaves. The concentration factor between soil and plant is specific for each individual nuclide.

Uptake in Green Vegetables:

U_v (in Ci per kg) =

$E_v \times C_s + 0.8 \times 29 \times COV_v^{-1}(IRR \times C_\ell + DEP \times C_a)$

Uptake in grain and root vegetables is assumed to take place primarily through the root system.

Uptake in Grain, Root Vegetables:

U_g (in Ci per kg) $= E_g \times C_s$

U_r (in Ci per kg) $= E_r \times C_s$

The radioactivity in eggs comes from feeding the hens with contaminated grain and drinking water.

Uptake in Eggs:

U_e (in Ci per egg) $= F_e$ ($Mc_g \times E_g \times C_s + Mc_w \times C_w$)

Uptake in fish takes place through the inflow of contaminated groundwater into the lake and the feedback of radioactivity from the runoff area and the bottom sediments.

Uptake in Fish:

U_f (in Ci per kg) = $E_f \times C_f$

7.4.4 Radiation doses

The radioactive elements which enter the biosphere via the groundwater expose man to ionizing radiation through radioactive decay both in the environment, which leads to external irradiation, and in the body, which leads to internal irradiation.

The slow and protracted turnover of the various elements leads to varying intakes of the different radioactive elements.

The dose factors which have been used in the calculations in this work and which describe how the intake of 1 Ci of a given nuclide can be translated into radiation doses refer to the soluble or transportable form which is ingested via food and drinking water and the insoluble or non-transportable form which is ingested via inhalation. The portion which is carried away from the lungs to the intestinal tract is assumed to be transportable.

Health effects /7-32/ depend upon a number of factors besides the radiation dose level, for example the energy which is generated by decay, that portion of the energy which is absorbed in the body, the range of the ionizing radiation in body tissue, ionization density, which tissue is exposed to irradiation and the time span over which exposure takes place.

Thus, the biological effect of the absorbed dose may vary widely. If the dose is given in rems, as in these calculations, however, the relative biological effectiveness of different types of radiation and exposure situations is taken into account.

Some organs are more sensitive to radiation and accumulate more of a given radioactive element. Moreover, the most vulnerable organs vary for the different nuclides.

Weighted whole-body dose

An attempt is made to take into account the combined effect of different doses to different organs on the human body by means of the so-called "whole-body dose", which consists of weighted dose contributions from the radiologically most important organs. The weight factors, v_i /7-31/, which are used in the dose calculations are given in table 7-3. These weight factors apply regardless of age and sex, and relate to an average dose in the population.

Thus, the weighted whole-body dose, D, is the sum of the contributions, $D_i \cdot v_i$, from different organs:

$$D = \Sigma D_i \cdot v_i \qquad (1)$$

The doses D_i to the individual organs for which weight factors are available can be calculated for most of the nuclides in

Table 7-3. Weight factors for calculation of whole-body dose.

Organ or tissue	Weight factor
Reproductive glands	0.25
Chest	0.15
Red bone marrow	0.12
Lung tissue	0.12
Thyroid gland	0.03
Bone tissue	0.03
Remaining organs (individual organ 1/5)	0.30
	1.00

question with atomic numbers below 84. For other nuclides, except for radium-226 (i.e., mainly isotopes of thorium, uranium and transuranic elements), the weighted whole-body dose is based on doses to certain critical organs and the whole-body dose, D_w, in accordance with former recommendations from ICRP /7-27, 7-28, 7-29/.

$$D = \sum_{i=1}^{\ell} D_i \cdot v_i + \left(1 - \sum_{i=1}^{\ell} v_i\right) \cdot D_w \qquad (2)$$

Most of the radium which is absorbed and remains in the body more than a few days is accumulated in the skeleton /7-30/. When radium-226 decays, most of the decay energy is transferred to alpha particles with very short ranges. The cell tissue which covers the bones thereby receives the highest doses, making it the critical organ in relation to its dose limit /7-27, 7-29/. The blood-forming organs in the bone marrow receive, on the average, 1/10th of the dose /7-32/ received by the bone-forming cells on the surfaces of the bone. The turnover of radium in the body's soft tissues is rapid /7-30/, as a result of which the doses there are only about 1/25th of those in the bones. It should therefore be expected that the whole-body dose will be lower than the dose for the critical organ. Only the oldest dose calculations from ICRP still include the whole-body dose for radium-226 /7-27, 7-28/. At that time, however, knowledge concerning the metabolism of radium in the human body was relatively uncertain, which can be seen from the fact that the whole-body dose is of the same magnitude as the dose to bones later calculated by ICRP /7-29/. As far as radium-226 is concerned, the use of the calculation principles in the formulae (2) above should therefore lead to a considerable overestimation of the dose. The calculations for this isotope have therefore been based on the dose to bones and bone marrow and the dose to soft tissures has been substituted for the whole-body dose /7-30, 7-32/.

The dose factors for the whole-body dose /7-26, 7-32/, organ doses and the weighted whole-body dose in accordance with new regulations /7-31/ are specified in table 7-4 for the nuclides in question.

Dose to individuals in the proximate zone

The critical group shall, according to the radiological definition, represent a limited number of individuals who may receive higher doses than average /7-31/. The paths of exposure for the three main types of inflow into the biosphere were defined in the preceding section.

With the groundwater connection between the repository and the inland ecosystem which is assumed, the critical group in the well alternative consists of individuals who are exposed both to the radioactive elements which reach the environment through the well and those which reach the environment through the nearby lake. In the lake alternative and the Baltic Sea alternative the critical group is exposed only to the activity which enters the biosphere through inflow to the lake or to the coastal Baltic Sea zone.

Collective dose and dose commitment

The collective dose is the sum of the various doses to all individuals in a given population. Model studies of the radioactive elements which are turned over within and between different ecosystems make it possible to calculate the collective doses to three different populations: the regional population (18 000), the Baltic Sea area population (10 million) and the global population (10 000 million) outside of the Baltic Sea area.

Which of these populations receives the highest collective dose varies from nuclide to nuclide. The point in time at which the exposure occurs is also of importance for the collective dose distribution. In an initial phase, the regional or Baltic Sea population often makes dominant contributions to the collective dose. Depending on whether the nuclide is, for example, bound relatively strongly to soil and sediment or is able to a greater extent to enter global cycles via lakewater and then seawater, either of these three populations may be dominant with respect to the total collective dose at the time of the maximum collective dose rate. The local population, which may consist of 2-20 individuals, does not make an appreciable contribution to the collective dose.

If the individual or collective doses from a given radioactive release are integrated in time, the dose commitment for an unlimited future is obtained. Such calculations have been carried out for all nuclides and paths of inflow.

With regard to the global exposure for nuclides from the repository, however, the consequence analysis in chapter 8 is based on the maximum accumulated collective dose for a period of 500 years - a time interval which can be obtained at different points in time, depending on the nuclide and the type of inflow into the biosphere. The choice of 500 years as a time interval for calculations of the maximum accumulated collective dose is based on the same principles applied by the radiation protection authorities in establishing directives for the evaluation of long-lived radioactive elements in discharges from nuclear power stations /7-33/.

Table 7-4 Dose factors for intake with food and water or through inhalation of 1 curie of some important nuclides.

	Whole-body* dose	Bone dose	Lung dose	Gonad dose	Thyroid dose	Weighted** whole-body dose
Dose via intake of food or water (rem /Ci)						
Sr 90	9.1×10^{5}	1.1×10^{7}		2.0×10^{3}		1.5×10^{6}
Zr 93	9.1×10^{-1}					1.7×10^{2}
Tc 99	4.6×10^{1}	1.2×10^{2}	1.4×10^{1}	4.6×10^{1}		5.5×10^{2}
I 129	9.1×10^{3}			3.4×10^{3}	1.1×10^{7}	3.4×10^{5}
Cs 135	4.6×10^{3}	1.8×10^{4}	1.8×10^{3}	4.6×10^{3}		7.3×10^{3}
Cs 137	4.6×10^{4}	1.1×10^{5}	1.1×10^{4}	4.6×10^{4}		5.5×10^{4}
Ra 226	3.0×10^{7}	3.0×10^{7}				2.8×10^{7}
Th 229	6.1×10^{4}	2.2×10^{6}				3.4×10^{5}
Th 230	6.1×10^{4}	2.2×10^{6}				3.4×10^{5}
U 233	4.6×10^{4}	5.4×10^{5}				1.1×10^{5}
U 234	4.6×10^{4}	5.2×10^{5}				1.1×10^{5}
Np 237	4.6×10^{4}	1.2×10^{6}				2.0×10^{5}
Pu 239	1.8×10^{4}	1.1×10^{6}				1.6×10^{5}
Pu 240	1.8×10^{4}	1.1×10^{6}				1.6×10^{5}
Am 241	4.6×10^{4}	1.1×10^{6}				2.2×10^{5}
Am 243	4.6×10^{4}	1.1×10^{6}				2.2×10^{5}
Dose via inhalation (rem /Ci)						
Sr 90	1.0×10^{6}	1.2×10^{7}		2.7×10^{3}		2.3×10^{6}
Zr 93	2.5×10^{3}	1.2×10^{5}				1.8×10^{4}
Tc 99	5.0×10^{1}	1.3×10^{2}	1.5×10^{1}	5.0×10^{1}		3.6×10^{2}
I 129	1.0×10^{4}			2.6×10^{3}	6.0×10^{6}	1.9×10^{5}
Cs 135	3.3×10^{3}	1.5×10^{4}	1.5×10^{3}	3.3×10^{3}		5.7×10^{3}
Cs 137	3.3×10^{4}	6.0×10^{4}	1.0×10^{4}	3.3×10^{4}		3.8×10^{4}
Ra 226	4.0×10^{7}	4.0×10^{7}				3.8×10^{7}
Th 229	1.0×10^{8}	6.0×10^{9}				9.0×10^{8}
Th 230	1.0×10^{8}	6.0×10^{9}				9.0×10^{8}
U 233	1.0×10^{6}	1.4×10^{7}				2.7×10^{6}
U 234	1.0×10^{6}	1.3×10^{7}				2.7×10^{6}
Np 237	1.0×10^{8}	3.0×10^{9}				5.0×10^{8}
Pu 239	2.0×10^{8}	6.0×10^{9}				9.5×10^{8}
Pu 240	2.0×10^{8}	6.0×10^{9}				9.5×10^{8}
Am 241	1.0×10^{8}	2.0×10^{9}				4.1×10^{8}
Am 243	1.0×10^{8}	2.0×10^{9}				4.1×10^{8}

* According to ICRP2 /7-27/
** According to ICRP26 /7-31/

7.4.5 Reliability of the model

The reliability of the calculated doses is dependent upon the structure of the model, the choice of exposure paths, approximations in the calculations and uncertainties in the utilized data.

Model design and paths of exposure

The model has been designed on the basis of previous experiences of radioecological calculation models /7-33 and 7-34/.

The 13 paths of exposure taken into account by the model cover the pathways for doses to man which have been found by experience to be the most relevant. Radioactive elements can be introduced into the food web via deposition on plants, uptake via root systems or concentration in animal products. The exposure paths permit this, but they also provide control of those doses which originate from radioactivity in the air, ground and water. The assumption that the concentration of radioactive elements is the same on the beach as in the bottom sediments can lead to overestimates of external exposure, especially as far as thorium-229 is concerned.

Numerical approximation

Uncertainties stemming from numerical approximation have been shown to be no more than 20%, in most cases 5%, of the dose values.

Variations in exchange between the reservoirs in the ecosystem

Transfer coefficients for the exchange between the reservoirs in the model have been calculated for each nuclide. These coefficient have been derived from empirical and calculated data from the literature. In some cases, the span in the interval is great. The dose load has therefore been based on values which generally give the higher dose load with regard to both the critical group and the populations. If other transfer coefficients are used, the doses can therefore deviate from the given result. The degree to which uncertainties in the transfer rates between different reservoirs affect the result with regard to doses to critical groups and the different populations has been investigated by variation of the transfer parameters.

Variations in the transfer coefficients significantly affect the doses in the well and lake alternatives for cesium-135, radium-226 and the uranium isotopes, resulting in considerable contributions to the total dose.

- The range of variation in the exchange between soil and groundwater or between sediment and water can involve a halving of the dose for these nuclides in the local or regional area.
- The concentration factors for fish vary depending on the type of ecosystem and on measuring uncertainties. In the case of cesium-135, the dose can vary by a factor of five in

either direction. In the lake alternative, the doses can vary by a factor of four for radium-226 and two for the uranium isotopes.

Variation in water turnover in the coastal zone in the Baltic Sea alternative can lead to a variation of the dose by a factor of two.

Variations in diet composition and uptake through the food chains

A diet composition has been established for the critical group. For cesium-135, radium-226 and uranium-233, water, fish and milk are the most important paths of exposure. A relatively high fish consumption, 50 kg per year and individual, has been assumed, where the fish has been taken from a given lake. A reduction of fish consumption by half leads to a dose reduction by half for cesium-135 and by less than one-third for radium-226 and uranium-233. Reasonable changes in the consumption of milk products have only a minor effect on the dose load.

Daughter products in decay chains

In decay chains where the daughter product is also radioactive, the distribution of the daughter product among different parts of the biosphere depends partly on the turnover of the parent nuclide. Uncertainties in the turnover of the parent nuclide can, in some cases, affect the dose calculations for the daughter nuclide. In view of its relatively high dose contribution the decay chain uranium-234 - thorium-230 - radium-226 is of particular interest.

Thorium is dispersed slowly through soil in relation to its physical decay rate. Variations in the rate of exchange between soil and groundwater therefore have a relatively insignificant effect on the amount of thorium in the soil. With the interface in an inland area, the amount of radium-226 to which the critical group and the regional population are exposed therefore depends primarily on how quickly uranium and radium are transported through the surface soil, since this has a considerable effect on the radium level both in the food chains and in the groundwater which can reach wells in the surrounding area.

Current studies of the transport of uranium and its daughter products indicate that uranium is leached much faster through typical Swedish soils than has been assumed in previous studies pertaining to vitrified waste. The field and laboratory studies /7-20, 7-21 and 7-35/ which have been carried out for strontium and radium indicate that radium is dispersed much more slowly than strontium through soils under very diverse conditions. In previous studies, however, radium has been assumed to migrate at the same speed as strontium. These changes in the transfer rates in the soil-groundwater system for uranium and radium have been found to lead to a reduction of the exposure of the critical group and the regional population which varies with the assumed type of inflow. In the main alternative discussed above, the doses from the intake of radium are reduced by half when the new transfer coefficients are used /7-26/. The exchange of radium

between sea and sediment greatly affects the global collective dose. Exchange between the oceans and their sediments can be estimated roughly on the basis of the retention times in the ocean of stable isotopes of chemical closely related nuclides among the alkaline soil metals such as strontium. Such estimates are, however, highly uncertain. A more precise measure can be obtained by basing the calculation on the radium inventory in the oceans, the amount of radium which enters the oceans through runoff, the amount which is generated indirect by decay of the uranium present in the oceans and the loss through physical decay of radium /7-26/. With the latter derivation of the transfer from ocean to sediment as a basis for the calculations, the collective dose to the world population which is obtained is only 1/20th of that obtained with the previously used estimate.

Variations in population distribution

Changes in the distribution of the regional population can affect the calculated collective doses. This applies especially to the relatively short-lived or poorly soluble nuclides for which the collective dose primarily derives from the regional load. The assumed population distribution of 20 persons per km^2 is the average for Sweden. An increase of the population, for example in a high-density area in the future, can lead to a limited increase of the collective doses depending on the critical paths of exposure for the different nuclides.

The yield of fish from the lake has been set at 60 000 kg/year, which entails a certain overestimation. Since fish consumption is generally the predominant path of exposure in the region, no increase of the regional collective load in the inland alternative can therefore be expected., in view of the limited supply of fish from the primary lake recipient.

If foodstuffs such as milk and meat constitute critical paths of exposure, an increase of population density can hardly lead to any increase of the dose to the region, since the increase in the population occurs at the expense of the cultivated acreage. In the case of nuclides for which drinking water constitutes the predominant path of exposure, the regional collective dose can be expected to be proportionate to that portion of the regional population which obtains its drinking water from the lake which is the primary recipient for the inflow.

The relevance of the model in a long-range perspective

The local ecosystem in particular can, over the time spans covered by the forecasts, undergo changes which have considerable effects on the exposure situation. The design of the model makes it possible to analyze the consequences of important changes, such as the drying-up of the lake which constitutes the primary recipient for material leached from the repository. The drying-up of large areas of the Baltic Sea can also be taken into account. In both cases, the change can give rise to new exposures through the use of the sediments in agriculture.

Some elements are enriched to relatively high levels in the sediment from the lake or the Baltic Sea. In the case of the radio-

active nuclides which give the dominant dose to the critical group or the collective dose to the population, the drying-up of these bodies of water and the change of the exposure paths do not lead to any increase of the annual doses, since the uptake of nuclides in agricultural products cultivated on the sediment does not contribute as much as the elimination of fish as a path of exposure takes away.

The nuclide cesium-135 is an exception. Individual doses through internal and external exposure of the population living in those areas of the Baltic Sea which may be dried up may be up to one order of magnitude higher than the doses given by the calculations based on an unchanged Baltic Sea. The contribution to the collective dose from the Baltic Sea area is, however, less than one-fifth of the total dose load. An elevated exposure of a future Baltic Sea population through cesium-135 would therefore lead to a doubling of the total dose commitment in the long run.

An increased utilization of the food resources of the oceans in the future could cause a shift towards a diet of a more marine character. Overexploitation of traditional fish populations has led to a search for other sources of nutrition from the sea. In addition to an increased utilization of fish species which have formerly not been fished, there are large nutrient reserves in the form of squid and krill. Algae, especially those of macroformate have been used in many countries as a food source for a long time.

Potential catches of krill may suffice for an annual consumption of 5-10 kg per individual on the average over a population of 10^{10} individuals. Great technical difficulties exist in catching these shrimp. There is little possibility of using plankton as a food source within the forseeable future. But the importance of macroalgae as a food source will increase.

If, assuming no change in the amount of protein in the diet, 10 kg meat are replaced in the future by 10 kg krill or algae, the increase in uptake and dose will be limited to a factor of 1-3 for most radioactive elements. The global collective doses from plutonium and americium especially may increase by a factor of 10-20 for krill and by a factor of 100-150 for algae, still assuming 10 kg. However, the global contribution to the collective doses in the inland alternatives (which yield doses which are several orders of magnitude higher than in the Baltic Sea alternative) is less than one percent. This entails a maximum increase by a factor of 3.

8 SAFETY ANALYSIS

8.1 GENERAL

There are special laws and regulations in Sweden which govern nuclear power activities and which provide a basis for the safety and protection of personnel, nearby residents and the environment.

The Swedish Nuclear Power Inspectorate and the National Institute of Radiation Protection are responsible for the enforcement of laws and regulations in this field. These organizations are the inspection authorities designated by the Atomic Energy Act and the Radiation Protection Act. The Nuclear Power Inspectorate is mainly responsible for examining the safety of facilities and the design of various safety systems. The National Institute of Radiation Protection deals with matters pertaining to radiation protection in the working environment and in the external environment.

The general criteria for safety and radiation protection which comprise the basis for the inspection work and licensing activities of the inspection authorities require that facilities, processes, safety systems and activities be designed in such a manner that:

- the radiation exposure of personnel, nearby residents and the regional and global population is low,
- the risk level resulting from accidents is low,
- every effort is made to minimize the radiation exposure within the bounds of reasonable cost.

The special rules and regulations issued by the authorities in different countries on the basis of these criteria are described in KBS technical report 41 /8-1/ and have been summarized in the KBS report on vitrified high-level reprocessing waste /8-2/.

The explication of the Swedish Stipulation Law (which specifies the criteria which must be fulfilled before new nuclear power plants can be commissioned) states that the final repository must be able to meet radiation protection requirements which aim at preventing radiation injuries. The final repository shall be designed in such a manner that the waste or the spent fuel can be isolated for as long a period of time as is required for its radioactivity to have decreased to a harmless level. The evaluation of the safety of the final repository shall take into considera-

tion the risk that the waste or the spent fuel might escape to the biosphere by means of natural processes, accidents or acts of war.

This chapter provides a safety analysis of the activities which are special for the direct final storage of spent fuel without reprocessing. The safety analysis is based on the technical descriptious and data provided in chapters 2 through 7. Those parts of the handling chain which are the same for spent fuel and for vitrified reprocessing waste /8-2/ are not dealt with here. These stages are: storage of spent nuclear fuel in water-cooled pools in a central fuel storage facility and associated handling and transport operations. The safety evaluation of these activities is the same as reported in /8-2/.

Section 8.2 gives the source strengths of radioactive elements in the spent fuel and in the metal components of the fuel assemblies as well as other important input data for the safety analysis. Safety in the handling and encapsulation of spent fuel as well as of the more long-term storage in water pools is dealt with in section 8.3.

Certain safety principles for final storage are discussed in section 8.4. The most important grounds for evaluating the safety of the final repository are described. The principle of multiple barriers is discussed and temperature conditions and radiation levels are reported briefly.

The results of dispersal calculations with respect to the mechanisms described in chapter 7 are reported in section 8.5.

The central issue, the possibility of release of radioactivity from the final repository and possible consequences in terms of radiation doses and health effects in both the short and the long run, is treated in section 8.6.

The probability of extreme events and their importance from the viewpoint of safety is dealt with in section 8.7. Extreme events in this case also include the risk of criticality resulting from a local accumulation of fissionable materials.

A summary safety evaluation is provided in section 8.8.

8.2 SOURCE STRENGTHS AND INPUT DATA

8.2.1 The spent fuel assemblies

The direct disposal of spent nuclear fuel is not preceded by any chemical treatment. This means that the spent fuel assemblies with uranium dioxide, cladding etc. are only treated mechanically and disassembled into their structural components. The types of fuel treated in the calculations are PWR fuel equivalent to the Westinghouse fuel for the Ringhals 2 reactor and BWR fuel equivalent to the ASEA ATOM fuel for the Forsmark 1 reactor (figure 2-1). The PWR assembly in figure 2-2 is a Ringhals 3 assembly with the fuel rods in a 17 x 17 lattice, whereas the Ringhals 2 assemblies have thicker rods in a 15 x 15 pattern. The quantities of

material are roughly the same. Table 8-1 presents fuel data for Ringhals 2, Ringhals 3 and Forsmark 1.

Table 8-1. Data for unirradiated fuel assemblies

Materials quantities (kg/assembly)	PWR (R2)	PWR (R3)	BWR (F1)
Uranium	452	461	178.0
Oxygen from UO_2	61	62	23.9
Springs	5	5	2.2
Cladding	100	110	49.0
Top tie plate (incl. handle)	8	8	1.6
Bottom tie plate	6	6	1.2
Guide tubes for control rods	9	9	
Spacer grids (7)	6	5	1.0
Spacer capture rod			0.8
Fuel channel			35.4
Transition piece			5.0
Total approx.	650 kg	666 kg	300 kg

Other data	PWR (R2)	PWR (R3)	BWR (F1)
Number of fuel rods per assembly	204	264	63
Rod diameter (mm)	10.72	9.50	12.25/11.75
Rod length (mm)	3 856	3 852	3 954
Assembly length (mm)	4 067	4 058	4 383
Assembly width (mm)	214	214	139

A more detailed description of nuclide formation and inventory, composition of the spent fuel and relative toxicity of the nuclides etc. is provided in /8-2/, section 3.1.

8.2.2 Radioactivity and residual heat in spent nuclear fuel

In high level waste from reprocessing, most of the heavy nuclides have been removed while most of the fission products have been left behind. Spent fuel contains, in addition to the fission products, all of the heavy elements, the residual uranium, the transuranium elements formed by successive neutron capture and their decay products. For more detailed discussion of formation, radioactivity and decay see section 3.2 in /8-2/ and also /8-3/ and /8-4/. Figure 8-1 shows the most important radioactive nuclides in spent fuel. The radioactivity content of the entire final repository after 100 000 years is broken down into nuclides with radioactivity greater than 1 curie in table 8-2.

Data for PWR fuel with a burnup of 33 000 MWd(t)/tU have been used in calculating the quantity of radioactive elements in the spent fuel. The calculation has been carried out using the ORIGEN computer program. Compared with more detailed reactor

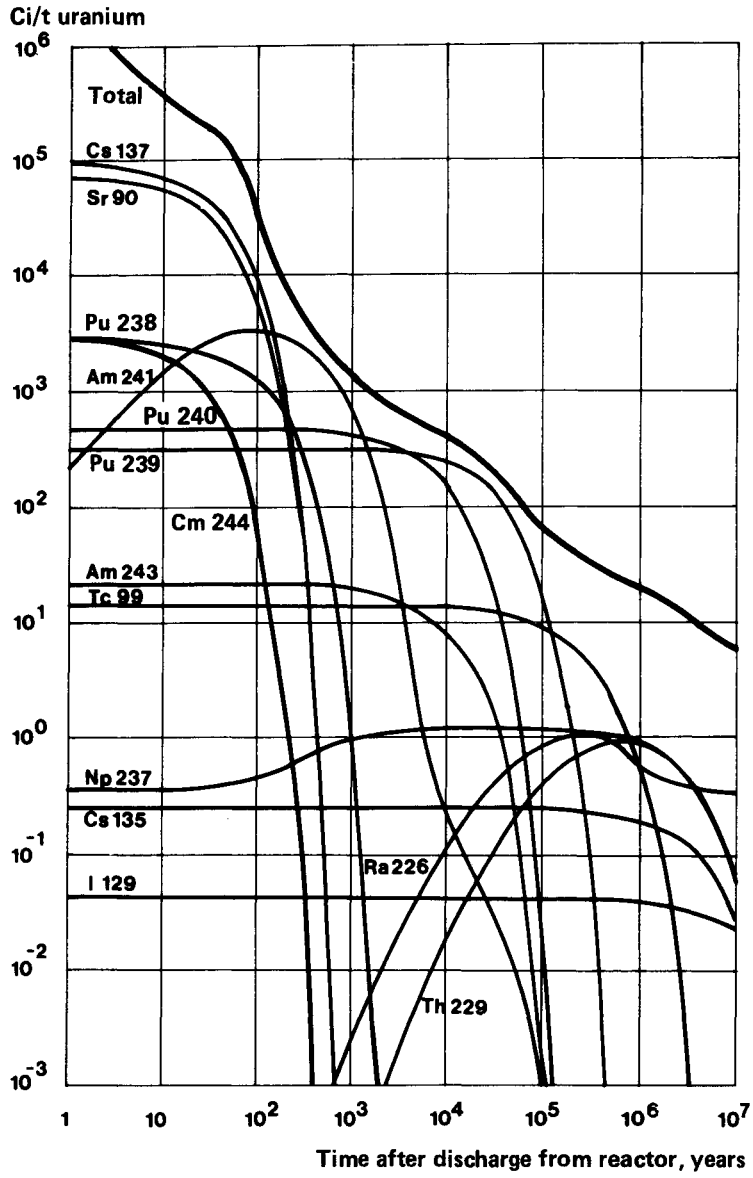

Figure 8-1. Radioactive elements in spent fuel. The graph shows the radioactive elements in PWR fuel with a burnup of 33 000 MWd (t)/tU, power density 34.4 MW (t)/tU and enrichment 3.1 % uranium-235.

physics computer programs, ORIGEN underestimates the quantity of heavy nuclides in the fuel. Table 8-3 presents a comparison between maximum calculated nuclide contents at any time in the spent PWR fuel obtained with ORIGEN and contents obtained with the more accurate program CASMO (ORIGEN has been used for the decay calculations here as well). A comparison with the CASMO values for BWR (27 600 MWd(t)/tU) shows that the ORIGEN values for PWR can be used for the total content for the final repository, since most of the Swedish reactors are of the boiling water type. As far as fission products are concerned, the total levels in the final repository are overestimated when the PWR-ORIGEN values are used. See /8-4/ for a more detailed discussion.

Figure 8-2 shows the residual heat in spent fuel at different points in time following discharge from the reactor. More detailed are presented in /8-2/ section 3.3 and in /8-5/.

Table 8-2. Long-lived fission products and heavy elements in 10 000 tons of spent PWR fuel after 100 000 years.

Nuclide	Half-life (years)	Radioactivity (Ci per 10 000 tonnes)
Se 79	65 000	1 400
Zr 93	1.5×10^6	18 000
Tc 99	210 000	100 000
Pd 107	7×10^6	1 200
Sn 126	100 000	2 800
I 129	17×10^6	380
Cs 135	3×10^6	2 500
Cm 245	8 260	1
Am 243	7 650	24
Am 241	433	1
Pu 242	379 000	13 000
Pu 241	14.6	1
Pu 240	6 760	180
Pu 239	24 400	200 000
Np 237	2.13×10^6	11 000
U 238	4510×10^6	3 100
U 236	23.9×10^6	4 100
U 235	710×10^6	260
U 234	247 000	14 000
U 233	162 000	3 800
Pa 231	32 500	210
Th 230	80 000	9 000
Th 229	7 300	3 800
Ra 226	1 600	9 000
Total for above		390 000
Total including decay chains		540 000

Table 8-3. Some environmentally important heavy nuclides in spent fuel. Comparison between fuel types and calculation programs.

Nuclide	Max Ci/tonne uranium		
	PWR[a]		BWR[b]
	ORIGEN	CASMO	CASMO
Ra 226	1.1	1.1	0.83
Th 229	0.85	1.1	0.67
Np 237	1.1	1.5	0.89
Pu 239	320	400	270
Pu 240	490	520	450
Am 241	3 300	4 700	2 900
Am 243	21	19	12

a) Burnup 33 000 MWd/tU b) Burnup 27 600 MWd/tU

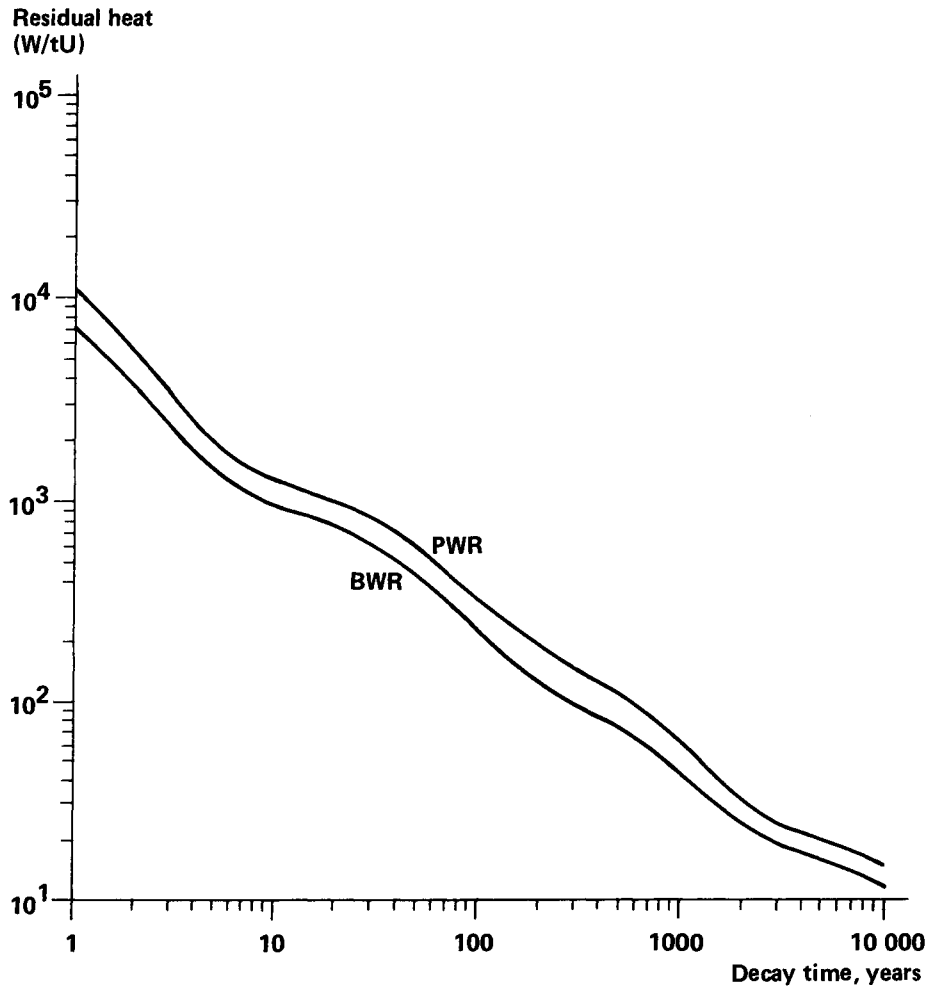

Figure 8-2. Residual heat in spent fuel from PWR and BWR. For the PWR fuel, it has been assumed that burnup is 33 000 MWd (t)/tU, power density is 38.5 MW (t)/tU and enrichment is 3.25 % uranium-235. The corresponding data for BWR fuel are 27 600 MWd (t)/tU, 22.0 MW (t)/tU and 2.75 % uranium-235.

8.2.3 Induced radioactivity in fuel assembly components

Besides the elements discussed above, other activation products are also formed in the fuel rods in the cladding and in the springs which hold the uranium dioxide pellets in place. Decay is demonstrated in table 8-4. The radioactivity in the cladding and in the springs represents a negligible addition to the radioactivity in the fuel itself.

In addition to fuel rods, the fuel assemblies also consist of a number of metal structural components, see table 8-1 and figures 2-1 and 2-2. According to the proposed handling method, the fuel rods are to be removed from the fuel assemblies and stored separately. The remaining metal components contain radioactive nuc-

Table 8-4. Induced radioactivity in cladding and springs, PWR

Radioactivity (Ci/tU) after	10 yrs	100 yrs	1 000 yrs	10 000 yrs	100 000 yrs	1 mill.yrs	10 mill.yrs
Cladding (zircaloy)	170	0.76	0.37	0.25	0.18	0.12	0.0018
Springs (stainless)	630	26	0.40	0.32	0.14	-	-
Total	800	27	0.77	0.57	0.32	0.12	0.0018

lides formed by activation in the reactor. But they do not contain any appreciable quantities of heavy nuclides or fission products. Tables 8-5 and 8-6 show radioactivity broken down into different components and table 8-7 shows radioactivity broken down into the most important nuclides. Figure 8-3 presents a

Table 8-5. Induced radioactivity in fuel assembly components,PWR

Radioactivity (Ci/tU) after	10 yrs	100 yrs	1 000 yrs	10 000 yrs	100 000 yrs	1 mill.yrs	10 mill.yrs
Top tie plates (stainless)	200	8.2	0.13	0.10	0.045	-	-
Bottom tie plates (stainless)	730	30	0.47	0.37	0.17	-	-
Guide tubes for control rods (zircaloy)	16	0.071	0.035	0.023	0.017	0.011	0.0002
Spacer grids (Inconel)	780	220	3.4	2.9	1.2	0.0009	
Total	1 700	260	4.0	3.4	1.4	0.012	0.0002
Borosilicate glass rods* (stainless cladding; Ci total)	53 000	1 500	25	19	8.3	0.0038	-

* The rods are only used in the first core

Table 8-6. Induced radioactivity in fuel assembly components, BWR

Radioactivity (Ci/tU) after	10 yrs	100 yrs	1 000 yrs	10 000 yrs	100 000 yrs	1 mill.yrs	10 mill.yrs
Rod bundles							
Top tie plates and handles (stainless)	110	10	0.16	0.13	0.057	-	-
Bottom tie plates (stainless)	120	11	0.17	0.14	0.060	-	-
Spacer grids (Inconel)	310	120	1.8	1.5	0.68	0.0003	-
Spacer capture rod (zircaloy)	0.68	0.075	0.0076	0.0054	0.0038	0.0021	-
Total	540	140	2.1	1.8	0.80	0.0024	-
Boxes							
Fuel channel (zircaloy)	59	1.2	0.53	0.34	0.23	0.15	0.0023
Transition piece (stainless)	110	11	0.16	0.13	0.057	-	-
Total	170	12	0.69	0.47	0.29	0.15	0.0023

Table 8-7. Induced radioactivity in fuel assembly components, broken down into nuclides.

Radioactivity (Ci/tU) after	Half-life (years)	10 yrs	100 yrs	1 000 yrs	10 000 yrs	100 000 yrs	1 mill.yrs	10 mill.yrs
PWR								
C-14	5 735	0.080	0.079	0.071	0.024			
Co-60	5.25	800	0.0057					
Ni-59	80 000	3.4	3.4	3.4	3.1	1.4	0.0006	
Ni-63	92	500	260	0.29				
Zr-93	$1.5 \cdot 10^6$	0.0086	0.0086	0.0086	0.0086	0.0082	0.0054	
Nb-93m*		0.0090	0.020	0.020	0.014	0.0082	0.0054	
BWR								
C-14	5 735	0.39	0.38	0.34	0.12			
Co-60	5.25	130	0.0009					
Ni-59	80 000	2.0	2.0	2.0	1.9	0.86	0.0004	
Ni-63	92	300	150	0.17				
Zr-93	$1.5 \cdot 10^6$	0.12	0.12	0.12	0.12	0.11	0.075	0.0012
Nb-93m*		0.054	0.12	0.12	0.12	0.11	0.075	0.0012

* Daughter of Zr93 and Mo 93

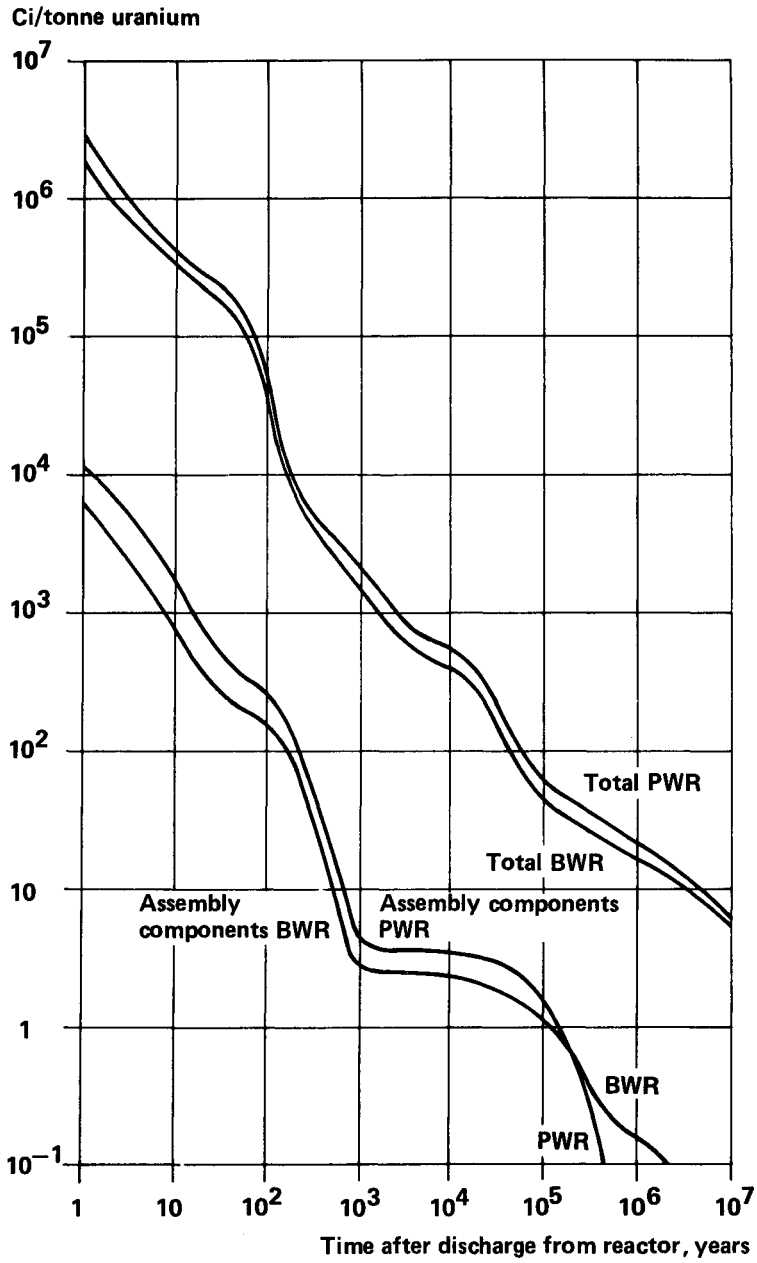

Figure 8-3. Radioactivity in spent fuel assemblies, total and in assembly components except for fuel rods. Fuel data as in figure 8-1 (PWR) and figure 8-2 (BWR).

comparison between the induced component radioactivity and the total activity in the fuel. Figure 8-4 shows a breakdown of the radioactivity into different nuclides (PWR).

The calculations of induced radioactivity in the structural material are presented in /8-6/.

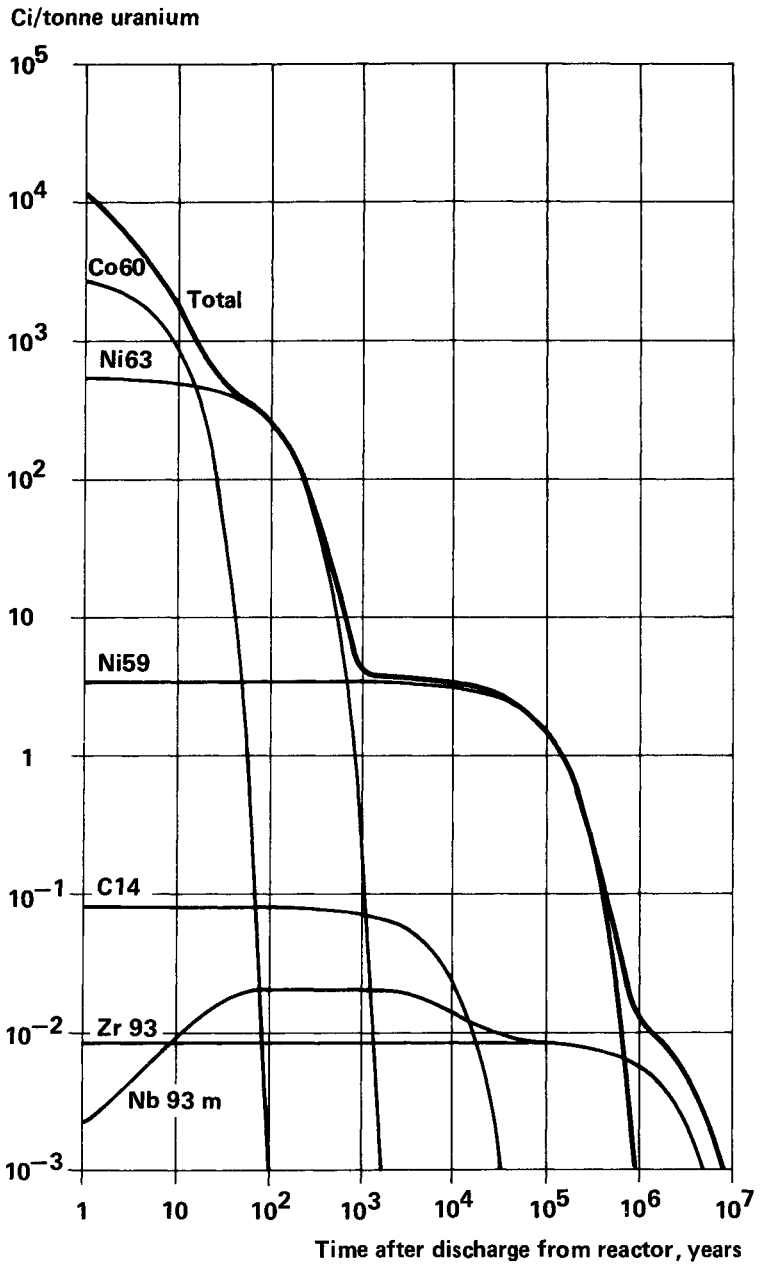

Figure 8-4. Radioactive elements in fuel assembly components from PWR. Fuel rods not included. Fuel data as for figure 8-1.

8.3 HANDLING AND ENCAPSULATION OF SPENT FUEL

8.3.1 General

Following is a summary of the safety aspects of such handling, storage and encapsulation procedures as are specific to the alternative of direct disposal of spent unreprocessed nuclear fuel. The facilities required for this alternative are an intermediate storage facility for spent fuel (long-term storage) and an encapsulation station.

A safety analysis of the central storage facility for spent fuel and of the transportation system was presented in a previous report /8-2/.

The safety aspects of the central storage facility are associated with the actual handling and short-term storage of the fuel in water pools and with the more protracted long-term storage. Safety with respect to handling and short-term storage has already been dealt with /8-2/. With regard to long-term storage in water pools, a special study has been carried out /8-7/, the results of which are summarized in section 8.3.2 below.

The processes involved in encapsulating spent fuel in highly durable containers suitable for final storage in rock have also been the subject of examination from the viewpoint of safety. The safety aspects of encapsulation and handling in connection therewith have been analysed in greater detail in two separate technical reports /8-8, 8-9/. A summary is provided in section 8.3.3.

Facilities, equipment and process technology are described in special reports which are summarized in section 2.3.

8.3.2 Long-term storage of spent fuel in water pools

The total time for which the spent fuel will be stored in water pools prior to direct final disposal is suggested to be 40 years.

Good experiences from the storage of fuel in water pools are available from many years of practice. No adverse effects on the canister or the fuel have been observed in connection with such storage. These experiences show /8-7/ that general corrosion after 100 years of storage in neutral pure water is scarcely more than 1 µm. Even with the assumption of other reasonable water chemistry, general corrosion will not occur to an extent which could jeopardize safety.

The possibilities of pitting, galvanic corrosion, crevice corrosion and galvanically induced hydration are also analysed in /8-7/. The results show that these mechanisms, if they take place at all, do not entail any problems for the type of storage in question.

Delayed fracture due to hydrogen embrittlement has not been observed on zircaloy-clad fuel in connection with storage. Theoretical analyses of the process indicates low crack growth which does not lead to failure.

During reactor operation, isolated fuel damage may occur as a result of stress corrosion cracking. This is caused by high stresses during operation and the simultaneous effects of certain elements (mainly iodine) which have been released from the fuel.

Since the stress in the cladding material is considerable lower during storage than during reactor operation and since the release of fission products decreases greatly after discharge of the fuel from the reactor, the conditions necessary for stress corrosion cracking do not exist during storage in the water pools.

Experimental studies of the inside of the cladding after many years of reactor operation and storage have shown the following:

- The build-up of oxide on the inner surface was scarcely measurable (approx. 1 µm) after 8 years of irradiation in the Halden reactor.
- Metallographic examination of fuel rods after 10 years of storage in England revealed nothing which could indicate ongoing or incipient degradation.

Damaged fuel is stored in different ways. The usual way is that fuel assemblies which contain leaking rods are placed in sealed water-filled containers in the pool. This method has been used for 5 years at WAK, Germany, and for 9 years at Windscale, England. At Mol, Belgium, damaged fuel is stored in sealed dry containers in pools. Damaged CANDU fuel has been stored at Mol in this manner for 9 years. At General Electric's Midwest Fuel Recovery Plant in the United States, damaged fuel is stored in the same manner as undamaged fuel without any problems. Damaged fuel is also stored in the same manner as undamaged fuel in pools at nuclear power plants.

Small quantities of radioactive elements can be released from damaged fuel rods during storage. But no further degradation of the fuel or the cladding has been noted in connection with the storage of such rods.

In connection with the long-term storage of damaged fuel, Cs-134 and Cs-137 constitute the main part of the release, which on the whole is very small. During an initial phase in the reactor's storage pool, the most accessible portion is released, after which leakage decreases. Most of the gaseous products which can leak out from damaged fuel have already been liberated during reactor operation. In view of the extensive and good experience available from the handling and storage of damaged fuel in reactor storage pools and the low leakage which persists after an initial period, it can be safely assumed that releases of radioactivity during long-term storage will not constitute a problem.

The portion of fission products which is easily accessible for leakage depends to a great extent on the specific power of the fuel during reactor operation. The total amount which is released is, of course, also dependent upon the number of damaged rods. The level of radioactivity in the storage pools is dependent upon the volume of the cleaning flow. The range of variation is 10^{-7} - 10^{-3} Ci/m^3 /8-7/.

If individual rods should be punctured during storage, this would lead to a small release of krypton-85. Experience shows, however, that this does not entail any radiation protection problems - not even in connection with normal fuel handling in the nuclear power stations.

8.3.3 Safety measures in the encapsulation station

A description of facilities, systems and procedures for handling and encapsulation is provided in section 2.3. Figure 2-5 shows the layout of the process building.

The facility is designed with a special emphasis on

- minimizing radiation doses for the personnel,
- preventing damage to the fuel resulting from accidents and improper handling,
- minimizing the dispersal of any released radioactivity to the environment.

The integrity and handleability of the spent fuel are not expected to deteriorate over the 40-year period of pool storage.

It has previously been shown that degradation mechanisms such as general corrosion, local corrosion, stress corrosion cracking, hydrogen embrittlement etc. are not expected to lead to any significant initiation of degradation within this period of time. The handleability of high-burnup fuel is good, and extensive experience and well-developed routines exist in Sweden for such handling. Experience shows that radiation exposure of personnel employed in fuel handling is small. Furthermore, these experiences are based on the handling of fuel immediately after reactor shutdown. The fuel which is handled in the encapsulation station will have decayed for 40 years, which leads to considerably more favourable radiation conditions.

The radiation doses are minimized primarily by remote handling of the fuel, either under water or in radiation-shielded cells. Handling in water takes place with at least 2.5 m of water coverage over the fuel, which provides fully adequate shielding of both gamma radiation and neutrons.

The various handling operations and equipment in the radiation-shielded encapsulation cells are remote-controlled from the control room. All activities are supervized via radiation-shielding windows from this room. The ventilation air from the encapsulation cells can be passed through filters if measurements show that it contains radioactive material. All radioactive areas are kept under negative pressure in relation to control rooms, other premises and the surrounding environment.

Even after the fuel has been encapsulated in the copper canister, handling is remote-controlled. Radiation shielding calculations for the lead-filled copper canister with its spent fuel are reported in /8-10/. The gamma dose rate on the container's cylindrical surface at the mid point is 20 mrems/h, while the neutron dose rate is 40-95 mrems/h. The corresponding dose rate on the lid above the fuel will reach a maximum of about 1 mrem/h. Thus, certain necessary short-term service work can be performed near the canisters without any excessive exposure.

All equipment in the encapsulation cells can be given service and maintenance by lifting the equipment out of the cells or taking it to a separate service cell. After a cell has been emptied of fuel, and decontaminated if required, the necessary maintenance can be carried out in the cell as well.

The cell walls bordering on the control rooms are thick enough so that no matter where the unshielded fuel is located in the cells, the dose rate in the control room will be very low. With conservative assumptions (copper canister without lead fill and with

only 10 years of decay of the spent fuel), the calculated dose rate outside the 1.3 m thick concrete walls is less than 0.1 mrem/h /8-11/.

Up to and including the reloading pool (see section 2.3 and figure 2-6), the fuel is stored inside the transport cask. The transport cask must be able to withstand a free fall from 9 m on to a hard surface, according to the IAEA transport regulations for type B packages. The handling of the cask is thus planned in such a manner that the cask is never lifted more than 9 m. For example, the cask is lifted down into the reloading pool in two stages. Horizontal movements of the transport cask within the receiving section are done by overhead crane over a reinforced section of floor. Lifting heights are kept to a minimum in connection with vertical movements.

The rods are removed from the fuel bundle in the dismantling position by means of a chuck tool which grips the end of the rod and fixes it in position. As an extra safety precaution, the chuck tool is attached to the slewing crane by a safety line in order to prevent the tool and the rod from being dropped.

As an extra safeguard against dropping of the copper canister with the fuel during welding of the canister lids, the welding machine is equipped with a pivot plate which is swung in under the canister. Normally, the canister is held in place by a gripping tool as the charging machine's lifting tackle is lowered.

The overhead cranes are equipped with redundant drive and brake equipment as needed.

If a fuel bundle is damaged during transport, it may be difficult to pick out individual rods. The bundle may be bent or deformed. The end tie plates may be knocked crooked, fuel rods may burst or spacers may be displaced. Reference /8-7/ describes how damaged fuel can be handled. In summary, it may be said that experience does not indicate any significant problems in connection with this handling. Equipment for vacuuming up dropped pellet fragments will be provided, for example in the form of sludge suction equipment.

Dropped pellet fragments are collected in filters which are then disposed of in the same manner as fuel rods. But it is unlikely that fuel pellets will be dropped out of damaged rods. It has, for example, proven to be very difficult to get pellets out of spent rods, in part owing to the fact the uranium dioxide swells.

During the lead casting operation in the encapsulation process, the fuel is heated to about 400°C. As a result, the internal gas pressure in the rods will increase. Thanks to the low fission gas pressure (~ 0.3 MPa) in the BWR rods, the effects of heating on the integrity of the cladding are negligible. The internal pressure of the PWR fuel can normally be about 5 MPa, which, after heating, can increase up to 12 MPa. This leads to an annular stress of about 110 N/mm^2. But the PWR cladding is designed to withstand stresses of 300 N/mm^2. Oxidation of the rods or the canister is impossible, since heating and cooling takes place under a protective gas.

Fuel handling and storage are designed to provide an ample margin

to criticality in all fuel configurations. K_{eff} is less than 0.95, even with fresh fuel in water and the most unfavourable configuration from the viewpoint of criticality, namely with fuel rods packed tightly in copper racks. Moreover, since it is the spent fuel that will be encapsulated, the margin to criticality is great.

The fire load is low throughout. In order to further reduce the fire hazard, the facility is devided into fire cells and equipped with an automatic fire alarm and fire ventilation as well as fire extinguishing systems adapted to the nature of the different areas.

8.3.4 Releases from the encapsulation station during normal operation

There may be some small leakage of radioactivity from the fuel to the water in the pool. This is taken care of by cleaning systems in the same way as in the reactor stations. Small quantities of krypton-85 and tritium are entrained in the ventilation air and released into the atmosphere. Traces of iodine and particulate activity may also be discharged to the air. But most remains in the water and is collected by the ion exchangers and filters in the cleaning systems. Most of the released radioactivity in the encapsulation cells is collected in filters installed in the exhaust ventilation ducts from these areas.

Normal operational releases resulting from handling of the fuel in the pools are not expected to exceed those from the central fuel storage facility. These have been reported previously /8-2/.

The fuel will to some extent be handled in dry condition, whereby any discharge of radioactivity will be to the air instead of to the water. However, all operations under dry conditions take place in the encapsulation cells, which are completely shielded off from the environment. The exhaust air from these cells is filtered in filter banks with more than 90% removal efficiency for iodine and 99.9% for aerosols.

8.3.5 Failures and accidents in the encapsulation station

The encapsulation station is designed in such a manner that the probability of accidents is very low. Those accidents which are nevertheless conceivable are limited to incidents which entail very small releases of radioactivity.

The possible types of failures and accidents and their frequency and consequences are analyzed in /8-8/. Additional information on some points is provided in /8-9/.

The following accidents have been studied:

- Fuel is dropped during handling
- Cladding is sawn through
- Mechanical fuel damages in connection with encapsulation
- Rack with fuel rods is dropped in casting cell
- Copper canister is damaged while being welded shut
- Copper canister is dropped

- Loss of vacuum and protective gas during heating and cooling in casting bell

External forces, including sabotage and acts of war, have also been considered.

8.3.6 Radiation doses

The consequences of releases to the environment as a result of accidents have been calculated /8-8/. The results can be summarized in brief by the following rounded-off figures, where the limits represent handling of BWR fuel or PWR fuel alone. For the time being, it is assumed that 20-30% of the fuel consists of PWR fuel. With a 40-years storage period, the releases of krypton-85 and tritium are even smaller.

Release	Kr-85 Ci	I-129 µCi	H-3 Ci	Aerosols (Pu) µCi
Annual average	10-200	2-25	0.1	-
Accident occuring several times a year	2-100	1-10	0.1	
Rare accident x)	100-2000	40-1200	4-10	4-40

x) Less than once every 10 years.

The other types of accidents dealt with in /8-9/ do not essentially alter the above figures.

The radiation dose at a distance of 1 km from the station has been calculated to be less than 0.4 µrem/year under normal operating conditions and 40 µrems in the event of a rare accident, i.e. well below the design goal (10 000 µrem/year) for nuclear power stations.

It has been deemed possible that the annual dose for personnel can, on the average, be kept lower than 200 mrems/year and no difficulty is foreseen in keeping the individual doses below the current limit value (5 000 mrems/year).

8.4 SAFETY PRINCIPLES FOR FINAL STORAGE

8.4.1 Safety-related grounds for evaluation of final storage

The Stipulation Law directs as one alternative that a reactor owner must demonstrate "how and where an absolutely safe final storage of spent, unreprocessed nuclear fuel can be effected". The special explication of the bill states that "the primary consideration here is whether the storage scheme can meet requirements for satisfactory radiation protection". Furthermore, "the storage site shall permit the isolation of the waste or the

spent nuclear fuel for as long a time as is required for the radioactivity to decay to a harmless level".

These very general criteria agree with the principles which are applied within other areas of nuclear power technology as well.

No specific safety criteria for final storage of radioactive waste have been established. However, work is being pursued within this area in many countries and in international cooperation. Pending the results of this work, existing rules which are more or less generally accepted for existing nuclear power installations must be applied. A review of current regulations is provided in /8-1/.

The following rules should be considered in connection with final storage:

- The ICRP rule that no individual, either now or in the future, shall be exposed to radiation doses which exceed the limits recommended by the ICRP. The present limit for individuals among the general public is 500 mrems per year from all activities which can give rise to irradiation, with the exception of the medical use of ionizing radiation. If a given radiation source can be expected to give rise to exposures over a series of years, the radiation dose from this source shall not exceed 100 mrems per year on the average, figured as a weighted whole-body dose.

- The design goal for new nuclear power plants in Sweden, a maximum of 10 mrems per year (weighted whole-body dose) to nearby residents.

- The maximum permissible radiation dose to nearby residents in Sweden in connection with the operation of nuclear power plants, namely 50 mrems per year (weighted whole-body dose).

- The recommended maximum permissible global weighted collective dose commitment applied in the Nordic countries of 1 manrem per year and MW installed electrical output (MWe), which applies to the entire nuclear fuel cycle. The collective dose commitment shall be calculated over a period of 500 years and distributed between 0.5 manrem/MWe-year for the operation of nuclear power plants and 0.5 manrem/MWe-year for the rest of the nuclear fuel cycle. The choice of the level of 1 manrem per year and MWe is based on the goal of a maximum of 10 mrems/year and individual with an assumed average global nuclear power production of 10 kW per person. (Note: In Sweden, the total installed electrical output is currently about 25 000 MWe, i.e. about 3 kW per person. Of this, some 0.5 kW per person is produced by nuclear power. 13 nuclear power units would increase this output to about 1.2 kW per person.)

In evaluating the final storage scheme, the fact that radioactive elements occur in nature and that ionizing radiation from these elements is a part of the natural environment of human beings should also be taken into consideration. Natural background radiation varies in Sweden between 70 and 140 mrems per year and in-

dividual /8-12/. Natural radiation levels of up to 1 300 mrem/year and individual exist at some places abroad /8-13/.

Of special interest in this context is the occurrence of natural radioactive elements in water. The following table gives some values for Sweden.

Contents of radioactive elements in water

Radioactive element	Contents in natural waters (pCi/l) in Sweden	
	Drinking water	Sea water[a)]
Radium-226	0.1-40	0.3
Uranium	0.1-1500[b)]	3
Potassium-40	ca 20	330

a) With 3.5% salinity

b) Applies to natural water (not necessarily drinking water)

A radium-226 level of 40 pCi/l in drinking water gives a radiation dose of about 40 mrems per year weighted whole-body dose in accordance with the calculation method used in this report. Radium-226 levels up to 256 pCi/l in groundwater near Helsinki are reported in a Finish study /8-14/.

8.4.2 Barriers

In order to meet the requirement for a long-term isolation of the radioactive substances and ensure a safe final storage, the waste is surrounded by a number of barriers.

These barriers are as follows:

- binding of the radioactive waste to a solid, poorly soluble substance,
- enclosure in canisters of a highly durable material,
- packing of the canisters in an impervious buffer material,
- final storage in stable bedrock with low groundwater flow,
- chemical barriers against the dispersal of the radioactive substances.

Each of these barriers provides protection against the release and dispersal of radioactive substances. But each barrier poses-ses different protective properties and functions which both reinforce and complement each other.

The binding of the radioactive elements to the uranium dioxide fuel is dealt with in chapter 6. The encapsulation of fuel rods is described in section 2.3 and the properties of the canister are described in chapter 5. The encapsulation of metallic waste and other types of waste is described in section 2.3 and the durability of the encapsulation is analyzed in section 6.10. The properties and function of the buffer material are described in

chapter 4, and the properties of the geological barrier in chapter 3. The retardation of radioactive elements by sorption is described in section 7.3.

The design of the final repository as far as spent fuel rods are concerned is illustrated by figures 2-17 and 2-22, and as far as other waste is concerned by figure 2-23.

8.4.3 Temperature conditions

In order to obtain the least possible disturbance of the natural environment in the rock which is selected for the final repository, a low heat load on the rock has been striven for. This has been achieved by a combination of a period of supervised storage of the fuel (40 years after discharge from the reactor) and a relatively widespread distribution of the fuel in the rock repository. This ensures that the temperature everywhere in the rock and in the buffer mass will be less than 100°C. Furthermore, the thermal gradient for groundwater flow will be so low that its impact on the groundwater flow through the repository will be insignificant.

Figure 8-5 gives the temperature on the surface of the hottest copper canister, the mean rock temperature in the centre of the final repository and the maximum rock temperature halfway between two canisters as a function of the time since commencement of final storage. The maximum canister temperature is less than 80°C, and the highest rock temperature halfway between two canis-

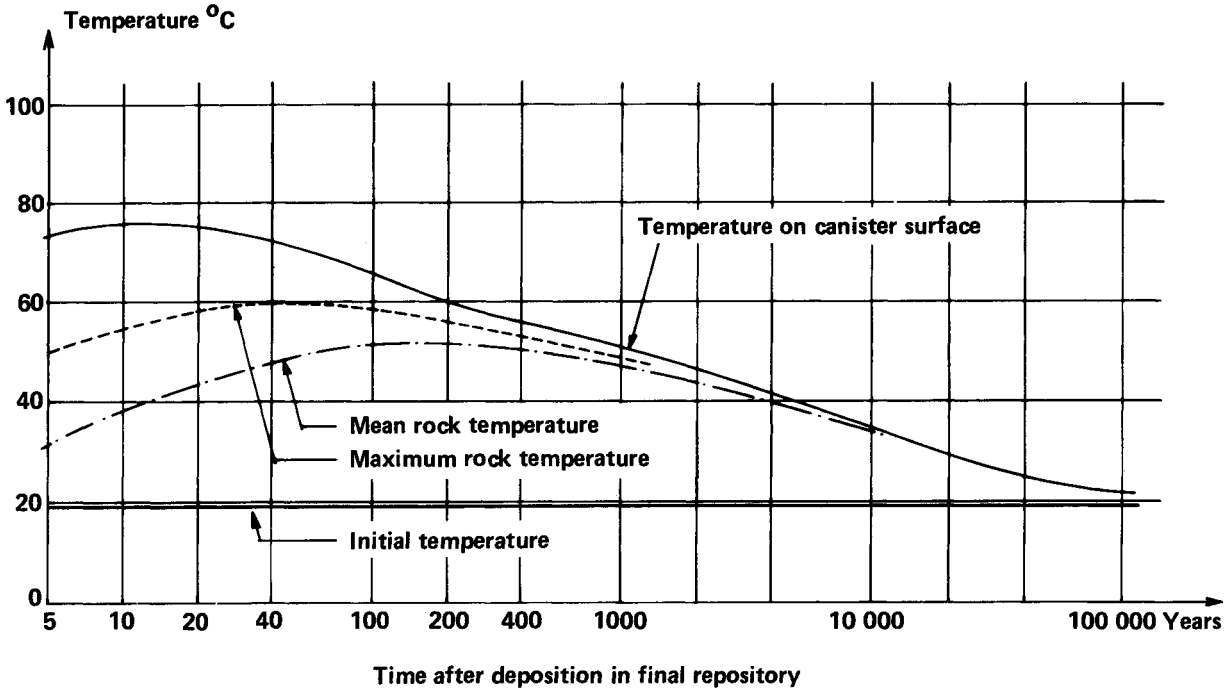

Figure 8-5. Temperatures on canister surface and in rock at different points in time after deposition in final repository.

ters near the centre of the final repository is close to 60°C. After 1 000 years, all temperatures have dropped to below 50°C. After approximately 100 000 years, the initial temperature level (20°C) has been largely restored. Thus, the expected service life of the canisters is considerably longer than the period of time during which any appreciable temperature elevation exists.

The heat generated by metal waste components resulting from the conditioning of spent unreprocessed nuclear fuel for final storage is so low that it is of no importance for the design of the final repository.

8.4.4 Radiation levels

The radioactive waste emits ionizing radiation. This radiation is strongest from the fuel rods. But the radiation is effectively shielded by the copper canister and the lead fill. The thickness of the canister wall, 200 mm, has been chosen with the aim of limiting the radiolysis effects in the buffer mass to an insignificant level. Figure 8-6 gives the maximum radiation dose rates on

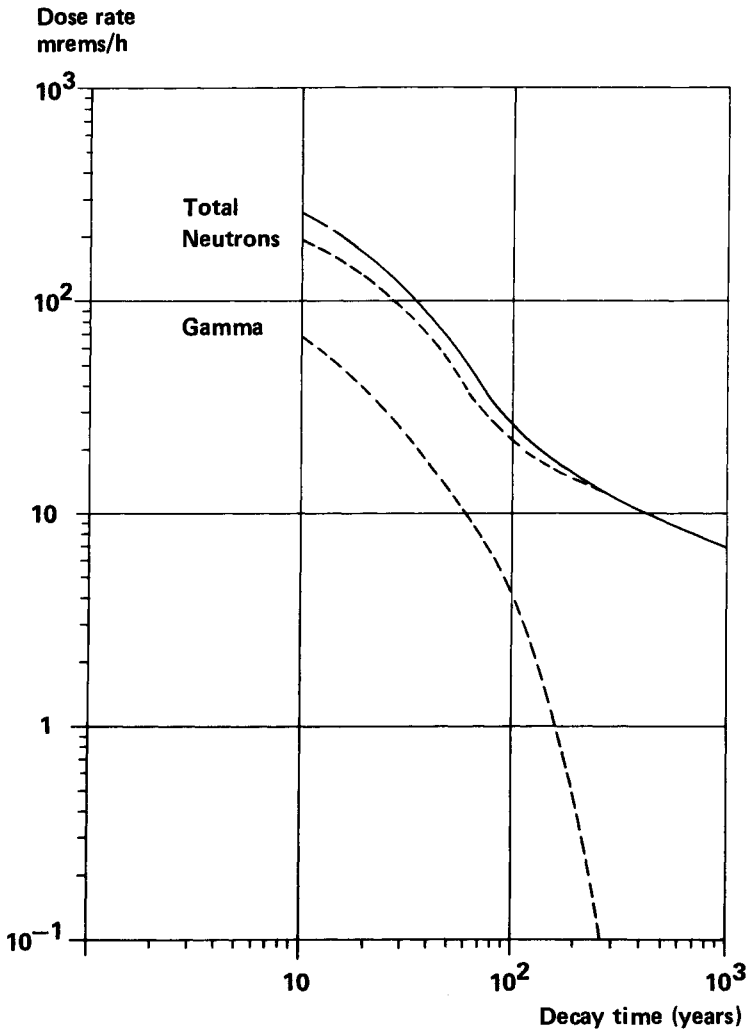

Figure 8-6. Radiation dose rates on surface of copper canister after different decay times.

the outside of the copper canister as a function of time for neutrons and for gamma radiation /8-10/.

The influence of radiation on corrosion of the canister and on leaching of the radioactive elements is described in chapters 5 and 6, respectively.

8.5 DISPERSAL CALCULATIONS

8.5.1 Calculation procedure and premises

The dispersal of radioactive elements through the rock and in the biosphere has been analyzed in accordance with the scheme illustrated in figure 8-7. This scheme is basically the same as that which was used for the safety analysis in the KBS report on the final storage of vitrified waste from reprocessing /8-2/.

The source strength calculations were described in section 8.2.

Nuclide transport through the rock has been calculated using a one-dimensional model which takes into account groundwater flow, axial dispersion, geochemical retardation of the different nuclides and chain decay /8-15/. The different model assumptions were discussed in section 7.2. The model exists in the form of a computer program, GETOUT /8-16, 8-17/, whose output is such that it can be used directly as input to the computer program BIOPATH.

This program calculates the transport of radioactive elements in the biosphere and radiation doses to man, as described in section 7.4. Three different cases for inflow to the biosphere have been studied: well, lake and Baltic Sea. See section 7.4.1.

The structure of the ecosystems, the transfer rates which control the exchange between the reservoirs in the ecosystems and the paths of exposure are assumed to be unchanged through all future time. Over the very long time spans covered by the study, however, changes in these parameters are possible. How such future variations will effect the results is discussed in 7.4.5.

8.5.2 Calculation cases

It is assumed that the final repository will accomodate some 7 000 canisters. The service life of a canister has been judged cautiously to be hundreds of thousands of years. Service life calculations show that the canister can be expected to remain intact for more than 1 million years. In the dispersal calculations, it has been conservatively assumed as a reference case that the first canisters start to be penetrated after 100 000 years. It is further assumed that the process of penetration of the canisters then proceeds at a uniform rate for 400 000 years, i.e. one canister is penetrated approximately every 60th year.

The dissolution of radioactive elements in a canister has been calculated in section 6.6 on the basis of the possible escape of dissolved elements through the buffer material and rock fissures. A minimum dissolution time of 1.8 million years after penetration

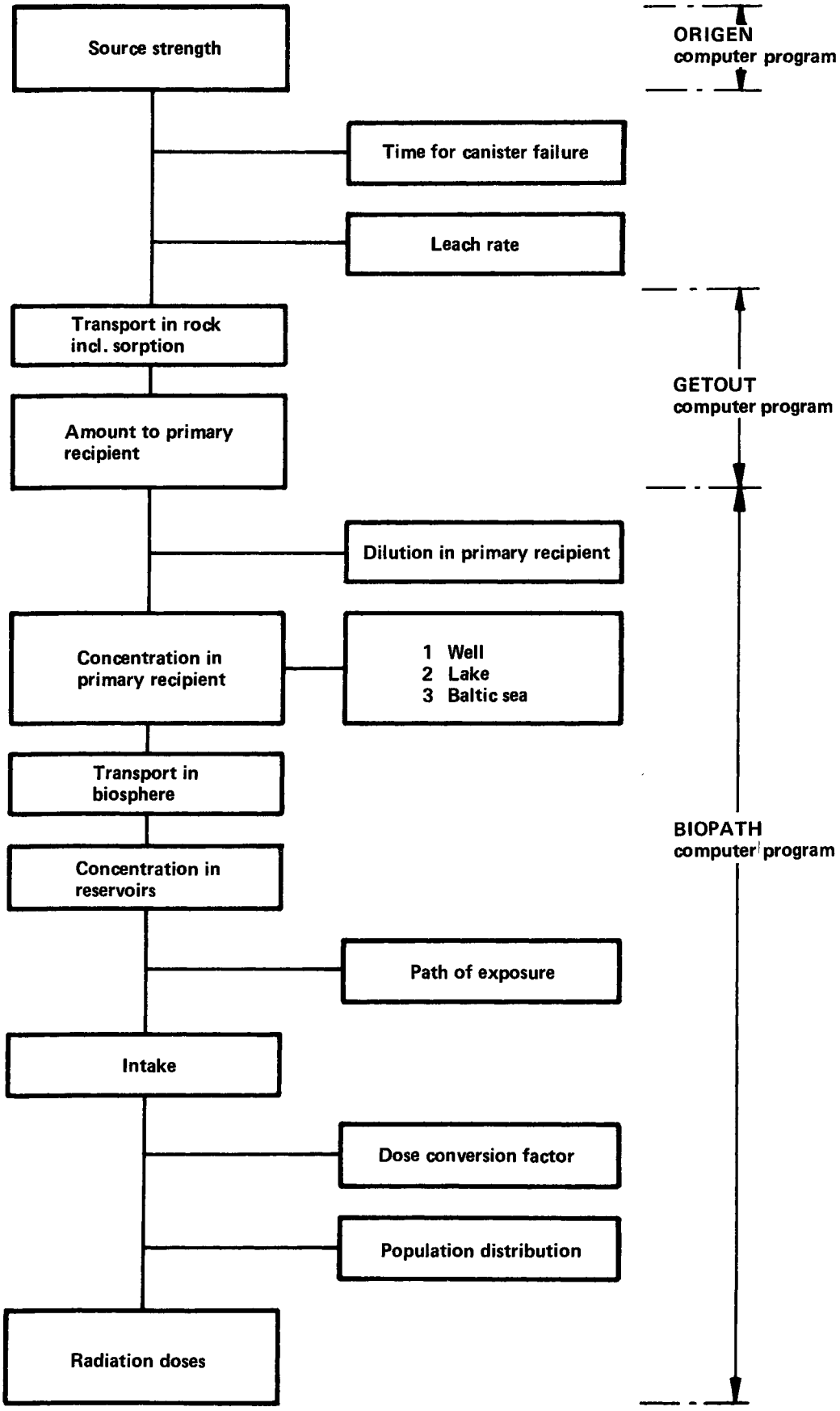

Figure 8-7. Scheme of calculation of radiation doses from the radioactive elements which might be released from a final repository for spent fuel.

of the canister is obtained with reasonably cautious assumptions. Very pessimistic assumptions give 500 000 years. It is cautiously assumed here as a reference case that dissolution will take 500 000 years.

With regard to the leaching of easily soluble substances which are not bound to the uranium dioxide matrix, see below.

With the above assumptions, the leach rate illustrated by curve A in figure 8-8 is obtained for the reference case. As the figure shows, the maximum leach rate is not reached until after 500 000 years. This maximum rate is the same as that which is obtained if an immediate penetration of all canisters after 100 000 years and a leaching time of 500 000 years is assumed - curve B in figure 8-8. In order to simplify the practical execution of the GETOUT and BIOPATH calculations, the premises which correspond to curve B in figure 8-8 have been used in these calculations as a main case. The effects of this approximation are discussed in section 8.5.4.

In addition the calculations have been carried out for a case with penetration of all canisters after 500 000 years and with a leaching period of 500 000 years.

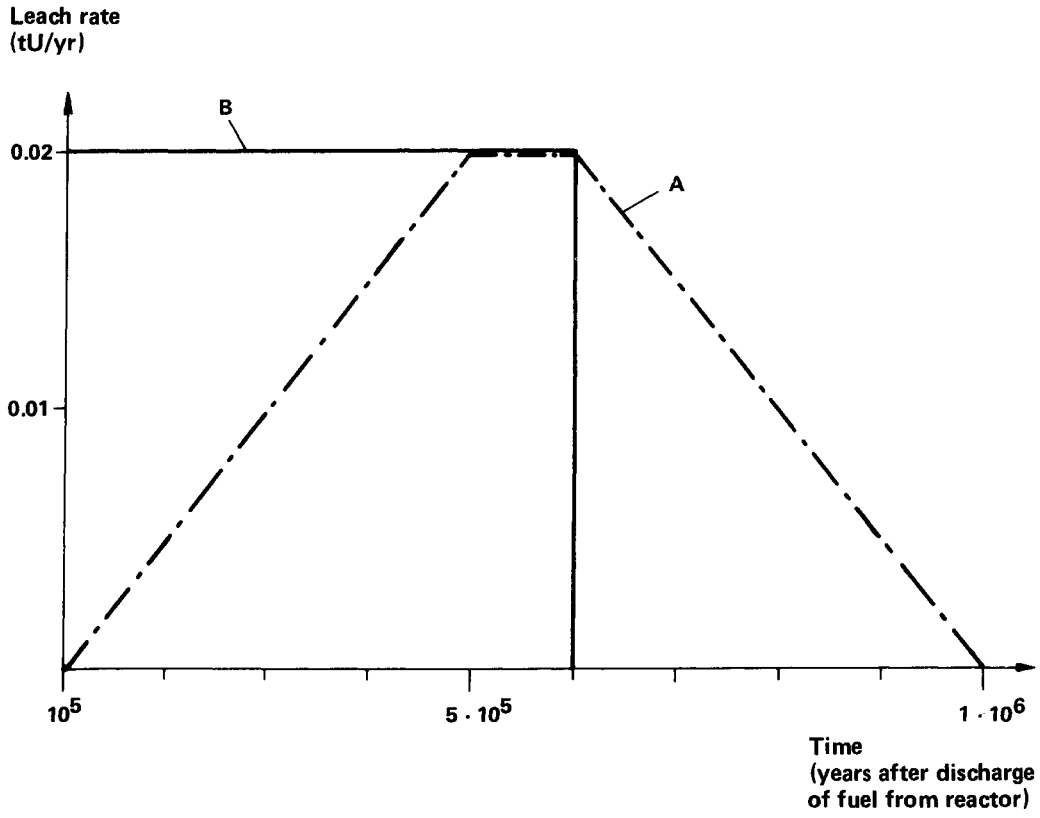

Figure 8-8. Leach rate for radioactive elements from the fuel as a function of time.

Curve A. Reference case for the safety analysis with uniform canister degradation during the period from 100 000 to 500 000 years and a dissolution time of 500 000 years for the fuel.

Curve B. Main case for the calculations with instantaneous canister degradation after 100 000 years and a dissolution time of 500 000 years for the fuel.

During the irradiation of the fuel in the reactor, certain of the fission products have been concentrated in the outer parts of the fuel pellets and in the space between the pellets and the zircaloy cladding, the cladding gap. This applies in particular to volatile elements and elements which are formed by the decay of volatile elements, e.g. iodine and cesium. In the event that water leaks into the canister, these elements could be dissolved much more quickly than the elements which are bound to the uranium dioxide matrix. The portion of the total contents of the canister which is more accessible for leaching in this manner has been assumed to be 10% for iodine, 1% for cesium and 0.1% for other elements /8-18/. Owing to the transport resistance (see section 6.5) in the immediate environment of the fuel, the effective leaching rate is limited even for the most soluble elements. It is shown in section 6.7 that, with reasonably conservative assumptions, the leaching rate for easily soluble elements decreases exponentially with a half-life of 2 000 years. This means that 50% will have leached out after 2 000 years and 75% after 4 000 years etc.

Since the 7 000 canisters are assumed to break down one by one over a 400 000 year period, 10% of the iodine, for example, will be released at a relatively uniform rate during these 400 000 years, while the portion which is more tightly bound to the uranium dioxide matrix will be released over a period of 500 000 years for each canister. During a certain period in connection with the breakdown of the last canisters, (500 000 years after deposition), the release of easily soluble iodine will take place at the same time as the slower release is taking place from all 7 000 canisters. The increase of the maximum rate of release for iodine which is thereby obtained from the entire repository is, however, only 2.5%. For other elements, the increase is less. Thus, a small quantity of readily accessible and easily soluble nuclides will not appreciably affect the maximum rate of release of radioactive elements from the final repository. The effects of a Gaussian canister life distribution have been explored in /8-19/.

As is explained in chapter 3, the transit time of the groundwater can be evaluated on the basis of 3-dimensional flow calculations and measurements of groundwater age. It is considered realistic to expect a transit time of at least 3 000 years for the groundwater. In addition, calculations have been carried out for a pessimistic case with a groundwater transit time of 400 years. This value was also used in the KBS safety analysis for the final storage of vitrified waste /8-2/.

Three different sets of retention factors for the radioactive elements have been given in table 7-2. The values for an oxidizing environment are the same as those which were used in /8-2/.

However, more recent studies have clearly shown that the chemical conditions at the final repository site will be reducing - see section 3.5. Table 7-2 gives two sets of retention factors which have been calculated for reducing chemical conditions, namely:

a = best estimate for reducing environment and slow groundwater transport

b = reducing environment with conservative assumptions regarding concentrations and short contact time.

In the calculations, set a) is combined with a water transit time of 3 000 years and set b) with the short water transit time of 400 years.

The following four calculation cases have been analyzed:

Case No.	Name	Canister penetration, years	Water transit time, years	Retention factor
1	Main case	100 000	3 000	a
2	Main case with longer canister life	500 000	3 000	a
3	Pessimistic case	100 000	400	b
4	Pessimistic case with longer canister life	500 000	400	b

In all cases, a leaching period of 500 000 years has been assumed. Furthermore, the effects of the variation of the groundwater transit time on the inflow of different nuclides to the primary recipient have been investigated in a parameter study for the main case with retention factors a) and for the pessimistic case with retention factors b).

Furthermore, calculations have been carried out for two highly unlikely cases with initial damage to a canister for the main case data concerning water transit time and retention factors and with a leaching period of 1 000 years for easily soluble substances.

8.5.3 Calculation results for dispersal through the rock

The results of the GETOUT calculations are reported in the form of figures and in tables.

Figures 8-9 and 8-10 show the inflow in Ci per year of different nuclides to the recipient area as a function of time after start of final storage. Figure 8-9 applies for the main case and 8-10 for the pessimistic case.

The maximum inflows and times for maxima are presented in Table 8-8 and include the calculation cases with delayed canister penetration (500 000 years after discharge from the reactor).

Owing to the longer groundwater transit time and the larger retention factors, the maximum inflows for many of the nuclides are

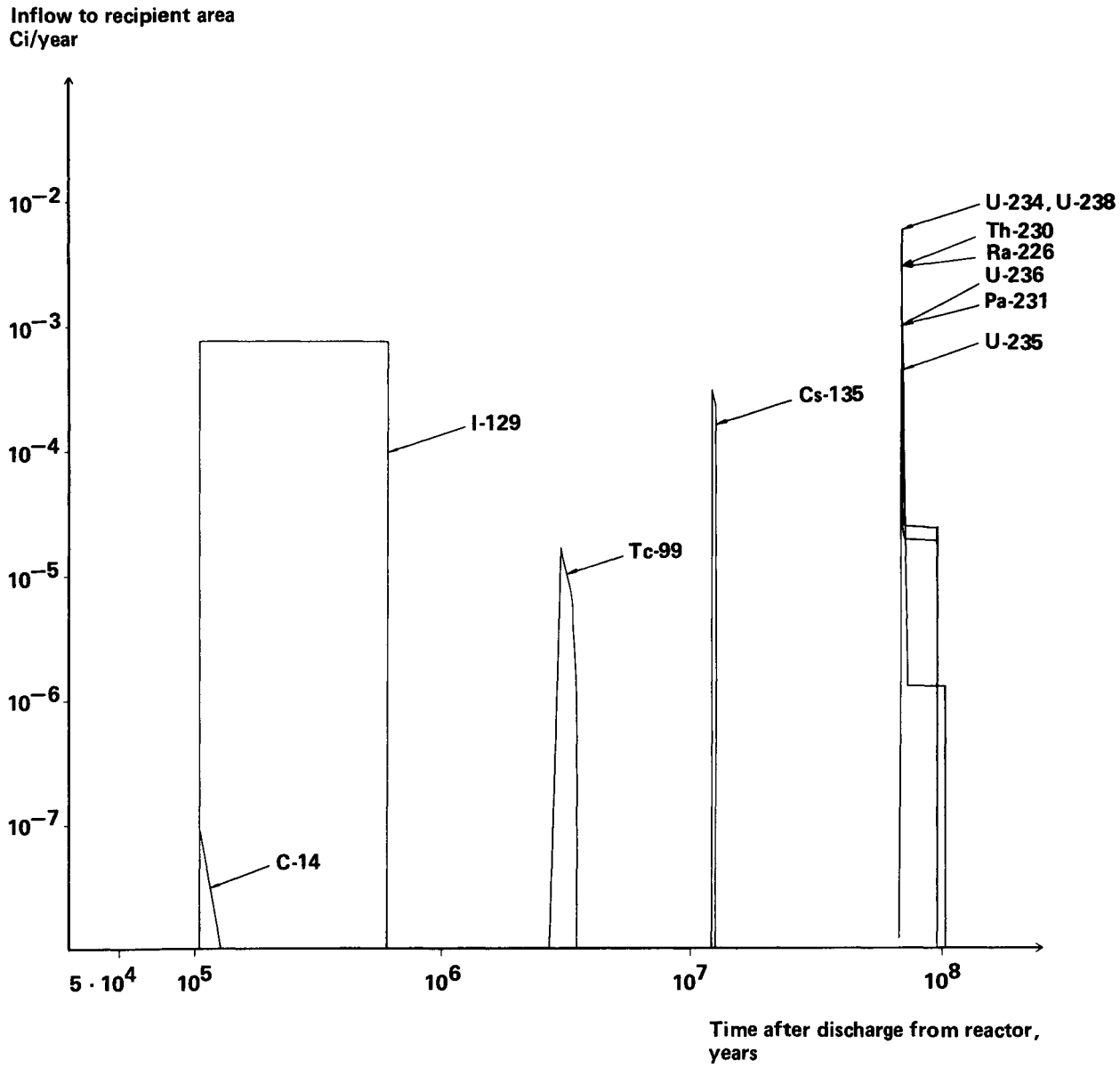

Figure 8-9. Results of GETOUT calculations. Inflow of radioactive elements to the recipient area in the main case.

considerably lower in the main case than in the pessimistic case. This applies to technetium-99, zirconium-93, radium-226, thorium-229, thorium-230, protactinium-231, uranium-233, uranium-236, neptunium-237 and plutonium-242. Of these, zirconium-93 and plutonium-242 decay completely (to a level of less than 10^{-15} Ci/year) in the main case.

As expected, the influence of the time of canister penetration is greatest for the nuclides whose half-lifes are less than or of the same order of magnitude as the range of variation for the time of canister penetration (400 000 years). In the main case, a significant effect is obtained only for carbon-14 (half-life 5 730 years) and technetium-99 (half-life 210 000 years). In the pessimistic case, the portion of the inflow of radium-226 which derives from plutonium-238 via uranium-234 in the fuel is reduced by half. With canister penetration 100 000 years after discharge

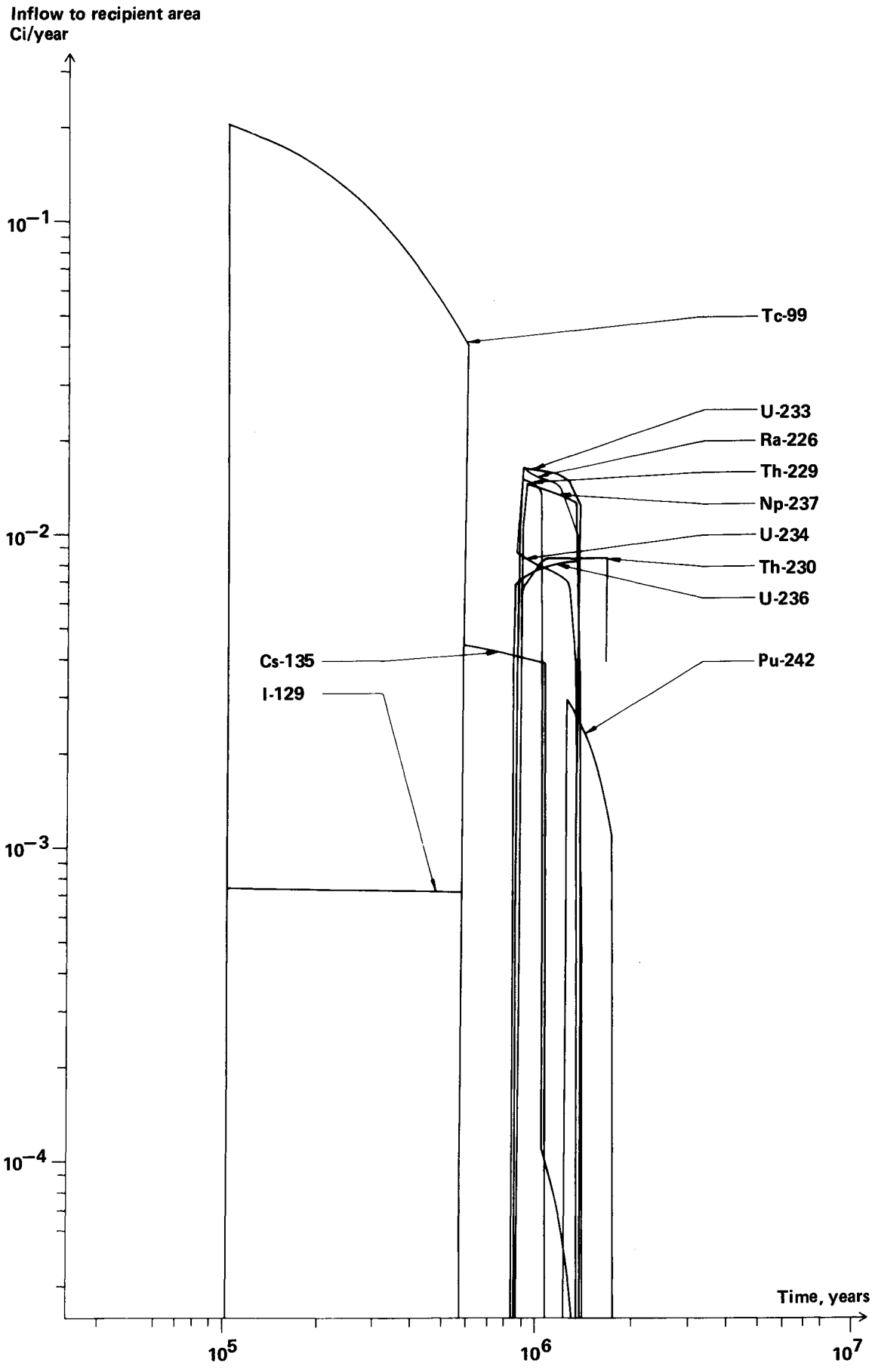

Figure 8-10. Results of GETOUT calculations. Inflow of radioactive elements to the recipient area for the pessimistic dispersal case.

Table 8-8. Maximum inflows, C_{max} (Ci/year) and times for maxima, T_{max} (years after discharge from the reactor), for the main case and the pessimistic case at two times for canister penetration.

Main case	Groundwater transit time 3 000 years and retention factors a) in section 8.5.2			
	Canister penetration after 100 000 years. Case 1		Canister penetration after 500 000 years. Case 2	
Nuclide	C_{max}	T_{max}	C_{max}	T_{max}
C-14	3.4×10^{-8}	1.0×10^{5}	-	-
Zr-93	-	-	-	-
Tc-99	1.7×10^{-5}	3.0×10^{6}	4.7×10^{-6}	3.4×10^{6}
I-129	7.5×10^{-4}	1.0×10^{7}	7.3×10^{-4}	5.0×10^{7}
Cs-135	3.0×10^{-3}	1.2×10^{7}	2.8×10^{-3}	1.3×10^{7}
Ra-226	3.0×10^{-11}	6.9×10^{7}	3.0×10^{-11}	6.9×10^{7}
Th-229	1.3×10^{-3}	6.9×10^{7}	1.1×10^{-3}	6.9×10^{7}
Th-230	3.1×10^{-4}	6.9×10^{7}	3.1×10^{-4}	6.9×10^{7}
Pa-231	9.7×10^{-12}	6.9×10^{7}	9.7×10^{-12}	6.9×10^{7}
U-233	3.9×10^{-3}	6.9×10^{7}	3.3×10^{-3}	6.9×10^{7}
U-234	6.2×10^{-4}	6.9×10^{7}	6.2×10^{-4}	6.9×10^{7}
U-235	4.7×10^{-4}	6.9×10^{7}	4.7×10^{-4}	6.9×10^{7}
U-236	9.9×10^{-3}	6.9×10^{7}	9.6×10^{-3}	6.9×10^{7}
U-238	6.2×10^{-12}	6.9×10^{7}	6.2×10^{-12}	6.9×10^{7}
Np-237	3.3×10	6.9×10^{7}	3.0×10	6.9×10^{7}
Pu-242	-	-	-	-
Pessimistic case	Groundwater transit time 400 years and rentention factors b) in section 8.5.2			
	Canister penetration after 100 000 years. Case 3		Canister penetration after 500 000 years. Case 4	
Nuclide	C_{max}	T_{max}	C_{max}	T_{max}
C-14	4.8×10^{-8}	1.0×10^{5}	-	-
Zr-93	1.5×10^{-2}	2.0×10^{6}	1.2×10^{-2}	2.4×10^{6}
Tc-99	2.1×10^{-1}	1.0×10^{5}	5.5×10^{-2}	5.0×10^{5}
I-129	7.5×10^{-4}	1.0×10^{5}	7.3×10^{-4}	5.0×10^{5}
Cs-135	4.4×10^{-3}	5.9×10^{5}	4.0×10^{-3}	9.9×10^{6}
Ra-226	1.6×10^{-2}	9.2×10^{5}	1.3×10^{-2}	1.4×10^{6}
Th-229	1.5×10^{-2}	9.1×10^{5}	1.4×10^{-2}	1.3×10^{6}
Th-230	8.5×10^{-3}	9.2×10^{5}	6.6×10^{-3}	1.3×10^{6}
Pa-231	5.1×10^{-3}	8.6×10^{5}	5.1×10^{-3}	1.3×10^{6}
U-233	1.6×10^{-2}	9.1×10^{5}	1.5×10^{-2}	1.3×10^{6}
U-234	8.7×10^{-3}	8.8×10^{5}	7.1×10^{-3}	1.3×10^{6}
U-235	5.2×10^{-4}	9.0×10^{5}	5.2×10^{-4}	1.3×10^{6}
U-236	8.0×10^{-3}	8.8×10^{5}	7.9×10^{-3}	1.3×10^{6}
U-238	6.3×10^{-3}	8.8×10^{5}	6.3×10^{-3}	1.3×10^{6}
Np-237	1.5×10^{-2}	9.3×10^{6}	1.3×10^{-2}	1.3×10^{6}
Pu-242	3.1×10^{-3}	1.3×10^{6}	1.5×10^{-3}	1.7×10^{6}

from the reactor, this contribution comprises 40% of the total radium inflow. In the main case, the entire radium inflow stems from U-238 (half-life 4 510 million years), which means that no change is obtained with a later canister penetration.

Table 8-9 shows the maximum inflow of the postulated easily so-

Table 8-9. Maximum inflows to the primary recipient for initial canister damage to one container according to the main case. Inflow is given for gap activity (10 % iodine, 1 % cesium and 0.1 % other nuclides) and for residual activity in the less soluble uranium dioxide matrix.

Nuclide	Dispersal according to main case		
	Leaching time 1 000 years for gap activity	Leaching time 500 000 years for uranium dioxide matrix	
	C_{max} (Ci/year)	C_{max} (Ci/year)	T_{max} (year)
C-14	1.4×10^{-6}	1.1×10^{-6}	3.1×10^{3}
Zr-93	-	-	-
Tc-99	1.8×10^{-10}	3.3×10^{-9}	2.9×10^{6}
I-129	5.3×10^{-6}	1.1×10^{-7}	3.1×10^{3}
Cs-135	5.7×10^{-9}	4.4×10^{-8}	1.2×10^{7}
Ra-226	2.7×10^{-9}	4.2×10^{-7}	6.9×10^{7}
Th-229	-	-	-
Th-230	2.7×10^{-9}	4.4×10^{-7}	6.9×10^{7}
Pa-231	7.4×10^{-10}	1.4×10^{-7}	6.9×10^{7}
U-233	-	-	-
U-234	2.0×10^{-9}	-	6.9×10^{7}
U-235	1.8×10^{-10}	6.7×10^{-8}	6.9×10^{7}
U-236	2.4×10^{-10}	1.5×10^{-7}	6.9×10^{7}
U-238	7.9×10^{-9}	8.7×10^{-7}	6.9×10^{7}
Np-237	-	-	-
Pu-242	-	-	-

luble fraction (10% iodine, 1% cesium and 0.1% others) to the primary recipient for the calculation case with initial canister damage.

In figure 8-11, the maximum inflow to the primary recipient is presented as a function of the water transit time for the main case data, and in figure 8-12, the same quantity is shown for the pessimistic case data.

With the aid of the figures, it is possible to analyze not only

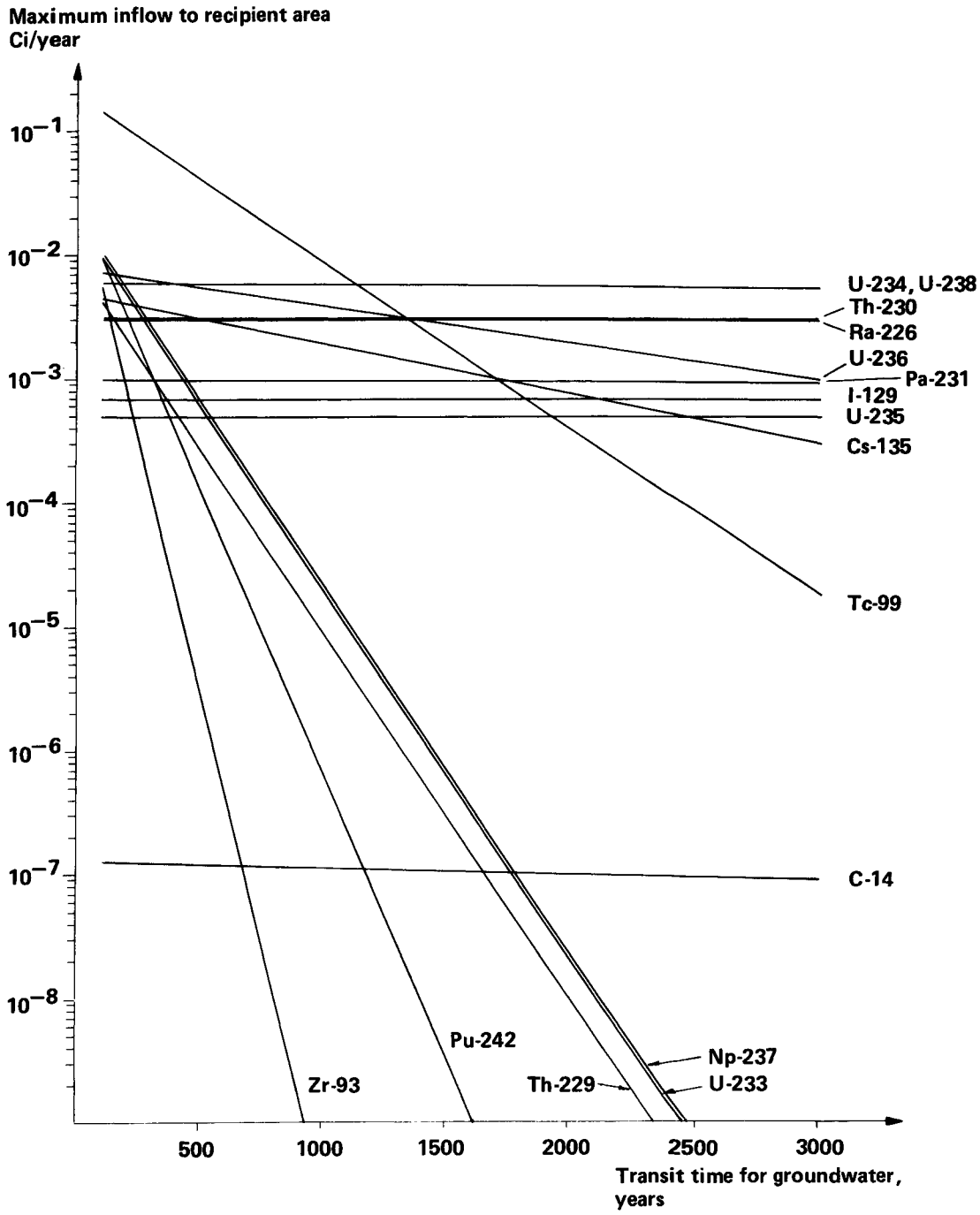

Figure 8-11. Maximum calculated inflow to recipient area for different nuclides at varying groundwater transit time. Retention factors as in the main case.

the sensitivity of the result to the groundwater velocity, but also the differences between the main case and the pessimistic case. In this way, the effect of the groundwater transit time can be isolated from the retention factors.

A more detailed analysis of these and several other calculation cases is provided in /8-19/, where the case with initial canister damage is also analyzed.

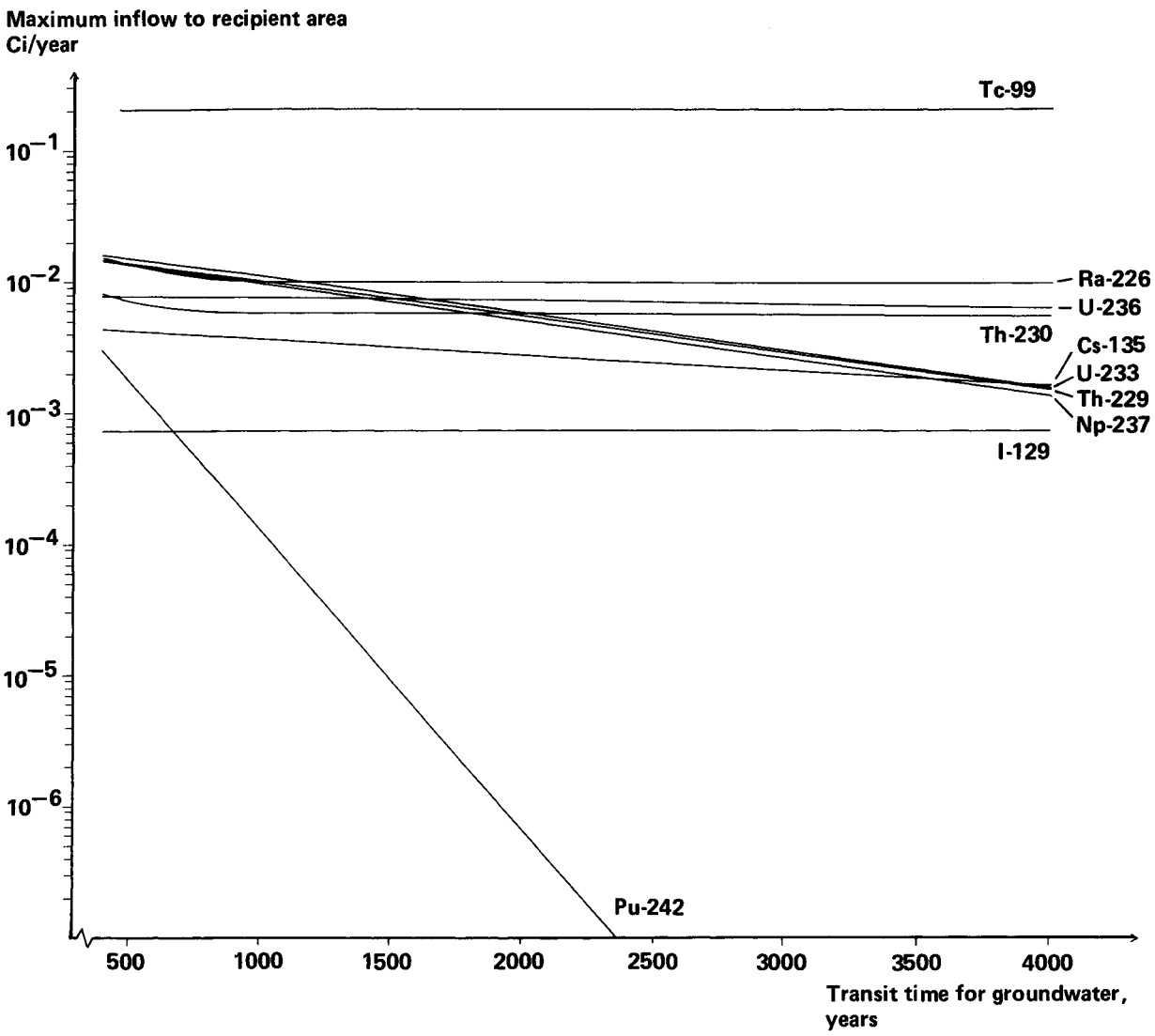

Figure 8-12. Maximum calculated inflow to recipient area for different nuclides at varying groundwater transit time. Retention factors as in the pessimistic dispersal case.

8.5.4 Sensitivity analysis of GETOUT calculations

As has already been noted, the distribution of canister penetrations in time has not been taken into consideration in the calculations. Nor have the organic complexing agents which have been found in groundwater (see section 7.2.5) or the effects of the statistical spread of the fissure widths (see section 7.3.6) been taken into consideration. The influence of these factors on the results in the main case and the pessimistic case are discussed below.

Distribution of canister penetrations in time

As is evident from figure 8-8, curve A, full leaching rate is not attained until after 500 000 years if the canister penetrations are assumed to be uniformly distributed between 100 000 years and 500 000 years. The inflows which were used for the main case and the pessimistic case are therefore slightly overestimated in relation to the basic assumption that the service life of the ca-

nisters is uniformly distributed. The size of the overestimation varies for different nuclides and is dependent upon the dominant half-life.

Many nuclides have long half-lives themselves or parent nuclides with long half-lives in relation to the 400 000 years during which the canister penetrations are assumed to occur. For these nuclides, the maximum inflows assuming uniformly distributed canister life will be the same as if the canisters had been penetrated after 500 000 years, i.e. at the time when the full dissolution rate is achieved according to curve A in figure 8-8.

Two nuclides, carbon-14 and technetium-99, decay more rapidly than the dissolution rate increases. This means that a maximum for radioactivity leached per unit time will be reached before 500 000 years. In the case of technetium-99, this maximum occurs after approx. 400 000 years and in the case of carbon-14 much earlier.

The maximum inflow of technetium, with the uniform distribution of canister penetrations in the reference case and with the dispersal data in the pessimistic case, is 0.058 Ci per year. This shall be compared with 0.21 Ci per year for the pessimistic calculation case (case 3) and 0.055 Ci per year in case 4 - see table 8-8. Owing to the relatively short half-life of carbon-14 (5 730 years), the maximum inflow of this isotope is completely negligible with uniformly distributed canister penetrations. For other nuclides in table 8-8, the corrections for uniformly distributed canister penetrations are negligible. See also the discussion concerning easily soluble elements in section 8.5.2.

Organic complexing agents

In groundwater at a depth of about 500 m, 0.5 milliequivalents of fulvic acids per litre has been measured /8-20/. These acids might act as complexing agents for heavy metals in the fuel, whereby the solubility and thus the leaching rate of the fuel could increase, and retardation decrease. See also section 7.2.5.

If it is cautiously assumed that one equivalent of fulvic acid is sufficient to bind one mole of heavy metal, a concentration of heavy metal complex in the groundwater corresponding to 120 g of heavy metal per cubic metre is obtained at the given fulvic acid level. It is shown in section 6.6 that a heavy metal concentration of 1 070 g per cubic metre groundwater gives a leaching time of 1.8 million years. Thus, fulvic acid complex would at most be able to reduce this leaching time by about 10% or to 1.6 million years.

Since the calculations have been carried out with a leaching time of 500 000 years, the possible effects of fulvic acids on the leaching time are covered well by the calculation cases.

The retardation of the nuclides in the rock is assumed in the GETOUT model to stem from ion exchange and adsorption processes in which mainly positive ions partake. However, some of the nuclides could conceivably migrate faster as neutral or negatively charged complexes of fulvic acid.

The most probable situation is that most of the fulvic acids are already bound to metals occuring naturally in the groundwater (for example bivalent iron) and that complexes of the waste nuclides with hydroxide in particular are much more prevalent than fulvic complexes /8-21/. In this case, the influence of the fulvic acids on the transport of radioactive elements will be negligible.

It may nevertheless be of interest to investigate the consequences of assuming conservatively, as above, that one equivalent of fulvic acid can bind one mole of heavy metal and that the retardation mechanism is rendered completely ineffective as regards the complex-bound heavy metal. If the fulvic acids form uniformly strong complexes with the most important heavy nuclides in the fuel - i.e. thorium, uranium, neptunium, and plutonium - then the fulvic acids will suffice to transport at most 60 kg of these nuclides during a period of 500 000 years. This results in the maximum inflows of actinides given in table 8-10. The complex-

Table 8-10. Maximum inflows of complex-bound heavy nuclides (Ci/year) to the recipient area. Dispersal scenario as in the main case.

Nuclide	Immediate canister penetration after 100 000 years	Uniformly distributed canister life
Th-229	1.7×10^{-7}	3.5×10^{-4}
Th-230	1.1×10^{-3}	1.4×10^{-3}
U-233	4.8×10^{-4}	1.0×10^{-3}
U-234	1.7×10^{-3}	8.2×10^{-4}
Np-237	1.2×10^{-3}	1.0×10^{-3}
Pu-239	2.2×10^{-2}	1.5×10^{-5}
Pu-240	4.1×10^{-5}	6.9×10^{-9}
Pu-242	1.6×10^{-3}	7.5×10^{-4}

bound fraction of actinides can be assumed to migrate with the speed of the water and the dose contributions from this fraction are added to the contributions from iodine-129 at the same time.

Even with very conservative assumptions concerning the chemical behavious of the fulvic acids with respect to the heavy metals, a maximum individual dose of 3 mrems/year is obtained (see also 8.6 and table 8-21).

Dispersion

Dispersion phenomena in the rock are discussed in section 7.3.6. It is mentioned there that a retarded nuclide may reach the recipient area after 20% of its mean transit at a concentration corresponding to 5% of its maximum concentration. In the pessimistic case, the inflow is not affected to any appreciable extent, since the transit times of most of the nuclides are relatively short in relation to their half-lives. An exception in this respect is plutonium-239, which, owing to more rapid transport in wide fis-

sures, can achieve an inflow of max 5×10^{-5} Ci/year if all canisters are assumed to be penetrated at once. In the event of uniformly distributed canister life, the inflow will be considerably lower.

In the main case, many nuclides decay to a very considerable extent. Among the fission products, this is true for zirconium-93, technetium-99 and cesium-135. In the case of the more important plutonium isotopes, their transit times are so long in relation to their half-lives that they decay virtually completely, despite the fissure width dispersion. The inflow of radium-226 and thorium-230 derives in the main case exclusively from uranium-238, which has such a long half-life that an earlier inflow does not increase the levels. As regards the decay chain neptunium-237 → uranium-233 → thorium-229, fissure width dispersion leads to an increased inflow compared to the main case (figure 8-9).

The retention time distribution for the fissure width dispersion given in /8-22/ and the parametric study of groundwater transit time presented in figure 8-11 have been used as a basis for estimating the maximum inflows due to dispersion phenomena. Table 8-11 gives the results for those nuclides which are significantly affected. The results are compared with the main case maximum inflows with no regard to dispersion.

Table 8-11. Comparison of the maximum inflows (Ci/year) with and without regard to fissure width dispersion for the main case.

Nuclide	With fissure width dispersion	Without fissure width dispersion
Zr-93	3×10^{-7}	-
Tc-99	3×10^{-3}	1.7×10^{-5}
Cs-135	7×10^{-4}	3.0×10^{-4}
Th-229	2×10^{-5}	1.3×10^{-11}
U-233	2×10^{-5}	3.9×10^{-12}
Np-237	3×10^{-5}	3.3×10^{-12}
Pu-242	1×10^{-5}	-

It should be pointed out that if the width of the chromatographic peaks is very small in relation to the transit time of the nuclides (see figure 8-9), a significant lowering of the height of the peaks is obtained due to the broadening of the peaks caused by dispersion. This has not been taken into account in table 8-11.

It should be further noted that the radial dispersion (perpendicular to the direction of flow) has not been included in any calculations or estimates. However, tracer tests at Studsvik /8-23/ indicate that radial dispersion in rock is considerable. If this dispersion were included, the inflows would be lower than those which are reported.

8.5.5 Results of BIOPATH calculations

The calculated maximum radiation doses to individuals in a so-called "critical group" and the maximum collective annual dose are given in tables 8-12 through 8-17. Predominant paths of exposure are also given in each table. The tables pertain to the following calculation cases:

Table	Case in table 8-8		Primary recipient
8-12	Main case	1	Well
13	"	1	Lake
14	"	1	Baltic Sea
15	Pessimistic case	3	Well
16	"	3	Lake
17	"	3	Baltic Sea

Radiation doses are not reported here for cases 2 and 4 - but see /8-24/, which also contains results from several other cases.

The following conclusions can be drawn from tables 8-12 to 8-17:

- in the well case, drinking water comprises the dominant path of exposure for most nuclides. However, fish is the most important source for cesium-135 and meat is the most important source for carbon-14 and iodine-129
- in the lake case, fish consumption or drinking water is the most important path of exposure
- in the Baltic coastal zone, the exposure situation is generally dominanted by fish consumption. As regards thorium-229, external exposure from fishing tackle and beach activities is responsible for most of the radiation dose
- different paths of exposure can dominate depending on whether the nuclide is carried out by groundwater from the repository or is generated via the decay of a long-lived parent nuclide which has already reached the biosphere (see e.g. Ra-226 and Th-229)
- for a given nuclide, the maximum dose to the critical group and the maximum collective annual dose to the population are often obtained at different points of time. Moreover, the dose to the critical group is often heavily dependent upon the type of inflow.

Calculations /8-24/ have also shown that:

- in the case of initial canister damage, iodine-129 and carbon-14 dominate with regard to both dose to critical groups and dose to population

Table 8-12. Maximum annual individual and collective doses with dominant paths of exposure. Inflow as in the main case according to 8.5.2. Primary recipient - well.

Nuclide	Max. ind. annual dose rems/year	Time years	Predominant paths of exposure 1	%	2	%	3	%	Max.coll. annual dose manrems/year	Time years
C-14	5.2×10^{-10}	1.0×10^{5}	meat	64	fish	30	water	3	5.0×10^{-4}	1.1×10^{5}
Tc-99	8.2×10^{-9}	3.0×10^{6}	water	50	milk	46	fish	2	4.9×10^{-5}	3.2×10^{6}
I-129	4.2×10^{-4}	1.0×10^{5}	meat	52	water	26	milk	20	1.7×10^{1}	5.8×10^{5}
Cs-135	6.8×10^{-6}	1.2×10^{7}	fish	65	water	14	meat	13	1.5×10^{-2}	1.2×10^{7}
Ra-226[a]	5.2×10^{-3}	6.9×10^{7}	water	59	milk	36	fish	2	1.1×10^{0}	6.9×10^{7}
Ra-226[b]	4.4×10^{-3}	6.9×10^{7}	water	55	fish	23	milk	20	1.2×10^{1}	6.9×10^{7}
Ra-226[c]	2.4×10^{-4}	6.9×10^{7}	water	100	fish	3×10^{-1}	milk	2×10^{-1}	2.2×10^{0}	6.9×10^{7}
Th-230	2.3×10^{-4}	6.9×10^{7}	water	88	meat	10	veget.	3	1.3×10^{-1}	6.9×10^{7}
Pa-231	4.9×10^{-4}	6.9×10^{7}	water	99	fish	1	meat	$2 \cdot 10^{-1}$	1.4×10^{0}	6.9×10^{7}
U-234	3.3×10^{-5}	6.9×10^{7}	water	83	meat	9	milk	3	1.2×10^{-1}	6.9×10^{7}
U-235	2.6×10^{-5}	6.9×10^{7}	water	83	meat	9	milk	3	4.2×10^{-2}	1.1×10^{8}
U-236	5.7×10^{-4}	6.9×10^{7}	water	83	meat	9	milk	3	3.9×10^{-2}	6.9×10^{7}
U-238	3.2×10^{-13}	6.9×10^{7}	water	83	meat	9	milk	3	2.3×10^{-1}	7.2×10^{7}
Np-237	3.4×10^{-13}	7.0×10^{7}	water	78	meat	17	veget.	2	8.0×10^{-12}	7.0×10^{7}

Table 8-13. Maximum annual individual and collective doses with dominant paths of exposure. Inflow as in the main case according to 8.5.2. Primary recipient - lake.

Nuclide	Max. ind. annual dose rems/year	Time years	Predominant paths of exposure 1	%	2	%	3	%	Max.coll. annual dose manrems/year	Time years
C-14	1.7×10^{-10}	1.0×10^{5}	fish	91	meat	9	milk	3×10^{-1}	5.0×10^{-4}	1.1×10^{5}
Tc-99	3.3×10^{-10}	3.0×10^{6}	milk	55	fish	42	meat	1	4.9×10^{-5}	3.2×10^{6}
I-129	1.9×10^{-5}	1.0×10^{5}	meat	57	milk	22	fish	20	1.7×10^{1}	5.8×10^{5}
Cs-135	4.9×10^{-6}	1.2×10^{7}	fish	91	water	9	meat	9×10^{-1}	1.5×10^{-2}	1.2×10^{7}
Ra-226[a]	4.3×10^{-4}	6.7×10^{7}	water	52	fish	24	milk	21	1.1×10^{0}	6.7×10^{7}
Ra-226[b]	4.4×10^{-3}	6.9×10^{7}	water	55	fish	23	milk	20	1.2×10^{1}	6.9×10^{7}
Ra-226[c]	2.4×10^{-4}	6.9×10^{7}	water	100	fish	3×10^{-1}	milk	2×10^{-1}	2.2×10^{0}	6.9×10^{7}
Th-230	4.6×10^{-4}	6.9×10^{7}	water	99	fish	1	meat	1×10^{-1}	1.3×10^{-1}	6.9×10^{7}
Pa-231	4.9×10^{-5}	6.9×10^{7}	water	99	fish	1	meat	2×10^{-1}	1.4×10^{0}	6.9×10^{7}
U-234	1.9×10^{-6}	6.9×10^{7}	water	57	fish	33	meat	8	1.2×10^{-1}	6.9×10^{7}
U-235	1.5×10^{-6}	6.9×10^{7}	water	57	fish	33	meat	8	4.2×10^{-2}	1.1×10^{8}
U-236	3.4×10^{-5}	6.9×10^{7}	water	57	fish	33	meat	8	3.9×10^{-2}	6.9×10^{7}
U-238	1.9×10^{-5}	6.9×10^{7}	water	57	fish	33	meat	8	2.3×10^{-1}	7.2×10^{7}
Np-237	1.5×10^{-14}	7.0×10^{7}	water	50	fish	29	meat	16	8.0×10^{-12}	7.0×10^{7}

Table 8-14. Maximum annual individual and collective doses with dominant paths of exposure. Inflow as in the main case according to 8.5.2. Primary recipient - Baltic sea.

Nuclide	Max.ind annual dose rems/year	Time years	Predominant paths of exposure 1	%	2	%	3	%	Max. coll. annual dose manrems/year	Time years
C-14	3.1×10^{-12}	1.0×10^{5}	fish	98	meat	2	milk	5×10^{-2}	5.0×10^{-4}	1.1×10^{5}
Tc-99	1.0×10^{-12}	3.0×10^{6}	fish	99	milk	1	fish.tackle	2×10^{-1}	4.8×10^{-5}	3.3×10^{6}
I-129	1.0×10^{-7}	1.0×10^{5}	fish	100	meat	4×10^{-1}	milk	2×10^{-1}	1.7×10^{1}	6.1×10^{5}
Cs-135	2.2×10^{-8}	1.2×10^{7}	fish	100	beach	1×10^{-3}	fish.tackle	4×10^{-3}	8.1×10^{-3}	1.3×10^{7}
Ra-226[a]	7.0×10^{-6}	6.7×10^{7}	fish	100	veget.	7×10^{-3}	fish.tackle	2×10^{-3}	1.1×10^{-1}	6.7×10^{7}
Ra-226[b]	3.0×10^{-5}	6.9×10^{7}	fish	90	fish.tackle	9	beach	1	1.1×10^{0}	6.9×10^{7}
Ra-226[c]	7.3×10^{-9}	6.9×10^{7}	fish	98	fish.tackle	2	beach	5×10^{-1}	1.7×10^{0}	6.9×10^{7}
Th-230	1.9×10^{-7}	6.9×10^{7}	fish	100	veget.	9×10^{-3}			9.7×10^{-5}	6.9×10^{7}
Pa-231	1.1×10^{-7}	6.9×10^{7}	fish	100	veget.	4×10^{-2}			2.0×10^{-2}	6.9×10^{7}
U-234	1.3×10^{-9}	6.9×10^{7}	fish	100	veget.	4×10^{-2}			8.2×10^{-2}	6.9×10^{8}
U-235	9.9×10^{-8}	6.9×10^{7}	fish	91	fish.tackle	6	beach	3	5.5×10^{-2}	1.0×10^{7}
U-236	2.2×10^{-7}	6.9×10^{7}	fish	100	veget.	4×10^{-2}			3.9×10^{-2}	7.0×10^{7}
U-238	1.2×10^{-7}	6.9×10^{7}	fish	100	veget.	4×10^{-2}			2.3×10^{-1}	7.2×10^{7}
Np-237	1.2×10^{-16}	7.0×10^{7}	fish	100	fish.tackle	2×10^{-1}	beach	4×10^{-2}	1.3×10^{-14}	7.0×10^{7}

a) Refers to the Ra-226 which reaches the biosphere directly via the groundwater from the repository.
b) Refers to the Ra-226 which is generated by the decay of Th-230 in the biosphere.
c) Refers to the Ra-226 which is generated by the decay chain U-234→Th-230→Ra-226 in the biosphere.

Table 8-15. Maximum annual individual and collective doses with dominant paths of exposure. Inflow as in the pessimistic case according to 8.5.2. Primary recipient - well.

Nuclide	Max.ind. annual dose rems/year	Time years	Predominant paths of exposure 1	%	2	%	3	%	Max. coll. annual dose manrems/year	Time years
C-14	6.8×10^{-10}	1.0×10^{5}	meat	64	fish	30	water	3	6.7×10^{-4}	1.1×10^{5}
Zr-93	3.4×10^{-6}	2.4×10^{6}	water	99	fish	2×10^{-1}	meat	3×10^{-2}	2.3×10^{-2}	2.5×10^{6}
Tc-99	9.9×10^{-5}	1.0×10^{5}	water	50	milk	46	fish	2	5.6×10^{-1}	3.9×10^{5}
I-129	4.2×10^{-4}	1.0×10^{5}	meat	52	water	26	milk	20	1.7×10^{1}	5.8×10^{5}
Cs-135	9.9×10^{-5}	5.9×10^{5}	fish	65	water	14	meat	13	2.0×10^{-1}	6.6×10^{5}
Ra-226[a]	3.4×10^{-2}	9.2×10^{5}	water	59	milk	36	fish	2	7.5×10^{0}	9.2×10^{5}
Ra-226[b]	2.5×10^{-2}	1.2×10^{6}	water	55	fish	23	milk	20	6.5×10^{1}	1.2×10^{6}
Ra-226[c]	4.1×10^{-4}	8.8×10^{5}	water	100	fish	3×10^{-1}	milk	2×10^{-1}	3.3×10^{0}	1.3×10^{6}
Th-229	1.3×10^{-2}	9.1×10^{5}	water	87	meat	10	veget.	3	1.8×10^{1}	9.6×10^{5}
Th-229[d]	9.2×10^{-4}	1.1×10^{6}	water	100	beach	5×10^{-1}	fish.tackle	5×10^{-2}	9.1×10^{-1}	1.3×10^{6}
Th-230	1.4×10^{-3}	9.2×10^{5}	water	88	meat	10	veget.	3	6.6×10^{0}	1.2×10^{5}
Pa-231	3.7×10^{-4}	8.6×10^{5}	water	99	fish	1	meat	2×10^{-1}	9.1×10^{0}	8.6×10^{5}
U-233	9.7×10^{-4}	9.2×10^{5}	water	83	meat	9	milk	3	3.1×10^{-1}	1.3×10^{5}
U-234	5.2×10^{-5}	8.8×10^{5}	water	80	meat	9	milk	3	1.9×10^{-2}	1.3×10^{6}
U-235	3.1×10^{-4}	9.0×10^{5}	water	83	meat	9	milk	3	1.8×10^{-1}	1.3×10^{6}
U-236	5.4×10^{-4}	1.0×10^{6}	water	83	meat	9	milk	3	3.0×10^{-1}	1.3×10^{6}
U-238	3.9×10^{-4}	9.4×10^{5}	water	83	meat	9	milk	3	1.9×10^{-1}	3.9×10^{6}
Np-237	1.6×10^{-3}	9.3×10^{5}	water	78	meat	17	veget.	2	7.0×10^{0}	1.4×10^{6}
Pu-242	5.6×10^{-4}	1.3×10^{6}	water	99	meat	2×10^{-1}	fish	2×10^{-1}	1.7×10^{0}	1.4×10^{6}

Table 8-16. Maximum annual individual and collective doses with dominant paths of exposure. Inflow as in the pessimistic case according to 8.5.2. Primary recipient - lake.

Nuclide	Max.ind. annual dose rems/year	Time years	Predominant paths of exposure 1	%	2	%	3	%	Max. coll. annual dose manrems/year	Time years
C-14	2.3×10^{-10}	1.0×10^{5}	fish	91	meat	9	milk	3×10^{-1}	6.7×10^{-4}	1.1×10^{5}
Zr-93	3.4×10^{-6}	2.4×10^{6}	water	99	fish	2×10^{-1}	meat	3×10^{-2}	2.3×10^{-2}	2.5×10^{6}
Tc-99	3.6×10^{-6}	1.0×10^{5}	milk	55	fish	42	meat	1	5.6×10^{-1}	3.9×10^{5}
I-129	1.0×10^{-5}	1.0×10^{5}	meat	57	milk	22	fish	20	1.7×10^{1}	5.8×10^{5}
Cs-135	7.2×10^{-3}	5.9×10^{5}	fish	91	water	9	meat	9×10^{-1}	1.9×10^{-1}	6.6×10^{5}
Ra-226[a]	2.8×10^{-2}	9.1×10^{5}	water	52	fish	24	milk	21	7.5×10^{0}	9.2×10^{5}
Ra-226[b]	2.5×10^{-2}	1.2×10^{6}	water	55	fish	23	milk	20	6.5×10^{1}	1.2×10^{6}
Ra-226[c]	4.1×10^{-4}	8.8×10^{5}	water	100	fish	3×10^{-1}	milk	2×10^{-1}	3.3×10^{0}	1.3×10^{6}
Th-229	7.7×10^{-3}	9.1×10^{5}	beach	73	fish.tackle	21	water	4	1.8×10^{1}	9.6×10^{5}
Th-229[d]	9.2×10^{-4}	1.1×10^{6}	water	100	beach	5×10^{-1}	fish.tackle	5×10^{-2}	9.1×10^{-1}	1.3×10^{6}
Th-230	1.1×10^{-3}	9.2×10^{5}	water	99	fish	1	meat	1×10^{-1}	6.6×10^{0}	1.2×10^{5}
Pa-231	3.7×10^{-4}	8.6×10^{5}	water	99	fish	1	meat	2×10^{-1}	9.1×10^{0}	8.6×10^{5}
U-233	5.7×10^{-5}	9.2×10^{5}	water	56	fish	32	meat	8	3.1×10^{-1}	1.3×10^{5}
U-234	3.1×10^{-5}	8.9×10^{5}	water	57	fish	33	meat	8	1.8×10^{-2}	1.3×10^{6}
U-235	1.8×10^{-6}	9.0×10^{5}	water	57	fish	33	meat	8	1.8×10^{-1}	1.3×10^{6}
U-236	3.2×10^{-5}	1.0×10^{6}	water	57	fish	33	meat	8	3.0×10^{-1}	1.3×10^{6}
U-238	2.3×10^{-5}	9.4×10^{5}	water	52	fish	33	meat	8	1.9×10^{-1}	3.9×10^{6}
Np-237	8.7×10^{-4}	9.3×10^{5}	water	50	fish	29	meat	16	8.8×10^{0}	1.4×10^{6}
Pu-242	5.6×10^{-4}	1.3×10^{6}	water	99	meat	2×10^{-1}	fish	2×10^{-1}	1.7×10^{0}	1.4×10^{6}

Table 8-17. Maximum annual individual and collective doses with dominant paths of exposure. Inflow as in the pessimistic case according 8.5.2. Primary recipient - Baltic sea.

Nuclide	Max.ind. annual dose rems/year	Time years	Predominant paths of exposure 1	%	2	%	3	%	Max. coll. annual dose manrems/year	Time years
C-14	4.4×10^{-12}	1.0×10^{5}	fish	98	meat	2	milk	5×10^{-2}	9.2×10^{-4}	1.0×10^{6}
Zr-93	9.8×10^{-9}	2.1×10^{6}	fish	65	fish.tackle	26	beach	9	1.5×10^{-1}	2.5×10^{5}
Tc-99	2.3×10^{-8}	1.0×10^{5}	fish	99	milk	1	fish.tackle	2×10^{-1}	5.5×10^{1}	3.9×10^{5}
I-129	1.0×10^{-7}	1.0×10^{5}	fish	100	meat	4×10^{-1}	milk	2×10^{-1}	1.7×10^{1}	5.9×10^{5}
Cs-135	3.2×10^{-7}	5.9×10^{5}	fish	100	beach	1×10^{-1}	fish.tackle	4×10^{-2}	4.5×10^{-2}	1.1×10^{6}
Ra-226[a]	3.2×10^{-5}	9.1×10^{5}	fish	100	veget.	7×10^{-3}	fish.tackle	4×10^{-3}	4.5×10^{-1}	1.1×10^{5}
Ra-226[b]	4.6×10^{-4}	1.2×10^{6}	fish	100	veget.	7×10^{-3}	fish.tackle	2×10^{-3}	7.5×10^{0}	9.2×10^{5}
Ra-226[c]	1.6×10^{-4}	1.2×10^{5}	fish	90	fish.tackle	9	beach	1	6.4×10^{0}	1.2×10^{6}
Th-229	1.2×10^{-8}	8.7×10^{5}	fish	98	fish.tackle	2	beach	5×10^{-1}	2.6×10^{0}	1.4×10^{5}
Th-229[d]	8.1×10^{-4}	9.6×10^{5}	fish.tackle	89	beach	10	fish	1	4.1×10^{-1}	9.5×10^{5}
Th-230	2.0×10^{-7}	9.6×10^{5}	fish.tackle	90	beach	10	fish	1×10^{-3}	6.4×10^{-1}	1.4×10^{6}
Pa-231	1.4×10^{-6}	9.2×10^{5}	fish	100	veget.	9×10^{-3}			6.9×10^{-4}	9.2×10^{5}
U-233	7.4×10^{-7}	8.5×10^{5}	fish	100	veget.	4×10^{-2}			1.3×10^{-1}	8.7×10^{6}
U-234	3.7×10^{-7}	9.2×10^{5}	fish	100	veget.	4×10^{-2}			1.9×10^{-1}	1.4×10^{6}
U-235	2.0×10^{-8}	8.8×10^{5}	fish	100	veget.	4×10^{-2}			1.2×10^{-1}	1.3×10^{6}
U-236	1.3×10^{-8}	9.0×10^{5}	fish	91	fish.tackle	6	beach	3	1.6×10^{-2}	2.7×10^{6}
U-238	1.8×10^{-7}	8.8×10^{5}	fish	100	veget.	4×10^{-2}			2.4×10^{-1}	1.4×10^{6}
Np-237	1.4×10^{-7}	8.8×10^{5}	fish	100	veget.	4×10^{-2}			2.0×10^{-1}	3.2×10^{6}
Pu-242	5.9×10^{-8}	9.3×10^{5}	fish	100	fish.tackle	2×10^{-1}	beach	4×10^{-2}	6.9×10^{-1}	1.4×10^{6}
	3.3×10^{-8}	1.3×10^{6}	fish	100	water	1×10^{-6}			1.8×10^{-2}	1.7×10^{6}

a) Refers to the Ra-226 which reaches the biosphere directly via the groundwater from the repository.
b) Refers to the Ra-226 which is generated by the decay of Th-230 in the biosphere.
c) Refers to the Ra-226 which is generated by the decay chain U-234→Th-230→Ra-226 in the biosphere.
d) Refers to the Th-229 which is generated by the decay of U-233 in the biosphere.

- in the case of slow canister degradation with leaching over a long time span, radium-226 and, in most cases, iodine-129 are responsible for a considerable portion of the dose to critical groups and the collective dose to populations.

The results of the radiation dose calculations are further analysed in section 8.6.

8.5.6 Calculation verification

The most important results from the computer runs with the programs mentioned in figure 8-7 have been checked in different ways. As was reported above (section 8.2), the source strengths have been checked against two other computer programs. A simple but effective verification of the maximum individual radiation dose from individual nuclides can be obtained as shown in table 8-18.

On the basis of the source strengths obtained from the tables in /8-3/, the inflows to the primary recipient are calculated with

Table 8-18. Table of simplified calculations of radiation doses to nearby residents for a number of nuclides.

	NUCLIDE					
Parameter	C 14	Tc 99	I 129	Cs 135	U 238	Np 237
Source strength (10 000 tonnes) at canister failure (Ci)	3.0×10^{-2}	1.03×10^{5}	3.8×10^{2}	2.5×10^{3}	3.1×10^{3}	1.1×10^{4}
Leaching time 500 000 years (outflow from repository)] (Ci/year)	6.0×10^{-8}	0.21	7.6×10^{-4}	4.9×10^{-3}	6.2×10^{-3}	2.2×10^{-2}
Total transit time for nuclides (retention factor x water transit time) (years)	3.0×10^{3}	2.9×10^{6}	3.0×10^{3}	1.2×10^{7}	6.9×10^{7}	6.9×10^{7}
Retardation (half-lives)	0.52	13.8	0	4	0	32.4
Inflow to recipient (Ci/year)	4.2×10^{-8}	1.5×10^{-5}	7.6×10^{-4}	3.0×10^{-4}	6.2×10^{-3}	3.9×10^{-12}
Inflow according to GETOUT (Ci/year)	3.4×10^{-8}	1.7×10^{-5}	7.5×10^{-4}	3.0×10^{-4}	5.6×10^{-3}	3.3×10^{-12}
To recipient area 50 % (Ci/year)	1.7×10^{-8}	8.5×10^{-6}	3.8×10^{-4}	1.5×10^{-4}	2.8×10^{-3}	1.7×10^{-12}
Recipient	WELL	WELL	WELL	LAKE [a]	WELL	WELL
- dilution (m^3/year)	5×10^{5}	5×10^{5}	5×10^{5}	2.5×10^{7}	5×10^{5}	5×10^{5}
- concentration (Ci/m^3)	3.4×10^{-14}	1.7×10^{-11}	7.6×10^{-10}	6.0×10^{-12}	5.6×10^{-9}	3.4×10^{-18}
Path of exposure	MEAT[b]	WATER [c]	WATER	FISH[d]	WATER	WATER
- relative importance (%)	63	49	26	65	83	78
- level (Ci/kg)	6.2×10^{-15}[e]	1.7×10^{-14}	7.6×10^{-13}	1.2×10^{-11}[f]	5.6×10^{-12}	3.4×10^{-21}
Intake (Ci/year)	2.8×10^{-13}	7.5×10^{-12}	3.3×10^{-10}	6.0×10^{-10}	2.5×10^{-9}	1.5×10^{-18}
Dose conversion factor (rem/Ci)	9.9×10^{2}	5.5×10^{2}	3.4×10^{5}	7.3×10^{3}	1.14×10^{5}	2.0×10^{5}
Individual dose (rem/year)	2.8×10^{-10}	4.1×10^{-9}	1.1×10^{-4}	4.4×10^{-6}	2.8×10^{-4}	3.0×10^{-13}
Total individual dose (incl. other paths of exposure) (rem/year)	4.4×10^{-10}	8.4×10^{-9}	4.2×10^{-4}	6.7×10^{-6}	3.4×10^{-4}	3.8×10^{-13}
Calculation with BIOPATH (rem/year)	5.2×10^{-10}	8.2×10^{-9}	4.2×10^{-4}	6.8×10^{-6}	3.2×10^{-4}	3.4×10^{-13}

a) exposure via fish from lake (65 %) and via well water (35 %)
b) consumption 45.6 kg/year, cattle take up carbon-14 through grazing and drinking
c) consumption 440 l/year
d) consumption 50 kg/year
e) uptake factor 1
f) concentration factor 2 000

the aid of the leaching rate and the nuclide transit time. The values can now be compared with corresponding values from the GETOUT model. All nuclides in the table exhibit good agreement with the GETOUT model.

The inflows and the dilution volume in the recipient determine the concentration and the intake per year. The relative importance of the paths of exposure /8-24/ and the dose conversion factor /8-24/ determine the size of the individual dose (weighted whole-body dose). The calculation result is then compared with the BIOPATH model, table 8-12.

8.5.7 Dispersal calculations for final storage of the fuel's metal components

During neutron irradiation in the reactor core, the fuel's metal components are activated. The source strength for the nuclides which are sufficiently long-lived to remain in significant quantities 10 years after discharge from the reactor are reported in section 8.2.

Immediately after discharge from the reactor, the radioactivity of the fuel is dominated by short-lived radionuclides such as cobalt-60, especially in those parts of the fuel which are made of stainless steel. But these nuclides have such short half-lives that they are of no importance for safety in the final repository.

In the period of time from a few decades up to around 1 000 years after discharge from the reactor, the radioactivity of the metal components is dominated by nickel-63. The half-life of nickel-63 is around 100 years, which means that it decays virtually completely in 1 000 years.

Besides cobalt-60 and nickel-63, the metal components contain significant quantities of nickel-59 (half-life 80 000 years), zirconium-93 (half-life 1.5 million years) and carbon-14 (half-life 5 735 years). The two last-named nuclides are mainly concentrated in the zircaloy boxes around the fuel assemblies from BWR reactors, while nickel-59 is found mainly in Inconel and stainless steel.

Zirconium-93 possesses low radiologic toxicity. There is a total of about 1 000 Ci in the metal components in the repository. In the well case, this radioactivity gives rise to a maximum of 0.01 mrem per year to the critical group if the dissolution time is 10 000 years.

The amount of carbon-14 in the metal components corresponds to approximately 60% of the amount in the rest of the fuel. Carbon is assumed to form easily soluble compounds which migrate with the velocity of the groundwater.

As is evident from section 6.10.5, the dissolution time is at least 2.5 million years, even with unfavourable assumptions. The final repository for metal components contains approximately 25 000 Ci nickel-59. Thus, a maximum of 0.01 Ci/year of the isotope is dissolved. The retention factor for nickel in granitic crystalline rock has been calculated on the basis of sorption

measurements /8-21/ to be 6 100 (see table 7-2). With a groundwater transit time of 400 years, the nuclide transit time for nickel is 2.4 million years, which corresponds to 30 half-lives. On the basis of these assumptions, the inflow to the primary recipient will be at most $9.3 \cdot 10^{-12}$ Ci/year. If the nuclide transit time is assumed to be only 40 years, the inflow will be $1.3 \cdot 10^{-3}$ Ci/year.

As is pointed out in section 8.6.3, the radiation doses from the final storage of metallic fuel assembly components are low.

8.6 CONSEQUENCE ANALYSIS

8.6.1 Probable sequence of events

The calculations and analyses of the life of the copper canister carried out in chapter 8 show that the canister can be expected to have a service life of more than one million years. During this period of time, most of the radioactive elements in the spent fuel decay. During the period of time after one million years, the radiotoxicity of the fuel is dominated by decay products of uranium, primarily radium-226. This means that, with the stated service life of the copper canister, the consequences of the final storage of the spent fuel will not be worse than the consequences of the storage of an equivalent amount of uranium-dioxide which has not been irradiated in any reactor. An exception from this rule is the release of iodine-129, which, even after one million years, can give rise to a certain dose in the biosphere if it is dispersed via groundwater. But this dose does not exceed 0.4 mrem per year in the well case. The dispersal of iodine-129 proceeds much faster than the dispersal of uranium, thorium and radium. The calculated doses from iodine-129 are, however, considerably lower than those from radium-226.

If the copper canister is assumed to have a shorter life than one million years, dispersal of radioactive elements could start earlier. However, the chemical environment in the final repository is such that dissolution of the fuel can be expected to proceed extremely slowly. Locally, radiolysis caused mainly by alpha radiation can occur, but only in an area in the immediate vicinity of the canisters. Otherwise, chemical conditions in the rock are such that the solubility of actinides is extremely low. See chapter 3. Furthermore, the buffer mass is very impervious, which means that material transport is controlled by diffusion. Even with cautious assumptions, the calculated time required for the dissolution of all of the uranium in a canister is millions of years. Under such circumstances, the consequences will still be equivalent to those obtained from the storage of unirradiated uranium. Iodine-229 can still give rise to certain early radiation doses which could not be obtained from unirradiated uranium.

Thus, the copper canister and the buffer mass constitute consecutive barriers to the dispersal of the radioactive substances in spent nuclear fuel for virtually an unlimited period of time to come. At the same time, they are to a certain extent redundant barriers, since the buffer mass prevents rapid dispersal even if the copper canister should be penetrated.

8.6.2 Consequences of dispersal from final repository for fuel

In evaluating the safety of the final repository, it is necessary to study the consequences of various courses of events which are less favourable than the most probable. Such courses of events include penetration of the canister at some given point in time and a relatively more rapid dissolution of the waste substances than is most probable.

As is reported in chapter 5, a group of corrosion experts have concluded that it is realistic to expect a service life of hundreds of thousands of years for the copper canister, with the exception of one expert, who is of the opinion that a service life of more than 1 000 to 10 000 years cannot be ensured.

The basic assumption in the calculations is that the first canisters start to be penetrated after 100 000 years and that the process of canister penetration then continues at a constant rate for 400 000 years.

Leaching-out of the fuel in a damaged canister is assumed to take 500 000 years. This assumption is justified in sections 6.6 and 8.5.2. Certain approximations of this reference case have been necessary in the calculations - see section 8.5.2.

With the assumptions of the reference case concerning canister penetration and leaching time, two different dispersal scenarios have been analyzed. The first, which is referred to as the main case (calculation case 1 in 8.5.2), assumes a water flow time from the repository to the biosphere of 3 000 years combined with a best estimate hypothesis concerning retention factors. The second case (calculation case 3) is referred to as the pessimistic case and assumes a water transit time of 400 years and more conservatively calculated retention factors. Calculation cases 2 and 4 correspond to the above-mentioned two cases 1 and 3, but with an assumed canister life of 500 000 years (see section 8.5.2).

The results of these calculation cases and the effects of different variations in the basic assumptions are discussed below.

The improbable cases with initial canister damage and an extremely rapid commencement of canister degradation are analysed separately.

Finally, the influence of complexing agents in the groundwater and the importance of dispersion resulting from varying fissure widths in the rock are discussed.

Main case

Figure 8-13 shows the calculated individual doses for the so-called "critical group" (nearby residents) which are assumed to live in the vicinity of the repository and take their drinking water from a well located nearby. It should be noted that the figure has logarithmic scales on both axies. During the time period from 100 000 to 1 million years, when the breakdown of the canisters and dissolution of the fuel are under way, the radiation dose has been calculated to be less than 0.5 mrem/year.

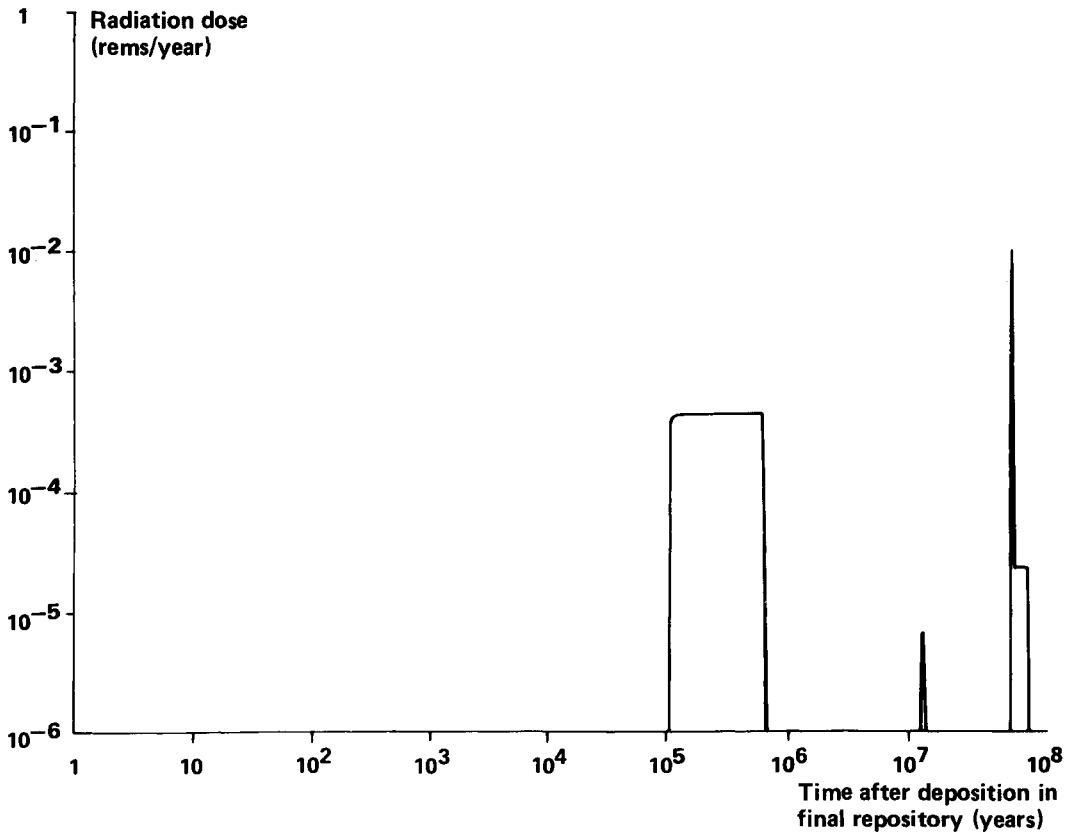

Figure 8-13. Calculated individual doses for critical group (nearby residents) for the main case with a well as the primary recipient.

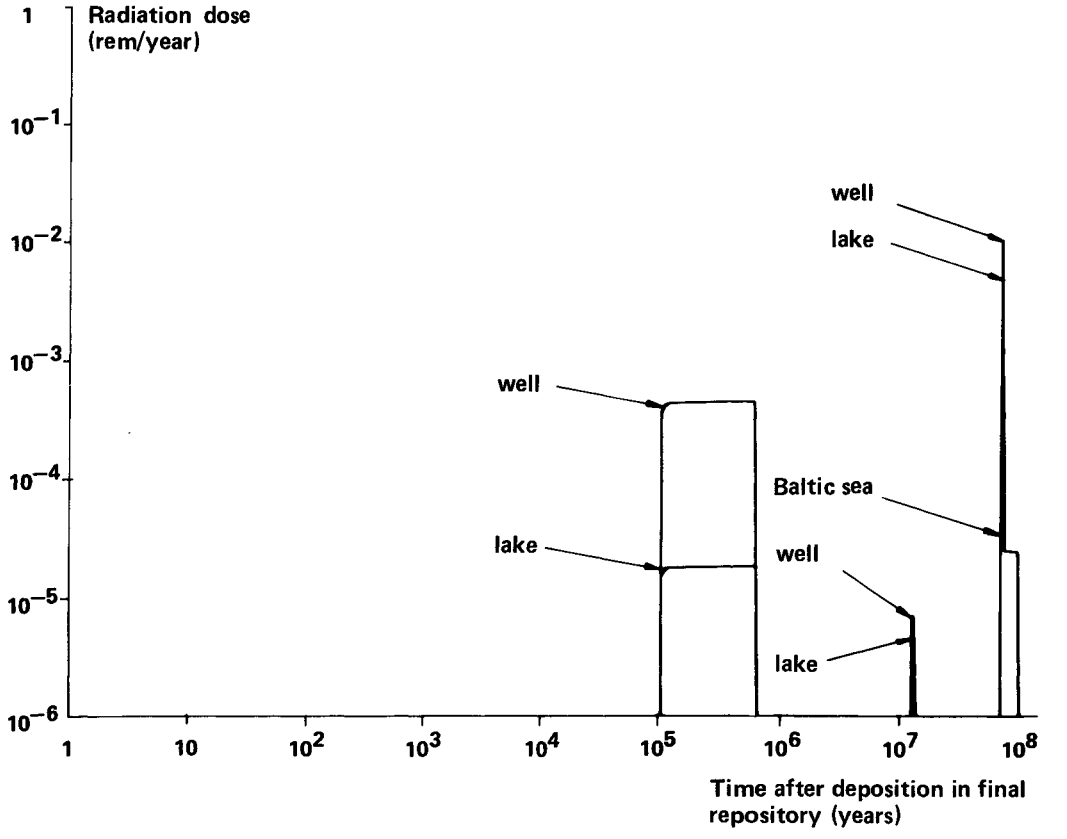

Figure 8-14. Calculated individual doses to critical groups (nearby residents) for different primary recipients. Main case.

Table 8-19. Maximum calculated individual doses to critical group for main case.

Nuclide	Time (years)	Well: maximum dose (rem/year)	Lake: maximum dose (rem/year)	Baltic Sea: maximum dose (rem/year)
C-14	1.0×10^{5}	5.2×10^{-10}	1.7×10^{-10}	3.1×10^{-12}
Tc-99	3.0×10^{6}	4.2×10^{-4}	1.9×10^{-5}	1.0×10^{-7}
I-129	1.0×10^{5}	4.2×10^{-4}	1.9×10^{-5}	1.0×10^{-7}
Cs-135	1.2×10^{7}	6.8×10^{-6}	4.9×10^{-6}	2.2×10^{-8}
Ra-226	6.9×10^{7}	9.8×10^{-3}	4.6×10^{-3}	3.0×10^{-5}
Th-230	6.9×10^{7}	2.3×10^{-4}	4.6×10^{-5}	1.9×10^{-7}
Pa-231	6.9×10^{7}	4.9×10^{-4}	4.9×10^{-4}	1.1×10^{-7}
U-234	6.9×10^{7}	3.3×10^{-4}	1.9×10^{-5}	1.3×10^{-7}
U-235	6.9×10^{7}	2.6×10^{-5}	1.5×10^{-6}	9.9×10^{-9}
U-236	6.9×10^{7}	5.7×10^{-5}	3.4×10^{-6}	2.2×10^{-8}
U-238	6.9×10^{7}	3.2×10^{-4}	1.9×10^{-5}	1.2×10^{-7}
Np-237	7.0×10^{7}	3.4×10^{-13}	1.5×10^{-14}	1.2×10^{-16}
Maximum total dose		0.011 rem/year	0.005 rem/year	0.00003 rem/year
Time for maximum total dose		69 million years	69 million years	69 million years

The dose stems primarily from iodine-129, which is not retarded in the rock. After more than 10 million years, cesium-135 has been calculated to give rise to a radiation dose of around 0.007 mrem/year. The largest doses for the reference case are not expected to occur until after 70 million years, with a total dose of around 10 mrem/year.

Figure 8-14 shows the calculated doses if the primary recipient is instead a lake or the Baltic Sea. The maximum doses in these cases are around 2 (lake) and 330 (Baltic Sea) times lower than in the well case.

Table 8-19 gives the maximum calculated individual doses to the critical group (nearby residents) for the three recipients and the times at which these doses are expected to occur. A breakdown is made according to important contributing nuclides. The importance of different paths of exposure is discussed in greater detail in section 8.5.5.

Radium-226 dominates completely for all recipients. In the well case, it dominates by a factor of around 20 over each of the nuclides protactinium-231, thorium-230, uranium-234 and uranium-238, which are all roughly equivalent in terms of radiation dose. In the lake case, radium-226 dominates by a factor of around 10 over the next nuclide, protactinium-231. For the Baltic Sea, this dominance is by two orders of magnitude.

The reason for this dominance is the assumption of a heavy local

precipitation of thorium-230 and a slow resuspension and dispersal. This also explains why the dose in the lake case is only around a factor of 2 lower than in the well case.

If it is assumed that canister degradation starts after 500 000 years (calculation case 2) and proceeds over a period of 400 000 years, the maximum inflows for dominant nuclides - and thereby the doses as well - are roughly equal to those in calculation case 1 (see table 8-8). An even longer canister life does not reduce the doses appreciably, since they are determined by the repository's content of uranium-238, with a half-life of 4 510 million years, and its daughter products, especially radium-226.

Pessimistic dispersal case

This case differs from the main case only with respect to the water transit time (400 years) and more conservative retention factors.

Figure 8-15 shows the calculated individual doses for the critical group (nearby residents) with a well next to the repository as their source of water. In this case, the dose is concentrated to the period from 100 000 years to around 3 million years following deposition. With these conservative assumptions, the maximum radiation dose is 70 mrem/year. The dominant nuclide is radium-226, followed by thorium-229, neptunium-237 and protactinium-231.

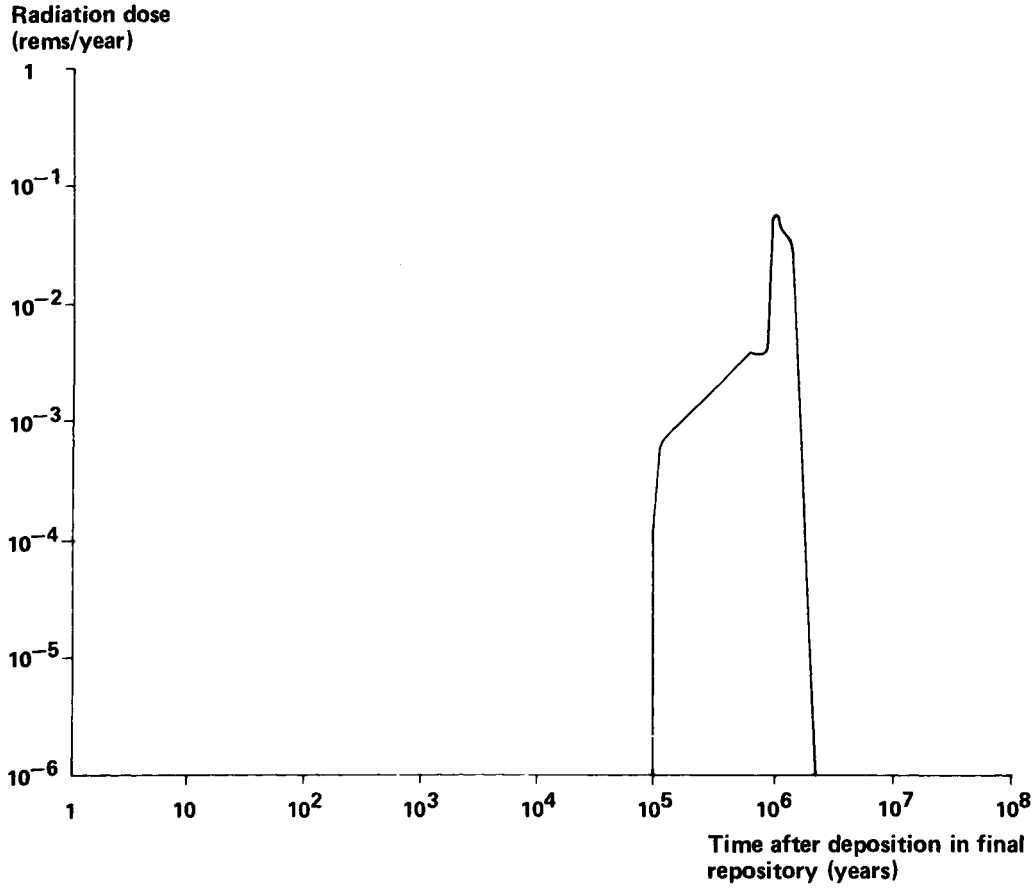

Figure 8-15. Calculated individual doses for critical group (nearby residents) for the pessimistic case with a well as the primary recipient.

An increase of the canister life with degradation beginning after 500 000 years does not lower the doses appreciably in this case either.

Initial canister damage

In view of the inspection and quality control measures which will be adopted in connection with canister fabrication, the probability of initial canister damage is judged to be very low. But in order to illuminate the consequences of such an event, a case with initial damage to one canister has been analysed. The results are illustrated in figure 8-16 and compared with the consequences of the slow degradation of all canisters in the main case. The maximum individual dose is caused by iodine-129, which appears after 3 300 years and is calculated to be 0.003 mrem/year in the well case (see table 8-20). The contributions from the retarded heavy nuclides, which are dominated by radium-226, are around 0.001 mrem/year and are scarcely visible in figure 8-16. For the pessimistic dispersal case, the contribution from iodine is nearly the same and the contribution from radium-226 is 1/7000th of the radiation dose from the entire repository, i.e. around 0.01 mrem/year. Plutonium-239 and other relatively short-lived nuclides decay virtually completely in the bedrock.

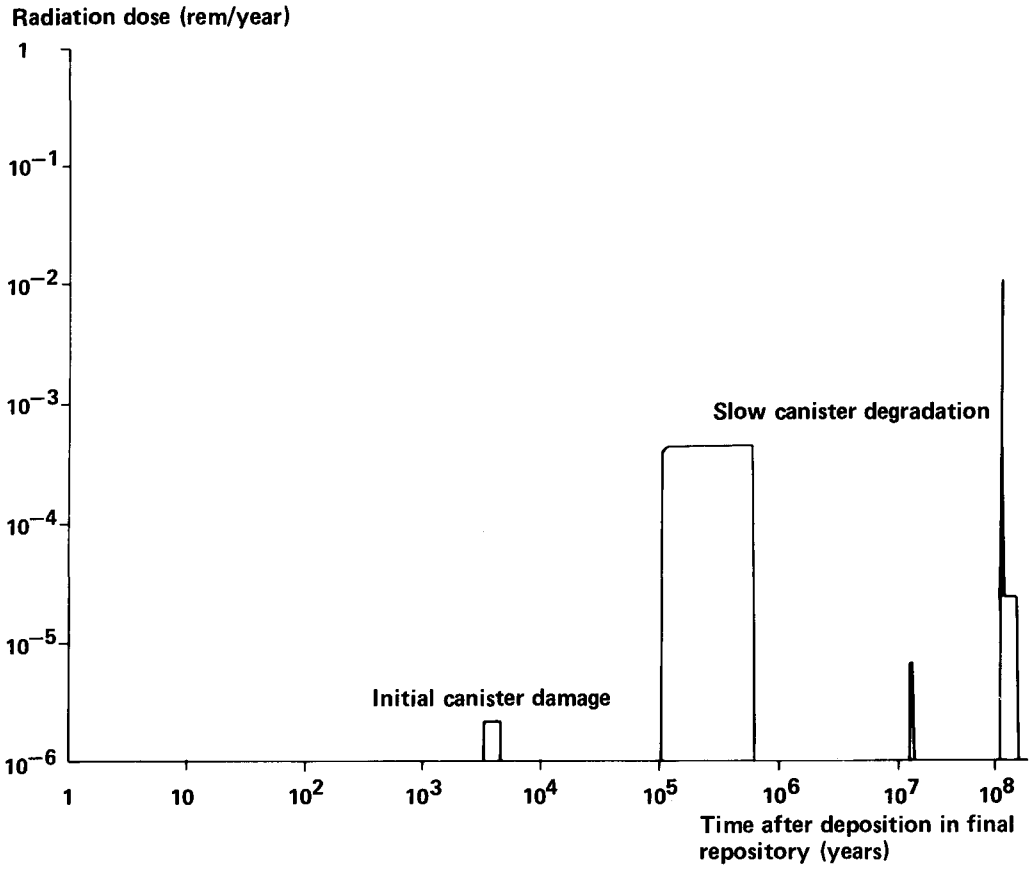

Figure 8-16. Calculated individual doses for critical group (nearby residents) with initial damage to one canister, compared with slow breakdown of all canisters. Primary recipient – well.

Table 8-20. Maximum calculated individual doses to critical group with initial canister damage. Other data as in main case and with well as primary recipient.

Nuclide	Maximum dose (rem/year)	Time (years)
C-14	1.5×10^{-8}	3.1×10^{3}
Tc-99	1.6×10^{-12}	2.9×10^{6}
I-129	2.9×10^{-6}	3.3×10^{3}
Cs-135	1.0×10^{-9}	1.2×10^{7}
Ra-226	8.9×10^{-7}	6.9×10^{7}
Th-230	7.5×10^{-8}	8.0×10^{7}
Pa-231	7.4×10^{-8}	6.9×10^{7}
U-235	3.7×10^{-9}	6.9×10^{7}
U-236	8.8×10^{-9}	6.9×10^{7}
U-238	5.2×10^{-8}	6.9×10^{7}
Maximum total dose		2.9×10^{-6} rem/year
Time for maximum total dose		3 300 years

Extremely early commenced canister degradation

One of the consulted corrosion experts was of the opinion that the possibility that the service life of the canister might be only a few thousand years cannot be excluded. As has already been pointed out in section 5.6.3, this is not consistent with the environment and the conditions which prevail in the final repository. If it is nevertheless assumed that an initial canister penetration occurs after 3 000 years, radiation doses from iodine-129 can occur after about 6 000 years at a level of around 0.5 mrem/year for the well case.

If it is still assumed that canister degradation proceeds at a uniform rate for 400 000 years, the same maximum radiation doses as in the main case are obtained. However, if the frequency of canister failure is assumed to be higher during a given period of time, the doses from more soluble components will increase. This applies especially to iodine-129. The reasonable hypothesis of a normal distribution with a maximum at 300 000 years /8-19/ leads to the conclusion that the frequency could be higher by a factor of 2-5. If it is cautiously assumed that the frequency is 10 times higher than that which corresponds to a uniform rate of degradation and that the entire iodine inventory in the fuel is available for leakage, then the radiaition dose from iodine-129 will be 10 times higher during this period. Only a small portion (around 10%) of the iodine is directly accessible for leaching, however.

Dissolution time

As is discussed in greater depth in chapter 6, the dissolution of the fuel is calculated to take at least 1.8 million years, owing to the limited flow rate and carbonate content of the water. In

the safety analysis, however, a period of 500 000 years has been cautiously assumed. If it is hypothetically assumed that the leaching time will be shorter, the radiation doses will be higher. The effects of different dissolution times have been studied with calculations for 10 000, 100 000 and 1 million years. These calculations have been carried out assuming a canister life of 10 000 years, a groundwater transit time of 400 years and the retention factors for an oxidizing environment which were used in the KBS report on vitrified waste /8-2/ (see also the first column in table 7-2).

In the least favourable case with a leaching time of 10 000 years and with the aforementioned pessimistic premises, a maximum calculated radiation dose in the well case of 100 - 150 mrem/year is obtained from heavy nuclides after 100 000 years, and around 20 mrem/year from iodine-129 after 10 000 years. The dose from the heavy nuclides is dominated by neptunium-237 with around 110 mrem/year /8-24/. With more realistic premises regarding to water transit time and retention factors, however, neptunium-237 will decay to a considerable degree, whereby the doses will also be lower.

Influence of organic complexing agents

The concentration of organic complexing agents in the groundwater is limited. Such agents can therefore only transport a small portion of the radioactive elements (see sections 7.2.5 and 8.5.4). At maximum inflows of complex-bound heavy metals (see section 7.2.5), the doses from plutonium-239 dominate with respect to the critical group. The total dose to the critical group from the maximum amount of complex-bound radioactive nuclides is, however, less than one-third of the maximum dose to the critical group in the main case (see table 8-21). Together with the iodine-129 dose, which is expected to appear at the same time, it amounts to around 3 mrem/year for the well case.

Table 8-21. Calculated individual doses for heavy nuclides dispersed via organic complexes in the groundwater. Data otherwise according to the main case. Primary recipient - well.

Nuclide	Inflow Ci/year	rems/year
Th-229	1.7×10^{-7}	1.5×10^{-7}
Th-230	1.1×10^{-3}	1.9×10^{-4}
U-233	4.8×10^{-4}	2.9×10^{-5}
U-234	1.7×10^{-3}	1.0×10^{-4}
Np-237	1.2×10^{-2}	1.4×10^{-3}
Pu-239	2.2×10^{-5}	1.9×10^{-6}
Pu-240	4.1×10^{-3}	3.7×10^{-4}
Pu-242	1.6×10^{-3}	1.4×10^{-4}

Fissure width dispersion

The calculations of inflow to the recipient have been carried out assuming a constant fissure width. A dispersion effect is obtained if the cracks exhibit a certain size variation. This will lead to a small portion of the inflow occurring sooner than average and possibly to a lower concentration maximum. An earlier inflow can result in considerably higher concentrations of relatively short-lived nuclides which would otherwise decay. The overall radiological consequences of an early inflow are, however, small. Table 8-11 shows the increase of inflow for the nuclides which are affected.

Table 8-22 shows that the individual doses which are obtained at

Table 8-22. Calculated individual doses at 20 % of the time for the calculated maximum dose as a result of fissure width dispersion. Primary recipient - well.

Nuclide	Inflow Ci/year	rem/year
Zr-93	3×10^{-7}	2×10^{-11}
Tc-99	3×10^{-5}	2×10^{-7}
Cs-135	7×10^{-4}	2×10^{-5}
Th-229	2×10^{-5}	2×10^{-5}
U-233	2×10^{-5}	1×10^{-6}
Np-237	3×10^{-5}	4×10^{-6}
Pu-242	1×10^{-5}	9×10^{-7}

20% of the time for maximum inflow as a result of fissure width dispersion constitute a small fraction of the maximum calculated radiation doses. The timetable is, however, altered radically, and the peak at about 70 million years shown in figure 8-13 is broadened and lowered considerably in analogy with what is shown in figure 7-3a. Fissure width dispersion has much less of an effect in the pessimistic dispersal case, in analogy with figure 7-3b.

Collective doses

Collective doses have been calculated for the different dispersal cases (see tables 8-12 to 8-17). They vary to only a relatively small extent with different premises.

In the main case, a maximum annual collective dose of 17 manrem/year is obtained after 580 000 years. This dose stems from iodine-129. After a very long period of time, radium-226 can also give rise to an equivalent collective dose: 15 manrem/year (see table 8-23). The maximum collective dose for the pessimistic case is 105 manrem/year, whereby radium-226 dominates.

Table 8-23. Maximum calculated collective doses for the main case.

Nuclide	Maximum collective dose (manrem/year)	Time (years)
C-14	5.0×10^{-4}	1.1×10^{5}
Tc-99	4.9×10^{-5}	3.2×10^{6}
I-129	1.7×10^{1}	5.8×10^{5}
Cs-135	1.5×10^{-2}	1.2×10^{7}
Ra-226	1.5×10^{1}	6.9×10^{7}
Th-230	1.3×10^{-1}	6.9×10^{7}
Pa-231	1.4×10^{0}	6.9×10^{7}
U-234	1.2×10^{-1}	6.9×10^{7}
Maximum total dose		17 manrem/year
Time for maximum total dose		5.8×10^{5} years and 6.9×10^{7} years
For case 3:(pessimistic dispersal)		
Maximum total dose		105 manrem/year
Time for maximum total dose		1.0×10^{6} years

Table 8-24 gives the collective dose commitments in the main case after different integration times. The collective dose for the most unfavourable 500-year period is 8 500 manrem. The possible health effects of this are discussed in section 8.6.4.

Table 8-24. Collective dose commitments in main case for different integration times.

Integration time (years)	Collective dose commitment (manrem)
$0 - 10^{5}$	0
$0 - 2 \times 10^{5}$	2.5×10^{5}
$0 - 10^{6}$	1.1×10^{7}
$0 - \infty$	2.0×10^{9}
For the worst 500-year period	8 500 manrem

8.6.3 Consequences of slow dispersal from final repository for the metal components of the fuel

Certain metal components from the fuel assemblies which have become radioactive due to neutron irradiation are stored in concrete moulds in a separate repository at a depth of 300 metres, as is described in section 2.4.5. The short-lived nuclides (cobalt-60 and nickel-63), with half-lives of 5.3 and 92 years, respectively) decay completely in the repository. In the case of nickel-59, with a half-life of 80 000 years, it is shown in sec-

tion 8.5.7 that the inflow to the recipient is negligible due to slow dissolution and to retardation in the rock. With conservative premises, the calculated inflow is $1.3 \cdot 10^{-3}$ Ci/year (see section 8.5.7), which corresponds to an individual dose in the well case of less than 0.002 mrem/year.

In the case of carbon-14, the radiation doses have been calculated with other even more conservative premises as regards retardation and leaching time. The critical path of exposure is via meat consumption. If it is assumed that the entire quantity of carbon-14 is completely dissolved over a period of 10 000 years and not retarded by the rock, the dose to the critical group will be around 1 mrem/year. A maximum dose of 0.01 mrem/year is obtained in a similar manner for zirconium-93.

8.6.4 Maximum health effects

Even for the most unfavourable cases with pessimistically chosen data in the calculations, the health hazards resulting from the escape of radioactive substances from the repository are very small, if any. This applies both for nearby residents and for the rest of the population for all future time. The risk to nearby residents can be illustrated by means of the following table, which gives the calculated increase in the cancer risk at the time of maximum radiation doses in the future.

Recipient	Present annual risk for cancer in Sweden	Additional risk due to leaching from repository	
		main case (case 1)	pessimistic case (case 3)
Well	3×10^{-3}	1×10^{-6}	6×10^{-6}
Lake	3×10^{-3}	5×10^{-7}	4×10^{-6}
Baltic Sea	3×10^{-3}	3×10^{-9}	1×10^{-7}

The additional risk is thus very small in relation to the natural cancer frequency, even for nearby residents and with conservative dispersal assumptions.

The total collective dose in the main case is 8 500 manrems during the worst 500-year period, which occurs after more than 500 000 years. This is equivalent to 0.03 manrem per MWe and year of operation.

The calculated collective doses in the main case and in the pessimistic case correspond to 2 and 10 cases of cancer, respectively, calculated for the population of the entire earth during a period of 500 years. The two nuclides iodine-129 and radium-226, which dominate in this case, are concentrated in the body primarily in the thyroid gland and the skeleton, respectively. The chromosomes in the reproductive organs therefore receive a relatively low dose from these nuclides. Table 7-4 shows the size of the dose to the gonads compared to the weighted whole-body dose for the nuclides. On the basis of the collective gonad dose,

the number of genetic defects is calculated to be no more than 0.1 case during a period of 500 years for the population of the entire world.

The present number of deaths due to cancer in Sweden is approximately 20 000 per year. Of all babies born in the country, approximately 3% are afflicted with natural genetically-caused defects, which is equivalent to some 3 000 cases per year at the present time in Sweden. The specified values for health effects have been calculated on the basis of internationally accepted principles concerning causal relationships between radiation doses and maximum health effects. However, this may lead to an overestimation of the actual health effects at the low dose values and dose rates in question here.

8.6.5 Comparisons with recommended limits and natural radioactivity

The maximum radiation dose for the critical group in the main case is calculated to be around 10 mrem/year. The ICRP recommended limit for the critical group which will be exposed to radiation over a number of years has recently been set at 100 mrem/year. Even with pessimistic assumptions concerning dispersal conditions, the calculated radiation doses from the final repository are below the ICRP recommended limit.

The calculated maximum radiation dose (10 mrem/year) in the main case is on a level with the design goal specified by the National Institute of Radiation Protection for nuclear power plants in Sweden. This limit is based on the principle that discharges of radioactive elements shall be kept as low as is reasonably achievable in view of the economic and social consequences of every effort to limit radioactive discharges.

It can also be of interest to compare calculated increased contents of radioactive elements in the primary water recipients directly with those which occur naturally in water, table 8-25. This comparison has special relevance in view of the fact that the dose-dominant nuclide is radium-226, which also occurs in nature.

8.7 INFLUENCE OF EXTREME EVENTS

In the preceding section 8.6, long-range safety has been discussed in relation to the slow degradation of the canisters which could take place in the final repository. In the following section, safety and the risk of certain extreme and special events are discussed.

8.7.1 Bedrock movements

In connection with the preparation of the previous report on vitrified waste, a number of different studies were conducted concerning the occurrence of earthquakes and bedrock movements and how these could affect a final repository at a depth of 500 metres in the Swedish bedrock.

Table 8-25. Content of radioactive elements in water.

Radioactive element	Concentrations in natural water in Sweden (pCi/l)		Calculated maximum increase of level in primary recipients near final repository in main case (pCi/l)	
	Drinking water	Sea water[a)]	Well	Lake
Radium-226	0.1-40	0.3	0.3	0.5
Uranium-238	0.1-1500[b)]	0.3	6	0.1
Potassium-40[c)]	ca 20	330	-	-
Cesium-135[c)]	-	-	0.3	0.006

a) With 3.5% salt content.

b) Includes U-235 and applies to natural water (not necessarily drinking water).

c) Potassium-40 and cesium-135 are biologically comparable but have somewhat different dose factors (24 000 and 7 300 rems/Ci, respectively).

The geological prerequisites for the safe final storage of spent nuclear fuel in Swedish bedrock are discussed in chapter 3.

Bedrock movements could conceivably damage the canisters and alter hydrological conditions. However, the properties of the copper and the buffer material allow a movement of serveral cm in the storage holes without the integrity of the canister being affected, as is discussed in /8-25/.

It is possible to obtain an idea of the frequency and the magnitude of rock movements over long periods of time by studying the fracture pattern in exposed rock outcroppings. In order to learn something about movements in shallower strata of solid rock, observations have been carried out in the Karlshamn area, the results of which are reported in greater detail in section 3.2. The greatest observed displacement was 2 cm. On the basis of the frequency distribution of the size of the displacements and under the assumption that the observed displacements have taken place in their entirety in a single deformation step, the probability of a displacement of 3 cm has been estimated. Transposed to a final repository, it would mean that one or a few canisters would be influenced over a period of 28 million years.

As is discussed in greater detail in chapter 3, the size and frequency of fracture movements have been greater than average during certain periods many millions of years ago. At the present time, Sweden is in a decidely stable period with a lower frequency of fracture movements. Moreover, the size of fracture move-

ments diminishes with increasing depth to a greater extent than is indicated by studies of subsurface rock.

As is discussed in greater detail in the same chapter, any fracture movements which may occur during the next few millions of years can only give rise to insignificant changes in the permeability of the rock.

Even if the permeability of the rock were to increase in connection with a fault movement which damaged a few canisters, the consequences would be greatly limited. The consequence of a hypothetical large fault movement which damages several canisters in the repository and a hypothetical coincidental increase of the water flow can be compared with the case of initial canister damage with modified premises. If it is assumed that 10 containers are damaged and that the water flow increases to the extent that full leaching takes place in 50 000 years (1 000 years for 10% of the iodine-129) and that the water transit time is reduced to 100 years, a maximum individual dose of around 0.006 mrem/year is obtained from iodine-129 100 years after such an event, and around 0.2 mrem/year from radium-226 after 200 000 years plus 0.2 mrem/year from plutonium-239. This assumes retention factors as in the pessimistic case. The doses for other nuclides will also be low /8-19 and 8-24/.

8.7.2 Criticality

The possibility that criticality, i.e. a self-sustaining chain reaction, could occur with the fissionable plutonium-239 and uranium-235 which is present in the repository is virtually nil. The question has been the subject of thorough analysis within the project and is dealt with in great detail in a technical report /8-26/. A brief summary is provided here.

Criticality with plutonium-239

In principle, sufficient plutonium-239 is present in a single canister from the start in order for criticality to be reached. But first some process involving penetrating water must separate the plutonium from the uranium in the fuel and collect it in concentrated form in a manner suitable for criticality. This is not feasible for a number of reasons.

Since the expected service life of the copper canisters is considerably longer than the half-life of plutonium-239, there will not be enough plutonium present for criticality if and when the copper canisters are penetrated. The case is therefore of interest only for a single container which could have initial canister damage.

Criticality inside a damage canister requires that the uranium present there be selectively dissolved and transported out of the canister before the plutonium-239 has had time to decay sufficiently.

Criticality outside of a damaged canister requires that uranium and plutonium be dissolved together and that plutonium be selec-

tively precipitated in the bentonite buffer outside of the canister. Selective leaching of plutonium is not possible for chemical reasons.

Neither internal nor external criticality with plutonium is a reasonable possibility, however, since it requires a more rapid dissolution (on the order of 50 000 years) of uranium or of uranium and plutonium than what is calculated to be possible (1.8 million years) under existing conditions with regard to water flow and carbonate levels. Furthermore, the plutonium must be distributed in a manner which is appropriate for criticality, which is very improbable.

Criticality also requires that large portions of the bentonite material around the canister be lost. This is considered to be impossible on the basis of existing knowledge of bentonite and rock properties.

Internal transport resistance in the canister will further impede the transport of material out of the canister.

In summary, the probability of plutonium criticality is extremely low. Furthermore, the consequences of a postulated criticality would be insignificant. The course of events is characterized by a slow heat generation and an increase of the temperature to a theoretical maximum of the boiling point of water (around 265°C at the pressure prevailing at a depth of 500 m). If the temperature tends to rise higher, water boils off and the reaction stops. The effects on nearby canisters will not be such that their integrity will be jeopardized. The amount of long-lived radiotoxic nuclides which are formed in connection with criticality is small in relation to the amount which is already present in the failed canister.

Criticality with uranium-235

Criticality with uranium-235 is not possible inside the canisters owing to neutron physics considerations. Such criticality is only possible in tunnel systems and storage holes outside of the canisters. Owing to the long half-life of uranium-235, the risk of criticality in this case does not apply only to an isolated initially damaged canister. Calculations show that the minimum critical mass in the tunnels is around 4 400 kg, which means that all of the uranium from at least four canisters must be accumulated within the critical geometry. The expected reducing environment, with bivalent iron in the bentonite, keeps uranium in the quadravalent state, which counteracts migration and local precipitation at any distance from the canisters. The risk of criticality can be completely eliminated by the addition of a few percent magnetite to the bentonite, thereby increasing neutron absorption to a sufficient level.

Even though the risk of criticality is thus extremely low or can be eliminated completely, the consequences of a hypothetical case have been calculated. A sudden, heavy release of energy is out of the question. Criticality can only be built up by a slow accumulation of uranium. The thermal power output from a hypothetical critical mass involving all of the uranium deposited in one of

the tunnels would be lower than 130 kW. The formation of fission products would be equivalent to that of 900 tonnes of deposited fuel, which would not increase the radiation doses to any great extent in relation to the main case without criticality.

In summary, it can be concluded that a number of extreme or improbable prerequisites must be postulated in order to achieve a critical configuration. The probability of this occurring is judged to be negligible. The consequences of hypothetical cases of criticality from both plutonium-239 and uranium-235 have, moreover, been calculated to be insignificant.

8.7.3 Meteorite impacts

If a meteorite should hit the surface of the earth directly above a final repository, a crater would be created which could weaken the geological barrier or, at worst, eliminate it completely.

According to Hartman /8-27/, who studied meteorite impacts which occurred during a period of 2 000 million years, the probability of a meteorite impact which would create a crater approximately 100 metres deep is approximately 10^{-13} per year and square kilometre. A more recent estimate /8-29/ puts the probability of a comparable event at 10^{-11} per km^2 and year. Historical experience also shows that a meteorite impact is not a risk which need to be considered in this context.

8.7.4 Acts of war and sabotage

In the long time perspective which is relevant for the final repository, acts of war cannot be considered to be "extreme events". On the other hand, the possibility that acts of war might lead to serious consequences for the safety of a finally sealed final repository at a depth of some 500 metres in the Swedish bedrock must be considered to be remote.

Ground detonations of nuclear devices of 10-50 megatons create craters in the rock with a depth of roughly 110-180 m /8-28/. The geological barrier would thus not be penetrated, but might well be weakened. In such a situation, however, this would be of subordinate importance, since any release of radioactivity from the final repository would represent only a fraction of the radioactivity caused by the bomb, which would remain in the area for a long period of time. Wartime damages to the final repository and the encapsulation station during the deposition stage are, naturally, conceivable. But the probability is low, since these facilities are not likely to be primary targets for military actions. The consequences of bomb hits and similar occurrences would also be limited compared to the other consequences of such acts of war.

Safeguards against sabotage acceptable to the authorities will be provided during intermediate storage, encapsulation and deposition in the final repository. After the final repository has been closed and sealed, effective acts of sabotage are impossible. Compared to other installations which experience has shown to be likely targets for sabotage in terrorist actions, the facilities described here are less attractive to potential saboteurs and are

most closely comparable to other industrial plants where environmentally hazardous material is handled.

8.7.5 Future disturbance by man

It is conceivable that the knowledge of where the final repository is located may be lost in the distant future and that man at that time may, for some reason, perform drilling or rock work which results in contact with the waste. The final repository is situated in one of our most common types of rock which does not contain any valuable minerals which could conceivably be considered for profitable extraction. The depth and low water content of the impervious rock selected for this purpose make it highly improbable that deep wells will be drilled for water near the repository in the future. No reason can be seen for seeking out such great depths for the construction of rock storage caverns or the like. Furthermore, the loss of the knowledge of the location of the final repository presupposes that our current civilization is destroyed as a result of some catastrophic event such as a global war of extermination or a new ice age. If the country were then repopulated again, the risks mentioned here would arise, but only after the new population had achieved a level of technological development which permitted advanced rock work. In such a case, it is probable that such a civilization would also possess the ability to detect the radioactivity in the final repository and act accordingly to prevent harm being done.

8.8 SUMMARY SAFETY EVALUATION

8.8.1 Handling, storage and transportation of spent fuel

Spent fuel and vitrified waste will behandled, stored and transported in accordance with international and national standards and regulations.

A good deal of experience has been gained both in Sweden and abroad in the handling and storage of spent fuel.

It is assumed that the central storage facility for spent fuel will be situated in a rock cavern with approximately 30 m of rock cover. The facility is designed with the primary objective of minimizing radiation doses to the personnel and preventing the release of radioactive substances to the environment.

The various measures which are adopted to ensure the radiological safety of the personnel - such as carefully designed radiation shielding, remote-controlled handling and ventilation, systems for monitoring direct radiation and airborne activity etc. - permit handling and storage to be affected with adequately low dose loads /8-2/.

Spent fuel and vitrified high-level waste will be transporated in accordance with international regulations in casks which can withstand severe transport accidents. The consequences of hypothetical leakage in connection with severe accidents have been analysed /8-2/.

Handling in connection with dismantling and encapsulation of the spent fuel in the encapsulation station entails risks which are, at the most, equal to but probably less than the risks involved in handling the fuel in the central fuel storage facility. This is true for both normal operation and more severe accidents. In the dry parts of the encapsulation station, i.e. the casting cell and the welding cell, fuel handling is completely shielded off from the environment and the exhaust air from these sections is filtered through banks of filters with a collection efficiency for iodine of more than 90%. Normal operational releases will be very small - less than 0.001 mrem/year to the nearby population. Accidents involving dropped fuel cassettes or copper canisters (in the casting cell) will, in the worst cases, give rise to krypton-85 releases which are comparable to those from similar accidents in the central fuel storage facility and aerosol releases of heavy nuclides which result in a maximum intake of 0.2 pCi of the dominating nuclide plutonium-238. These releases give rise to completely negligible individual doses.

Handling of the spent, unreprocessed nuclear fuel can thus be ascribed a very high level of safety.

8.8.2 Final storage of spent, unreprocessed nuclear fuel

The spent nuclear fuel is isolated by means of encapsulation in copper canisters which are packed in highly-compacted bentonite in sound rock at a depth of 500 m. Rock tunnels and shafts are sealed with a mixture of 80-90% quartz sand and 10-20% bentonite. Metal scrap etc. from the spent fuel is embedded in concrete and stored in special rock tunnels at a depth of 300 m in sound rock. The tunnels are back-filled with concrete. The safety analysis of such a final storage method shows the following:

1. The groundwater chemistry in the Swedish bedrock at the depths for the final repositories (300-500 m) is reducing. The groundwater is virtually oxygen-free. The buffer material - highly-compacted bentonite - possesses extremely low water permeability, so material transport through the buffer mass is controlled by diffusion.

   The avaiable quantity of oxidants which can attack copper is low and the supply rate of oxidants is extremely slow. The copper canister can therefore be expected to have a virtually unlimited life and thereby prevent the dispersal of radioactive substances.

2. The probable consequence of final storage of the spent nuclear fuel in the described manner is that it will not lead to any dispersal of radioactive substances to the biosphere for a very long period of time - more than one million years. This means that the long-term consequences of the final storage of spent unreprocessed nuclear fuel are equivalent to the long-term consequences of the storage of unirradiated uranium dioxide in the same manner.

3. On the basis of a statement by a group of specialists, it is judged realistic to anticipate a minimum service life of hundreds of thousands of years for a copper canister with a wall thickness of 200 mm.

4. Over a time span of 100 000 years, the following important radioactive nuclides decay virtually completely: americium-241, plutonium-238 and -241, strontium-90, cesium-137 and carbon-14. Americium-243, plutonium-239 and -240 also decay to an appreciable extent.

5. If the copper canisters should be penetrated after a few hundred thousand years, some leaching of radioactive substances to the groundwater could take place. This would proceed extremely slowly and would probably take millions of years, even under pessimistic assumptions. After approximately one million years, the toxicity of the waste will be dominated by radium-226, which is a daughter product of uranium-238 with a half-life of 4 510 million years. Uranium-238 and its decay products will therefore persist, even over periods of time which are long by geological standards.

6. For a case with conservatively chosen data, but representing probable assumptions concerning water transit time and nuclide retardation (the main case), a maximum calculated radiation dose to individuals of approx. 10 mrems per year is obtained after 70 million years. The corresponding global collective dose is approx. 17 manrems/year.

7. For a case with very pessimistically chosen data for all important parameters (pessimistic case), a maximum calculated radiation dose to individuals of approx. 70 mrems per year is obtained after 1 million years. Corresponding global collective dose is approx. 105 manrems/year.

8. The health hazards are extremely small, if any, for the pessimistic case as well.

9. The calculated increase of the level of radioactive elements in the recipients to which waste products could conceivably spread is, even in unfavourable cases, comparable to natural levels of such elements.

10. Radiation doses from the final repository for spent fuel rods calculated in accordance with the main case and the pessimistic case are presented in figure 8-17. The natural radiation level in Sweden and certain limit values recommended or prescribed for nuclear power plants by the authorities are given for comparison.

11. The final storage of other waste obtained in the handling of spent unreprocessed nuclear fuel does not give rise to any dose increment of importance for the overall safety evaluation (maximum 1 mrem/year).

12. A number of extreme or highly improbable or unreasonable circumstances must be postulated in order for criticality in or adjacent to the repository to be reached. The probability of this happening is judged to be extremely small. If it is nevertheless assumed that criticality occurs, the process will proceed slowly and the consequences will be insignificant compared with those reported for the final storage scheme as a whole.

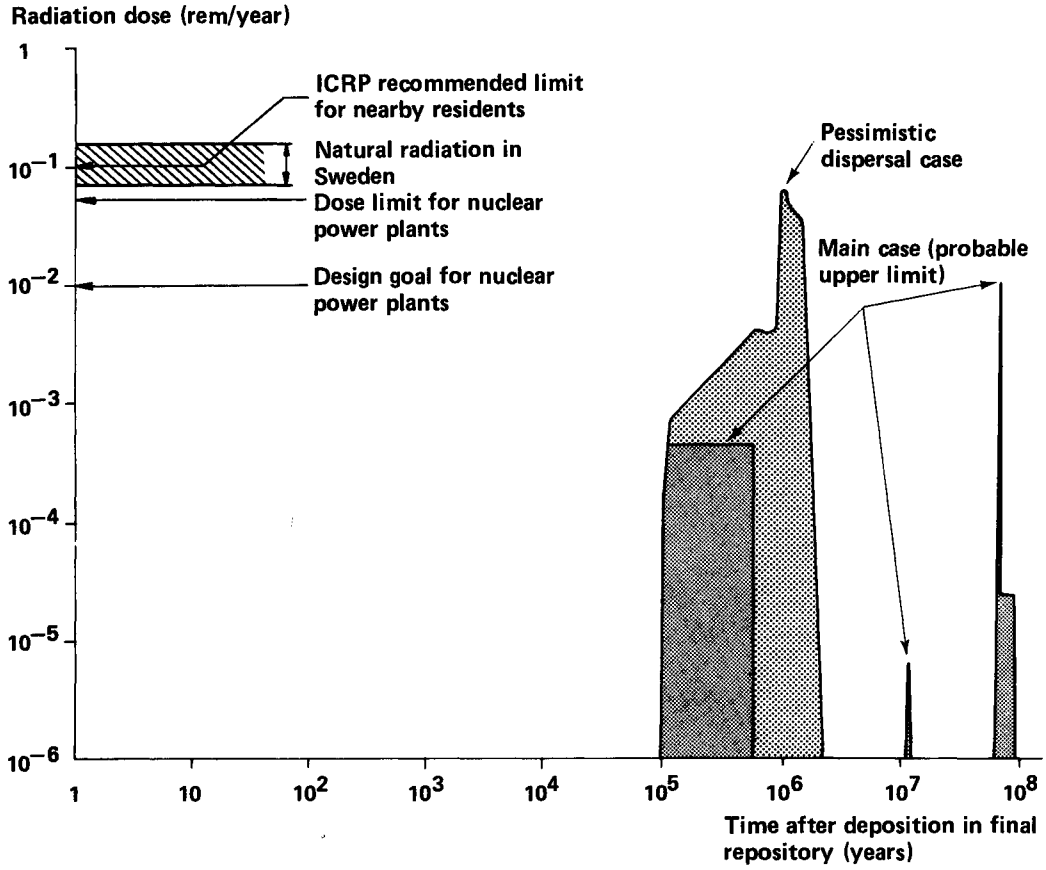

Figure 8-17. Comparison of calculated maximum radiation doses for persons living near the final repository with natural background radiation and with recommended or prescribed limits for nuclear power plants.

13. Even in those cases where a number of unfavourable assumptions have been made, the calculated changes in the background radiation are less than normally occurring natural variations. These natural variations do not have any effects on either man or ecological systems which can be demonstrated today. The calculated maximum radiation doses due to leakage from a final repository are below the limit values recommended by the International Commission on Radiological Protection (ICRP). The proposed method for the final storage of spent fuel is therefore deemed to be absolutely safe.

REFERENCES

CHAPTER 2

2-1 Svensk Kärnbränsleförsörjning AB (The Swedish Nuclear Fuel Supplies Company)
Centralt lager för använt kärnbränsle. Bilaga till lokaliseringsansökan enligt byggnadslagen och koncessionsansökan enligt atomenergilagen
("Central storage facility for spent nuclear fuel. Appendix to siting application in accordance with Building Act and licensing application in accordance with Atomic Energy Act")
(1977-11-30)

2-2 VESTERLUND G, OLSSON T
Degraderingsmekanismer vid bassänglagring och hantering av utbränt kraftreaktorbränsle
("Degredation mechanisms in connection with pool storage and handling of spent nuclear reactor fuel")
ASEA-ATOM
KBS Technical Report 68, 1978-01-18

2-3 LÖNNERBERG B
Konstruktionsstudier - direktdeponering
("Design studies - direct deposition")
ASEA-ATOM
KBS Technical Report 39, September 1978

2-4 BERGSTRÖM J, GILLANDER L, HANNERZ K, KARLSSON L, LÖNNERBERG B, NILSSON G, OLSSON S, SEHLSTEDT S
Tillverkning av kopparkapsel för slutförvaring av använt bränsle
("Fabrication of copper canisters")
ASEA, ASEA-ATOM
KBS Technical Report 81, JUNE 1978

2-5 LÖNNERBERG B, ENGELBREKTSON A, NERETNIEKS I
Hantering och slutförvaring av aktiva metalldelar
("Handling and final storage of radioactive metal components")
ASEA-ATOM, VBB
KBS Technical Report 82, JUNE 1978

2-6 TARANDI T
Temperaturberäkningar för slutförvar för använt bränsle
("Temperature calculations for spent fuel")
VBB
KBS Technical Report 46, June 1978

2-7 PUSCH R
Bergspricktätning med bentonit
("Rock fissure sealing with bentonite")
Luleå Institute of Technology
KBS Technical Report 71, 1977-11-16

2-8 PUSCH R
Small-scale bentonite injection test on rock
Luleå Institute of Technology
KBS Technical Report 75, 1978-03-02

2-9 FINNÉ A, ENGELBREKTSON A
Utformning av bergrumsanläggningar
("Design of rock cavern facilities")
KBS, VBB
KBS Technical Report 38, December 1977

2-10 ENGELBREKTSON A
Hantering av kapslar med använt bränsle i slutförvaret
("Handling of canisters for spent fuel in the final repository")
VBB
KBS Technical Report 83, April 1978

2-11 ENGELBREKTSON A, ODEBO U
Tillverkning och hantering av bentonitblock
("Fabrication and handling of bentonite blocks")
ASEA, VBB
KBS Technical Report 84, June 1978

2-12 FAGERSTRÖM H, LUNDAHL B
Hantering av buffertmaterial av bentonit och kvarts
("Handling of buffer material of bentonite and quartz")
VBB, Stabilator
KBS Technical Report 37, October 1977

2-13 BERGSTRÖM S, FAGERLUND G, ROMBÉN L
Bedömning av egenskaper och funktion hos betong i samband med slutlig förvaring av kärnbränsleavfall i berg
("Evaluation of properties and function of concrete in connection with final storage of nuclear fuel waste in rock")
The Swedish Cement and Concrete Research Institute
KBS Technical Report 12, 1977-06-22

2-14 NERETNIEKS I, ANDERSSON K, HENSTAM L
Utläckning av Ni-59 från ett bergförvar
("Leakage of Ni-59 from a rock repository")
Royal Institute of Technology
KBS Technical Report 101, 1978-04-24

CHAPTER 3

3-1 ÅBERG G
Precambrian geochronology of south-eastern Sweden
Proceedings of the Geological Society, Stockholm 100, 1978

Allmänna framställningar av Sveriges geologi ges av MAGNUSSON N H, LUNDQVIST G, REGNELL G
("General descriptions of the geology of Sweden are provided by Magnusson N H, Lundqvist G, Regnell G")
Sveriges Geologi (The Geology of Sweden)
Norstedts, Stockholm 1963

LUNDEGÅRDH P H, LUNDQVIST J, LINDSTRÖM M
Berg och jord i Sverige
("Rock and soil in Sweden")
Almqvist and Wiksell, Stockholm 1970

3-2 Zeitschrift für Angewandte Geologie;
Bd 23, H 9, 1977

3-3 SCHERMAN S
Förarbeten till platsval, berggrundsundersökningar
("Preliminary studies for site choice, bedrock studies")
Geological Survey of Sweden
KBS Technical Report 60, January 1978

KLOCKARS C-E, PERSSON O
Berggrundvattenförhållanden i Finnsjöområdets nordöstra del
("Groundwater conditions in the northeastern sector of the Finnsjö district")
Geological Survey of Sweden
KBS Technical Report 60, January 1978

3-4 MAGNUSSON K-Å, DURAN O
Geofysisk borrhålsmätning
("Geophysical borehole survey")
KBS Technical Report 61, January 1978

3-5 SWAN G
The mechanical properties of the rocks in Stripa, Kråkemåla, Finnsjön and Blekinge
Luleå Institute of Technology
KBS Technical Report 48, 1977-09-14

3-6 LAGERBÄCK R, HENKEL H
Studier av neotektonisk aktivitet i mellersta och norra Sverige, flygbildsgenomgång och geofysisk tolkning av recenta förkastningar
("Studies of neotectonic activitiy in central and northern Sweden, review of aerial photographs and geophysical interpretation of recent faults")
Geological Survey of Sweden
KBS Technical Report 19, September 1977

3-7 RÖSHOFF K, LAGERLUND E
Tektonisk analys av södra Sverige, Vättern - Norra Skåne
("Tectonic analysis of southern Sweden, Lake Vättern - Northern Skåne")
University of Lund and Luleå Institute of Technology
KBS Technical Report 20, September 1977

3-8 FLODÉN T
Tectonic lineaments in the Baltic from Gävle to Simrishamn
University of Stockholm
KBS Technical Report 59, 1977-12-15

3-9 STEPHANSSON O
Deformationer i sprickigt berg
("Deformations in fissured rock")
Luleå Institute of Technology
KBS Technical Report 29, 1977-09-28

3-10 PUSCH R
The influence of rock movements on the stress/strain situation in tunnels or boreholes with radioacitve canisters embedded in a bentonite/quartz buffer mass
Luleå Institute of Technology
KBS Technical Report 22, 1977-08-22

PUSCH R
Experimental determination of the stress/strain situation in a sheared tunnel model with canister
Luleå Institute of Technology
KBS Technical Report 76, 1978-03-02

3-11 BERGMAN S G A
Spänningsmätningar i Skandinavisk berggrund - förutsättningar, resultat och tolkning
("Stress measurements in Scandinavian bedrock - premises, results and interpretation")
KBS Technical Report 64, November 1977

3-12 KBS
Kärnbränslecykelns slutsteg. Förglasat avfall från upparbetning
("Handling of spent nuclear fuel and final storage of vitrified high-level reprocessing waste")
II Geology, Stockholm, November 1977

3-13 WESSLEN A
Hur stort kan ett bergrum göras?
("How large can a rock cavern be made?")
Teknisk Tidskrift, 1975:3

3-14 RINGDAL F, GJÖYSTDAL H, HUSEBYE E S
Seismotectonic risk modelling for nuclear waste disposal in the Swedish bedrock
Royal Norwegian Council for scientific and industrial research
KBS Technical Report 51, October 1977

3-15 EHRENBORG J
Geologic interpretation of bedrock from a landsat colour composite
Proceedings of the Geological Society, Stockholm, 99, p 58-62, 1977

3-16 de MARSILY G, LEDOUX E, BARBREAU A, MARGAT J
Nuclear Waste Disposal: Can the geologist guarantee isolation?
Science 197: 4303, p 519-527, 1977

3-17 NORDENSKÖLD C E
Morfologiska studier inom övergångsområdet mellan Kalmar-slätten och Tjust
("Morphological studies of the transitional area between the Kalmar plain and Tjust")
Dissertation VIII, Lund Institute of Geography , Lund 1944

3-18 MÖRNER N-A
Rörelser och instabilitet i den svenska berggrunden
("Movements and instability in the Swedish bedrock")
University of Stockholm
KBS Technical Report 18, August 1977

3-19 LUNDEGÅRDH P H
Berggrunden i Gävleborgs län
("The bedrock in Gävleborg County")
Geological Survey of Sweden, Ser Ba, 22, Stockholm 1967

3-20 RUDBERG S
The sub-cambrian peneplain in Sweden and its slope gradient
Zeitschrift für Geomorphologie, Supplementband 9, p 157-167, Stuttgart 1970

3-21 ASKLUND B
Bruchspaltenbildungen im südöstlischen Östergötland nebst einer Übersicht der geologischen Stellung der Bruschspalten Südostschwedens
("Fracture formation in southeastern Östergötland plus a survey of the geological state of the fractures of southern Sweden")
Proceedings of the Geological Society, Stockholm, 45, p 249-285, 1923

3-22 WELIN E
Uranium disseminations and vein fillings in iron ores of northern Upland, central Sweden
Proceedings of the Geological Society, Stockholm, 86, p 51-82, 1964

3-23 RATIGAN J L
Rock mechanics analyses
Hagconsult AB
KBS Technical Report 54:04, September 1977

3-24 STEPHANSSON O, MÄKI K, GROTH T, JOHANSSON P
Finit elementanalys av bentonitfyllt bergförvar
("Finite element analysis of bentonite-filled rock repository")
Luleå Institute of Technology
KBS Technical Report 104, June 1978

3-25 BJERHAMMAR A
The gravity field in Fennoscandia and postglacial crustal movements
Department of Geodesy, Royal Institute of Technology
KBS Technical Report 17, August 1977

3-26 KUKLA J
Correlation between loesses and deep sea sediments
Proceedings of the Geological Society, Stockholm, 92, p 148-180, 1970

3-27 PUSCH R
Inverkan av glaciation på en deponeringsanläggning belägen i urberg 500 m under markytan
("Influence of glaciation on a waste repository situated in primary bedrock 500 m below the surface of the ground")
Luleå Institute of Technology
KBS Technical Report 89, 1978-03-16

3-28 GEIJER P, MAGNUSSON N H
Mullmalmer i svenska järngruvor
("Hematite ores in Swedish iron mines")(Engl. summary)
Geological Survey of Sweden, Ser C 338, 1926

3-29 MAGNUSSON N H
Malm i Sverige 1
("Ore in Sweden 1") (p 278-280); 320 p
Almqvist and Wiksell, Stockholm 1973

3-30 DOWDING C H
Seismic stability of underground openings
Rockstore, intern. symp., preprint 2, p 23-30, Stockholm 1970

3-31 YAMAHARA H, HISATOMI Y, MORI T
A study on the earthquake safety of rock cavern
Rockstore, intern. symp., preprint 2, p 159-164
Stockholm 1977

3-32 BÅTH M
An earthquake catalogue of Fennoscandia for the years 1891-1950
Geological Survey of Sweden, Ser C, 545, 1956

3-33 KULHANEK O, WAHLSTRÖM R
Earthquakes of Sweden 1891-1957, 1963-1972
Dept of Seismology, University of Uppsala
KBS Technical Report 21, September 1977

3-34 BÅTH M
Earthquakes in Sweden in 1951 to 1976; and
Energy and tectonics of Fennoscandian earthquakes
Typescripts from the Dept of Seismology, University of Uppsala, 1978

3-35 KVALE A
Earthquakes; in Geology of Norway, p 490-506,
O Holtedahl ed., 540 p
Geological Survey of Norway, No. 208, Oslo 1960

3-36 HULT A, GIDLUND G, THOREGREN U
Permeabilitetsbestämningar
("Permeability determinations")
Geological Survey of Sweden
KBS Technical Report 61, January 1978

3-37 GIDLUND G
Analyser och åldersbestämningar av grundvatten på stora djup
("Analyses and age determinations of groundwater at great depths")
Geological Survey of Sweden
KBS Technical Report 62, 1978-02-14

3-38 OLKIEWICZ A, HANSSON K, ALMÉN K-E, GIDLUND G
Geologisk och hydrogeologisk grunddokumentation av Stripa försöksstation
("Geological and hydrogeological ground documentation at the Stripa research station")
Geological Survey of Sweden
KBS Technical Report 63, February 1978

3-39 CARLSSON H
Bergspänningsmätningar i Stripa gruva
("Measurements of rock stresses in the Stripa mine")
Luleå Institute of Technology
KBS Technical Report 49, 1977-08-29

3-40 LINDGREN W
Mineral deposits (p 525)
McGraw-Hill, New York, 1933

3-41 LARSSON I, LUNDGREN T, WIKLANDER U
Blekinge kustgnejs. Geologi och hydrogeologi
("The Blekinge coastal gneiss, geolgy and hydrogeology")
Department of Land Improvment and Drainage, Royal Institute of Technology, Swedish Geotechnical Institute and Geological Survey of Sweden
KBS Technical Report 25, August 1977

3-42 ÅKERBLOM G
From the Geological Survey of Sweden´s archives for uranium prospecting, 1977

3-43 LINDBLOM U
Groundwater movements around a repository, Phase 1
Hagconsult AB
KBS Technical Report 06, 1977-02-28

3-44 GRUNDFELT B
Translation and development of the BNWL Geosphere model
Kemakta Konsult AB
KBS Technical Report 10, 1977-02-05

3-45 Investigations of groundwater flow in rock around repositories for nuclear waste

STOKES J
Groundwater flow due to topographical and geological effects

THUNVIK R
Local groundwater depression around a repository

STOKES J, THUNVIK R
Three dimensional model of groundwater flow governed by topography
Department of Land Improvment and Drainage, Royal Institute of Technology
KBS Technical Report 47, 1978-02-28

3-46 Groundwater movements around a repository
Hagconsult AB
Technical Report 54:01-06, September-October 1977

01 STILLE H, BURGESS A, LINDBLOM U
Geological and geotechnical conditions

02 RATIGAN J L
Thermal analyses

03 BURGESS A
Regional groundwater flow analyses

05 RATIGAN J L, BURGESS A, SKIBA E L, CHARLWOOD R
Repository domain groundwater flow analyses

06 LINDBLOM U et al
Final report

3-47 NERETNIEKS I
Retardation of escaping nuclides from a final depository
Department of Chemical Engineering, Royal Institute of Technology
KBS Technical Report 30, 1977-09-14

3-48 GRUNDFELT B
Transport av radioaktiva ämnen med grundvatten från ett bergförvar
("Transport of radioactive elements in groundwater from a rock repository")
Kemakta Konsult AB
KBS Technical Report 43, November 1977

3-49 NILSSON L Y
Korttidsvariationer i grundvattnets trycknivå
("Short-term variaions in the pressure level of the groundwater")
Department of Land Improvment and Drainage, Royal Institute of Technology
KBS Technical Report 91, September 1977

3-50 HÄGGBLOM H
Calculations of nuclide migration in rock and porous media penetrated by water
AB Atomenergi
KBS Technical Report 52, 1977-09-14

3-51 HÄGGBLOM H
A three-dimensional method for calculating the hydraulic gradient in porous and cracked media
AB Atomenergi
KBS Technical Report 69, 1978-01-26

3-52 GRUNDFELT B
Nuklidvandring från ett bergförvar för utbränt bränsle
("Nuclide migration from a rock repository for spent fuel")
Kemakta Konsult AB
KBS Technical Report 77, 1978-08-31

3-53 SNOW D T
Rock racture spacings, openings and porosities
Journ. Soil Mech. Found. Div., AICLE, 94, p 73-91. 1968

3-54 MARINE W I
The permeability of fractured crystalline rock at the Savannah River plant near Aiken, South Carolina
US Geol. Survey Prof. Paper 575-B, p 203-211, 1967

3-55 LARSSON I, FLEXER A, ROSÉN B
Effects of groundwater caused by excavation of rock store caverns
Eng. Geol. 11, p 279-294, 1977

3-56 STILLE H, LUNDSTRÖM L
Large scale permeability test of the granite in the Stripa mine and thermal conductivity test
Hagconsult 1978

3-57 WEBSTER D S, PROCTOR J F, MARINE I W
Two-well tracer test in fractured crystalline rock
US Geol. Survey Water Supply Paper 1544-I, 1970

3-58 HEIMLI P
Bergarters porositet, permeabilitet, fuktutvidgelse og kapilaritet
("The porosity, permeability, moisture swelling and capillarity of different types of rocks")
Geological Institute of Engineering Geology
Norwegian Institute of Technology, Trondheim, 1974

3-59 BRACE W F, ORANGE A S
Electrical resistivity changes in saturated rocks during fracture and frictional sliding
Journ. Geophys. Res. 73, p 1433-1445, 1968

3-60 JESSOP A M, ROBERTSON P B, LEWIS T J
A brief summary of thermal conductivity of crystalline rocks
Canad. Dept. of Energy, Mines and Resources Rep. 76-4
1976

3-61 JESSOP A M
Written message to KBS; Reg. No. 42.08, 77-11-17

3-62 MALMQVIST L, ÖQUIST U
Measurements of the complex impedance of rock samples at the frequency 1 Hz; Manuscript 1978

3-63 KELLER G V, FRISCHKNECHT F C
Electrical methods in geophysical prospecting (p 27)
Pergamon Press, Oxford 1966

3-64 FAURE G
Principles of Isotope Geology
J Wiley & Sons, New York, 1977

3-65 MOOK W G
The dissolution-exchange model for dating groundwater with ^{14}C; in interpretation of environmental isotope and hydrochemical data in groundwater hydrology
- 213-225
Internat. Atom. Energy Agency, Vienna 1976

3-66 ERIKSSON E, HOLTAN H
Hydrokemi, kemiska processer i vattnets kretslopp ("Hydrochemistry, chemical processes in the water cycle"), p 52
Nordic IHD Report No. 7, Oslo 1974

3-67 STUIVER M, POLACH H A
Reporting of ^{14}C data; Radiocarbon, 19, p 355-363
1977

3-68 VOGEL J C
Carbon-14 dating of groundwater; in Isotope Hydrology 1970; p 225-239
Internat. Atom. Energy Agency, Vienna 1970

3-69 WENNER C G, MÖLLER Å, KJELLIN B
Vattnets beskaffenhet i svenska brunnar ("The nature of the water in Swedish wells")
Water, 30, p 370-389

3-70 LAAKSO M
Kalliokaivojen veeden laatu ja antoisuus;
Maataloushallituksen insinööriosasto;
Maaja Vesitekn. Tutkimustoimustu, Tied 2, 86 p,
Helsinki 1966

3-71 LAHERMO P
On the hydrogeology of the coastal region of south-eastern Finland
Geol. Survey of Finland, Bull. 252, 44 p, 1971

3-72 FETH J H, ROBERTSON C E, POLZER W L
Sources of mineral constituents in water from granitic rocks, Sierra Nevada, California and Nevada
US Geol. Survey Water Supply Paper 1535-I, 1964

3-73 PACES T
Steady state kinetics and equilibrium between groundwater and granitic rock
Geochim. et Cosmochim. Acta. 37, p 2641-2663, 1973

3-74 RENNERFELT J
Sammansättning av grundvatten på större djup i granitisk berggrund
("Composition of groundwater deep down in granitic bedrock")
Orrje & Co
KBS Technical Report 36, 1977-11-07

3-75 JACKS G
Groundwater chemistry at depth in granites and gneisses
Department of Land Improvement and Drainage, Royal Institute of Technology
KBS Technical Report 88, April 1978

3-76 RENNERFELT J, JACKS G
Probable composition of groundwater in the crystalline bedrock at great depth
Technical Report 90, subappendix A:1, 1978

3-77 KBS
Handling of spent nuclear fuel and final storage of vitrified high-level reprocessing waste
I General, p 62-63, Solna 1977

3-78 GERMANOV A I, PANTELEYEV V M
Behaviour of organic matter in groundwater during infiltrational epigenesis
Internat. Geology Rev., 10, - 826-832

3-79 LISITSYN A K, KUZNETSOVA E C
Role of microorganisms in development of geochemical reduction barriers where limonitization bedded zones wedge-out
Internat. Geology Rev., 9, p 1180-1191

3-80 BROTZEN O
On the occurrence of uranium in ancient conglomerates
Econ. Geol. 53, p 489-491, 1958

3-81 HOSTETLER P B, GARRELS R M
Transportation and precipitaiton of uranium and vanadium at low temperatures
Econ. Geol. 57, p 137-157, 1962

3-82 BATULIN S G, GOLEVIN E A, ZELENOVA O I et al
Exogeneous epigenetic uranium deposits
Atomizdat, 1965

3-83 DAHL A R, HAMATER J L
Genesis and characteristics of the Southern Powder Basin uranium deposits, Wyoming, USA, in Formation of uranium-ore deposits, p 201-215
Proc. Symp. Internat. Atom. Energy, Vienna 1974

3-84 ALLARD B, KIPATSI H, RYDBERG J
Sorption av långlivade radionuklider i lera och berg ("Sorption of long-lived radionuclides in clay and rock")
Part I
Department of Nuclear Chemistry, Chalmers University of Technology
KBS Technical Report 55, 1977-10-10

3-85 ALLARD B, KIPATSI H, TORSTENFELT B
Sorption av långlivade radionuklider i lera och berg ("Sorption of long-lived radionuclides in clay and rock")
Part II
Department of Nuclear Chemistry, Chalmers University of Technology
KBS Technical Report 98, 1978-04-20

3-86 COWAN G A
Migration paths for Oklo reactor products and applications to the problem of geological storage of nuclear wastes
Proc. Techn. Comm. on Nat. Fiss. React.,
Internat. Atom. Energy Agency, Paris 1977

3-87 BROOKINS D G
The Oklo phenomenon
Proc. Techn. Comm. on Nat. Fiss. React.,
Internat. Atom. Energy Agency, Paris 1977

3-88 TOVERUD Ö
Chemical and mineralogical aspects of some geochemical anomalies in glacial drift and peat in northern Sweden
Geological Survey of Sweden, Ser C, 729, 1977

3-89 BERGSTRÖM J
Seasonal variations and distribution of dissolved iron in an aquifer
Nordic Hydrology, 5, p 1-31, 1974

3-90 ERIKSSON E, KHUNAKASEM V
The chemistry of groundwater in Groundwater problems, Eriksson, Gustafsson, Nilsson Ed, Pergamon Press, London 1968

3-91 GRENTHE I
Determination of redox potential in groundwater from Stripa and Finnsjö Lake
Department of Inorganic Chemistry, Royal Institute of Technology
KBS Technical Report 90, appendix B5, 1978

3-92 TARDY Y, GARRELS R M
A method of estimating the Gibbs energi of formation of layer silicates
Geochim. Cosmochim. Acta, 38, p 1101-1116, 1974

3-93 BRUSEWITZ A M, SNÄLL S, AHLBERG P, LUNDGREN T
Lerzoner i berganläggningar
("Clay zones in rock facilities")
Internal reports No. 5, Swedish Geotechnical Institute, Stockholm 1974

3-94 ARMANDS G
Geochemical prospecting of a uraniferous bag deposit at Masungsbyn, northern Sweden; in Geochemical prospecting in Fennoscandia, p 127-154, A Kvalheim ed. 350 p,
Interscience, New York, 1967

3-95 ADAMEK P M, WILSON M R
Recognision of a new uranium province from the Precambrian of Sweden;
IAEA-TC-25/16, in Recognition and evaluation of uraniferous areas, p 199-215,
Internat. Atom. Energy Ag., Vienna 1977

3-96 WELIN E
Uranium mineralizations and age relationships in the precambrian bedrock of central and southeastern Sweden
Proceedings of the Geological Society, Stockholm, 88, p 34-67, 1966

3-97 PAČES T
Chemical equilibria and zoning of subsurface water from Jáchymov ore deposit, Czechoslovakia
Geochim. Cosmochim. Acta, 33, p 591-609, 1969

3-98 MILLER L J
The chemical environment of pitchblende
Econ. Geol., 53, p 521-545, 1958

3-99 RAFAELSKY R P
The experimental investigation of the conditions of uranium transport and deposition by hydrothermal solutions
Proc. 2nd United Nations internat. conf. peaceful uses atom. energy, 2, p 432-444, Geneva 1958

3-100 RAFAELSKY R P, KUDINOVA K F
Experimentelle Untersuchung der Reduktion und Fällung von Uran durch Mineralien
("Experimental investigation of the reduction and precipitation of uranium through mineralization")
Kernenergie, 3, p 535-538, 1960

CHAPTER 4

4-1 PUSCH R, JACOBSSON A
Egenskaper hos bentonitbaserat buffertmaterial
("Properties of bentonite-based buffer material")
Luleå Institute of Technology
KBS Technical Report 32, 1978-06-10

4-2 PUSCH R
Highly compacted Na bentonite as buffer substance
Luleå Institute of Technology
KBS Technical Report 74, 1978-02-25

4-3 NERETNIEKS I
Transport of oxidants and radionuclides through a clay barrier
Royal Institute of Technology
KBS Technical Report 79, 1978-02-20

4-4 PUSCH R
Self-injection of highly compacted bentonite into rock joints
Luleå Institute of Technology
KBS Technical Report 73, 1978-02-25

4-5 KNUTSSON S
Värmeledningsförsök på buffertsubstans av kompakterad bentonit
("Thermal conductivity tests on buffer material of compacted bentonite")
Luleå Institute of Technology
KBS Technical Report 72, 1977-11-16

4-6 TARANDI T
Temperaturberäkningar för slutförvar för använt bränsle
("Temperature calculations for final repository for spent nuclear fuel")
VBB
KBS Technical Report 46, June 1978

4-7 Le BELL J C
Colloid Chemical Aspects of the "Confined bentonite concept"
Institute of Surface Chemistry
KBS Technical Report 97, 1978-03-07

4-8 STEPHANSSON O, MÄKI K, GROTH T, JONASSON P
Finit elementanalys av bentonitfyllt bergförvar
("Finite element analysis of bentonite-filled rock repository")
Luleå Institute of Technology
KBS Technical Report 104, July 1978

CHAPTER 5

5-1 TARANDI T
Temperaturberäkningar för slutförvar för använt bränsle
("Temperature calculations for final repository for spent fuel")
VBB
KBS Technical Report 46, June 1978

5-2 GRENTHE I
Thermodynamic aspects of copper encapsulation and the corrosive environment in a waste repository
Appendix B to KBS Technical Report 90, 1978-03-31

5-3 NERETNIEKS I
Transport of oxidants and radionuclides through a clay barrier
Royal Institute of Technology
KBS Technical Report 79, 1978-02-20

5-4 EKBOM L
Calculation of the quantity of oxidants present in a waste repository with copper canisters
Appendix D to KBS Technical Report 90, 1978-03-31

5-5 LUNDGREN K
Strålningsnivå och till vatten deponerad strålningsenergi utanför kapslar i slutförvaret
("Radiation level and radiant energy imparted to water outside of canisters in the final repository")
ASEA-ATOM
KBS Technical Report 106, 1978-05-29

5-6 RENNERFELT J
Sammansättning av grundvatten på större djup i granitisk berggrund
("Composition of groundwater deep down in granitic bedrock")
Orrje & Company
KBS Technical Report 36, 1977-11-07

5-7 HANNERZ K, HYDEN L
Removal of free oxygen in the bentonite-sand mixture by a deoxidant
ASEA-ATOM, Technical Memorandum 78-25, 1978-04-05

5-8 RENNERFELT J, JACKS G
Probable composition of groundwater in crystalline bedrock at great depth
Subappendix A1 to KBS Technical Report 90, 1978-03-31

5-9 EKBOM L
Statistical evaluation of copper corrosion in soil from tests conducted by Denison and Romanoff
Appendix E to KBS Technical Report 90, 1978-03-31

5-10 KJELLBERT N
Nuklidhalter i använt LWR-bränsle och i högaktivt avfall från återcykling av plutonium i PWR
("Nuclide levels in spent LWR fuel and in high-level waste from the recycling of plutonium in PWR")
KBS Technical Report 111, 1978-07-26

5-11 VESTERLUND G
Spänningar och deformationer i bränslekapsling under slutlagring
("Stresses and deformations in fuel canister during final storage")
ASEA-ATOM, Bulletin RB 78-99

5-12 The Swedish Corrosion Institute and its reference group
Copper as an encapsulation material for unreprocessed nuclear waste - evaluation from the viewpoint of corrosion
KBS Technical Report 90, 1978-03-31

5-13 WRANGLÉN G
Special statement
Appended to KBS Technical Report 90, 1978-03-31

5-14 NILSSON F
Some aspects on the mechanical safety of a canister for nuclear fuel waste.
Royal Institute of Technology
KBS Technical Report 66, February 1978

CHAPTER 6

6-1 PEARSON R L, WADSWORTH M E
A kinetic study of the dissolution of UO_2 in carbonate solution
Trans of The Metallurgical Society of AIME, June 1958, p 294-300

6-2 SCHORTMANN W W, DESESA M A
Kinetics of the Dissolution of Uranium Dioxide in Carbonate-Bicarbonate Solutions.
Proceedings of the United Nations International Conference of the Peaceful use of Atomic Energy.
Genève 1958, Vol 3, p 333-341.

6-3 GRANDSTAFF D E
A kinetic study of the dissolution of uraninite
Econ Geology 71 (1976), p 1493-1505.

6-4 KATAYAMA Y B
Leaching of irradiated LWR fuel pellets in deionized and typical ground water
BNWL-2057, July 1976

6-5 KATAYAMA Y B, MENDEL J E
Leaching of irradiated LWR fuel pellets in deionized water, sea brine, and typical ground water
PNL-SA-6416
American Nuclear Society Winter Meeting
Nov 22 - Dec 2, 1977, San Francisco
TANSAO 27 (1977) p 447

6-6 FORSYTH R S, EKLUND U-B
Lakning av bestrålat UO_2-bränsle
("Leaching of irradiated UO_2 fuel")
AB Atomenergi
KBS Technical Report 70, 1978-02-24

6-7 NILSSON G
Accelererad utlösning av uran från alfaaktiv UO_2
("Accelerated dissolution of uranium from alpha-active UO_2")
Studsvik, Work Report FL-1, 1978-04-27

6-8 CHRISTENSEN H
Radiolys av vatten med alfa-strålning vid förvaring av direktdeponerat bränsle
("Radiolysis of water by alpha radiation in repository for direct disposal of unreprocessed nuclear fuel")
Studsvik Work Report, MC-78/259, 1978-04-14

6-9 CHRISTENSEN H
Radiolys av vatten vid förvaring av direktdeponerat bränsle
("Radiolysis of water in repository for direct disposal of unreprocessed nuclear fuel
Oxidation by hydrogen peroxide")
Studsvik Work Report MC-78/264, 1978-05-02

6-10 RENNERFELT J
Sammansättning av grundvatten på större djup i granitisk berggrund
("Composition of groundwater deep down in granitic bedrock")
Orrje & Company
KBS Technical Report 36, 1977-11-07

6-11 KJELLBERT N
Kompletterande källstyrkestudier för KBS
("Supplementary emission rate studies for KBS")
Studsvik Work Report SM-78/25

6-12 ALLARD B, KIPATSI H, RYDBERG J
Sorption av långlivade radionuklider i lera och berg, del 1
("Sorption of long-lived radionuclides in clay and rock, Part 1")
Chalmers Institute of Technology
KBS Technical Report 55, 1977-10-10

6-13 ALLARD B, KIPATSI H, TORSTENFELT B
Sorption av långlivade radionuklider i lera och berg, del 2
("Absorption of long-lived radionuclides in clay and rock, Part 2")
Chalmers Institute of Technology
KBS Technical Report 98, 1978-04-20

6-14 BAZIN J, JOUAN J, VIGNESOULT N
Compartment et état physico-chimique des produits de fission, dans les éléments combustibles pour reacteur à eau pressurisée.
No 196 Oct 1974, p 56
Bulletin d´Information Scientifiques et Techniques

6-15 FRIED S et al
Migration of plutonium and americium in the lithosphere
Argonne National Lab., Ill. USA (1976)
Symposium on Environmental Behavior of Actinides, CONF-7604126-1, New York April 1-5, 1976

6-16 BIRD R B, STEWARD W F, LIGHTFOOT E N
Transport Phenomena, John Wiley" N Y 1960

6-17 Handling of spent nuclear fuel and final storage of vitrified high-level reprocessing waste, Volume IV, Stockholm 1977

6-18 PUSCH R
Highly compacted Na Bentonite as buffer substance
Luleå Institute of Technology
KBS Technical Report 74, 1978-02-25

6-19 HÄGGBLOM H
Calculation of nuclide migration in rock and porous media, penetrated by water
AB Atomenergi
KBS Technical Report 52, 1977-09-14

6-20 REID R C, PRAUSNITZ J M, SHERWOOD T K
The properties of gases and liquids, 3rd ed, McGraw-Hill, N Y 1977

6-21 NERETNIEKS I, SKAGIUS C
Diffusivitetsmätningar av metan och väte i våt lera
("Diffusivity measurements of methane and hydrogen in wet clay")
Royal Institute of Technology
KBS Technical Report 86, 1978-01-09

6-22 NERETNIEKS I, SKAGIUS C
Diffusivitetsmätningar i våt lera av Na-lignosulfonat, Sr^{2+}, Cs^{+}
("Diffusivity measurements in wet clay, Na-lignosulphonate, Sr^{2+}, Cs^{+}")
Royal Institute of Technology
KBS Technical Report 87, 1978-03-16

6-23 NERETNIEKS I
Retardation of escaping nuclides from a final depository
Royal Institute of Technology
KBS Technical Report 30, 1977-09-14

6-24 NERETNIEKS I
Transport of oxidants and radionuclides through a clay barrier
Department of Chemical Engineering
Royal Institute of Technology
KBS Technical Report 79, 1978-02-20

6-25 PAČES T
Chemical equilibria and zoning of subsurface water from Jachymov ore deposit. Czechoslovakia, Geochimica et Cosmochimica, Acta 33, 1969, p 591

6-26 COWAN G A
Migration paths for Oklo reactor products and applications to the problem of geological storage of nuclear wastes
IAEA Symp Dec 19-21, 1977, Paris

6-27 JACOBSSON A, PUSCH R
Deponering av högaktivt avfall i borrhål med buffertsubstans
("Deposition of high-level waste in boreholes containing buffer material")
Luleå Institute of Technology
KBS Technical Report 03, 1977-04-15

6-28 NERETNIEKS I, ANDERSSON K, HENSTAM L
Utläckning av Ni-59 från ett bergförvar
("Leakage of Ni-59 from a rock repository")
Royal Institute of Technology
KBS Technical Report 101, 1978-04-24

6-29 GRENTHE I et al
Jämvikter i systemet Ni-H_2O-Cl^- - CO_3^{2-} - SO_4^{2-} - F^- vid olika redoxpotential och temperatur
("Equilbria in the system Ni-H_2O - Cl^- - CO_3^{2-} - SO_4^{2-} - F^- at different redox potentials and temperatures")
Report to KBS 1977, 12, from Department of Inorganic Chemistry, Royal Institute of Technology

CHAPTER 7

7-1 HULT A, GIDLUND G, THOREGREN U
Permeabilitetsbestämningar
("Permeability determinations")
Geological Survey of Sweden
KBS Technical Report 61, January 1978

7-2 LINDBLOM et al
Groundwater movements around a repository. Final report
Hagconsult AB
KBS Technical Report 54:06, October 1977

7-3 STOKES J, THUNVIK R
Investigations of groundwater flow in rock around repositories for nuclear waste
Royal Institute of Technology
KBS Technical Report 47, April 1978

7-4 NERETNIEKS I
Retardation of escaping nuclides from a final depository
Royal Institute of Technology
KBS Technical Report 30, 1977-09-14

7-5 SNOW D T
Rock fracture spacings, openings and porosities.
Soil J. Mechanics and foundations division.
AIChE 94 no SM 1 Jan 1968 p 73-91

7-6 BIRD R B, STEWART W E, LIGHTFOOT E N
Transport Phenomena Wiley 1960

7-7 LANDSTRÖM O, KLOCKARS C E, HOLMBERG K E, WESTERBERG S
Fältförsök rörande spårämnens transport med grundvatten i sprickförande berggrund
("Field study concerning transport of tracers with the groundwater in fissured bedrock")
Geological Survey of Sweden, bedrock bureau, 1977

7-8 NERETNIEKS I
Transport of oxidants and radionuclides through a clay barrier
Royal Institute of Technology
KBS Technical Report 79, 1978-02-20

7-9 RENNERFELT J
Sammansättning av grundvatten på större djup i granitisk berggrund
("Composition of groundwater deep down in granitic bedrock")
Orrje & Company
KBS Technical Report 36, 1977-11-07

7-10 Le BELL J
Colloid chemical aspects of the "Confined bentonite concept"
Institute of Surface Chemistry
KBS Technical Report 97, 1978-03-07

7-11 NERETNIEKS I
Some aspects on colloids as means for transporting radionuclides
Royal Institute of Technology
KBS Technical Report 103, 1978-08-08

7-12 PUSCH R
Highly compacted Na bentonite as buffer substance
Luleå Institute of Technology
KBS Technical Report 78, 1978-02-25

7-13 HÄGGBLOM H
Calculations of nuclide migration in rock and porous media penetrated by water
AB Atomenergi
KBS Technical Report 52, 1977-09-14

7-14 DAVYDOV Y P
Nature of colloid of radioactive elements
Radiochimiya 9 (1) 1967 p 89

7-15 KEPAK F
Adsorption and colloidal properties of radioactive elements in trace concentrations
Chem. Rev. 71 nr 4 1971 p 357

7-16 KEPAK F
Colloidal forms of radionuclides and their separation from water solution
J Radioanalytical Chem. 21 1974 p 489-495

7-17 MARSILY G, LEDOUX E, BARBREAU A, MARGAT J
Nuclear Waste Disposal: Can the Geologist Guarantee Isolation? Science 197 no 4304 1977 p 519

7-18 DEVELL L, HESBÖL R
Lakningsbar spaltaktivitet
("Leachable gap activity")
AB Atomenergi
KBS Technical Report 109, Ocotber 1978

7-19 HÄGGBLOM H
Diffusion of soluble materials in a fluid filling a porous medium
AB Atomenergi
KBS Technical Report 09, 1977-03-24

7-20 ALLARD B, KIPATSI H, RYDBERG J
Sorption av långlivade radionuklider i lera och berg, del 1
("Sorption of long-lived radionuclides in clay and rock, Part I")
Chalmers Institute of Technology
KBS Technical Report 55, 1977-10-10

7-21 ALLARD B, KIPATSI H, TORSTENFELT B
Sorption av långlivade radionuklider i lera och berg, del 2
("Absorption of long-lived radionuclides in clay and rock, Part II")
Chalmers Institute of Technology
KBS Technical Report 98, 1978-04-20

7-22 GRUNDFELT B
Transport av radioaktiva ämnen med grundvatten från ett bergförvar
("Transport of radioactive elements in groundwater from a rock repository")
Kemakta Konsult AB
KBS Technical Report 43, 1977-12-13

7-23 GRUNDFELT B
Nuklidvandring från ett bergförvar för utbränt bränsle ("Nuclide migration from a rock repository for spent nuclear fuel")
Kemakta Konsult AB
KBS Technical Report 77, 1978-08-31

7-24 KBS
Handling of spent nuclear fuel and final storage of vitrified high-level reprocessing waste
Volume IV Safety Analysis
KBS, Stockholm, November 1977

7-25 BERGMAN R, BERGSTRÖM U, EVANS S
BIOPATH - Datorprogram för kompartmentanalys av stråldoser och ekologiska omsättningar ("BIOPATH - computer programme for compartment analysis of radiation doses and ecological turnovers")
Unpublished material
AB Atomenergi

7-26 BERGMAN R, BERGSTRÖM U, EVANS S
Dos och dosinteckning från grundvattenburna radioaktiva ämnen vid direktförvaring av använt kärnbränsle ("Dose and dose committment from groundwater-borne radioactive elements in the final storage of spent nuclear fuel")
AB Atomenergi
KBS Technical Report 100, 1978-10-06

7-27 ICRP publication 2, Permissible Dose for Internal Radiation, 1959

7-28 ICRP publication 6, Permissible Dose for Internal Radiation, 1964

7-29 ICRP publication 10, Evaluation of Radiation Doses to Body Tissues from Internal Contamination due to Occupational Exposure, 1968

7-30 ICRP publication 20, Alkaline Earth Metabolism in Adult Man, 1972

7-31 ICRP publication 26, Recommendations of the International Commission on Radiological Protection, 1977

7-32 UNSCEAR, 1977
Sources and Effects of Ionizing Radiation, Report to the general assembly 1977

7-33 BERGMAN R, McEWAN C
Dose and dose committment due to Carbon-14 from the nuclear industry
AB Atomenergi 1977 (S-548)

7-34 BERGMAN R, BERGSTRÖM U, EVANS S
Kompartmentmodell för omsättning av vattenburna utsläpp i brackvattensystem
("Compartment model for turnover of water-borne releases in brackish water systems")
AB Atomenergi 1977 (S-549)

7-35 BURKHOLDER H
"Nuclear Waste Partitioning Incentives" in Proc. NRC Wkshp. Mgt. Rad. Waste: Waste Partitioning as an alternative, NF-CONF-001 (1976)

7-36 Limitation of releases of radioactive substances from nuclear power stations
Swedish Nuclear Power Inspectorate, FS 1977-2

7-37 BERGMAN R, BERGSTRÖM U, EVANS S
Ekologisk transport och stråldoser från grundvattenburna radioaktiva ämnen
("Ecological transport and radiation doses from groundwater-borne radioactive substances")
AB Atomenergi
KBS Technical Report 40, 1977-12-20

7-38 Handling of spent nuclear fuel and final storage of vitrified high-level reprocessing waste
Volume II, Geology
KBS, Stockholm, November 1977

7-39 JACKS G
Groundwater chemistry at depth in granites and gneisses
Royal Institute of Technology
KBS Technical Report 88, April 1978

CHAPTER 8

8-1 GYLLANDER C, JOHNSON S, ROLANDSON S
Säkerhet och strålskydd inom kärnkraftområdet. Lagar, normer och bedömningsgrunder
("Safety and radiation protection in the fields of nuclear power. Laws, standards and grounds for evaluation")
AB Atomenergi and ASEA-ATOM
KBS Technical Report 41, 1977-10-13

8-2 Handling of spent nuclear fuel and final storage of vitrified high-level reprocessing waste
Part IV Safety Analysis
KBS, Stockholm, November 1977

8-3 KJELLBERT N A
Källstyrkor i utbränt bränsle och högaktivt avfall från en PWR beräknade med ORIGEN
("Emission rates in spent fuel and high level waste from a PWR, calculated using ORIGEN")
AB Atomenergi
KBS Technical Report 01, 1977-04-05

8-4 KJELLBERT N A
Nuklidhalter i använt LWR-bränsle och i högaktivt avfall från återcykling av plutonium i PWR
("Nuclide levels in spent LWR fuel and in high-level waste from the recycling of plutonium in PWR")
AB Atomenergi
KBS Technical Report 111, 1978-07-26

8-5 EKBERG K, KJELLBERT N A, OLSSON G
Resteffektstudier för KBS
("Decay power studies for KBS")
Del 1 Litteraturgenomgång
("Part I Review of the literature")
Del 2 Beräkningar
("Part II Calculations")
AB Atomenergi
KBS Technical Report 07, 1977-04-19

8-6 KJELLBERT N A
Neutroninducerad aktivitet i bränsleelementdetaljer
("Neutron-induced radioaktivity in fuel assembly components")
AB Atomenergi
KBS Technical Report 105, 1978-03-30

8-7 VESTERLUND A, OLSSON T
Degraderingsmekanismer vid bassänglagring och hantering av utbränt kraftreaktorbränsle
("Degradation mechanisms in connection with pool storage and handling of spent nuclear reactor fuel")
ASEA-ATOM
KBS Technical Report 68, 1978-01-18

8-8 CARLESON G
Säkerhetsanalys av inkapslingsprocesser
("Safety analysis of encapsulation processes")
AB Atomenergi
KBS Technical Report 65, 1978-01-27

8-9 NORDESJÖ E
Säkerhetsanalys av hanteringsförfarandet vid inkapsling av utbränt bränsle i kopparkapsel
("Safety analysis of the handling procedure in the encapsulation of spent nuclear fuel in copper canisters")
ASEA-ATOM
KBS Technical Report 112, 1978-03-20

8-10 LUNDGREN K
Strålningsnivå och till vatten deponerad strålningsenergi utanför kapslar i slutförvaret
("Radiation level and radiant energy imparted to water outside of canisters in the final repository")
ASEA-ATOM
KBS Technical Report 106, 1978-05-29

8-11 LUNDGREN K
SLUK - Slutlig förvaring av utbränt kärnbränsle
Strålskärmsberäkningar ASEA-ATOM
("SLUK - final storage of spent fuel. Radiation shielding calculations")
ASEA-ATOM RF 77-370

8-12 Energi Hälsa Miljö
Bilaga 2: Hälso- och miljöverkningar vid användning av kärnkraft
("Medical and environmental effects of nuclear power")
National Institute of Radiation Protection, report to Energy and Environment Committee regarding the medical and environmental risks associated with nuclear power, 1977

8-13 Report of the United Nations Scientific Committee on the effects of atomic radiation.
Supplement No 16 (A/5216) 1968

8-14 Natural radioactivity of groundwater in the Helsinki area.
Institute of Radiation Physics, Helsinki
Report SFL-A19, November 1973

8-15 GRUNDFELT B
Transport av radioaktiva ämnen med grundvattnet från ett bergförvar
("Transport of radioactive elements in groundwater from a rock repository")
Kemakta Konsult AB
KBS Technical Report 43, 1977-12-13

8-16 LESTER D H, JANSEN G, BURKHOLDER H C
Migration of Radionuclide Chains through an Adsorbing Medium
AICHE symposium series 71, 202 (1975)

8-17 BURKHOLDER H C et al
Incentives for partitioning High-Level Waste
BNWL-1927 (1975)

8-18 DEVELL L, HESBÖL R
Lakningsbar spaltaktivitet
("Leachable gap activity")
AB Atomenergi
KBS Technical Report 109, October 1978

8-19 GRUNDFELT B
Nuklidvandring från ett bergförvar för utbränt bränsle
("Nuclide migration from a rock repository for spent fuel")
Kemakta Konsult AB
KBS Technical Report 77, 1978-08-31

8-20 JACKS G
Groundwater chemistry at depth in granites and gneisses
Royal Institute of Technology
KBS Technical Report 88, April 1978

8-21 ALLARD B, KIPATSI H, TORSTENFELT B
Sorption av långlivade radionuklider i lera och berg
Del 2
("Sorption of long-lived radionuclides in clay and rock")
Part II
Chalmers Institute of Technology
KBS Technical Report 98, 1978-04-20

8-22 NERETNIEKS I
Retardation of Escaping Nuclides from a Final Depository
Royal Institute of Technology
KBS Technical Report 30, 1977-09-14

8-23 LANDSTRÖM O, KLOCKARS C E, HOLMBERG K E, VESTERBERG S
Fältförsök rörande spårämnens transport med grundvatten i sprickförande berggrund
("Field study concerning transport of tracers with groundwater in fissured bedrock")
Geological Survey of Sweden, bedrock bureau, 1977

8-24 BERGMAN R, BERGSTRÖM U, EVANS S
Dos och dosinteckning från grundvattenburna radioaktiva ämnen vid slutförvaring av använt kärnbränsle
("Dose and dose committment from groundwater-borne radioactive elements in the final storage of spent nuclear fuel")
AB Atomenergi
KBS Technical Report 100, 1978-10-06

8-25 PUSCH R
Highly compacted Na bentonite as buffer substance
Luleå Institute of Technology
KBS Technical Report 74, 1978-02-25

8-26 BEHRENZ P and HANNERZ K
Criticality in a spent fuel repository in wet crystalline rock
ASEA-ATOM
KBS Technical Report 108, 1978-05-30

8-27 HARTMAN W K
Terrestial and Lunar Flux of Large Meteorites in the Last Two Billion Years
Icarus 4, 157-65, 1965

8-28 Fortifikationshandbok, del 1, Vapenverkan
("Fortification handbook, part I, Effects of Weapons")
Swedish Defence Staff and Fortification Inspectorate
Stockholm 1973

8-29 GRIEVE R A F, DENCE M R
The Terrestrial Cratering Record: II The Crater Production Rate (Submitted to Icarus 1978)

APPENDIX 1 ALUMINIUM OXIDE CANISTER FOR FINAL STORAGE OF SPENT NUCLEAR FUEL, Status report, May 1978

SUMMARY

Ceramic materials can also be used for the encapsulation of spent fuel for final storage. According to a method proposed by ASEA, the fuel rods are enclosed in canisters of aluminium oxide. This material occurs as a mineral in nature in the form of corundum and sapphire.

Aluminium oxide canisters for the enclosure of spent nuclear fuel are prefabricated by hot isostatic pressing (HIP). The canister consists of a container and a lid. After the fuel rods are placed in the container, the container and its lid are sealed together by means of hot isostatic pressing to produce a completely tight, seamless aluminium oxide canister. The canister can then be deposited deep down in the bedrock, surrounded by a quartz-bentonite mixture, in a manner similar to that described for the copper canister.

Fabrication of full-size aluminium oxide canisters has been demonstrated in the spring of 1978 at ASEA's high-pressure laboratory in Robertsfors, see figure B1-1.

Experiments and calculations performed to date show that a canister of aluminium oxide with a wall one decimetre thick can resist the action of the groundwater for a period of time corresponding to the most long-lived waste elements. Canister durability is affected only very slightly by the surrounding environment. Calculations of canister life are verified by knowledge of how naturally occurring aluminium oxide resists severe conditions. Erosion deposits of corundum and sapphire on river bottoms and in shore gravel show that this mineral possesses very high resistance to chemical and mechanical action over geologically long periods of time.

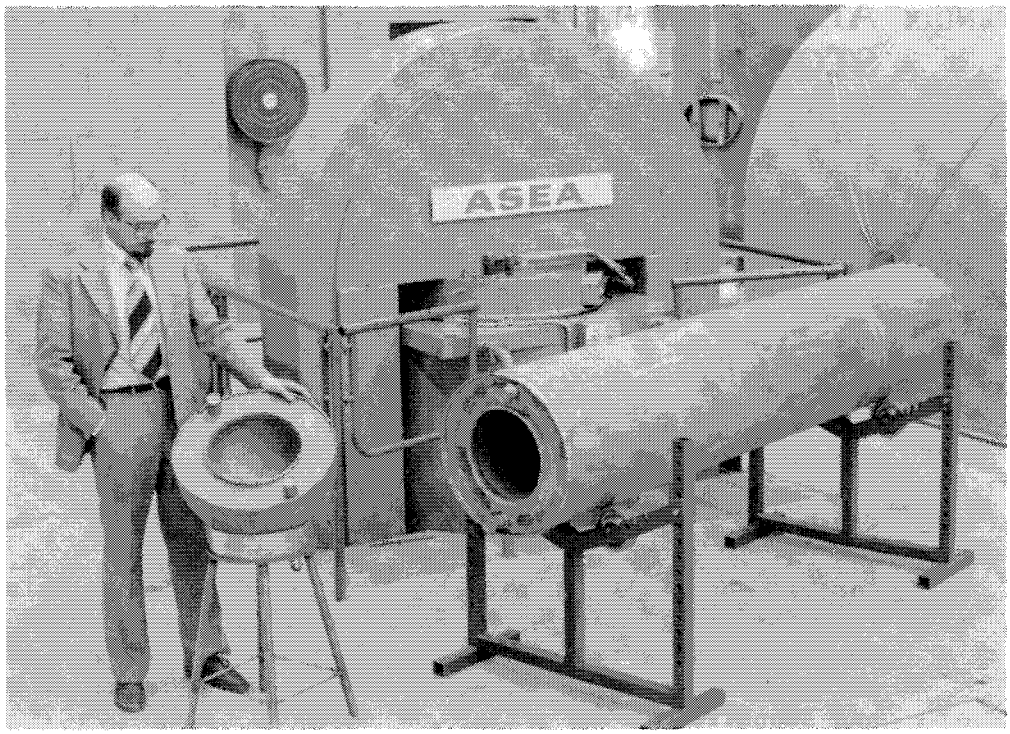

Figure B1-1. Full-size canister of aluminium oxide for direct disposal of spent nuclear fuel. In the background, the QUINTUS press for hot-isostatic pressing.

CONTENTS

B1.1 INTRODUCTION

In direct disposal the spent fuel is deposited in the final repository without prior reprocessing. The proposed handling sequence (see I:4) includes enclosure of the spent fuel in corrosion-resistant canisters. These canisters are intended to be deposited in a final repository at a suitable site deep down in the bedrock. The canister will thereby comprise one of a number of barriers against dispersal of the radioactive material. It is therefore essential to demonstrate that the canister material possesses high resistance to all types of attack in the storage environment in question.

Materials which have proved themselves to be extremely durable exist in nature. The method for the enclosure of spent nuclear fuel which has been proposed and developed by ASEA is based on the use of such a naturally occuring material, namely aluminium oxide. This material occurs as a mineral in the form of corundum and sapphire. Canisters for enclosing the fuel are fabricated by means of hot isostatic pressing, a high-pressure technique with which ASEA has many years of experience. In this technique, a combination of high pressure and high temperature is used to produce bodies of metallic or ceramic materials. The method is currently being used commercially for the manufacture of tool steel and cemented carbide products.

ASEA has been conducting development work with aluminium oxide over the past years at its high-pressure laboratory in Robertsfors, Sweden, where a new laboratory facility has been built. During the spring of 1978 this laboratory has produced full-scale aluminium oxide canisters, suitable for the encapsulation of spent nuclear fuel for final storage.

The development status of the method as of May 1978 is described in the following. Section 2 describes the fundamental characteristics of the method. The properties of the aluminium oxide are described in section 3, and the fabrication of the aluminium oxide canister in section 4. Section 5 gives an account of the active steps of the encapsulation method: preparation of the fuel rods and filling and sealing of the canisters. Deposition in the final repository is described briefly in section 6. Section 7 deals with the quality and properties of the canister in the final repository environment. In conclusion, section 8 defines the outlines and important aspects of the continued development work.

B1.2 FUNDAMENTAL METHODOLOGY

B1.2.1 Canister material

In the final storage of unreprocessed spent nuclear fuel, very high demands are imposed on the long-term durability of the canisters in which the fuel is enclosed. Good mechanical properties are required, but the chemical stability of the canister under the conditions which prevail in the final repository is particularly essential. The necessity of predicting these conditions for a very long period of time to come can be greatly reduced if the canister material can be shown to possess suffi-

cient stability in many of the conceivable natural environments (dry, wet, oxidizing, reducing, salty, acidic, basic or containing organic material).

It is also an advantage if canister durability can be based on the primary material's own resistance. Naturally, the long-term stability of the canister is calculated using the best available scientific methodology. Knowledge of how the chosen material has resisted severe conditions for a corresponding period of time in the past can provide convincing verification of such a calculation. Only naturally occuring materials, i.e. minerals, fulfill this last requirement.

The material should in itself be thermodynamically stable in the temperature and pressure range which will be encountered in the final repository. This means that spontaneous transformation to another structure without the action of other substances cannot occur. For technical reasons of fabrication, the same structure should be stable at the temperatures and pressures which are used during fabrication.

An extensive evaluation of minerals has been carried out. This has shown that aluminium oxide of the so-called alpha type - corundum or sapphire in mineral form - fulfills the above requirements.

Next to diamond, corundum and sapphire are among the hardest minerals known. Deposits of these in the form of weathered materials on river bottoms and in shore gravel exhibit very high mechanical and chemical durability, even over geologically long periods of time.

In nature, corundum and sapphire have often been formed from aluminium hydroxides, which, owing to their low degree of solubility compared to other minerals, are concentrated in erosion remains. When such materials have been brought down to great depths in the earth's crust, aluminium oxide in the form of corundum or sapphire has been formed by metamorphism under high temperature and pressure, with the release of water from the aluminium hydroxide (B1-1). In the pure state, such minerals are colourless or white, but if the erosion remains contain small amounts of other substances, the product is coloured, for example red ruby (chromium), blue sapphire (titanium) and black emery (iron).

This natural process is simulated in the fabrication of the aluminium oxide canister. Water is removed in connection with the production of the aluminium oxide powder and during its preparation prior to compaction to a completely dense material. This compaction is carried out under high pressure and temperature by means of hot isostatic pressing.

B1.2.2 Canister fabrication

The method used for fabricating the canister, hot isostatic pressing (HIP), is one of several high-pressure methods which are possible with the use of ASEA's QUINTUS presses.

Hot isostatic pressing is a process in which a completely enclosed powder can be moulded into fully dense bodies of the de-

sired shape and size. A flexible container, normally made of mild steel or glass, is filled with a granular material of the desired composition (e.g. metallic or ceramic material). The container is evacuated and sealed. The container is then subjected to high pressure and temperature for several hours. The pressure is applied to the container via a gas as the pressure medium so that the pressure acts perpendicular to the surface of the container at all points.

Since the pressure is applied from all directions, the resultant product is homogeneous and of exactly the same shape as the original container. As the pressure level is relatively high - 100 - 300 MPa - most materials can be compacted into virtually completely pore-free bodies at only 50 - 70% of their melting temperature.

Hot isostatic pressing can be used not only for producing dense bodies from granular material, but also for joining large bodies to each other without the use of any additional material. Such joining can be carried out at combinations of pressure, temperature and time corresponding to those reqiured to produce pore-free bodies from powder made of the material in question.

Both the method of fabricating dense bodies and the method of joining large bodies to each other are used in the ASEA method for encapsulating spent nuclear fuel.

Figure B1-2 illustrates schematically the design of a hot isostatic press. The high-pressure chamber consists of a cylinder made of high-grade steel. It is prestressed by wires of high-strength steel wound around the cylinder in a number of layers. This arrangement subjects the steel cylinder to compressive stress, which remains on the pressure side even under a maximum internal pressure in the high-pressure chamber. The tensile stresses are taken up by the wires. This method of winding the cylinder with wire provides a built-in, very high redundancy so that the high-pressure chamber cannot burst.

At each end of the steel cylinder is a steel lid with high-pressure seals. The lids are kept in place during pressing by a frame which is prestressed with wound wire in the same manner as the steel cylinder. The frame is moved aside when the high-pressure chamber is opened.

The pressure in the high-pressure chamber is created by pumping in a gas, usually argon, with the aid of compressors. Inside the chamber is a resistance-type furnace designed to withstand the high pressure. With the aid of sophisticated temperature control, the temperature can be maintained at 1 400^{o}C with an accuracy of ± 10^{o}C within the entire work chamber.

Hot isostatic pressing achieved its main industrial breakthrough in the 1970s. The method is used today for the production of tool steel, cemented carbide products and articles made of superalloys. There is, for example, a plant for the production of tool steel by this method at Söderfors in Sweden. The steel billets produced in this plant weigh nearly 2 tonnes apiece.

ASEA has delivered more than 40 QUINTUS hot isostatic presses with up to 40 000 tonnes press force. Presses of the type and

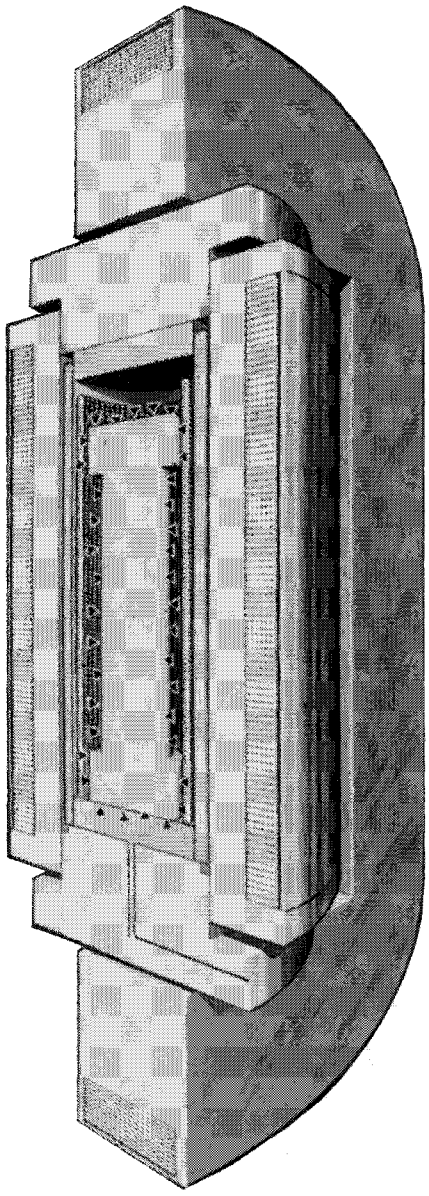

Figure B1-2. Cross-section of a hot isostatic QUINTUS press.

size which are required for the production of canisters suitable for the enclosure of spent nuclear fuel have already been put into production. Another feature of the method is that scaling up problems are small compared with other fabrication methods. This is due partly to the isostatically applied pressure and partly to the fact that the necessary temperature level is relatively low compared to conventional methods.

B1.2.3 Encapsulation method

Encapsulation and final storage of spent nuclear fuel in accordance with the method proposed here can be described briefly as follows (fig. B1-3):

1 By means of hot isostatic pressing of aluminium oxide powder, a container and a lid as shown in fig. B1-4 are fabricated. The container and lid are transferred to the encapsulation station.

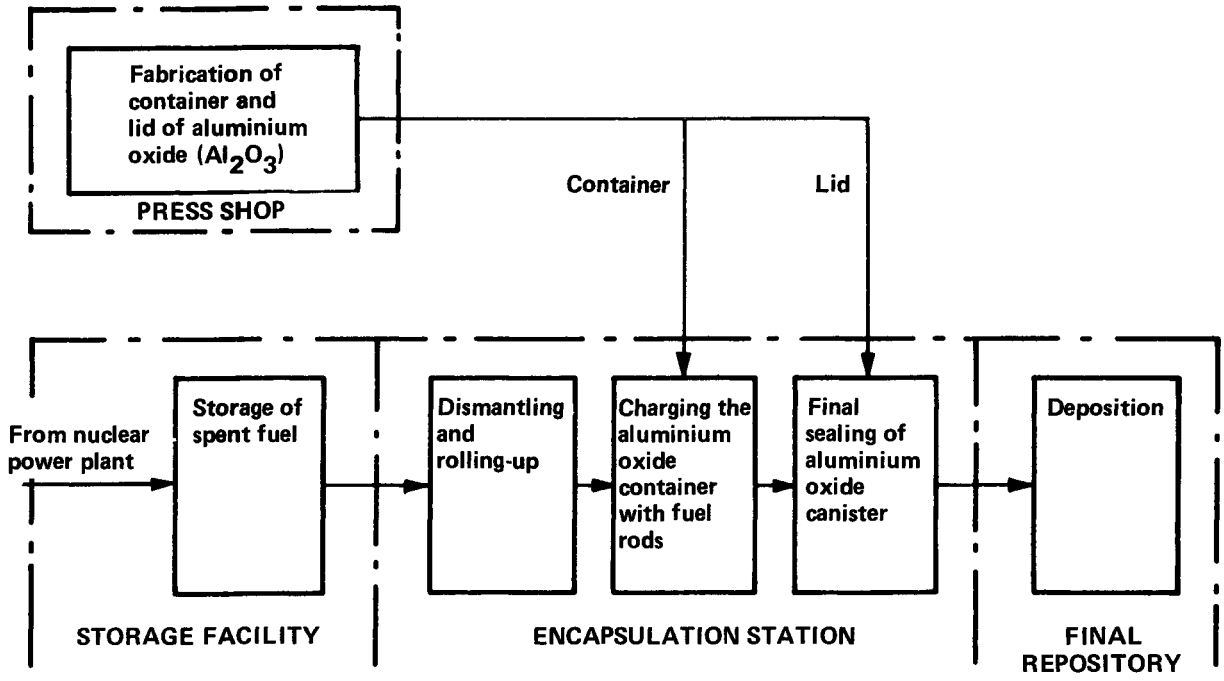

Figure B1-3. Block diagram illustrating encapsulation of spent nuclear fuel in aluminium oxide canister.

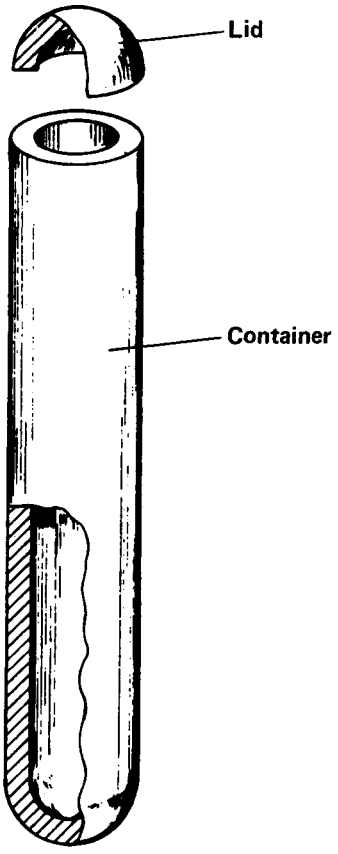

Figure B1-4. Schematic drawing of container and lid of aluminium oxide for encapsulation of spent nuclear fuel.

2 Fuel assemblies are dismantled, after which the fuel rods are rolled up and placed in a steel container.

3 The steel container with fuel rods is placed in the aluminium oxide container and the lid is put on.

4 The aluminium oxide container and the lid are joined, enclosed by a thin metal shell, by hot isostatic pressing into a completely seamless, monolithic body.

5 The sealed aluminium oxide canister is transported to the final repository and deposited.

B1.3 ALUMINIUM OXIDE: PROPERTIES AND PERFORMANCE

The aluminium oxide (Al_2O_3) which is used is of the alpha type of high purity (> 99.8%). The characteristic properties of this material are listed in table B1-1.

Aluminium oxide occurs in a number of different crystalline structures. Of these, only alpha-aluminium oxide is inherently thermodynamically stable. All other forms of aluminium oxide are transformed to alpha-aluminium oxide upon to heating to temperatures above 1 000°C.

Alpha-aluminium oxide is hydrated upon contact with water (see section 7.2), but its reaction with water is extremely slow at the temperatures prevailing in the final repository. Its high hardness indicates very strong bonds between the atoms. In flowing 80°C water with a pH of 8.5 containing chloride ions, its dissolution rate has been measured at less than 0.07 µm per year, equivalent to 0.07 mm in 1 000 years /B1-7/. At the lower temperature which prevails in the final repository after this period of time, the dissolution rate is at least 10 times lower. Even in boiling, very acidic (20% hydrochloric, sulphuric or nitric acid) or basic (20% sodium hydroxide) solutions, the measured corrosion rate is less than 0.1 mm/year /B1-2/.

High purity is of decisive importance for achieving high strength and high chemical resistance. Aluminium oxide with a purity of more than 99.8% has been used in the development work. The composition of this material is given in table B1-2. Even purer powder is available on the market. On the basis of results obtained so far, however, the powder grade which is now used is adequate.

Fine-grained alpha-aluminium oxide normally contains approx. 0.5% water, which is adsorbed on the surface of the powder grains. The pretreatment of the powder prior to the hot isostatic pressing drives this water off (see section 4).

Aluminium oxide of the alpha-type is an intermediate product in the manufacture of aluminium and is obtained by calcining gibbsite (α-Al_2O_3 . 3 H_2O). A complete transformation to alpha-aluminium oxide is obtained after approx. 1 hour at 1 200 - 1 300°C. Other uses of alpha-aluminium oxide include: as an abrasive, in the porcelain and ceramics industry for the production of technical porcelain, in high-temperature-resistant materials etc.

Table B1-1. Characteristic properties of alpha-aluminium oxide (Al_2O_3) (purity > 99.8%).

Property		Consequence
1	High chemical resistance	
1.1	Extremely high corrosion resistance	Groundwater affects canister's integrity very slowly
	- lower solubility in water at pH values in final repository than most other minerals	
	- dissolution rate extremely slow at temperatures in final repository	
1.2	Difficult to reduce	Not affected by hydrogen or carbon
1.3	Aluminium in its highest oxidation state	Not affected by oxygen
2	High stability	
	- thermodynamically stable from room temperature up to melting point (>2 000°C)	Spontaneous transformation to other structure without action of other substances impossible.
	- a single-phase material	Mechanical and chemical properties well-defined
3	High strength and hardness	
	- flexural strength approx. 500 MN/m^2	
	- hardness near that of diamond	

Resources of bauxite and other aluminium-bearing raw materials are virtually inexhaustable. The cost of high-purity alpha-aluminium oxide powder is currently around SKr 5/kg.

Table B1-2. Composition of aluminium oxide

Designation: Alcoa A15 Superground
Mean particle size: 2.5 μm

Trace substances	Typical analysis according to manufacturer	Own analysis
Na_2O	0.08%	0.07%
K_2O	data lacking	0.001
SiO_2	0.05	0.012
CaO	0.03	0.011
MgO	0.01	0.017
Fe_2O_3	0.01	0.016
Cr_2O_3	0.0002	< 0.01
MnO	< 0.0015	< 0.01
B_2O_3	< 0.001	< 0.02

B1.4 FABRICATION OF ALUMINIUM OXIDE CONTAINER AND LID

B1.4.1 Pretreatment of aluminium oxide powder

Fabrication of the aluminium oxide container and the aluminium oxide lid can be completely geographically separated from the encapsulation plant. This facbrication process does not involve the use of any radioactive materials. Only the shape of the final product differentiates the production chains for containers and lids. The following description therefore concerns only the container, but the same process is used for the lid as well.

The production chain is shown in fig. B1-5. Treatment of the aluminium oxide powder prior to hot isostatic pressing includes the following stages:

a) Granulation

In order to minimize shrinkage during the final hot isostatic compaction, the filling density of the powder in the steel container must be maximal. This is achieved by granulation of the powder to a grain size varying from 0.005 mm to about 3 mm.

b) Drying

The water bound to the surface of the powder grains must be driven off prior to compaction. This is done by calcination at 1 100°C. Any organic grinding additives which may remain from the manufacturing process are then also removed.

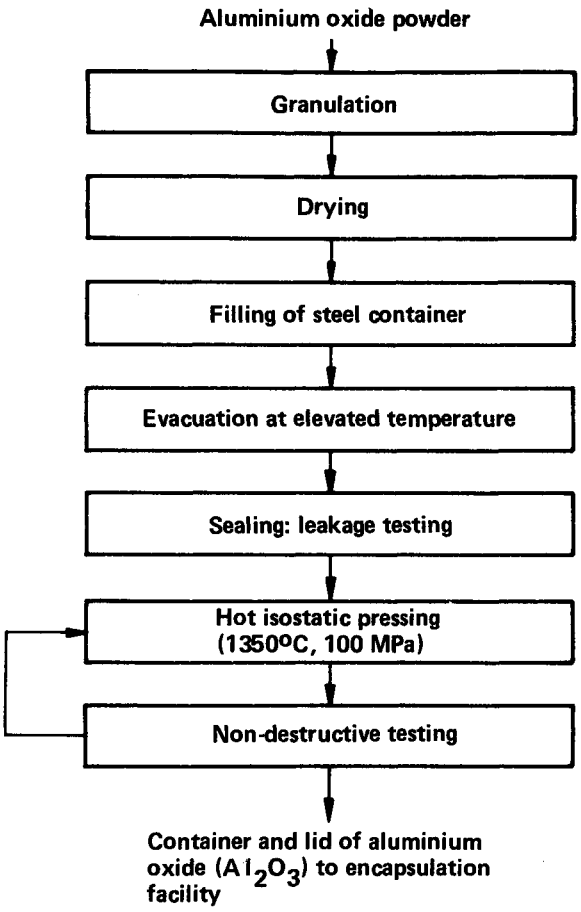

Figure B1-5. Schematic diagram of production chain for aluminium oxide canister for spent nuclear fuel.

c) Filling of preformed steel containers

The dried powder is packed into preformed steel containers. (The container determines the appearance of the canister and the lid in fig. B1-4.) The containers are made of unalloyed steel with a low carbon content and with a wall thickness of 3 mm. The containers are welded and thoroughly cleaned internally.

The powder can be packed so that a very homogeneous fill is achieved. Powder of optimal grain size distribution can be packed to more than 60% density in the container.

d) Evacuation at elevated temperature

The powder is porous after packing. In order to prevent residual porosity after pressing, the air must be evacuated. This is done at about 700°C so that the moisture and the gases which have been adsorbed on the powder grains during the packing operation are driven off as well.

Evacuation is carried out to a final pressure of 0.1-1 kPa (1-10 mbar) in the powder. The water content after evacuation is below 0.01%.

e) Sealing and leakage testing

Evacuation of the powder takes place through a tube mounted

on the steel container. When evacuation is finished, this tube is sealed by means of welding. All welds are then subjected to rigorous testing in order to ensure that the steel container is hermetically sealed.

B1.4.2 Hot isostatic pressing of aluminium oxide container

During the hot isostatic pressing, the powder in the steel container is subjected to a combination of high pressure and high temperature. Control of temperature and pressure is of vital importance for the ultimate performance of the hot isostatically compacted aluminium oxide material. Optimal pressing parameters have been determined on the basis of an extensive trial programme with small test bodies and 1/3-scale containers.

The powder container is placed in the press, after which the pressure and the temperature are raised to about 100 MPa and 1 350°C. After a holding time at these parameters, the aluminium oxide powder has been compacted to full density. The container is then allowed to cool slowly. The cooling rate is decisive in ensuring that a stress-free aluminium oxide material will be obtained.

The hot isostatically pressed aluminium oxide container is examined by means of nondestructive testing methods such as ultrasonic testing or proof testing.

Ultrasound can be used to inspect containers with internal flaws and surface cracks larger than about 1 mm. This test can be performed through the surrounding steel shell.

Proof testing can be carried out in order to ensure that the aluminium oxide container does not have surface cracks in the aluminium oxide larger than a given size. The maximum permissible crack depth is determined, in view of the risk of delayed fracture, by the required life of the canister in the final repository. A 100% reliable method to detect such critical surface cracks is to test-load the aluminium oxide material, a procedure known as proof testing.

A proof testing method has been developed whereby stresses in the aluminium oxide are created by imposing a temperature differential between the inner and outer walls of the container. Flawless containers are not affected by these stresses while defects immediately fail. An apparatus for testing 1/3-scale containers is currently being put into operation.

According to fracture mechanics theory, a relationship can be established for approved containers between proof stress and guaranteed container life with respect to delayed fracture in the final repository, see section 7.2.

B1.4.3 Small-scale and 1/3-scale trials

The development work has mainly been conducted at ASEA's high-pressure laboratory in Robertsfors. Available equipment in 1977 has permitted the production of aluminium oxide bodies of maximum

diameter 170 mm and length about 800 mm (roughly 1/3 scale, see section 4.4).

The fabrication of small-scale and 1/3-scale test bodies has been done for the following reasons:

- to serve as a basis for optimizing powder treatment methods and pressing parameters
- to permit the selection of methods and equipment for the full-scale facility (see section 4.4)
- to produce representative material for material characterization and
- to permit the testing of methods and equipment for production control.

All process stages in fig. B1-5 have been tested, mainly through manual handling. The sealing process has also been tested on 1/3 scale (see section 5.2).

B1.4.4 Full-scale facility

A new large plant has been built during 1977 at ASEA's high-pressure laboratory at Robertsfors. The production and sealing of aluminium oxide canisters 500 mm in diameter and 3 000 mm in length, suitable for the enclosure of spent nuclear fuel, can be demonstrated in this plant. The plant was commissioned in early 1978.

The plant is intended only as a pilot plant for testing the process. The installed equipment for powder treatment is more mechanized than previously used laboratory equipment. As a result, the quality of the canisters can be made even better and more uniform. A QUINTUS press for 1 400^{o}C and 160 MPa is included in the plant.

The plant is now in operation and full-scale experiments have been started. The first of a series of full-sized aluminium oxide containers was recently taken out of the QUINTUS press following hot isostatic pressing, see fig. B1-6.

The experimental facility provides excellent opportunities for both demonstrating and optimizing the production method for full-sized aluminium oxide containers.

B1.5 ENCAPSULATION OF SPENT NUCLEAR FUEL

B1.5.1 General

In the current form of the process, spent nuclear fuel will be encapsulated in aluminium oxide canisters in two stages:

1) Reduction of length of nuclear fuel rods

   By means of a specially developed method, the over 4-m-long fule rods are rolled up so that they fit in the 3-m-long aluminium oxide canister. This length reduction can be ac-

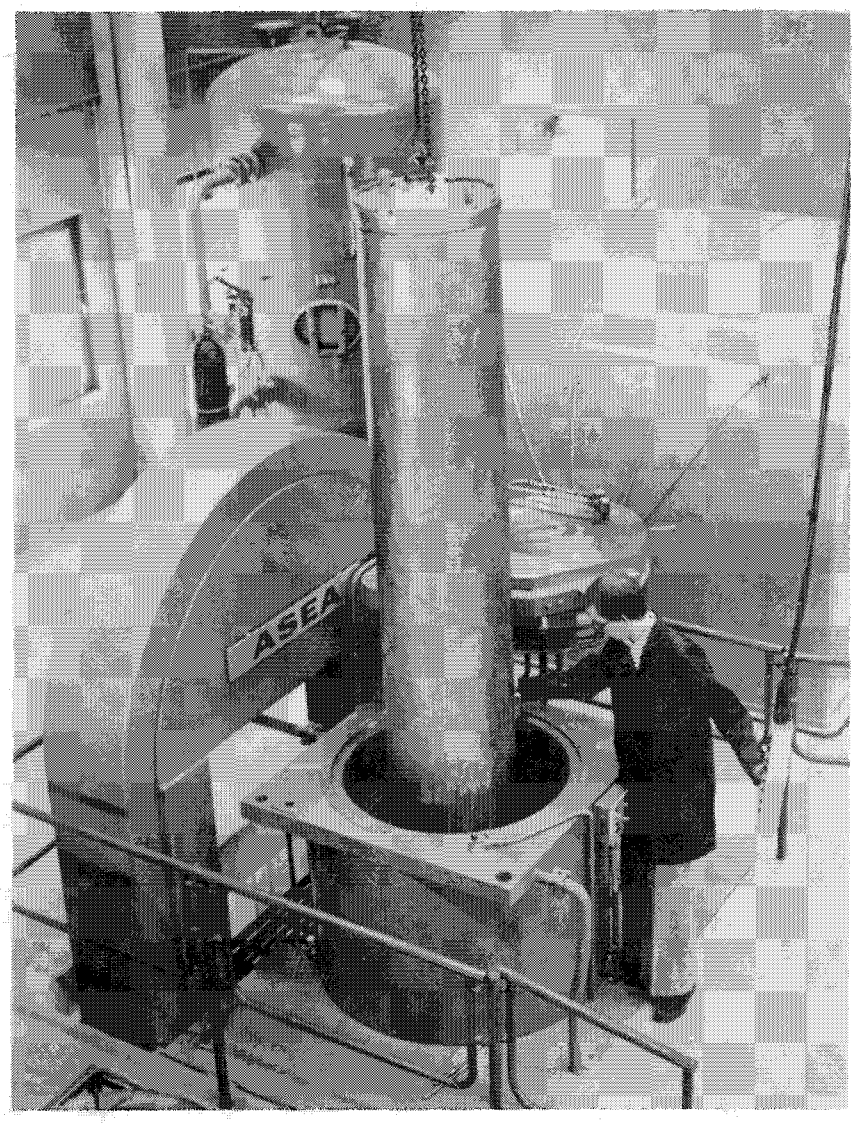

Figure B1-6. A full-size aluminium oxide container is lifted up out of the QUINTUS press. The container is 2.5 metres long and has a diameter of 500 mm.

complished without releasing the fission gases present in the spent nuclear fuel (see section 5.2).

2) Sealing of aluminium oxide canister

In a specially developed hot isostatic pressing operation, the aluminium oxide container is joined together with the aluminium oxide lid without the use of any filler material. The joint between the container and the lid merges together so that a completely seamless (monolithic) canister is obtained (see section 5.3).

The encapsulation plant is to be built in direct connection with the final repository. The fuel bundles can be transported from the receiving section under water into the encapsulation plant. The encapsulation process is carried out in a series of stages in adjacent concrete cells with walls thick enough that an acceptable radiation level is obtained outside of the cell wall.

The projected annual capacity of the encapsulation plant for fuel corresponds to 300 tonnes of uranium per year. With 200 days of operation per year, this means 1.5 tonnes of uranium per day of operation. An aluminium oxide canister with the above-specified dimensions can hold approximately 144 BWR fuel rods or 174 PWR fuel rods, which means that 4-5 aluminium oxide canisters will be sealed per day of operation.

B1.5.2 Reduction of fuel rod length

This process consists of the following stages (see fig. B1-7):

- dismantling of fuel bundles,
- encapsulation of fuel rods in pairs in steel sheaths,
- rolling-up of steel sheaths into coils,
- packing of coils into a stainless steel cylinder.

Dismantling of the fuel bundles, section 2.3, is done with the same handling technique currently used in nuclear power plants.

The fuel rods are placed in pairs in a sheath made of stainless steel sheet with a thickness of 1 mm, open at the top and with a drainage hole in the bottom. Each sheath also contains a 1 mm thick strip made of spring steel, tack-welded to one wall of the sheath. The entire sheath is brought into the first cell under-water, after which it is lifted up, drained and dried. The steel sheath is evacuated to vacuum and sealed. The sheath is then leakage-tested with helium. Then follows the length reduction stage.

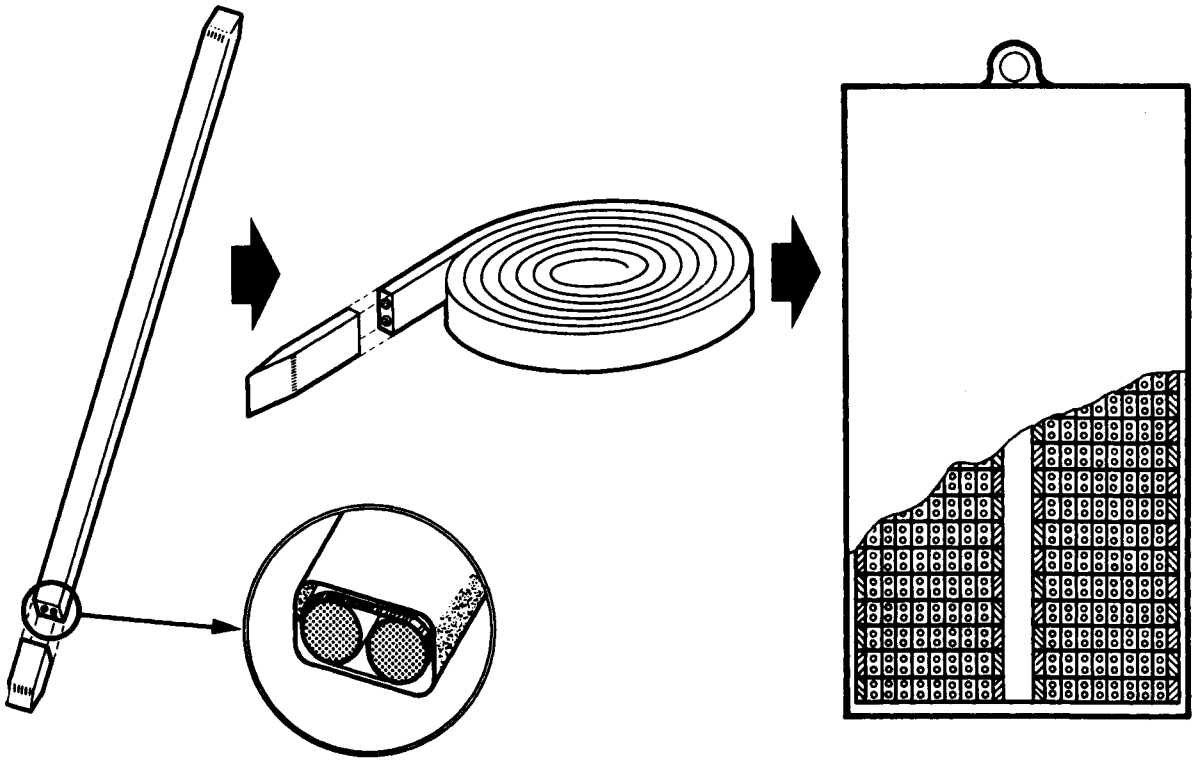

Figure B1-7. The fuel rods are encapsulated in pairs in steel sheaths which are then rolled up. The resultant coils are packed in a cylinder of stainless steel.

In order to reduce the length of the fuel rods, the sheath, with the steel strip to protect it on the outside, is rolled on a centre tube with a diameter of 100 mm to a flat coil with an outside diameter of max 300 mm. When the first, tight turn is rolled, the zircaloy cladding on the fuel rods will be split and the fuel pellets will be crushed into different-sized fragments. The liberated fission gas will fill the steel sheath to a pressure of max. 0.2 MPa. The steel sheath will remain intact owing to the protective effect of the steel strip, which prevents sharp parts of the fuel from penetrating the steel sheath.

The coiled sheaths are packed one by one into a stainless steel cylinder with a wall thickness of 5 mm, a diameter of 300 mm and a length of 2 000 mm. The cylinder holds a total of 72 BWR (87 PWR) sheaths, equivalent to approx. 400 kg (300 kg) uranium. After evacuation, the steel cylinder is sealed and tested for leakage. The steel cylinder is then placed in the prefabricated aluminium oxide container.

This method of reducing the length of the spent nuclear fuel rods by coiling has been tested within ASEA-ATOM. Trial bendings have been carried out both with normal and ambrittled, unirradiated fuel rod dummies and with fuel rods which have been irradiated at the Oskarshamn station to 23 MWd/kgU /B1-5/.

The smallest radius of curvature and thereby the highest stress in the material is obtained in the innermost turn. It is therefore sufficient to show that rods can be rolled around a cylinder with a diameter of 100 mm. No negative effects have been found following such rolling. Figure B1-8 shows a spiral of a steel sheath containing a fuel rod with natural uranium and normal encapsulation.

With regard to the necessity of reducing the length of the fuel rods, the following can be said:

In the introductory phase of the project, encapsulating fuel rods of full length in aluminium oxide canisters was rejected on geological grounds. Movements in the bedrock could give rise to

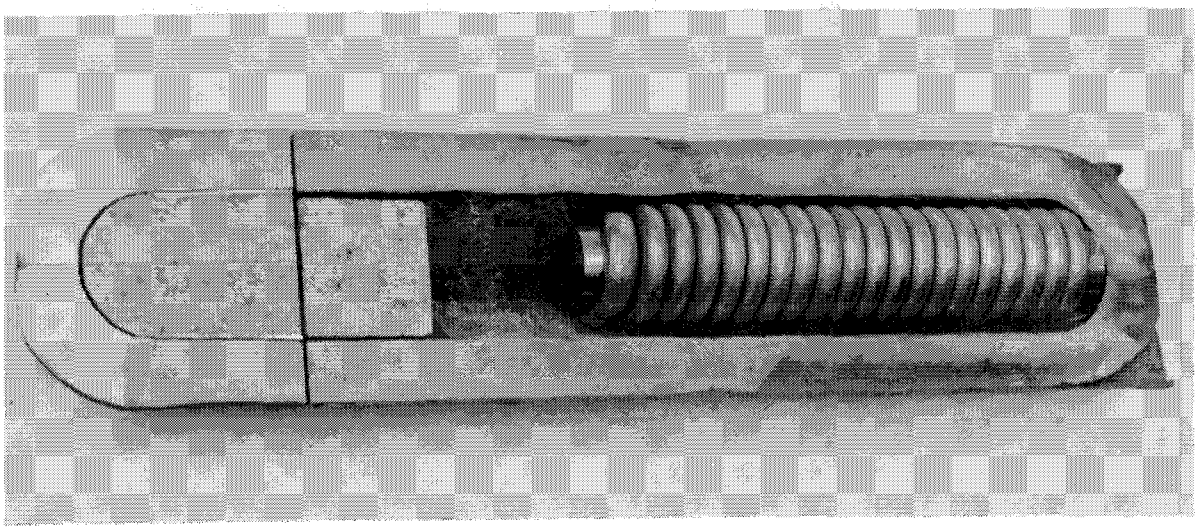

Figure B1-8. The sealing process has been tested at 1/3-scale. The photograph shows a sealed container which has been cut in half. In the container is a dummy fuel rod which has been bent into a spiral.

unacceptable stresses in such a long (approx 5 m) aluminium oxide canister. Since more knowledge has been gained concerning bedrock movements and the deposition procedure has been modified the importance of reducing the length of the fuel rods has diminished. It has nevertheless been decided to continue the development work on an encapsulation process which permits the encapsulation of spent fuel rods in roughly 3 m long aluminium oxide canisters, since QUINTUS presses of the necessary size are already available today. However, nothing in the process prevents the fabrication of aluminium oxide canisters large enough to enclose full-length fuel rods.

B1.5.3 Sealing of canister

Hot isostatic pressing is also used to join together the aluminium oxide container and lid. The seam between the container and the lid thereby disappears so that a completely seamless canister is obtained. The procedure is illustrated schematically in fig. B1-9.

The steel cylinder with the coiled fuel rods is lowered down into the prefabricated aluminium oxide container (internal dimensions 300 x 2 800 mm). The flat end surface of the container, as well as the aluminium oxide lid, has previously been machined to precision flatness. The method currently used for this, surface grinding with a diamond tool, achieves a flatness within ±25 µm, which has proven to be fully adequate. The joint surfaces must be thoroughly cleaned in order to prevent inclusions of foreign material in the joint.

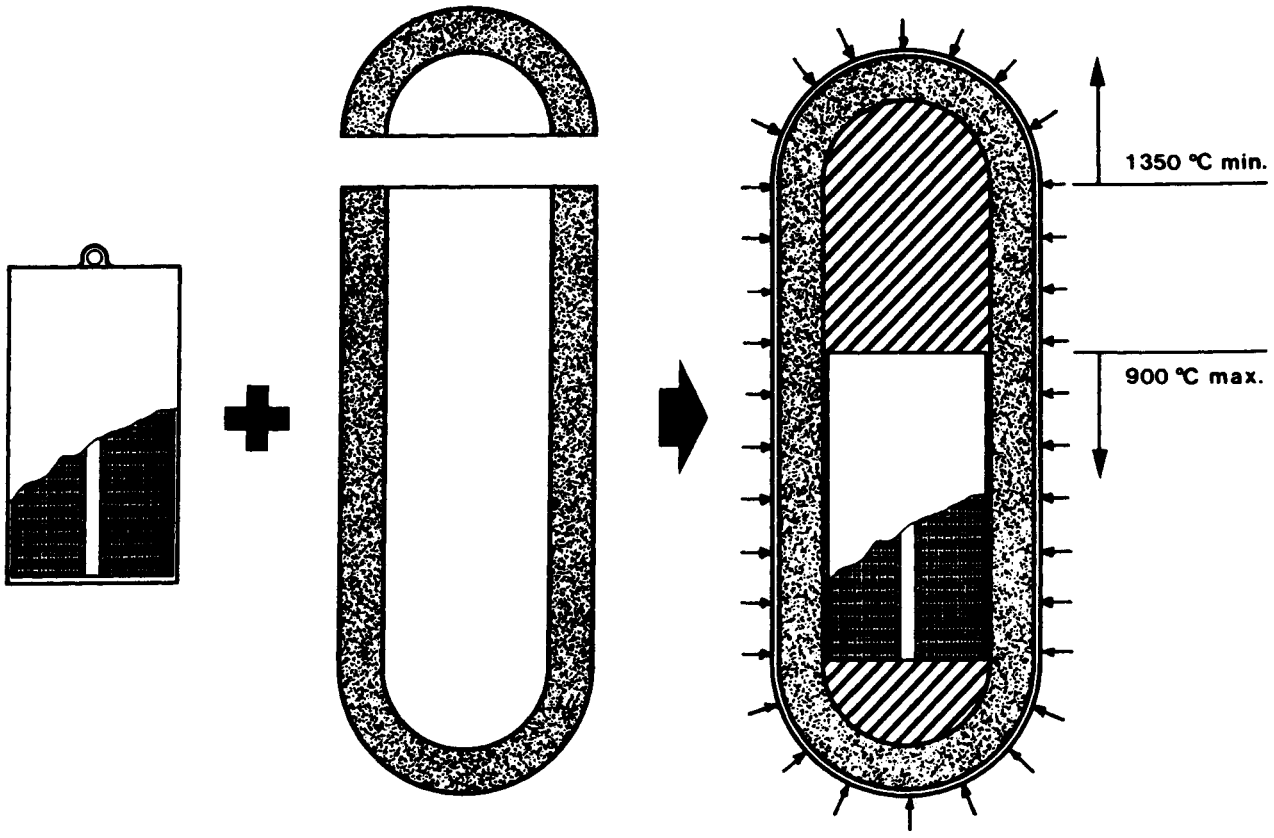

Fig B1-9. The stainless steel cylinder with fuel rods is placed in the container. The lid and the container are sealed by means of hot isostatic pressing to produce a completely seamless canister.

On top of the steel cylinder, the aluminium oxide container is filled with an approximately 300 mm thick heat-insulating mass of fibrous aluminium silicate. On top of this, a 500 mm thick magnesium oxide support block is placed. The lid is emplaced and fitted precisely in position. The container and the lid are enclosed in a gas-tight 3 mm thick shell fitted with lifting devices. The shell is evacuated and sealed. The canister is then ready for the final sealing operation.

The canister is sealed in a QUINTUS press, designed for radioactive conditions and equipped with a specially developed furnace. A temperature of at least 1 350°C is required in the joint for joining the lid to the container. This high temperature is combined with an external pressure of approx. 70 MPa, which results in a pressure of about 100 MPa at the surfaces of the joint. At the same time, the steel cylinder with its nuclear fuel should preferably be kept below 900°C. The specially-developed furnace permits such a temperature gradient to be created in the canister.

The parts of the canister which are not heated to above 1 000°C can withstand the external pressure with plenty of margin. However, in those parts of the canister which attain maximum temperature, i.e. near the joint, there is some creep deformation resulting from stresses caused by the external pressure and thermal stresses. In these parts, certain residual stresses remain in the material after pressing. The size of these residual stresses must be limited in order to prevent slow crack growth.

Very extensive theoretical calculations have been carried out in order to:

- determine the optimum pressing parameters for the sealing operation, and from these to
- calculate stress distributions, both during heating and cooling, as well as to
- calculate maximum residual stresses after the sealing operation.

The appearance of the cooling curve is particularly important in determining the quality of the final canister. The temperature of the canister must decline slowly after decompression so that residual stresses can relax.

The sealing process has been tested on small and 1/3 scale. Fig. B1-8 shows a sealed container which has been sawn up axially. Flexural strength tests on material taken from the joint area show that the joint can be just as strong as the parent material (see section 7.1).

A gradient furnace for sealing full-scale canisters is under development at ASEA's workshops at Robertsfors. Sealing of full-size canisters will be demonstrated during the first half of 1978.

After the joining operation, the joint is inspected with ultrasound. Joining trials on 1/3 scale carried out to date have shown that fully acceptable joints can be obtained.

Approved canisters are transported from the encapsulation station

to the final repository for deposition or, alternatively, to an intermediate storage facility for further decay of the radioactive material. If an imperfect joint is obtained, the canister can be subjected to the joining process once again without being opened. Alternatively, canisters with serious defects can be sawn up with diamond tools. The steel cylinder, still completely intact, can then be placed in a new aluminium oxide container which is then sealed by the procedure described above.

B1.5.4 Safety and environment

A comprehensive analysis of radiological safety in connection with the encapsulation of spent nuclear fuel, like that previously done for the copper canister, /B1-4/ has been carried out for the aluminium oxide canister.

Both radioactivity releases to the ventilation system and the dose load on the staff of the facility and the external environment have been calculated for normal annual releases and for conceivable incidents.

All calculated figures for radioactivity releases and dose loads are very low. For example, the global dose commitment from radioactivity releases to the external environment is about 10^{-3} man-rems/year. The difference in dose commitment between the two encapsulation procedures can, for the most part, be regarded as negligible.

The use of the QUINTUS press in a radioactive environment with full remote control is not expected to entail any appreciable technical complications.

B1.6 DEPOSITION

The aluminium oxide canisters are intended to be deposited in vertical holes in the bottom of horizontal tunnels in a manner similar to that described for the lead/titanium canister for vitrified waste and for the copper canister. A bed of 90% quartz and 10% bentonite is placed in the bottom of the hole. This bed is packed in the moist state and given an indentation which matches the bottom of the canister. The canister is then seated in this indentation, after which plastic clay containing bentonite and with a relatively high moisture content is used to fill the spaces around and above the canister. The hole is temporarily covered until all holes in a tunnel have been filled and the tunnel is backfilled.

The properties of the bed material are such that possible rock movements will not give rise to stresses in the canister which could affect its life.

B1.7 CANISTER MATERIAL AND CORROSION

B1.7.1 Properties of the hot isostatically compacted aluminium oxide

The chemical composition of the aluminium oxide material is given in table B1-2. The table applies to aluminium oxide in powder form, but is also representative for the hot isostatically pressed material.

The material is compacted to virtually theoretical density. A density of 3.97 t/m^3, which is more than 99.5% of the theoretical density, is representative for material produced thus far.

The aluminium oxide is a very hard material. A microhardness of 2 100 H_V has been measured. High-speed steel normally has a hardness of 750 - 800 H_V.

Both flexural strength and creep strength have been measured at room temperature and at elevated temperatures. Flexural strength lies between 450 and 500 MN/m^2 at room temperature, which is equivalent to the strength of unalloyed steel.

Specimens have been taken from both special material characterization bodies and 1/3-scale containers. The values apply to material produced using the best pressing parameters available today. Specimens taken from the joint area exhibit a flexural strength which is just as high as that of the parent material.

Creep strength has been tested at Stal Laval's laboratory at Finspång. A total of 25 specimens have been measured at temperatures between 1 000 and 1 350°C. The measurement results have been used as a basis for the creep deformation calculations mentioned in section 5.3.

The material's thermal conductivity has been determined from room temperature of up to 1 400°C. Its coefficient of thermal conductivity ranges from about 38 W/m, °C at room temperature to about 7 W/m, °C at 1 500°C. Stainless steel has a coefficient of thermal conductivity of 16 W/m, °C at room temperature.

A method for determining residual tensile stresses in the outer surface of the aluminium oxide container has been developed. Figure B1-10 shows measured residual stresses as a function of the distance from the joint for a 1/3-scale container. It can be seen that the maximum tensile stress is less than 25 MN/m^2 and that calculation for this case gives a conservative result. Calculation based on a longer relaxation time after joining also gives reassuringly low values.

B1.7.2 Properties of the canister in the repository environment

After deposition, the aluminium oxide canister constitutes one of several barriers against the dispersal of radioactive material in the biosphere. It is therefore essential to be able to predict the properties of the aluminium oxide material under the conditions created by the repository environment.

After deposition, the aluminium oxide canister will be subjected

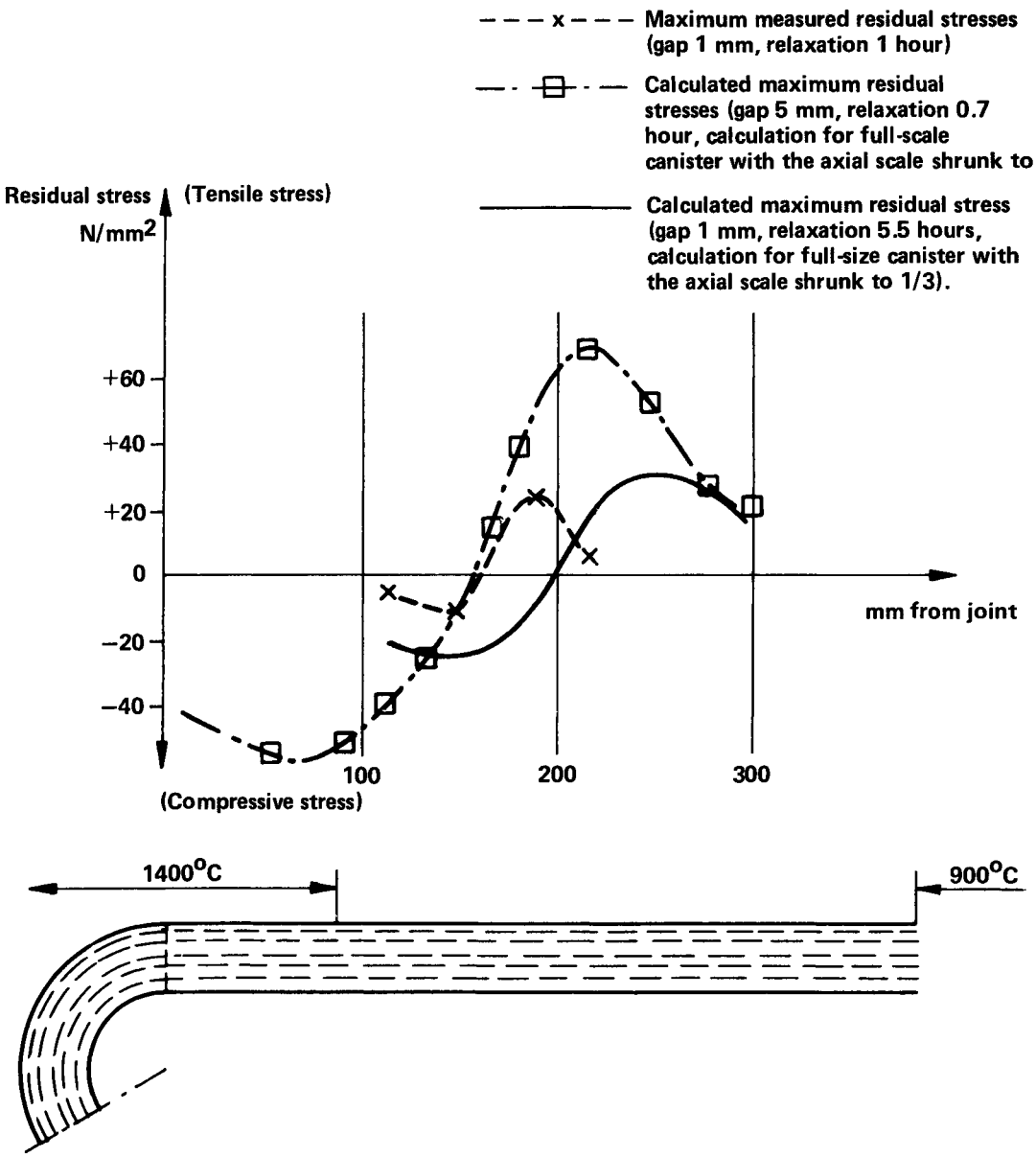

Figure B1-10. Residual stresses in the aluminium oxide on the outer surface of the canister after sealing of a 1/3-scale canister. Measurements carried out on the upper half of the canister shown in figure B1-8.

to the action of the surrounding groundwater. Since aluminium is in its highest oxidation state and the oxide is very difficult to reduce, no redox reactions will take place in the aqueous environment. The aluminium oxide will, however, be hydrated on surfaces in contact with water. The reaction with water is extremely slow at the temperatures and pHs which prevail in the final repository.

In the groundwater, which contains dissolved substances such as quartz, solubility will be even lower than in pure water owing to the formation of poorly soluble compounds of the aluminium silicate type. Studies show that compounds of the same type as the clay minerals in the bed will be formed /B1-3/.

Experiments are being conducted both in Sweden and abroad to verify the durability of the aluminium oxide material produced by hot isostatic compaction. The effects of groundwater of the type which may be found in the final repository are being determined.

In order to obtain measurable affects, the experiments are being carried out at elevated temperature, 100 - 350°C. A growth rather than an erosion of the surface has been obtained in the type of groundwater in question.

On the basis of experiments and geological assessments carried out to date, it has been concluded that a canister of aluminium oxide with 100 mm thick walls can resist the action of the groundwater for at least 1 million years. Growth or erosion will be uniformly distributed over the canister surface /B1-6/.

The only mechanism which could lead to local corrosion of the aluminium oxide in an aqueous environment is a form of slow crack growth which can lead to delayed fracture.

In order for such fracture to be able to occur in the aluminium oxide canister after deposition, two factors are required: a defect of sufficiently stress-raising character in surfaces exposed to the water and a certain minimum tensile stress. This tensile stress may be a residual stress from fabrication or a stress in the canister caused by rock movements. On the basis of fracture mechanics theory, and with knowledge of the maximum defects on the surfaces of the aluminium oxide canister and the residual tensile stresses in these surfaces at the time of deposition, the minimum life of the canister in the final repository as determined by delayed fracture can be predicted.

Both calculations and measurements of maximum residual tensile stresses show that these stresses can, with the use of suitable pressing parameters, be kept at a sufficiently low level. With the proposed deposition technique, stresses caused by any movements which might occur in the bedrock can only add slightly to this stress level. Furthermore, it is judged possible to achieve such high canister quality that the risk of delayed fracture will not be crucial in determining the life of the canister.

B1.8 CONTINUED DEVELOPMENT WORK

The present report constitutes a status report from a development project which has been under way for approximately two years. Results obtained to date show that encapsulation and deposition of spent nuclear fuel in aluminium oxide canisters at great depth in the Swedish bedrock meets stringent environmental and safety requirements. Some development work still remains to be done before an economically optimal process can be demonstrated practically.

The continued development work will include the demonstration of the sealing process in full scale.

REFERENCES

B1-1 HARKER, ALFRED
Metamorphism. A Study of the Transformations of Rock-Masses, p 63.
Methuen & Co Ltd, London, 1932.

B1-2 THE SWEDISH CORROSION INSTITUTE AND ITS REFERENCE GROUP
Bedömning av korrosionsbeständigheten hos material avsedda för kapsling av kärnbränsleavfall. Lägesrapport 1977-09-27 samt kompletterande yttranden, bilaga 11.
("Evaluation of the corrosion resistance of material intended for the encapsulation of nuclear fuel waste")
Status report, 1977-09-27, and supplementary statements, appendix 11.
KBS Technical Report 31

B1-3 HESS, P C
Amer. J. Sci. 264 (4), p 300, 302-323 (1966).

B1-4 CARLESON, GÖRAN
Säkerhetsanalys av inkapslingsprocesser.
("Safety analysis of encapsulation processes")
AB Atomenergi 1978-01-27
KBS Technical Report 65

B1-5 OLSSON, T
Metod att bocka bestrålade bränslestavar.
("Method for bending irradiated fuel rods")
ASEA-ATOM 1978-03-29
KBS Technical Report 102

B1-6 FYFE, W S
University of Western Ontario,
letter 78-04-11

B1-7 INGRI, N and ÖHMAN, L-O
Bestämning av korrosionshastigheten för Al_2O_3 i natriumvätekarbonatbuffrat, klorhaltigt vatten vid 80°C och pH 8,5.
("Determination of corrosion rate for Al_2O_3 in chloridic water buffered with sodium bicarbonate at 80°C and pH 8.5.")
Department of Inorganic chemistry, University of Umeå, August 1978
(Unpublished)

APPENDIX 2 LIST OF KBS TECHNICAL REPORTS

01 Källstyrkor i utbränt bränsle och högaktivt avfall från en PWR beräknade med ORIGEN
("Emission rates in spent fuel and high-level waste from a PWR, calculated using ORIGEN")
Nils Kjellbert
AB Atomenergi, 1977-04-05

02 PM angående värmeledningstal hos jordmaterial
("Memorandum concerning the thermal conductivity of soil")
Sven Knutsson
Roland Pusch
Luleå Institute of Technology, 1977-04-15

03 Deponering av högaktivt avfall i borrhål med buffertsubstans
("Deposition of high-level waste in boreholes containing buffer material")
Arvid Jacobsson
Roland Pusch
Luleå Institute of Technology, 1977-05-27

04 Deponering av högaktivt avfall i tunnlar med buffertsubstans
("Deposition of high-level waste in tunnels containing buffer material")
Arvid Jacobsson
Roland Pusch
Luleå Institute of Technology, 1977-06-01

05 Orienterande temperaturberäkningar för slutförvaring i berg av radioaktivt avfall, Rapport 1
("Preliminary temperature calculations for the final storage of radioactive waste in rock, Report 1")
Roland Blomqvist
AB Atomenergi, 1977-03-17

06 Groundwater movements around a repository, Phase 1, State of the art and detailed study plan
Ulf Lindblom
Hagconsult AB, 1977-02-28

07 Resteffekt studier för KBS ("Decay power studies for KBS")
Del 1 Litteraturgenomgång ("Part 1 Review of the literature")
Del 2 Beräkningar ("Part 2 Calculations")
Kim Ekberg
Nils Kjellbert
Göran Olsson
AB Atomenergi, 1977-04-19

08 Utlakning av franskt, engelskt och kanadensiskt glas med högaktivt avfall
("Leaching of French, English and Canadian glass containing high-level waste")
Göran Blomqvist
AB Atomenergi, 1977-05-20

09 Diffusion of soluble materials in a fluid filling a porous medium
Hans Häggblom
AB Atomenergi, 1977-03-24

10 Translation and development of the BNWL-Geosphere Model
Bertil Grundfelt
Kemakta Konsult AB, 1977-02-05

11 Utredning rörande titans lämplighet som korrosionshärdig kapsling för kärnbränsleavfall
("Study of suitability of titanium as corrosion-resistant cladding for nuclear fuel waste")
Sture Henriksson
AB Atomenergi, 1977-08-24

12 Bedömning av egenskaper och funktion hos betong i samband med slutlig förvaring av kärnbränsleavfall i berg
("Evaluation of properties and function of concrete in connection with final storage of nuclear fuel waste in rock")
Sven G Bergström
Göran Fagerlund
Lars Rombén
The Swedish Cement and Concrete Research Institute, 1977-06-22

13 Urlakning av använt kärnbränsle (bestrålad uranoxid) vid direktdeponering
("Leaching of spent nuclear fuel (irradiated uranium oxide) following direct deposition")
Ragnar Gelin
AB Atomenergi, 1977-06-08

14 Influence of cementation on the deformation properties of bentonite/quartz buffer substance
Roland Pusch
Luleå Institute of Technology, 1977-06-20

15 Orienterande temperaturberäkningar för slutförvaring i berg av radioaktivt avfall, Rapport 2
("Preliminary temperature calculations for the final storage of radioactive waste in rock, Report 2")
Roland Blomqvist
AB Atomenergi, 1977-05-17

16 Översikt av utländska riskanalyser samt planer och projekt rörande slutförvaring
("Review of foreign risk analyses and plans and projects concerning final storage")
Åke Hultgren
AB Atomenergi, August 1977

17 The gravity field in Fennoscandia and postglacial crustal movements
Arne Bjerhammar
Stockholm, August 1977

18 Rörelser och instabiliteter i den svenska berggrunden
("Movements and instability in the Swedish bedrock")
Nils-Axel Mörner
University of Stockholm, August 1977

19 Studier av neotektonisk aktivitet i mellersta och norra Sverige, flygbildsgenomgång och geofysisk tolkning av recenta förkastningar
("Studies of neotectonic activities in central and northern Sweden, review of aerial photographs and geophysical interpretation of recent faults")
Robert Lagerbäck
Herbert Henkel
Geological Survey of Sweden, September 1977

20 Tektonisk analys av södra Sverige, Vättern - Norra Skåne
("Tectonic analysis of southern Sweden, Lake Vättern - Northern Skåne")
Kennert Röshoff
Erik Lagerlund
University of Lund and Luleå Institute of Technology, September 1977

21 Earthquakes of Sweden 1891 - 1957, 1963 - 1972
Ota Kulhánek
Rutger Wahlström
University of Uppsala, September 1977

22 The influence of rock movement on the stress/strain situation in tunnels or boreholes with radioactive canisters embedded in a bentonite/quartz buffer mass
Roland Pusch
Luleå Institute of Technology, 1977-08-22

23 Water uptake in a bentonite buffer mass
A model study
Roland Pusch
Luleå Institute of Technology, 1977-08-22

24 Beräkning av utlakning av vissa fissionsprodukter och aktinider från en cylinder av franskt glas
("Calculation of leaching of certain fission products and actinides from a cylinder made of French glass")
Göran Blomqvist
AB Atomenergi, 1977-07-27

25 Blekinge kustgnejs. Geologi och hydrogeologi
("The Blekinge coastal gneiss, Geology and hydrogeology")
Ingemar Larsson Royal Institute of Technology
Tom Lundgren Swedish Geotechnical Institute
Ulf Wiklander Geological Survey of Sweden
Stockholm, August 1977

26 Bedömning av risken för fördröjt brott i titan
("Evaluation of risk of delayed fracture of titanium")
Kjell Pettersson
AB Atomenergi, 1977-08-25

27 A short review of the formation, stability and cementing properties of natural zeolites
Arvid Jacobsson
Luleå Institute of Technology, 1977-10-03

28 Värmeledningsförsök på buffertsubstans av bentonit/pitesilt
("Thermoconductivity experiments with buffer material of bentonite/pitesilt")
Sven Knutsson
Luleå Institute of Technology, 1977-09-20

29 Deformationer i sprickigt berg
("Deformations in fissured rock")
Ove Stephansson
Luleå Institute of Technology, 1977-09-28

30 Retardation of escaping nuclides from a final depository
Ivars Neretnieks
Royal Institute of Technology, Stockholm, 1977-09-14

31 Bedömning av korrosionsbeständigheten hos material avsedda för kapsling av kärnbränsleavfall. Lägesrapport 1977-09-27 samt kompletterande yttranden
("Evaluation of corrosion resistance of material intended for encapsulation of nuclear fuel waste. Status report, 1977-09-27, and supplementary statements")
Swedish Corrosion Research Institute and its reference group

32 Egenskaper hos bentonitbaserat buffertmaterial
("Properties of bentonite-based buffer material")
Roland Pusch
Arvid Jacobsson
Luleå Institute of Technology, 1978-06-10

33 Required physical and mechanical properties of buffer masses
Roland Pusch
Luleå Institute of Technology, 1977-10-19

34 Tillverkning av bly-titan kapsel
("Fabrication of lead-titanium canister")
Folke Sandelin AB
VBB
ASEA-Kabel
Swedish Institute for Metals Research
Stockholm, November 1977

35 Project for the handling and storage of vitrified high-level waste
Saint Gobain Techniques Nouvelles, October 1977

36 Sammansättning av grundvatten på större djup i granitisk berggrund
("Composition of groundwater deep down in granitic bedrock")
Jan Rennerfelt
Orrje & Co, Stockholm, 1977-11-07

37 Hantering av buffertmaterial av bentonit och kvarts
("Handling of buffer material of bentonite and quartz")
Hans Fagerström, VBB
Björn Lundahl, Stabilator
Stockholm, October 1977

38 Utformning av bergrumsanläggningar
("Design of rock cavern facilities")
Arne Finné, KBS
Alf Engelbrektson, VBB
Stockholm, December 1977

39 Konstruktionsstudier, direktdeponering
("Design studies, direct deposition")
Bengt Lönnerberg
ASEA-ATOM, Västerås, September 1978

40 Ekologisk transport och stråldoser från grundvattenburna radioaktiva ämnen
("Ecological transport and radiation doses from groundwater-borne radioactive substances")
Ronny Bergman
Ulla Bergström
Sverker Evans
AB Atomenergi, 1977-12-20

41 Säkerhet och strålskydd inom kärnkraftområdet.
Lagar, normer och bedömningsgrunder
("Safety and radiation protection in the field of nuclear power. Laws, standards and grounds for evaluation")
Christina Gyllander
Siegfried F Johnson
Stig Rolandson
AB Atomenergi and ASEA-ATOM, 1977-10-13

42 Säkerhet vid hantering, lagring och transport av använt kärnbränsle och förglasat högaktivt avfall
("Safety in the handling, storage and transportation of spent nuclear fuel and vitrified high-level waste")
Ann Margret Ericsson
Kemakta, November 1977

43 Transport av radioaktiva ämnen med grundvatten från ett bergförvar
("Transport of radioacitve elements in groundwater from a rock repository")
Bertil Grundfelt
Kemakta, 1977-12-13

44 Beständighet hos borsilikatglas
("Durability of borosilicate glass")
Tibor Lakatos
Glasteknisk Utveckling AB, Växjö, December 1977

45 Beräkning av temperaturer i ett envånings slutförvar i berg för förglasat radioaktivt avfall
("Calculation of temperatures in a single-level final repository in rock for vitrified radioactive waste")
Report 3
Roland Blomquist
AB Atomenergi, 1977-10-19

46 Temperaturberäkningar för använt bränsle
("Temperature calculations for spent fuel")
Taivo Tarandi
VBB, June 1978

47 Investigations of groundwater flow in rock around repositories for nuclear waste
John Stokes
Roger Thunvik
Department of agricultural hydrotechnics, Royal Institute of Technology, 1978-02-28

48 The mechanical properties of the rocks in Stripa, Kråkemåla, Finnsjön and Blekinge
Graham Swan
Luleå Institute of Technology, 1977-08-29

49 Bergspänningsmätningar i Stripa gruva
("Measurements of rock stresses in the Stripa mine")
Hans Carlsson
Luleå Institute of Technology, 1977-08-29

50 Lakningsförsök med högaktivt franskt glas i Studsvik
("Leaching trials with high-level French glass at Studsvik")
Göran Blomqvist
AB Atomenergi, November 1977

51 Seismotectonic risk modelling for nuclear waste disposal in the Swedish bedrock
F Ringdal
H Gjöystdal
E S Husebye
Royal Norwegian Council for scientific and industrial research, October 1977

52 Calculations of nuclide migration in rock and porous media penetrated by water
H Häggblom
AB Atomenergi, 1977-09-14

53 Mätning av diffusionshastighet för silver i lera-sand-blandning
("Measurement of rate of diffusion of silver in clay-sand-mix")
Bert Allard
Heino Kipatsi
Chalmers University of Technology, 1977-10-15

54 Groundwater movements around a repository

54:01 Geological and geotechnical conditions
Håkan Stille
Anthony Burgess
Ulf E Lindblom
Hagconsult AB, September 1977

54:02 Thermal analyses
Part 1 Conduction heat transfer
Part 2 Advective heat transfer
Joe L Ratigan
Hagconsult AB, September 1977

54:03 Regional groundwater flow analyses
Part 1 Initial conditions
Part 2 Long term residual conditions
Anthony Burgess
Hagconsult AB, October 1977

54:04 Rock mechanics analyses
Joe L Ratigan
Hagconsult AB, September 1977

54:05 Repository domain groundwater flow analyses
Part 1 Permeability perturbations
Part 2 Inflow to repository
Part 3 Thermally induced flow
Joe L Ratigan
Anthony Burgess
Edward L Skiba
Robin Charlwood
Hagconsult AB, September 1977

54:06 Final report
Ulf Lindblom et al
Hagconsult AB, October 1977

55 Sorption av långlivade radionuklider i lera och berg
("Sorption of long-lived radionuclides in clay and rock")
Part 1
Bert Allard
Heino Kipatsi
Jan Rydberg
Chalmers University of Technology, 1977-10-10

56 Radiolys av utfyllnadsmaterial
("Radiolysis of filler material")
Bert Allard
Heino Kipatsi
Jan Rydberg
Chalmers University of Technology, 1977-10-15

57 Stråldoser vid haveri under sjötransport av kärnbränsle
("Radiation doses in the event of a failure during the transport of nuclear fuel by sea")
Anders Appelgren
Ulla Bergström
Lennart Devell
AB Atomenergi, 1978-01-09

58 Strålrisker och högsta tillåtliga stråldoser för människan
("Radiation hazards and maximum permissible radiation doses for human beings")
Gunnar Walinder
FOA, Stockholm, 1977-11-04

59 Tectonic Lineaments in the Baltic from Gävle to Simrishamn
Tom Flodén
University of Stockholm, 1977-12-15

60 Förarbeten till platsval, berggrundsundersökningar
("Preliminary studies for site choice, bedrock studies")
Sören Scherman

Berggrundvattenförhållanden i Finnsjöområdets nordöstra del
("Groundwater conditions in the northeastern sector of the Finnsjö district")
Carl-Erik Klockars
Ove Persson
Geological Survey of Sweden, January 1978

61 Permeabilitetsbestämningar
("Permeability determinations")
Anders Hult
Gunnar Gidlund
Ulf Thoregren

Geofysisk borrhålsmätning
("Geophysical borehole survey")
Kurt-Åke Magnusson
Oscar Duran
Geological Survey of Sweden, January 1978

62 Analyser och åldersbestämningar av grundvatten på stora djup
("Analyses and age determinations of groundwater at great depths")
Gunnar Gidlund
Geological Survey of Sweden, 1978-02-14

63 Geologisk och hydrogeologisk grunddokumentation av Stripa försöksstation
("Geological and hydrogeological documentation at the Stripa research station")
Andrei Olkiewicz
Kenth Hansson
Karl-Erik Almén
Gunnar Gidlund
Geological Survey of Sweden, February 1978

64 Spänningsmätningar i Skandinavisk berggrund - förutsättningar, resultat och tolkning
("Stress measurements in Scandinavian bedrock - premises, results and interpretation")
Sten G A Bergman
Stockholm, November 1977

65 Säkerhetsanalys av inkapslingsprocesser
("Safety analysis of encapsulation processes")
Göran Carleson
AB Atomenergi, 1978-01-27

66 Några synpunkter på mekanisk säkerhet hos kapsel för kärnbränsleavfall
(Viewpoints on the mechanical reliability of a canister for nuclear waste")
Fred Nilsson
Royal Institute of Technology, Stockholm, February 1978

67 Mätning av galvanisk korrosion mellan titan och bly samt mätning av titans korrosionspotential under γ-bestrålning
("Measurement of galvanic corrosion between titanium and lead and measurement of corrosion potential of titanium under gamma radiation")
3 technical memorandums
Sture Henriksson
Stefan Poturaj
Maths Åsberg
Derek Lewis
AB Atomenergi, January-February 1978

68 Degraderingsmekanismer vid bassänglagring och hantering av utbränt kraftreaktorbränsle
("Degradation mechanisms in connection with pool storage and handling of spent nuclear reactor fuel")
Gunnar Vesterlund
Torsten Olsson
ASEA-ATOM, 1978-01-18

69 A three-dimensional method for calculating the hydraulic gradient in porous and cracked media
Hans Häggblom
AB Atomenergi, 1978-01-26

70 Lakning av bestrålat UO_2-bränsle
("Leaching of irradiated UO_2 fuel")
Ulla-Britt Eklund
Ronald Forsyth
AB Atomenergi, 1978-02-24

71 Bergspricktätning med bentonit
("Rock fissure sealing with bentonite")
Roland Pusch
Luleå Institute of Technology, 1977-11-16

72 Värmeledningsförsök på buffertsubstans av kompakterad bentonit
("Thermal conductivity tests on buffer material of compacted bentonite")
Sven Knutsson
Luleå Institute of Technology, 1977-11-18

73 Self-injection of highly compacted bentonite into rock joints
Roland Pusch
Luleå Institute of Technology, 1978-02-25

74 Highly compacted Na bentonite as buffer substance
Roland Pusch
Luleå Institute of Technology, 1978-02-25

75 Small-scale bentonite injection test on rock
Roland Pusch
Luleå Institute of Technology, 1978-03-02

76 Experimental determination of the stress/strain situation in a sheared tunnel model with canister
Roland Pusch
Luleå Institute of Technology, 1978-03-02

77 Nuklidvandring från ett bergförvar för utbränt bränsle
("Nuclide migration from a rock repository for spent fuel")
Bertil Grundfelt
Kemakta konsult AB, Stockholm, 1978-08-31

78 Bedömning av radiolys i grundvatten
("Evaluation of radiolysis in groundwater")
Hilbert Christenssen
AB Atomenergi, 1978-02-17

79 Transport of oxidants and radionuclides through a clay barrier
Ivars Neretnieks
Royal Institute of Technology, Stockholm, 1978-02-20

80 Utdiffusion av svårlösliga nuklider ur kapsel efter kapselgenombrott
("Diffusion of poorly soluble nuclides from a canister following canister penetration")
Karin Andersson
Ivars Neretnieks
Royal Institute of Technology, Stockholm, 1978-03-07

81 Tillverkning av kopparkapsel för slutförvaring av använt bränsle
("Fabrication of copper canisters for final storage of spent nuclear fuel")
Jan Bergström
Lennart Gillander
Kåre Hannerz
Liberth Karlsson
Bengt Lönnerberg
Gunnar Nilsson
Sven Olsson
Stefan Sehlstedt
ASEA, ASEA-ATOM, June 1978

82 Hantering och slutförvaring av aktiva metalldelar
("Handling and final storage of radioactive metal components")
Bengt Lönnerberg
Alf Engelbrektsson
Ivars Neretnieks
ASEA-ATOM, VBB (The Swedish Hydraulic Engineering Co., Ltd.), Royal Institute of Technology, June 1978

83 Hantering av kapslar med använt bränsle i slutförvaret
("Handling of canisters for spent fuel in the final repository")
Alf Engelbrektsson
VBB (The Swedish Hydraulic Engineering Co., Ltd.), April 1978

84 Tillverkning och hantering av bentonitblock
("Fabrication and handling of bentonite blocks")
Alf Engelbrektsson et al
VBB, ASEA, ASEA-ATOM, Gränges Mineralprocesser, June 1978

85 Beräkning av kryphastigheten hos ett blyhölje innehållande en glaskropp under inverkan av tyngdkraften
("Calculation of the creep rate of a lead jacket containing a glass body under the influence of gravity")
Anders Samuelsson

Förändring av krypegenskaperna hos ett blyhölje som följd av en mekanisk skada
("Alteration of creep properties of a lead jacket as a result of mechanical damage")
Göran Eklund
Institute of Metals Research, September 1977 - April 1978

86 Diffusivitetsmätningar av metan och väte i våt lera
("Diffusivity measurements of methane and hydrogen in wet clay")
Ivars Neretnieks
Christina Skagius
Royal Institute of Technology, Stockholm, 1978-01-09

87 Diffusivitetsmätningar i våt lera Na-lignosulfonat, Sr^{2+}, Cs^{+}
("Diffusivity measurements in wet clay, Na-lignosulphonate Sr^{2+}, Cs^{+}")
Ivars Neretnieks
Christina Skagius
Royal Institute of Technology, Stockholm, 1978-03-16

88 Groundwater chemistry at depth in granites and gneisses
Gunnar Jacks
Royal Institute of Technology, Stockholm, April 1978

89 Inverkan av glaciation på deponeringsanläggning belägen i urberg 500 m under markytan
("Influence of glaciation on a waste repository situated in primary bedrock 500 m below the surface of the ground")
Roland Pusch
Luleå Institute of Technology, 1978-03-16

90 Copper as an encapsulation material for unreprocessed nuclear waste - evaluation from the viewpoint of corrosion
Final report, 1978-03-31
The Swedish Corrosion Research Institute and its reference group

91 Korttidsvariationer i grundvattnets trycknivå
("Short-term variations in the pressure level of the groundwater")
Lars Y Nilsson
Royal Institute of Technology, Stockholm, September 1977

92 Termisk utvidgning hos granitoida bergarter
("Thermal expansion of granitoid rocks")
Ove Stephansson
Luleå Institute of Technology, April 1978

93 Preliminary corrosion studies of glass ceramic code 9617 and a sealing frit for nuclear waste canisters
I D Sundquist
Corning Glass Works, 1978-03-14

94 Avfallsströmmar i upparbetningsprocessen
("Waste flows in reprocessing")
Birgitta Andersson
Ann-Margret Ericsson
Kemakta, March 1978

95 Separering av C-14 vid upparbetningsprocessen
("Separation of C-14 in reprocessing")
Sven Brandberg
Ann-Margret Ericsson
Kemakta, March 1978

96 Korrosionsprovning av olegerat titan i simulerade deponeringsmiljöer för upparbetat kärnbränsleavfall ("Corrosion testing of unalloyed titanium in simulated deposition environments for reprocessed nuclear fuel waste")
Sture Henriksson
Marian de Pourbaix
AB Atomenergi 1978-04-24

97 Colloid chemical aspects of the "confined bentonite concept"
Jean C Le Bell
Institute of Surface Chemistry, 1978-03-07

98 Sorption av långlivade radionuklider i lera och berg Del 2 ("Absorption of long-lived radio nuclides in clay and rock Part 2")
Bert Allard
Heino Kipatsi
Börje Torstenfelt
Chalmers University of Technology, 1978-04-20

99 Lakning av högaktivt franskt glas ("Leaching of high-level radioactive French glass")
Status report 1978-06-01
Göran Blomqvist
AB Atomenergi, 1978-06-19

100 Dos och dosinteckning från grundvattenburna radioaktiva ämnen vid slutförvaring av använt kärnbränsle ("Dose and dose committment from groundwater-borne radioactive elements in the final storage of spent nuclear fuel")
Ronny Bergman
Ulla Bergström
Sverker Evans
AB Atomenergi, 1978-10-06

101 Utläckning av Ni-59 från ett bergförvar ("Leakage of Ni-59 from a rock repository")
Ivars Neretnieks
Karin Andersson
Lennart Henstam
Royal Institute of Technology, Stockholm, 1978-04-24

102 Metod att bocka bestrålade bränslestavar ("Method for bending irradiated fuel rods")
Torsten Olsson
ASEA-ATOM, 1978-03-29

103 Some aspects on colloids as a means for transporting nuclides
Ivars Neretnieks
Royal Institute of Technology, Stockholm, 1978-08-08

104 Finit elementanalys av bentonitfyllt bergförvar
("Finite element analysis of bentonite-filled rock repository")
Ove Stephansson
Kenneth Mäki
Tommy Groth
Per Johansson
Luleå Institute of Technology, July 1978

105 Neutroninducerad aktivitet i bränsleelementdetaljer
("Neutron-induced radioacitvity in fuel assembly components")
Nils A Kjellberg
AB Atomenergi, 1978-03-30

106 Strålningsnivå och till vatten deponerad strålningsenergi utanför kapslar i slutförvaret
("Radiation level and radiant energy imparted to water outside of canisters in the final repository")
Klas Lundgren
ASEA-ATOM, 1978-05-29

107 Blyinfodrad titankapsel för upparbetat och glasat kärnbränsleavfall - Bedömning ur korrosionssynpunkt
("Lead-lined titanium canister for reprocessed and vitrified nuclear fuel waste - Evaluation from the viewpoint of corrosion")
The Swedish Corrosion Institute and its reference group
Final report
1978-05-25

108 Criticality in a spent fuel repository in wet crystalline rock
Peter Behrenz
Kåre Hannerz
ASEA-ATOM, 1978-05-30

109 Lakningsbar spaltaktivitet
("Leachable gap activity")
Lennart Devell
Rolf Hesböl
AB Atomenergi, October 1978

110 In situ experiments on nuclide migration in fractured crystalline rocks
Ove Landström
Carl-Erik Klockars
Karl-Erik Holmberg
Stefan Westerberg
Studsvik Energiteknik and
The Geological Survey of Sweden
July 1978

111 Nuklidhalter i använt LWR-bränsle och i högaktivt avfall från återcykling av plutonium i PWR
("Nuclide levels in spent LWR fuel and in high level waste from the recycling of plutonium in PWR")
Nils Kjellberg
AB Atomenergi, 1978-07-26

112 Säkerhetsanalys av hanteringsförfarandet vid inkapsling av utbränt bränsle i kopparkapsel
("Safety analysis of the handling procedure in the encapsulation of spent fuel in copper canisters")
Erik Nordesjö
ASEA-ATOM, 1978-03-20

113 Studier av keramiska material för inkapsling av högaktivt avfall
("Studies of ceramic material for encapsulation of high-level waste")
Lennart Hydén et al
ASEA-ATOM, September 1978

114 γ-radiolysis of organic compounds and α-radiolysis of water
Hilbert Christensen
Studsvik Energiteknik AB, 1978-09-07

115 Accelererad utlösning av uran från α-aktivt UO_2
("Accelerated dissolution of uranium from α-active UO_2")
Gösta Nilsson
Studsvik Energiteknik AB, 1978-04-27

116 Lakning av Al_2O_3 under simulerande deponeringsbetingelser
("Leaching of Al_2O_3 under simulated repository conditions")
Britt-Marie Svensson
Lennart Dahl
Studsvik Energiteknik AB, 1978-06-02

117 Lakning av Al_2O_3 i dubbeldestillerat vatten
("Leaching of Al_2O_3 in twice-distilled water")
Britt-Marie Svensson
Göran Blomqvist
Studsvik Energiteknik AB, 1978-05-29

118 Slutrapport Al_2O_3 kapsel
("Final report on Al_2O_3 canister")
The Swedish Corrosion Institute and its reference group

119 Slutförvaring av aktiverade ståldetaljer i betong
("Final storage of activated steel components in concrete")
Lars Rombén
Kyösti Tuutti
The Swedish Cement and Concrete Research Institute, 1978-07-14

120 Some notes in connection with the KBS studies of final disposal of spent fuel
Ivars Neretnieks
Royal Institute of Technology, September 1978